LIPID NANOPARTICLES AS A NOVEL STRATEGY TO DELIVER BIOACTIVE MOLECULES

frontiers Research Topics

About Frontiers

Frontiers is more than just an open-access publisher of scholarly articles: it is a pioneering approach to the world of academia, radically improving the way scholarly research is managed. The grand vision of Frontiers is a world where all people have an equal opportunity to seek, share and generate knowledge. Frontiers provides immediate and permanent online open access to all its publications, but this alone is not enough to realize our grand goals.

Frontiers Journal Series

The Frontiers Journal Series is a multi-tier and interdisciplinary set of open-access, online journals, promising a paradigm shift from the current review, selection and dissemination processes in academic publishing. All Frontiers journals are driven by researchers for researchers; therefore, they constitute a service to the scholarly community. At the same time, the Frontiers Journal Series operates on a revolutionary invention, the tiered publishing system, initially addressing specific communities of scholars, and gradually climbing up to broader public understanding, thus serving the interests of the lay society, too.

Dedication to Quality

Each Frontiers article is a landmark of the highest quality, thanks to genuinely collaborative interactions between authors and review editors, who include some of the world's best academicians. Research must be certified by peers before entering a stream of knowledge that may eventually reach the public - and shape society; therefore, Frontiers only applies the most rigorous and unbiased reviews.
Frontiers revolutionizes research publishing by freely delivering the most outstanding research, evaluated with no bias from both the academic and social point of view. By applying the most advanced information technologies, Frontiers is catapulting scholarly publishing into a new generation.

What are Frontiers Research Topics?

Frontiers Research Topics are very popular trademarks of the Frontiers Journals Series: they are collections of at least ten articles, all centered on a particular subject. With their unique mix of varied contributions from Original Research to Review Articles, Frontiers Research Topics unify the most influential researchers, the latest key findings and historical advances in a hot research area! Find out more on how to host your own Frontiers Research Topic or contribute to one as an author by contacting the Frontiers Editorial Office: frontiersin.org/about/contact

LIPID NANOPARTICLES AS A NOVEL STRATEGY TO DELIVER BIOACTIVE MOLECULES

Topic Editors:
Alan Talevi, National University of La Plata, Argentina
Guillermo Raul Castro, Consejo Nacional de Investigaciones Científicas y Técnicas (CONICET), Argentina
Nelson Duran, State University of Campinas, Brazil

Table of Contents

frontiers in Chemistry

Editorial: Lipid Nanoparticles as a Novel Strategy to Deliver Bioactive Molecules

Alan Talevi [1,2]*, Nelson Duran [3] and Guillermo Raul Castro [4]

[1]Laboratory of Bioactive Research and Development (LIDeB), Department of Biological Sciences, Faculty of Exact Sciences, University of La Plata (UNLP), La Plata, Argentina, [2]Consejo Nacional de Investigaciones Científicas y Técnicas (CONICET), Buenos Aires, Argentina, [3]Laboratory of Urogenital Carcinogenesis andImmunotherapy, Department of Structural and Functional Biology, Institute of Biology, University of Campinas (UNICAMP), Campinas, Brazil, [4]Laboratorio de Nanobiomateriales, Centro de Investigacióny Desarrollo enFermentaciones Industriales (CINDEFI), Departamento de Química, Facultad de Ciencias Exactas, Universidad Nacional deLa Plata (UNLP)-CONICET (CCT La Plata), La Plata, Argentina

Editorial on the Research Topic

Lipid Nanoparticles as a Novel Strategy to Deliver Bioactive Molecules

Lipid nanoparticles are so far among the most successful nanodelivery systems, considering the significant proportion of marketed nanocarriers that correspond to this category. High loading capacity, biocompatibility, and environmentally friendly obtention techniques can be mentioned among their most prominent specific advantages. The current research topic on *Lipid Nanoparticles as a Novel Strategy to Deliver Bioactive Molecules* encompasses original and review articles on a wide range of lipid nanoparticle-related topics, from encapsulation of gene therapies to novel characterization approaches. The collection of articles also expresses the increasing versatility of these nanosystems, owing to the use of hybrid and functionalized carriers.

The review article "Solid lipid nanoparticles for drug delivery: pharmacological and biopharmaceutical aspects" provides a literature survey on original publications from the last 7 years, considering only those articles where pharmacodynamic and/or pharmacokinetic studies have been performed. The article focuses on biopharmaceutical aspects of nanosystems administered through different routes, from oral absorption to enhanced brain penetration, including a critical view on current uncertainties and future directions.

The article "Surface Plasmon Resonance as a Characterization Tool for Lipid Nanoparticles used in Drug Delivery" describes recent work on the use of surface plasmon resonance to predict the potential interactions of lipid nanoparticles with biological proteins, including constituents of the protein corona that may trigger elimination by the mononuclear phagocyte system, thus conditioning their bioavailability.

For their part, Muraca et al. reviewed the use of lipid nanosystems for the delivery of therapeutics against a group of three trypanosomatid-caused neglected diseases: African trypanosomiasis, Chagas disease, and leishmaniasis. The article "Trypanosomatid-caused conditions: State of the art of therapeutics and potential applications of lipid-based nanocarriers" concludes that lipid nanocarriers could improve the efficacy–safety balance of known treatments, diminishing cytotoxicity and organ toxicity, especially in the case of leishmaniasis. However, it also underlines that last generation systems are still to be widely explored in the field of neglected conditions.

In the work entitled "Functional hybrid nanoemulsions for sumatriptan intranasal delivery," Ribeiro et al. developed nanostructures composed of biopolymers and copaiba essential oil for the delivery of sumatriptan for intranasal administration. The work tried to solve bioavailability issues of

that antimigraine active pharmaceutical ingredient. From the biopolymers screened, alginate was selected to produce a nanoemulsion of sumatriptan with the oil. The nanoemulsions displayed high entrapment efficiency in the range of 69 to 41%, high stability during at least for one year, and improved kinetic release compared to free drug. Also, tests on zebrafish larvae did not show changes in behavior either in their morphology.

An interesting work entitled "Optimizing the intracellular delivery of therapeutic anti-inflammatory TNF-α siRNA to activated macrophages using lipidoid-polymer hybrid nanoparticles" presented by Lokras et al. applied quality by design methodology to optimize RNA interference as strategy to silence the overexpression of pro-inflammatory cytokines such as tumor necrosis factor-alpha (TNF-α) induced by macrophages during lung pathologies like chronic obstructive pulmonary disease (COPD). A hybrid platform used for the intracellular delivery of TNF-α siRNA was the lipid-like transfection agent lipidoid L5 and poly(D,L-lactide-co-glycolide) successfully assayed in lipopolysaccharide-activated murine macrophage cell line RAW 264.7. Importantly, kinetic release of fluorescent siRNA from LPNs *in vitro* and *in vivo* demonstrated not only sustained release of siRNA from the nanoparticles but also a correlation between cell uptake and *in vivo* distribution. In a related review ("Advances in Lipid Nanoparticles for mRNA-Based Cancer Immunotherapy"), Guevara et al. summarize recent advances in the development of lipid particles for the delivery of mRNA-based immunotherapies, with a focus on cancer treatment. They also highlight a diversity of immunotherapeutic approaches through mRNA delivery and discuss the main factors affecting *in vivo* transfection efficiency and tropism of mRNA-loaded lipid nanoparticles.

In another relevant work called "Rapamycin-loaded lipid nanocapsules induce selective inhibition of the mTORC1-signaling pathway in glioblastoma cells," Garcion et al. developed lipid nanocapsules containing rapamycin, a poorly water-soluble inhibitor of mTOR phosphorylation at Ser(2448), for potential application in cancer, particularly in glioblastomas combined with radiotherapy. Inhibition of mTOR phosphorylation down regulates a serine protein kinase (Akt) involved in the regulation of the progression of cancer cells. The work suggests that the new developed nanocarrier for rapamycin could be used as radiosensitizer and could be used for local–regional or peripherical administration for the treatment of glioblastomas.

In the work entitled "*In silico* and *in vitro* evaluation of mimetic peptides as potential antigen candidates for prophylaxis of leishmaniasis," Guedes et al. performed the liposomal encapsulation of synthetic peptides with antigenic activity against *Leishmania* spp. Six peptides obtained from *Leishmania* spp. membranes and histones were synthetized by the phage display technique. The entrapped peptide was administered to New Zealand rabbits and used to determine humoral immunogenic protection against *L. braziliensis* or *L. infantum*. The peptide mixture triggered IFN-γ, IL-12, IL-4, and TGF-β, which induced Th1 and Th2 cellular immune response by polarization of T CD4$^+$ cells and high expression of iNOS in infected rabbits. These promissory results will be extended for the treatment of other pathologies and imply a new approach for the development of novel type of vaccines.

AUTHOR CONTRIBUTIONS

All authors listed have made a substantial, direct, and intellectual contribution to the work and approved it for publication.

Advances in Lipid Nanoparticles for mRNA-Based Cancer Immunotherapy

Maria L. Guevara[1], Francesca Persano[2] and Stefano Persano[3*]

[1] Barts Cancer Institute, Queen Mary University of London, London, United Kingdom, [2] Department Matematica e Fisica 'Ennio De Giorgi', Università del Salento, Lecce, Italy, [3] Nanomaterials for Biomedical Applications, Istituto Italiano di Tecnologia (IIT), Genova, Italy

Over the past decade, messenger RNA (mRNA) has emerged as potent and flexible platform for the development of novel effective cancer immunotherapies. Advances in non-viral gene delivery technologies, especially the tremendous progress in lipid nanoparticles' manufacturing, have made possible the implementation of mRNA-based antitumor treatments. Several mRNA-based immunotherapies have demonstrated antitumor effect in preclinical and clinical studies, and marked successes have been achieved most notably by its implementation in therapeutic vaccines, cytokines therapies, checkpoint blockade and chimeric antigen receptor (CAR) cell therapy. In this review, we summarize recent advances in the development of lipid nanoparticles for mRNA-based immunotherapies and their applications in cancer treatment. Finally, we also highlight the variety of immunotherapeutic approaches through mRNA delivery and discuss the main factors affecting transfection efficiency and tropism of mRNA-loaded lipid nanoparticles *in vivo*.

Keywords: monoclonal antibodies, CAR T cells, cancer vaccines, lipid nanoparticles, therapeutic mRNA, cancer immunotherapy

INTRODUCTION

mRNA-based therapeutics have emerged as a highly appealing new class of drugs, revolutionizing cancer immunotherapy by finding application in different types of anticancer approaches, such as therapeutic vaccines, monoclonal antibodies, immunomodulatory drugs and CAR cell therapies (Van Lint et al., 2012; Kranz et al., 2016; Pardi et al., 2018; Foster et al., 2019; Hoecke and Roose, 2019). In comparison to other functional biomolecules such as plasmid DNA (pDNA) and recombinant proteins, mRNA exhibits several therapeutic benefits, thereby rendering it highly desirable for the development of a new generation of cancer immunotherapy drugs (Pastor et al., 2018).

Firstly, mRNA possesses a superior safety profile indeed, unlike pDNA, mRNA cannot integrate into the genome and thus avoids potential insertional mutagenesis (Sahin et al., 2014). Moreover, mRNA efficiently transfects both mitotic and non-mitotic cells, as it does not require to enter into the nucleus since it exerts its function in the cytoplasmic compartment (Sahin et al., 2014).

Translatability and stability of mRNA as well as its immunostimulatory activity are further intrinsic features that make it the most attractive type of therapeutic agent emerged in the last decade, especially for cancer immunotherapy (Pastor et al., 2018; Guevara et al., 2019b).

Finally, large-scale production of Good Manufacturing Practice (GMP)-grade mRNA is relatively simple, fast and inexpensive, since mRNA is synthesized in a cell-free system, and its manufacturing can be obtained in standardized and controlled conditions (Sahin et al., 2014; Pardi et al., 2018; Guevara et al., 2019b).

Despite the enormous potential of mRNA-based therapies, only recently has their therapeutic application become possible, as a consequence of the considerable progresses of nanomedicine in the design of non-viral vectors for gene delivery (Guan and Rosenecker, 2017; Kaczmarek et al., 2017). In this regard, various type of nanoparticles have been investigated as mRNA delivery systems, but lipid nanoparticles have been the most extensively explored for mRNA-based immunotherapy, enabling a variety of new antitumor treatments currently in preclinical development and some undergoing clinical trials (Gómez-Aguado et al., 2020).

The use of lipid-based nanocarriers has addressed key issues for mRNA transfection into target cells by improving its protection from degradation in the extracellular compartments, as well as by facilitating cellular uptake and delivery to an appropriate intracellular compartment (Wadhwa et al., 2020). Herein, we will provide an overview on the recent advances in the field of lipid-based nanoparticles and on the design of mRNA delivery platforms for various forms of cancer immunotherapy.

LIPID-BASED NANOPARTICLES FOR MRNA DELIVERY: BASIC FORMULATION AND STRUCTURAL ORGANIZATION

The encapsulation of mRNA into a carrier is essential to fully harness its therapeutic power by ensuring protection from extracellular RNase degradation and simultaneously promoting cellular uptake and endosomal escape of mRNA (Guan and Rosenecker, 2017; Guevara et al., 2019b).

To enable mRNA encapsulation, protection, and transfection, amine-containing nanomaterials are commonly used as non-viral platforms (Kranz et al., 2016; McKinlay et al., 2017; Oberli et al., 2017; Persano et al., 2017; Zhang et al., 2019). Lipid-base formulations represent the most developed tool for mRNA delivery (Wadhwa et al., 2020).

Lipoplexes, consisting of cationic liposomes interacting electrostatically with the negative charges of the phosphate backbone of mRNA, were the earliest lipid-based delivery systems successfully employed to introduce mRNA molecules into target cells (**Figure 1**) (Felgner and Ringold, 1989; Kranz et al., 2016). However, after a first brief phase of great enthusiasm, lipoplexes have shown important concerns, such as high instability, relatively low transfection efficiency and poor customizable composition, given that they are often formulated with an excess of cationic charges not only to promote mRNA binding but also to facilitate the interaction with the anionic phospholipids in the plasma membrane and subsequently promote its uptake by endocytosis (Li and Huang, 1997; Xue et al., 2015; Guevara et al., 2019b; Wahane et al., 2020).

These drawbacks have limited further application of nucleic acid-loaded lipoplexes, thus shifting the current interest on lipid nanoparticles, which have demonstrated superior stability, structural plasticity and enhanced gene delivery (Xue et al., 2015; Guevara et al., 2019b).

A typical lipid nanoparticle formulation is composed of pH-responsive lipids or cationic lipids bearing tertiary or quaternary amines to encapsulate the polyanionic mRNA; neutral helper lipids such as zwitterionic lipid [i.e., 1,2-dioleoyl-sn-glycero-3-phosphoethanolamine (DOPE) or 1,2-distearoyl-sn-glycero-3-phosphocholine (DSPC)] and/or sterol lipid (i.e., cholesterol) to stabilize the lipid bilayer of the lipid nanoparticle and to enhance mRNA delivery efficiency; and a polyethylene glycol (PEG)-lipid to improve the colloidal stability in biological environments by reducing aspecific absorption of plasma proteins and forming a hydration layer over the nanoparticles (Cullis and Hope, 2017; Guevara et al., 2019b). The morphology of lipid nanoparticles is not like a traditional liposome, characterized by a lipid bilayer surrounding an aqueous core, indeed, they possess an electron-dense core, where the cationic/ionizable lipids are organized into inverted micelles around the encapsulated mRNA molecules (**Figure 1**) (Cullis and Hope, 2017; Guevara et al., 2019b).

Recently, lipid-polymer hybrid nanoparticles have emerged as novel mRNA delivery systems combining the advantages of biodegradable polymeric nanoparticles and liposomes (Persano et al., 2017; Islam et al., 2018; Guevara et al., 2019b). Lipid-polymer hybrid nanoparticles consist of a biodegradable mRNA-loaded polymer core coated with a lipid layer (Persano et al., 2017; Islam et al., 2018; Guevara et al., 2019b). Usually, the lipid envelope is organized into a lipid bilayer or lipid monolayer containing a mixture of cationic or ionizable lipids, helper lipids, and pegylated lipid (**Figure 1**).

Lipid-polymer hybrid nanoparticles, thanks to their structural design, can offer a series of benefits such as small size, high nucleic acid condensation efficiency, large functionalizable surface that can be easily modified by the binding of different functional groups, and prolonged blood circulation time (Guevara et al., 2019b). In addition, the specific physicochemical properties of hybrid lipid-polymer nanostructures can potentially result in a different interaction of the delivered mRNA with innate RNA sensors, consequently altering the immunogenicity and safety profile of lipopolyplex-based immunotherapies (Van der Jeught et al., 2018).

The above benefits of hybrid lipid-polymer formulations have been highlighted in a recent study were an mRNA-loaded lipid-polymer platform functionalized with mannose receptor targeting moieties to promote dendritic cell (DC) targeting *in vivo* was employed (Van der Jeught et al., 2018). The formulation exhibited excellent hemocompatibility and the expression of the mRNA cargo was preferentially restricted to splenic antigen presenting cells (APCs) upon systemic administration. Furthermore, vaccination with the lipopolyplex formulation elicited a potent T-cell-mediated immune response and manifested superior effectiveness in inhibiting tumor growth compared to intravenous immunization with a lipoplex-based mRNA vaccine (Van der Jeught et al., 2018). Early innate

FIGURE 1 | Schematic representation of the different types of lipid-base nanovectors: lipoplex, lipid nanoparticle, lipid-polymer hybrid nanoparticle where the lipid shell can be organized as a bilayer or monolayer.
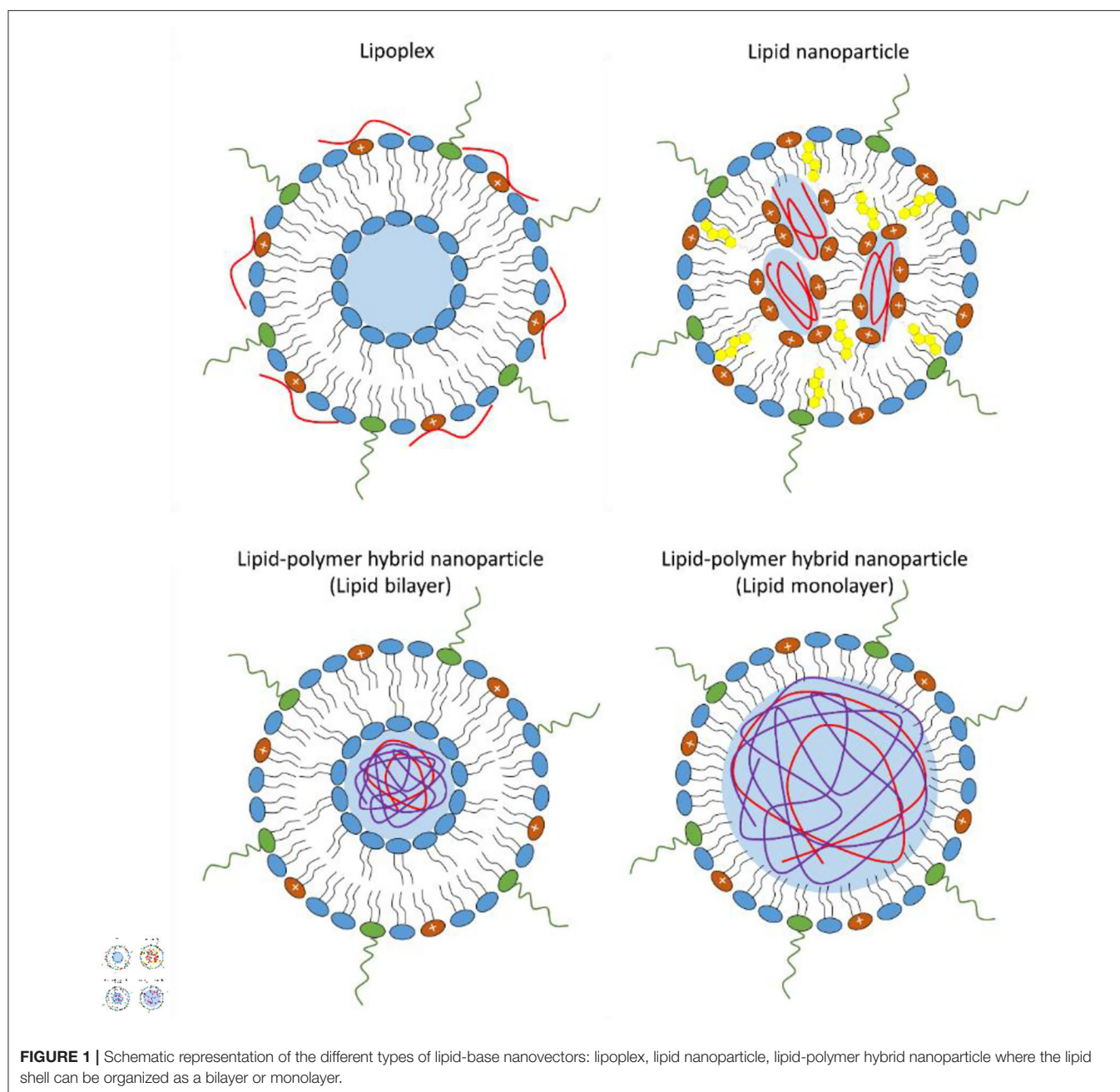
responses to hybrid lipid-polymer vaccine formulation were characterized by a type I interferon (IFN) response in the spleen. Nevertheless, unlike conventional lipoplexes, the hybrid lipid-polymer nanovaccine did not rely on type I IFN responses to generate cytotoxic T-cell effectors (Van der Jeught et al., 2018). This unlooked behavior of lipopolyplex nanostructures could enable the preparation of new anticancer therapeutic vaccines with a more moderate pro-inflammatory profile, but with an equal capacity to promote a potent immune response, representing a valid alternative to the lipid formulated mRNA vaccines currently under investigation in early phase clinical trials.

CELLULAR INTERNALIZATION AND ENDOSOMAL ESCAPE OF MRNA-LOADED LIPID-BASED NANOPARTICLES

Although the mechanism that leads to the internalization of RNA-loaded lipid-based nanoparticles has not been fully clarified, experimental insights revealed that the process involves clathrin-dependent endocytosis followed by micropinocytosis, that is the major uptake mechanism (Gilleron et al., 2013; Wang and Huang, 2013). The initial interaction of nanoparticles with the cell plasma membrane of the target cells can be promoted or accelerated by the presence of positive charges or active

targeting ligands on the outer surface, which can interact with the negatively charged cell membrane components or with specific proteins exposed at the cell membrane of the target cell (Hajj and Whitehead, 2017).

Once the lipid nanoparticles are engulfed into the cell, they follow the conventional endocytic route, trafficking first into early endosomes, then into late endosomes, and finally into lysosomes where the RNA is enzymatically degraded. It has been estimated that only a small fraction (1–2%) of lipid nanoparticles can evade the endosomal pathway before they reach the lysosomes and this tend to vary between cell types (Gilleron et al., 2013). The proton sponge effect was initially considered the dominant mechanism leading to the endosomal escape of the RNA-loaded lipid nanoparticles. However, increasing evidence indicates that the endosomal escape mechanism of lipid nanoparticles is much more complex, and involves the docking of the lipid nanoparticles at the endosomal membrane, triggering membrane fusion and destabilization of the endosomal lipid bilayer, with consequent release of the genetic cargo into the cytosol (Zelphati and Szoka, 1996; Gilleron et al., 2013).

Previous studies revealed that endosomal escape occurs mainly from early endosomes or macropinosomes before their fusion with lysosomes, since late endosomes and lysosomes are characterized by lower leakiness, due to the variation in the lipid composition occurring during endosome maturation (Gilleron et al., 2013; Wang and Huang, 2013). These changes in the cell membrane lipid composition consist in a decrease of the cholesterol content, the hydrolysis of sphingomyelin and increased levels of phosphatidylcholine in the membranes of late endosomes and lysosomes. However, a recent study suggested that late endosome/lysosome formation could be essential for the functional delivery of mRNA (Patel et al., 2017). Indeed, Rab7A-deficient cells exhibited not significant changes in mRNA-uptake but a strong decrease in the transfection efficiency compared to wild-type cells. Conversely, the absence of Rab4A or Rab5A, both localized at the early/recycling endosomes, had limited effects on cell transfection efficiency. Interestingly, the authors showed that mRNA electroporation of Rab7A knockout cells was not able to rescue the basal transfection efficiency obtained in wild-type cells, and provided evidence that the late endosome/lysosome structure can positively control the translation of the delivered mRNA by serving as hub for the mammalian target of rapamycin complex 1 (mTORC1)-mediated signaling pathway (Patel et al., 2017).

Recently, Maugeri et al. showed that after endocytosis a small fraction of mRNA-loaded lipid nanoparticles can immediately evade the endocytic route and be consigned to the recycling pathway to be expelled by exocytosis (Maugeri et al., 2019). After secretion, the mRNA packed into extracellular vesicles can be transferred in other cells *in vitro* and blood/organs *in vivo* and produce new copies of protein (Maugeri et al., 2019).

All these findings suggest that mRNA transfection mediated by lipid nanoparticles is an overly complex process, strongly influenced by several factors, such as uptake mechanism, endosomal maturation, endosomal recycling, and may vary widely between different cell types. Inefficient endosomal escape efficacy and precise tissue/cell targeting efficiency

remain the major challenges for mRNA delivery by lipid-based nanoplatforms. A better understanding of the mechanisms regulating the biodistribution, internalization and endosomal escape of mRNA-loaded lipid nanoparticles will help in the development of next generation nanoparticle-based mRNA immunotherapies with increase efficacy, safety, and clinical translatability.

LIPID COMPOSITION OF LIPID-BASED NANOPARTICLES FOR MRNA DELIVERY

Cationic Lipids

Cationic lipids are amphiphilic molecules, consisting of a positively charged polar head group, and a hydrophobic tail domain, that in aqueous solution spontaneously self-assemble into higher order aggregates (**Figure 2**) (Guevara et al., 2019b). Thanks to their cationic amino groups, they can electrostatically interact with the negatively charged phosphate groups of mRNA molecules and allow their entrapment in a lipid-based nanoparticle (Guevara et al., 2019b).

The use of delivery systems based on permanently cationic lipids have proven to be effective for mRNA *in vitro* transfection and was described for the first time more than 30 years ago (Felgner and Ringold, 1989; Malone et al., 1989). In this study, a relative high transfection efficiency was achieved using a lipoplex structure, obtained by complexing mRNA with a liposome containing the synthetic cationic lipid, N-[1-(2,3-dioleyloxy)propyl-N,N,N-trimethylammonium chloride (DOTMA), and the helper lipid DOPE (Malone et al., 1989). After this encouraging early result, further mRNA therapeutic development was abandoned, due to its high fragility and the inadequate knowledge at that time on the potential of non-viral vectors in protecting and efficiently deliver RNA molecules into eukaryotic cells (Guevara et al., 2019b). The recent revival interest in the use of mRNA-based immunotherapies has encouraged an advancement on the design of cationic lipid-based nanocarriers mostly for cancer immunotherapy (Guevara et al., 2019b).

On this regard, the study from 2016 by Kranz et al. has represented the culmination of several years of interdisciplinary research on mRNA-based drug optimization and has provided the bases for the development of novel mRNA-based cancer immunotherapies (Kranz et al., 2016). The authors showed that mRNA-lipoplexes composed of DOTMA/DOPE or 1,2-dioleoyl-3-trimethylammonium-propane (DOTAP)/DOPE lipids, formulated by gradually decreasing their surface charge from positive to negative, were able to protect antigen-encoding mRNA from extracellular ribonucleases, efficiently accumulating in the spleen and delivering the mRNA into DCs upon systemic administration, with the consequent induction of an antigen-specific immune response (Kranz et al., 2016).

More recently, Cheng et al. reported the percentage of permanently cationic lipid contained in the formulation as the main factor affecting bio-distribution of pH-independent cationic lipid nanoparticles (Cheng et al., 2020). Surprisingly,
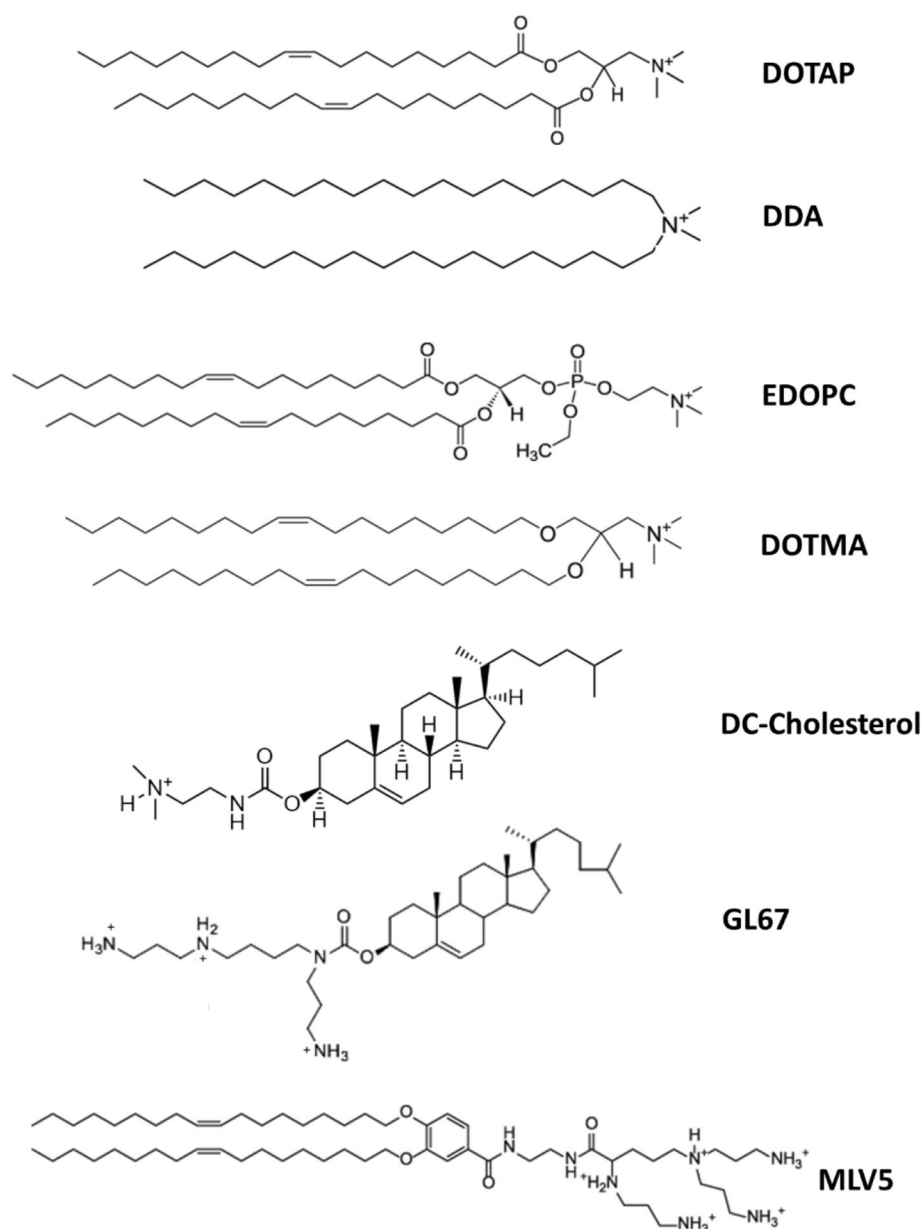
FIGURE 2 | Chemical structure of the major cationic lipids utilized for mRNA delivery.

by increasing the percentage of DOTAP lipid from 5 to 100%, the expression of the encapsulated luciferase-encoding mRNA shifted progressively from liver to spleen, and then to lung, demonstrating that the percentage of cationic lipid can be opportunely tailored for tissue-specific delivery via an intravenous administration route (Cheng et al., 2020).

Cationic lipid-based nanoparticles have seen a widespread use in the delivery of therapeutic mRNA, not only for their ability to form stable complexes with nucleic acids, but also because they have revealed intrinsic immunogenic properties attributable to the interaction with innate immune components, thus

serving as immune adjuvants to enhance the immunogenicity of formulations.

For instance, the immunogenicity of the cationic lipid dimethyldioctadecylammonium (DDA) was illustrated already more than 50 years ago by Gall (Gall, 1966). DDA can act as a vaccine adjuvant, enhancing both cell-mediated and humoral immunity, and it has shown to be effective in different vaccine platforms, including mRNA-based vaccines (Henriksen-Lacey et al., 2010; Blakney et al., 2019). The adjuvant activity of DDA has been attributed to its positive surface charge and its ability to interact and stabilize antigens by ionic interactions. This was

demonstrated by using fluorescently labeled ovalbumin (OVA) as a model antigen (Korsholm et al., 2007). The adsorption of the antigen onto DDA liposomes enhanced its uptake by APCs, in addition to increasing its immunogenicity as confirmed by the significant upregulation in the expression of maturation markers of APCs, all this resulted in the improvement of their effectiveness in antigen presentation (Korsholm et al., 2007). Similarly, both DOTAP- and DOTMA- based nanostructures have been reported to induce the activation of TLRs and NLRP3 inflammasome pathways (Lonez et al., 2014). Therefore, delivery platforms containing permanently cationic lipids can be opportunely designed and tuned to obtain novel mRNA-based immunotherapies with superior immunogenicity and therapeutic efficacy.

Ionizable Lipids and Lipid-Like Polymers

A second generation of transfecting lipids was developed due to the necessity of novel delivery systems for siRNA molecules with improved safety profile and able to accumulate more efficiently at the target site, avoiding sequestration by blood-filtering organs like liver and spleen, a phenomenal frequently observed mostly with positively charged nanoparticles (**Figure 3**) (Blanco et al., 2015).

In the first half of the 1990s, Cullis developed the first pH-responsive cationic lipid, bearing the unique feature that its net charge changed in response to the pH of its surroundings, acquiring a net positive charge in an acidic pH and maintaining a neutral charge in a physiological pH (Bailey and Cullis, 1994). Thus, mRNA encapsulation into pH-responsive lipid nanoparticles is achieve only in acidic conditions. Nanoparticles formulated with these lipids have a minimal positive charge density in the bloodstream, and therefore tend to display a superior biocompatibility and a reduced off-target accumulation (Tam et al., 2013). Several ionizable lipids have been proposed, initially for siRNA delivery and, recently, their application has been extended to mRNA delivery (**Figure 3**).

The initial difficulties encountered in achieving efficient mRNA delivery by using lipid formulations designed for siRNA delivery pointed out that delivery systems should be specifically tailored for mRNA, as it has different features compared to siRNA. Therefore, previously proposed lipid formulations have been re-optimized and new ionizable synthetic lipids have been introduced with the aim of enhancing the delivery and translation of mRNA *in vivo*, and thus improving its therapeutic effect.

Several studies conducted in this area have allowed to identify the pKa value as the dominant factor affecting the transfection efficiency of ionizable lipids, with an optimal pKa range of 6.2–6.5 (Cullis and Hope, 2017). DLin-MC3-DMA (MC3), having an optimized pKa value of 6.44, represents one of the most powerful pH-dependent cationic lipids that has been synthesized for RNA delivery, and it has been successfully employed for protein replacement therapy of genetic diseases such as the neurodegenerative disease Friedreich's ataxia (Tam et al., 2013; Nabhan et al., 2016; Arteta et al., 2018). MC3-based lipid nanoparticles encapsulating either luciferase or farataxin encoding mRNA and intrathecally injected in mice resulted

in high protein expression into dorsal root ganglion neurons (Nabhan et al., 2016).

Lipid-like materials also known as lipidoids, represent a new generation of ionizable lipids characterized by protonable tertiary-amino groups and highly hydrophobic side chains, which play a significant role in determining transfection efficiency (**Figure 3**). Indeed, experimental observations helped to clarify the huge impact that the chemical structure of the tail portion of cationic lipids could have on the transfection efficiency of lipid-based nanoparticles. In this regard, a recently conducted screening study revealed that longer and unsaturated alkyl tails could enhance mRNA delivery efficiency (Fenton et al., 2016).

Similarly, a biodegradable ionizable lipid obtained by modifying the hydrophobic tail of MC3 lipid through the introduction of ester and alkyne groups, in addition to showing an improved tolerability, displayed an enhanced transfection efficiency. In particular, Miao et al. observed that the incorporation of an unsaturated alkyne group, rather than double bounds, in the non-polar tail of the ionizable lipid can improve the fusogenicity with the endosomal membrane, and consequently facilitate endosomal escape and mRNA release into the cytosol (Miao et al., 2020). Additionally, its co-formulation with cKK-E12 pH-responsive cationic lipid synergistically boosted mRNA delivery into hepatocytes, offering early evidence that novel and more efficient delivery systems could be potentially obtained from the co-formulation of distinct ionizable lipids. cKK-E12-based lipids have been shown to enhance the serum stability and protein binding of the particles (Miao et al., 2020).

Ionizable lipid-based nanoparticles were recently utilized to facilitate the development of several mRNA-based immunotherapies for cancer treatment. For instance, Oberli et al. demonstrated the efficacy of ionizable lipid-based nanoparticles for antigen encoding mRNA-based anti-tumor vaccination (Oberli et al., 2017). Interestingly, the authors reported that unmodified mRNA led to a significantly higher number of antigen-specific CD8$^+$ T cells in peripheral blood, compare to modified mRNA, upon subcutaneous administration. Finally, the anti-tumor vaccine obtained by loading a TRP-2 encoding mRNA into ckk-E12-based lipid nanoparticles significantly suppressed tumor growth and extended the survival of B16 F10 tumor-bearing mice, and the addition of LPS into the formulation further improved this effect (Oberli et al., 2017). A similar formulation was proposed in a recently published study by Stadler et al. showing that antibody-encoding mRNA delivery can enable antibody-mediated cancer immunotherapy (Stadler et al., 2017). Systemically-administered modified-mRNA encoding for a bispecific antibody directed against the T cell receptor (TCR)–associated CD3 complex and a tumor-associated antigen loaded into a hybrid polymer/lipid-based formulation was shown to significantly impair tumor growth in a murine tumor model (Stadler et al., 2017).

Helper Lipids and Stealth Lipids

In addition to charged or ionizable materials, lipid-based nanoformulations typically comprise supplementary components including cholesterol, for improving nanoparticle's

FIGURE 3 | Chemical structure of the most common ionizable lipids and lipidoids used for mRNA delivery.
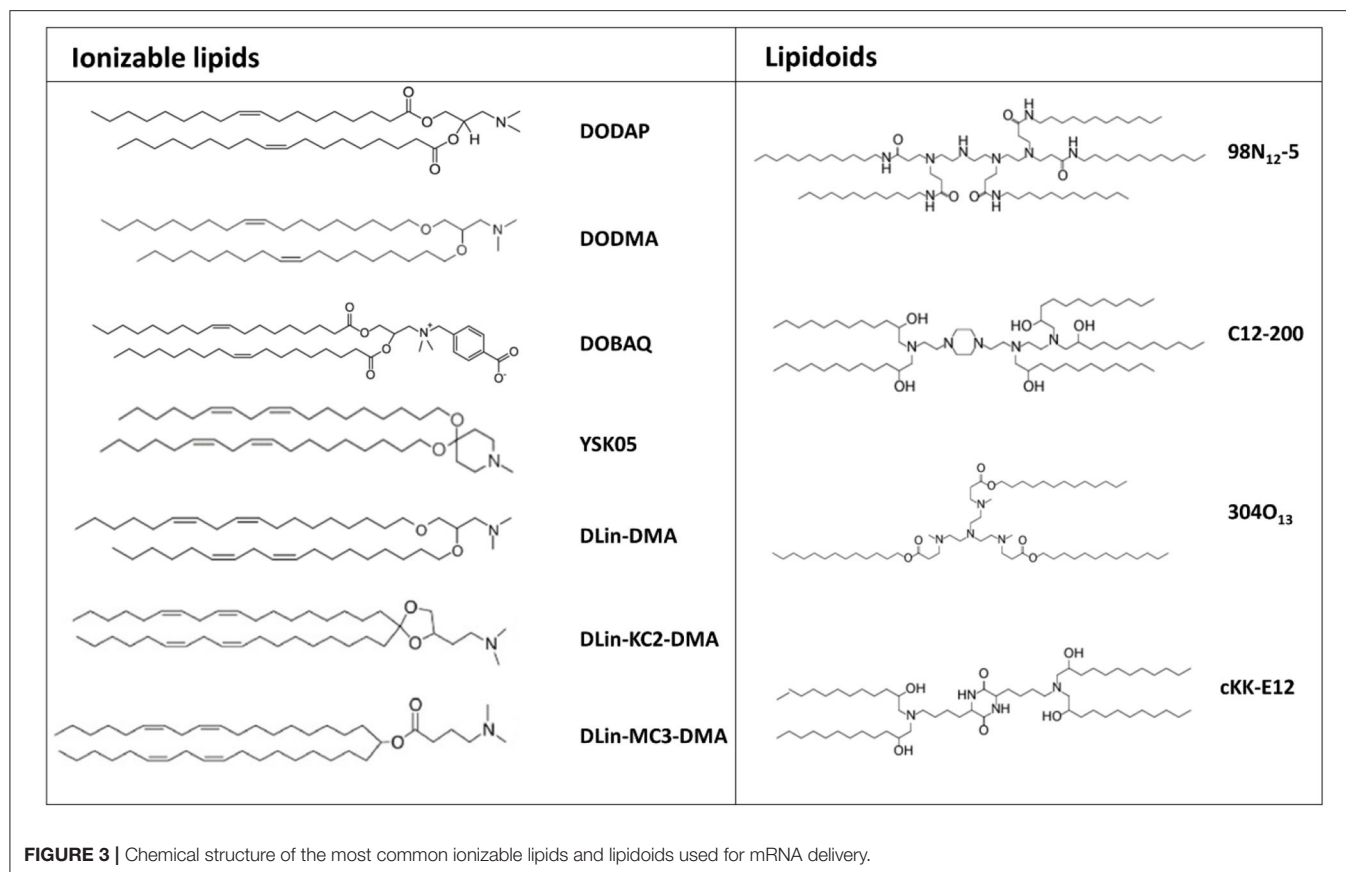
stability; helper lipid, such as DSPC and DOPE, to facilitate the maintenance of the lipid bilayer structure and to promote endosomal release; and a PEG-conjugated lipids to prevent opsonization by serum proteins, thus enhancing the circulation time of nanoparticles (**Figure 4**) (Guevara et al., 2019b).

The ratio between the different types of lipids in the formulation of nanoparticles can substantially affect their efficacy as mRNA delivery systems (Oberli et al., 2017). Compared with lipid-based nanoparticles developed for achieving efficient siRNA delivery, a vector optimized for mRNA encapsulation and release generally requires a reduced amount of ionizable cationic lipid and cholesterol, and higher amounts of helper lipid and PEG-lipid (Weng et al., 2020).

The addition of cholesterol into the formulation has been shown to the enhance transfection efficiency of lipid-base nanoparticles, potentially by promoting membrane fusion and endosomal escape and, as expected, the percentage of cholesterol has a considerable influence on intracellular gene delivery (Pozzi et al., 2012). Patel et al. reported that the inclusion of a naturally occurring cholesterol analogous (C-24 alkyl phytosterols) into lipid-based nanoformulations enhances mRNA delivery (Patel et al., 2020). In this regard, the length of the alkyl tail, the flexibility of sterol ring and the polarity associated with the hydroxyl group were found essential to maintain a high transfection efficiency. Interestingly, the structural examination of lipid nanoparticles containing phytosterols revealed a polymorphic shape and various degrees of multilamellarity, polymorphism and lipid partitioning (Eygeris et al., 2020). The modification of the tail with methyl and ethyl groups led to an increase of multilamellarity (>50% increase compared to cholesterol), whereas the addition of a double bond promoted lipid partitioning (>90% increase compared to cholesterol) (Eygeris et al., 2020). Lipid nanoparticles displaying multilamellar and polymorphic structures showed higher gene transfection.

Previous studies showed that by replacing DSPC, a helper lipid commonly included in siRNA lipid-based formulations, with DOPE, the mRNA delivery efficacy is strongly enhanced (Ball et al., 2018). This may be because phosphocholine-containing lipids usually inhibit membrane fusion-mediated endosomal escape, while unsaturated lipids, such as DOPE, can undergo a conformational change from a stable lamellar phase to an unstable hexagonal phase leading to membrane fusion (Harper et al., 2001; Sato et al., 2020).

However, Sato et al. reported that lipid nanoparticles formulated with a combination of a pH-sensitive cationic lipid with a hydrophobic tail longer than C18 and egg sphingomyelin (ESM), a phosphocholine-containing phospholipid, exhibited a dose-dependent transfection efficiency, while lipid nanoparticles with a classical scaffold length (=C18) failed in transfecting cells *in vitro*, demonstrating that the inhibitory effect of phosphocholine lipids on endosomal escape can be overcome

FIGURE 4 | Chemical structure of the most common helper and stealth lipids employed for the preparation of formulated mRNA.
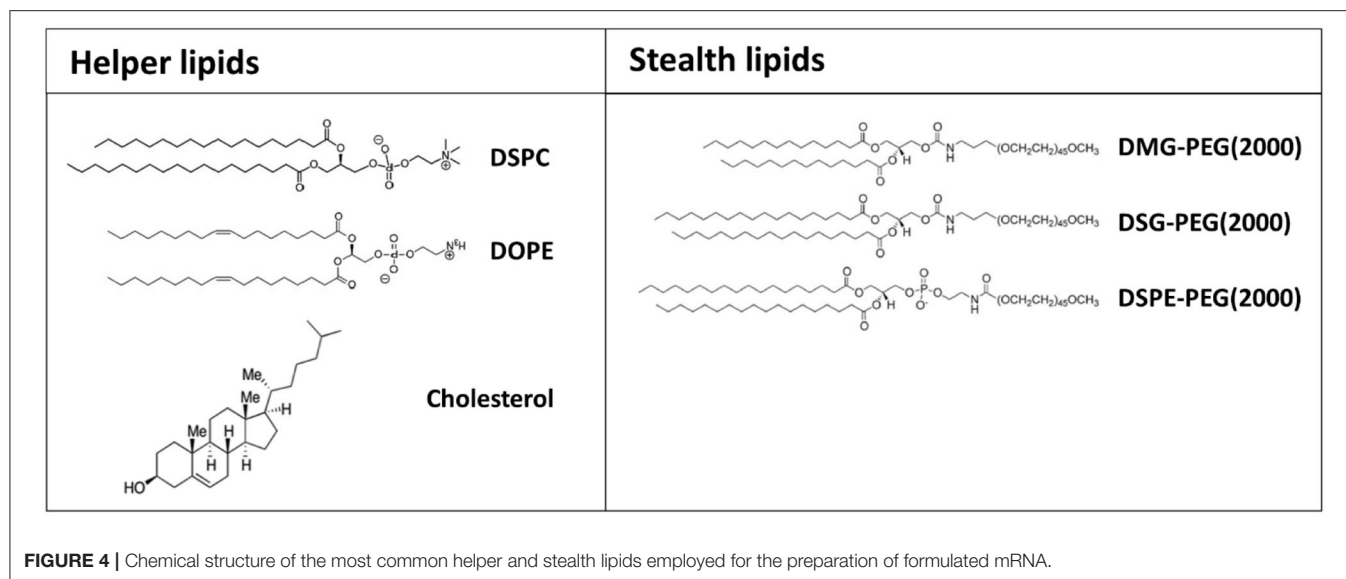
by modifying the structure of the hydrophobic scaffold (Sato et al., 2020).

In order to prevent aggregation and favor a prolonged circulation time of nanoparticles in the bloodstream upon their systemic administration the coating of nanoparticles with a PEG-lipid through a process known as "PEGylation" is a commonly employed strategy. PEGylated nanoparticles are often referred as "stealth" nanoparticles, due their ability to avoid opsonization by serum proteins and detection by the reticuloendothelial system (RES) (Li and Huang, 2009).

The selection of the appropriate PEG-lipid is a crucial step in the design of mRNA delivery platforms and can have a huge impact on the carrier activity by shaping its pharmacokinetics. It has been demonstrated that the lipid anchor length determines how long the PEG-lipid remains incorporated in the lipid shell. PEG-lipids with longer anchors are stably included on the surface of the lipid layer and require more time to dissociate from it, thus preventing undesired interactions with proteins and cells, and consequently prolonging nanoparticles' blood circulation time (Zhu et al., 2017). On the other hand, PEGylation with PEG-lipids with longer anchors can negatively affect the uptake efficiency of nanoparticles by inhibiting their interaction with the plasma membrane of the target cells (Zhu et al., 2017). Moreover, PEGylated nanoparticles can be rapidly clear from the circulation upon secondary exposure, as consequence of antibody-mediated immune responses against the PEG component (Judge et al., 2006). Therefore, the use of PEG-lipids with shorter anchors, such as PEGylated 1,2-dimyristoyl-sn-glycerol (PEG-DMG, a C14-based lipid), which are gradually released from the surface of nanoparticles, appears to be an extremely successful approach to achieve high colloidal stability and cargo delivery into target cells (Tam et al., 2013). The reason for this is that the PEG-lipid is embedded into the lipid layer by hydrophobic interactions; hence, spontaneous de-PEGylation is a process that can be partially controlled changing their hydrophobic properties (Zhu et al., 2017).

PEG-lipids have been also extensively exploited to facilitate lipid-based nanoparticles' functionalization with specific targeting ligands that can promote their precise accumulation at the target site. For instance, to target DCs *in vivo*, mannose, which binds with high affinity to the Lectin Receptor DC-SIGN exposed on the surface of DCs, can be introduce in the formulation (Wang et al., 2018). Likewise, intravenously administrated anti-PECAM-1 antibody conjugated lipid nanoparticles have been successfully employed to achieve higher protein expression in the lungs compared to non-targeted counterparts (Parhiz et al., 2018).

Lipidic immune adjuvants have emerged as novel class of lipids that have been introduced into lipid-based mRNA formulations to further increase the immunogenicity of mRNA-based immunotherapies and "guide" the immune responses (Verbeke et al., 2017; Guevara et al., 2019a). In this regard, the Anderson group has developed multifunctional ionizable lipid-like materials capable of simultaneously facilitate mRNA delivery *in vivo* and act as immune adjuvants to potentiate anti-tumor immunity by promoting the activation of the stimulator of IFN genes (STING) pathway (Miao et al., 2019).

Taken together, these findings corroborate the importance of helper lipids and PEG-lipids in determining the fate and efficacy of lipid-based nanoparticles carrying mRNA, and emphasize the need for a deeper understanding of the relationship between the structural properties of lipid-based formulations and their endosomal escape activity and immunogenicity, thus enabling the design of high performing mRNA-based immunotherapeutics.

Lipid-Based Nanoparticles' Preparation Techniques

The method used for the preparation of lipid-based nanoparticles has been shown to be critical at determining the efficacy of lipid-based nanoformulations, as it has a direct impact on both their

size and encapsulation efficiency (Cullis and Hope, 2017). Lipid-based nanoparticles are usually formed by ethanol injection nanoprecipitation technique, where the desired lipids dissolved in ethanol at an appropriate ratio, and the mRNA dissolved in an acidic aqueous buffer, are mixed together (Reichmuth et al., 2016; Cullis and Hope, 2017). The acidic pH is necessary to ensure the protonation of ionizable lipids (cationic lipids have a head group with a permanent positive charge) so that, after mixing of the two solutions, electrostatic interactions drive the formation of inverted micelles containing the mRNA surrounded by cationic lipids (**Figure 5**) (Cullis and Hope, 2017). The fast increase of solution's polarity promotes the aggregation of the inverted micelles, which is followed by the deposition of the other lipids on the surface of the nascent lipid-based nanoparticles (**Figure 5**) (Cullis and Hope, 2017). The PEG-lipid, that is the most hydrophilic lipid in the mixture, would be the last component to self-associate on the particle's surface to form an outer shell that stabilizes the nanoparticles (Cullis and Hope, 2017). Following the mixing step, nanoparticles are dialyzed against an aqueous buffer in order to increase the pH to a physiological value (Cullis and Hope, 2017).

Based on this method, the size of the resulting nanoparticles would be strongly influenced by the rate at which the polarity of the ethanol solution changes, which in turn is influenced by the mixing rate and the volumetric ratio between the aqueous and lipid phases. Therefore, a rapid mixing of the ethanol–lipid phase with excess water is essential for the preparation of uniform and small lipid-based nanoparticles (Cullis and Hope, 2017). In some cases the nanoprecipitation technique has been performed by replacing the ethanol with a different organic solvent, such as tert-butanol (t-But) or acetonitrile, with a consequent size reduction and improved polydispersity index of the nanoparticles (Matsui et al., 2015; Islam et al., 2018). Further factors that may significantly influence the size of the synthesized nanoparticles are the ratio of "core" lipid (cationic or ionizable lipid) to "surface" lipid in the lipid mix, the amount of PEGylated lipid contained in the formulation and the lipid composition (Cullis and Hope, 2017).

Nanoprecipitation technique has been successfully applied not only for the preparation of lipid nanoparticles but also for the synthesis of mRNA-loaded hybrid polymer-lipid nanoparticles (Kaczmarek et al., 2016).

New approaches for the synthesis of lipid-based nanoparticles directly mix the organic phase, containing the lipids, with the mRNA dispersed in the aqueous phase using a fluidic device (Cullis and Hope, 2017). The advantage of this strategy is that the flow and hence, the mixing rates, can be easily controlled through pumps. In this way, it has been possible to obtain nanoparticles with a diameter up to 70 nm and high encapsulation efficiency (Cullis and Hope, 2017; Oberli et al., 2017). However, nanoparticles generated with early fluidic devices based on macroscopic mixing techniques have often shown high polydispersity and poor reproducibility. For this reason, microfluidic chip devices have been recently developed for the synthesis of mRNA lipid-based nanoformulations (Cullis and Hope, 2017; Thomas et al., 2018). The use of microfluidic mixing devices can ensure a rapid mixing of the aqueous and organic phases, with a consequent fast increase of the polarity of the solution. The time required for mixing in the microfluidic mixer (tm) decreases with the flow velocity (U), according to the following formula: $t_{mix} \sim \lambda/[U \ln(Ul/D)]$, where λ and l are parameters determined by the geometry of the microfluidic chip and D is the diffusion coefficient (Reichmuth et al., 2016; Cullis and Hope, 2017).

The effect of flow rate on the size and polydispersity of lipid-based nanoparticles has been investigated, and previously published studies report that size and polydispersity decrease with an increasing flow rate (Belliveau et al., 2012; Reichmuth et al., 2016). However, an increment in flow rate above 2 ml/min has no effect on nanoparticle's size (Belliveau et al., 2012; Reichmuth et al., 2016). Additionally, Zhigaltsev et al. tested the influence of aqueous/ethanol flow rate ratios on size and polydispersity, and identified a flow rate ratio of 3:1 as the limit value at which smaller and more uniform nanoparticles can be obtained (Zhigaltsev et al., 2012). All together, these findings suggest that an aqueous flow rate of 1.5 ml/min and an ethanol flow rate of 0.5 ml/min represent the best conditions to ensure the synthesis of monodisperse limit-sized nanoparticles.

The microfluidic mixer approach represents an innovative synthesis strategy that offers several advantages compare to other synthesis methods, allowing large-scale production of lipid-based nanoparticles with high encapsulation efficiency, small size and high monodispersity, and facilitates the manufacturing process of commercial mRNA drugs, according to GMP standards.

mRNA to Deliver Different "Immunotherapeutic Messages"

mRNA-based gene therapy holds the promise to revolutionize the field of cancer immunotherapy by addressing current manufacturing limitations and offering novel therapeutic solutions.

The relative rapidity of its production is considered one of the central advantages of mRNA compared with other immunotherapeutic strategies. Indeed, the synthesis of mRNA-based treatments can be achieved within weeks using a cell-free and scalable process, once the sequence encoding the immunogene is available (Wadhwa et al., 2020).

Besides the manufacturing advantages, the use of mRNA technology can avoid any risk of genomic integration, since mRNA translation occurs in the cytosol and it is degraded naturally after gene expression (Granot and Peer, 2017; Guevara et al., 2019b). These characteristics indicate that mRNA-based immunotherapy has the potential to be safer than other strategies and is thus a promising immunotherapeutic platform.

Currently, mRNA constructs have been employed to express tumor associated antigens (TAA) and neoantingens for the development of therapeutic and prophylactic vaccines, for the in-situ production of potent monoclonal antibodies and for the engineering of CAR T cells (Kranz et al., 2016; Rybakova et al., 2019; Wilk et al., 2020). The application of mRNA for these strategies will be discuss in the next sections.

Additionally, a number of clinical trials are now examining the efficacy of nanoformulated mRNA cancer immunotherapies for

FIGURE 5 | Schematic representation of the mechanism driving the self-assembly of mRNA-loaded lipid-based nanoparticles.
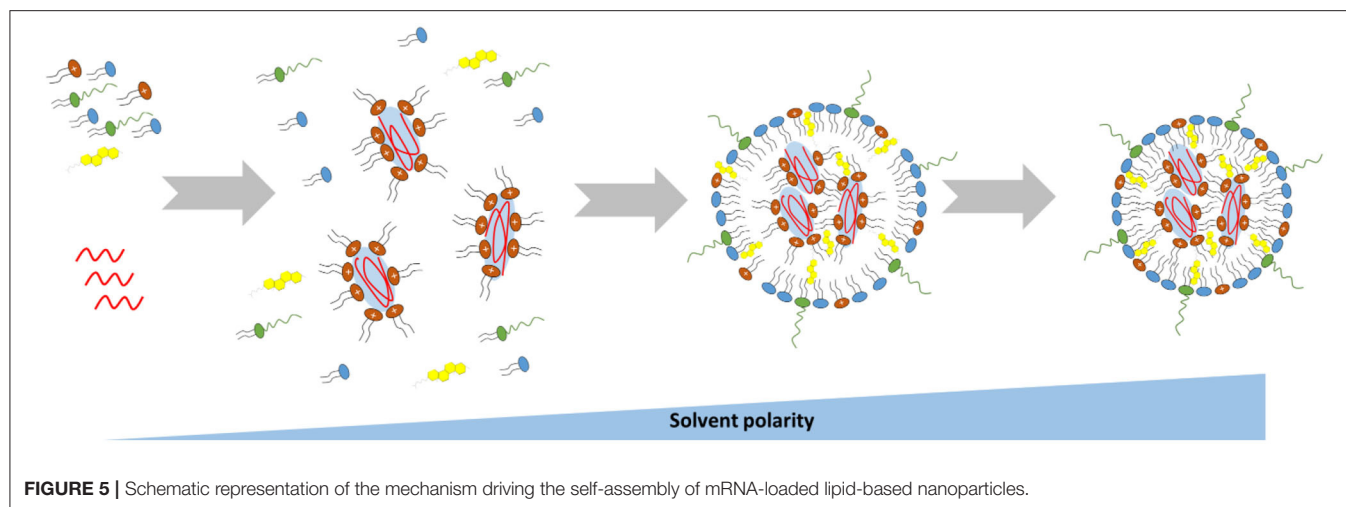
different types of solid tumors and hematological malignancies (see **Table 1**).

mRNA General Structure

Currently, two different types of mRNA platforms have been proposed for cancer immunotherapy, non-amplifying mRNA (conventional mRNA) with an open reading frame (ORF) flanked by 5′ and 3′ untranslated regions (UTRs), and self-amplifying mRNA (saRNA) derived from the positive-stranded alphavirus RNA genome (**Figure 6**) (Kowalski et al., 2019). In saRNA, genes encoding structural proteins are replaced by genes coding for proteins of therapeutic value, whereas viral genes containing the information for proteins forming the replication machinery are maintained (Kowalski et al., 2019).

Major advantages of conventional mRNA include its relatively small size compared to saRNA (∼2–3 kb vs. ∼10 kb), the absence of viral genes thus minimizing the risk of eliciting undesired immunogenic effects in the patient, its simple and scalable manufacturing procedures, and the fact that its sequence can be easily engineered to improve its therapeutic efficacy and minimize any adverse effects (Pardi et al., 2018; Kowalski et al., 2019). On the other hand, saRNA can produce multiple copies of itself, thereby achieving effective gene expression and protein translation with a much lower number of molecules compared to conventional mRNA (Kowalski et al., 2019).

Both types of mRNAs are synthesized in a cell-free system, using an *in vitro* transcription (IVT) method, which requires the generation of pDNA containing the sequence for a DNA-dependent RNA polymerase promoter (T7 or SP6), followed by the sequence corresponding to the mRNA construct (Weissman, 2014; Zhong et al., 2018; Kowalski et al., 2019). After enzymatic linearization, the pDNA can serve as a template for the transcription of mRNA using a DNA-dependent RNA polymerase. Once the transcription reaction is completed the pDNA is degraded by treatment with DNase. The addition of the 3′ poly(A) tail can be achieved during the transcription process or enzymatically after transcription via poly-A polymerase, while enzymatic addition of the 5′ cap can be carried out by using

guanylyl transferase and 2′-O-methyltransferase to introduce a Cap 0 (N7MeGpppN) or Cap 1 (N7MeGpppN2′-OMe) structure, respectively (Weissman, 2014; Zhong et al., 2018; Kowalski et al., 2019).

mRNA sequence and its secondary structures can be potentially recognized by several innate immune receptors to promote the release of type I IFN, with a consequent inhibition of protein translation (De Beuckelaer et al., 2016). However, innate immune activation can be prevented by using modified mRNA, incorporating non-standard nucleotides such as pseudouridine (Ψ), 5-methylcytidine (5 mC), cap-1 structure and optimized codons, thus improving its translation efficiency (Holtkamp et al., 2006; Pardi et al., 2018).

The purity of the mRNA is a crucial factor that influences its performance. It has been shown that DNA-dependent RNA polymerases yield abortive initiation products, as well as double-stranded RNA resulting from self-complementary, which can lead to type I IFN and inflammatory cytokines production upon pattern recognition receptors recognition (Jackson et al., 2020). Karikó et al., in this regard, showed that the removal of impurities from synthetic mRNA by high-pressure liquid chromatography (HPLC) can minimize innate immune activation with a consequent significant increase of levels of expression of the reporter gene (Karikó et al., 2011).

Lipid Nanoparticles for mRNA-Based Vaccines

The main objective of a therapeutic anti-cancer vaccine is to stimulate cell-mediated immune responses by targeting tumor antigens that are restricted or preferentially expressed in malignant cells (Pardi et al., 2018).

Adoptive transfer approaches, based on the administration of *ex-vivo* mRNA-transfected DCs, were the first form of mRNA-based vaccines to be proposed and clinically investigated (Baldin et al., 2020). Most of these clinical studies employed DCs generated from peripheral blood monocytes (Baldin et al., 2020). However, thanks to the recent advancements in separation techniques for primary DCs, the new generation of DC vaccines

Treatment	Phase	mRNA-encoded protein	Tumor	Identifier
Vaccine	1	Four mRNAs encoding New York Esophageal Squamous Cell Carcinoma-1 (NY-ESO-1), Melanoma-associated antigen 3 (MAGE-A3), tyrosinase, and transmembrane phosphatase with tensin homology (TPTE)	Advanced malignant melanoma	NCT02410733
Vaccine	1	mRNA-4157 targeting 20 tumor-associated antigens (TAAs) that are specifically expressed by the patient's cancer cells	Resected solid tumors including melanoma, bladder carcinoma, and non-small-cell lung carcinoma (NSCLC), and in combination with pembrolizumab in patients with unreseactable solid tumors	NCT03313778
Immune modulator	1/2	mRNA-2416 encoding OX40 ligand (OX40L)	Alone or in combination with durvalumab for patients with solid tumors or lymphoma.	NCT03323398
Immune modulator	1	mRNA-2752 encoding OX40L, IL-23 and IL-36γ	Alone or in combination with duvalumab for patients with triple negative breast cancer, head and neck squamous cell carcinoma, non-hodgkin lymphoma, and urothelial cancer	NCT03739931
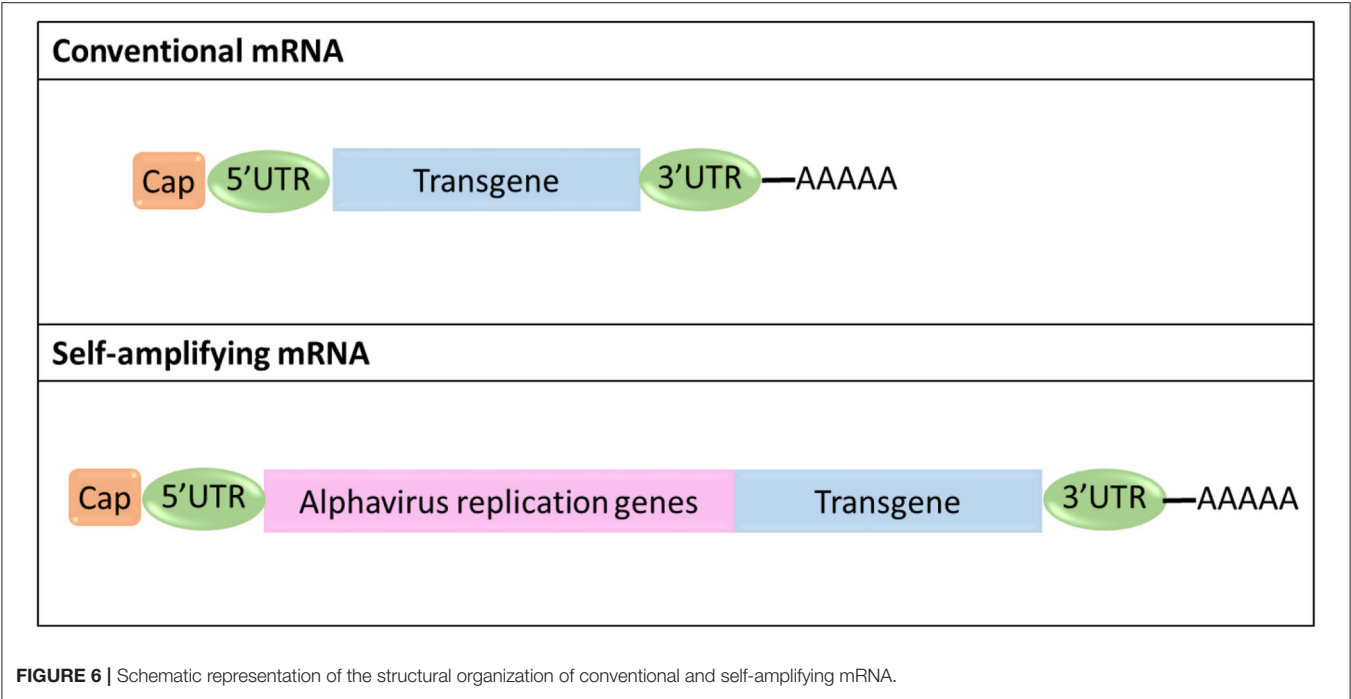
FIGURE 6 | Schematic representation of the structural organization of conventional and self-amplifying mRNA.

is focusing on the isolation of specific primary DC subsets, due to their superior immunostimulatory functions (Baldin et al., 2020).

Despite DC vaccines have shown encouraging outcomes in preclinical studies, their clinical efficacy remains limited. Additionally, there are multiple technical challenges associated with their manufacturing procedures (Farkona et al., 2016; Baldin et al., 2020). For instance, a large amount of patient's peripheral blood needs to be collected for the isolation and generation of DCs. This is a key issue when dealing with oncological patients, given that the cytotoxic effects of chemotherapy may further reduce the number of DCs and monocytes in the peripheral blood (Farkona et al., 2016; Baldin et al., 2020).

In the second decade of the twenty first century, direct *in vivo* transfection of DCs with a tumor antigen-encoding mRNA, appeared as a valid strategy to overcome limitations faced with

the development of DC vaccines (Baldin et al., 2020). Since then, the field has been rapidly expanding, leading to the development of mRNA-based vaccines that are currently in clinical trials, and to the establishment of biotech companies across the globe focusing on mRNA technologies for cancer immunotherapy.

It is known that the efficacy of DC vaccines is strongly influenced by the efficiency of DCs to migrate toward secondary lymphoid organs after their administration to patients. However, *ex-vivo* activated DCs often fail to reach the lymph nodes and their functionality is affected by tolerogenic signals, impairing the ability of DCs to efficiently prime tumor-specific cytotoxic T cells (CTLs) (Turnis and Rooney, 2010; Farkona et al., 2016; Baldin et al., 2020). The release of the antigen directly into secondary lymphoid organs offers the possibility to reduce the risk that mRNA-transfected mature DCs receive inactivating

signals before that they can encounter and present the antigen to naïve T cells (Kreiter et al., 2010). In addition, this kind of approaches can easily bypass all the technical limitations associated with the preparation of DC vaccines, since the isolation or generation of DCs is not necessary. First efforts in the delivery of antigen-mRNA demonstrated that local injection of naked mRNA into lymph nodes could promote antigen-specific anti-tumor immunity (Kreiter et al., 2010). However, its efficacy was negatively affected by the low uptake of naked mRNA by local DCs and the incapacity of free mRNA to escape from the endosomal compartment and reach the cytosol of the cells following its endocytosis. All these issues, together with the concerns related to the feasibility of direct intranodal injection of mRNA, has promoted the development of non-viral vectors opportunely designed for mRNA vaccine delivery.

Different types of nanoparticles have been proposed for mRNA delivery, but lipid-based nanoparticles have shown the most promising results and currently represent the gold standard for precise *in vivo* delivery of mRNA into immune cells (Kranz et al., 2016; Oberli et al., 2017; Persano et al., 2017; Miao et al., 2020). A proof-of-concept study using this approach was reported by Kranz et al. in 2016, demonstrating that DCs can be passively targeted *in vivo* using intravenously injected mRNA-lipoplexes based on DOTMA/DOPE or DOTAP/DOPE formulations by optimizing the mRNA/cationic lipid ratio, obtaining nanoparticles with a negative net charge (Kranz et al., 2016). The loading of TAA-mRNA onto the lipoplex nanostructure efficiently protected the mRNA from extracellular ribonucleases and enhanced its uptake and expression by different DC subsets and macrophages in various lymphoid organs. Finally, the authors showed that mRNA-lipoplex vaccine can induce both a type-I-IFN-mediated innate immune response as well as a potent adaptive response, resulting in a strong tumor growth inhibition.

After this study reported the successful application of lipid-based non-viral vectors for anticancer mRNA-based vaccines, other types of lipid-based nanostructures have been successfully employed, such as lipid nanoparticles and hybrid lipid-polymer formulations. For instance, Oberli et al. proposed a lipid nanoparticle-based formulation for the *in vivo* delivery of mRNA vaccines into APCs (Oberli et al., 2017). The efficacy of the vaccine was tested in a B16F10 melanoma murine model, detecting a strong anti-tumor cell-mediated immune response after a single dose. Treatment of B16F10 melanoma tumors with the nanovaccine containing mRNA coding for TAAs (gp100 or TRP-2) resulted in a decrease of the tumor volume and the prolongation of survival of treated mice. Likewise, Persano et al. reported the development of a hybrid lipid-polymer nanoformulation, consisting of poly-(β-amino ester) polymer/mRNA core coated with 1,2-dioleoyl-sn-glycero-3-ethylphosphocholine (EDOPC)/DOPE/1,2-distearoyl-sn-glycero-3-phosphorylethanolamine (DSPE)-PEG(2000), for mRNA vaccine delivery (Persano et al., 2017). This hybrid nanostructure was efficiently internalized by DCs via micropinocytosis and promoted their maturation through a mechanism that involves innate immunity activation by Toll-like receptor 7/8 signaling (Persano et al., 2017). The vaccination

of mice bearing lung metastatic B16-OVA tumors with OVA-mRNA/lipopolyplex resulted in a significant reduction in the number of lung metastases (Persano et al., 2017).

Recently, mRNA-based nanovaccines have been explored for the development of a new class of anticancer vaccine, referred as personalized vaccines that are based on tumor neoantigens deriving from non-synonymous mutations occurring in cancer cells. In this direction, mRNA-based nanovaccines are attracting a growing interest, as they hold the unique potential to facilitate the co-release of multiple neoantigens by incorporating different epitope sequences within the same molecule. Kreiter et al. have provided evidences that neoantigens are immunogenic when delivered via mRNA platforms and currently several clinical trials are ongoing testing mRNA encoding for neoantigens for the treatment of various solid tumors, including NSCLC, colorectal and pancreatic cancer (Kreiter et al., 2010; Kowalski et al., 2019).

A deeper understanding of the mechanisms involved in the activation and setting up of immune responses has helped to determine the crucial role that a specific immune adjuvants included in a vaccine formulation can play in determining the therapeutic outcome of a vaccine in patients. Indeed, even if non-modified mRNA has well-recognized immune adjuvanting properties associated to its ability to interact with innate immune receptors, it is also true that mRNA vaccines can benefit from their combination with immune adjuvants directed to re-modulate the immunosuppressive microenvironment or to provide additional signals that can reinvigorate vaccine-induced immune responses (Verbeke et al., 2017; Guevara et al., 2019a). This is particularly relevant for oncological patients, as they tend to have a compromised immune system and may involve elderly adults that display features of immunosenescence (Crooke et al., 2019). In this regard, lipid nanoformulations have shown to efficiently assist in the co-delivery of antigen-mRNA with immune adjuvants, promoting the development of potent and effective anti-cancer vaccines. Haabeth et al., for instance, demonstrated that intratumoral injection of charge-altering releasable transporters (CART)-mRNA complexes resulted in high expression of the transduced transgene, with an efficient transfection of dendritic cells, macrophages, and T cells at the injection site (Haabeth et al., 2019). The co-delivery of OX40L-, CD80-, and CD86-encoding mRNAs resulted in a localized upregulation of pro-inflammatory cytokines, robust T cells priming, and migration of immune cells toward the draining lymph node or to distant tumors. This therapeutic approach significantly inhibited tumor growth and promoted tumor eradication in two different murine tumor models.

The field of mRNA-based nanovaccine is rapidly progressing and it currently represents the most advanced application of mRNA technology with multiple clinical trials ongoing in different tumor settings, including melanoma, bladder carcinoma and NSCLC (see **Table 1**).

The first successful application of a therapeutic nanovaccine based on multiple mRNAs encoding four tumor antigens (NY-ESO-1, MAGE-A3, tyrosinase, and TPTE) was tested in advanced malignant melanoma patients (NCT02410733, phase I). The study showed that all patients developed de novo T cell responses against the administered tumor antigens.

Additionally, this multiple mRNA nanovaccine was successfully evaluated in combination with checkpoint inhibitor in patients with unresectable solid tumors (Kranz et al., 2016).

These early positive indications highlight the potential of mRNA nanovaccines, and provide evidences that this strategy may be at the point of development to be incorporated into clinical practice. However, the enormous therapeutic potential of mRNA is still limited by the need for improved targeting and transfection efficiency of lipid-based mRNA delivery systems.

Lipid Nanoparticles for the Delivery of mRNA Coding for Monoclonal Antibodies

Monoclonal antibodies represent one of the most studied class of cancer immunotherapy and they have received clinical approval for the treatment of an increasing number of human malignancies (Hoecke and Roose, 2019). Antibody-based cancer immunotherapy has been applied to target specific proteins express on tumor cells and immune cells or molecules released into the extracellular environment. Depending on the protein they are targeting, antibodies have different mechanisms of action and effects (Suzuki et al., 2015).

Cancer treatment based on monoclonal antibodies targeting immune checkpoints is largely considered the most promising area of cancer immunotherapy currently in development (Park et al., 2018). Several types of immune checkpoints monoclonal antibodies have been discovered in the last years and some of them, such as anti-programmed cell death 1 (PD-1)/programmed cell death-ligand 1 (PD-L1) and cytotoxic T-lymphocyte-associated protein 4 (CTLA-4) inhibitors, have already received approval for clinical use while many others are under clinical trials (Park et al., 2018).

Although monoclonal antibodies have generally exhibited great therapeutic efficiency in the context of diverse solid tumors, their use is associated with several disadvantages that limit their extensive application in the clinic. These challenges are mainly related to the manufacturing process of antibodies, which requires the use of engineered mammalian cells followed by complex and time-consuming procedures in order to obtain an antibody completely free from cell culture supernatant, viruses and other potential contaminants (Hoecke and Roose, 2019; Schlake et al., 2019). Furthermore, monoclonal antibodies are characterized by a wide variety of post-translational modifications, which can strongly impact their therapeutic properties (Hoecke and Roose, 2019; Schlake et al., 2019). Therefore, after synthesis and purification, the quality of antibodies needs to be assess using many expensive analytical techniques (Hoecke and Roose, 2019; Schlake et al., 2019). All these challenges render antibody-based therapies poorly affordable.

In the recent years, mRNA technology has emerged has an elegant solution to circumvent the limitations associated with the preparation of antibody-based drugs (see **Table 1**) (Hoecke and Roose, 2019; Schlake et al., 2019). With this innovative approach, by administrating the antibody-encoding mRNA directly to patients, it is possible to achieve *in situ* production of the therapeutic product, overcoming all the problems associated to

its synthesis and purification (Hoecke and Roose, 2019; Schlake et al., 2019).

A proof of the feasibility of using mRNA as a platform for antibody-based immunotherapy was reported by Pardi et al. In this work, modified mRNAs encoding both the light and heavy chains of a neutralizing antibody direct against HIV-1 (VRC01), were co-encapsulated into lipid nanoparticles and intravenously administrated (Pardi et al., 2017). Passive vaccination with mRNAs-loaded nanoparticles led a robust antibody expression in the liver, resulting in an effective prophylactic response in a HIV-1 murine model (Pardi et al., 2017). Using a similar strategy, Stadler et al. reported a new class of drug that employs a modified mRNA formulated into lipid nanoparticles to promote *in situ* production of bispecific antibodies termed RiboMABs. RiboMAB targeting CD3 and TAAs link T cells to cancer cells, enhancing the anti-tumor activity of effector cells (Stadler et al., 2017).

A single dose of mRNA-loaded nanoparticles, administrated intravenously, was sufficient to promote rapid production of bispecific antibodies and their secretion into circulation. Treatment with RiboMAB completely eliminated the tumor and remarkably, in a control experiment, to achieve a similar degree of tumor eradication the recombinant bispecific antibody had to be administered three times (Stadler et al., 2017).

All the above-mentioned studies have delivered the mRNA intravenously, exploiting liver cells as a sort of bioreactor to translate the mRNA and release antibodies systemically. In contrast, Tiwari et al. achieved local expression of antibodies directed against the respiratory syncytial virus (RSV) by delivering formulated mRNA encoding antibody in the lungs via intratracheal aerosols (Tiwari et al., 2018). The authors showed that by using this delivery approach, up to 45% of the lung cells expressed the antibody, leading to a significant reduction of RSV infection in challenged mice (Tiwari et al., 2018).

These studies demonstrate the potential of mRNA-based lipid nanovectors as platforms for the *in situ* production of antibodies, and how their use may revolutionize the field. Particularly exciting is the fact that this technology may reduce the cost and the number of doses currently require for treatments with recombinant monoclonal antibody-based therapies, thus rendering them more accessible to a larger portion of patients.

Lipid Nanoparticles to Harness mRNA Therapeutic Potential for CAR T Cell Therapy

CAR T-cell therapy represents the most advanced personalized cancer immunotherapy and has received approval from the FDA and the European Medicine Agency (EMA) for its clinical implementation in the context of hematological cancers, including acute lymphoblastic leukemia and diffuse large B-cell lymphoma (Mohanty et al., 2019; Vitale and Strati, 2020). Thus, CAR T cell therapy is one of the first successful examples of cell engineering and personalized adoptive cell transfer immunotherapy to become available in clinic.

In this strategy, T cells are isolated from the patient and genetically modified to introduce a chimeric antigen receptor that binds a tumor protein that is express uniquely or mostly by

TABLE 2 | Overview of formulated mRNA strategies for monoclonal antibody and CAR cell therapies.

Type of immunotherapy	Nanocarrier composition	Ex-vivo or in vivo transfection	Transgene	Tumor	References
Monoclonal antibody	C14-4/DOPE/Chol/PEG-lipid (35:16:46.5:2.5 mol/mol)	In vivo	Anti-HER2 antibody	MDA-MB-231 cells (Breast cancer)	Rybakova et al., 2019
	Polymer/lipid formulation	In vivo	CLDN6 × CD3 bispecific antibody	OV-90 cells (Ovarian cancer)	Stadler et al., 2017
	L319/DSPC/chol/PEG-DMG (50:10:38.5:1.5 mol/mol)	In vivo	Anti-CD20 antibody (Rituximab)	Raji cells (Burkitt's lymphoma)	Thran et al., 2017
CAR cell therapy	C14-4/DOPE/Chol/PEG-lipid (35:16:46.5:2.5 mol/mol)	Ex-vivo	CD19	Nalm6 cells (Acute lymphoblastic leukemia)	Billingsley et al., 2020
	CART synthetic lipid-based nanoparticles	Ex-vivo and in vivo	GFP and Luciferase	ND	McKinlay et al., 2018
	CART synthetic lipid-based nanoparticles	Ex-vivo	CD19	Nalm6 cells (Acute lymphoblastic leukemia)	Wilk et al., 2020

the target malignant cells. Afterward, CAR T cells are expanded and re-infused into patients to attack and destroy chemotherapy-resistant cancer cells (Jackson et al., 2016).

Although this therapeutic approach is currently restricted to the treatment of non-solid tumors, thanks to the recent advancement in the field and the introduction of novel technologies, the scientific community is largely sure that in the next future it would be possible to extend this treatment regime to the treatment of solid tumors.

Despite its tremendous potential, previous studies with CAR cell therapy have pointed out several limitations concerning safety issues, complex manufacturing procedures and high costs, that can hinder the wide application of this technology (Hartmann et al., 2017; Zhao et al., 2018).

Regarding the collateral effects, they have been mostly associated to unwanted immunological immune responses that can lead to macrophage activation syndrome, neurotoxicity and cytokine release syndrome. Concerns have been also raised regarding the use of viral vectors for transducing T cells with CAR sequences, particularly due to their immunogenicity and the potential risk of insertional mutagenesis, besides their limited size insert capacity (Hartmann et al., 2017; Zhao et al., 2018).

While immunological toxicity may be mitigated by treatment with anti-IL-6 receptor antibodies, manufacturing challenges remain unsolved, justifying the need for novel lymphocyte transfection strategies for the development of safer and more accessible CAR cell therapies (Brudno and Kochenderfer, 2016).

Recently, mRNA technology has emerged as a potential solution to overcome these challenges. Indeed, mRNA allows the transient expression of CAR, since mRNA molecules are subject to decay after translation, thus preventing any risk of genomic vector integration (Wiesinger et al., 2019). Furthermore, the structure of the mRNA can be easily customized with specific sequences or modifications to maximize transfection and translation.

Currently, electroporation is standardly employed in clinical practice to deliver mRNA encoding CAR into T cells. However, electroporation has several disadvantages that can strongly affect the quality of the CAR T cells produced (Billingsley et al., 2020). Indeed, the application of pulsed electric fields can

irreversibly compromise the cell plasma membrane's integrity. All this can result in low viability, aberrant gene expression profile and reduced transgene expression in the surviving transfected cells. At the end of the last decade, non-viral delivery systems have been explored as an alternative approach for lymphocytes' transfection (Billingsley et al., 2020). In particular, ionizable lipid nanoparticle delivery platforms have showed outstanding efficacy in preclinical studies (see **Table 2**). In line with the above, Billingsley et al. recently reported the development of ionizable lipid nanoparticles for ex vivo mRNA delivery into human T cells. The designed nanovector was exploited to achieve CAR-encoding mRNA delivery into primary human T cells to produce functional CAR T cells with enhanced tumor killing activity (Billingsley et al., 2020).

Interestingly, recent studies have highlighted the great potential of mRNA-based lipid nanoformulations to deliver genetic material to the target cells directly in vivo, thus avoiding the complications associated with the ex-vivo manipulation of T cells. This kind of strategies can offer the unprecedented possibility to easily transfect T cells using a practical and broadly applicable approach.

CONCLUSIONS AND FUTURE PROSPECTIVE

Synthetic mRNA has gained a growing interest as a therapeutic molecule for preventing or treating multiple malignancies or non-oncological diseases. The idea to use mRNA as therapeutic molecule was born due to the number of benefits that its implementation can offer over traditional treatments.

As mentioned in the previous sections, oppositely to pDNA-based gene therapy, mRNA holds a superior safety profile, given that it does not need to reach nucleus to exert its function, thus avoiding any risk of genomic integration. In addition, mRNA expression is time-restricted and can be tightly regulated. Most importantly, mRNA-based therapy can allow a rapid and affordable manufacturing of therapeutics as its synthesis is achieved using cell-free systems.

Despite this, mRNA is chemically unstable and susceptible to hydrolysis catalyzed by nucleases. The great structural fragility of mRNA limited its use as therapeutic agent in the past. Recent advances in non-viral delivery systems and the development of novel effective transfecting nanomaterials have provided solutions to these challenges.

Nowadays, lipid-based nanoformulations represent the most advanced and widely employed delivery system for the development of mRNA-based therapies. With several mRNA-based anti-cancer treatments currently in preclinical and clinical studies, it is evident that cancer immunotherapy is the field in which mRNA-based technology can better exert its enormous therapeutic power.

The application of lipid-based nanovectors has enabled the integration of mRNA-based technology in many pre-existing anti-cancer immunotherapeutic approaches, such as therapeutic vaccines, monoclonal antibodies and CAR cell therapy.

However, further research is needed to clarify the reasons behind the low mRNA transfection efficiency of non-viral vectors, especially in those cells that are considered hard to transfect, such as lymphocytes and monocytes. Recent published works have shown how the co-formulation of mRNA with drugs known to affect that endocytic pathway, can significantly enhance gene delivery (Patel et al., 2017; Kon et al., 2020). Modulating intracellular transport mechanisms for mRNA internalization and endosomal escape will potentially lead to the development of next generation of drug delivery systems by enabling high transfection efficiency with limited toxicity.

Additionally, a deeper understanding of key parameters, such as hydrophobicity and fusogenicity of the formulation, which strongly dictate the transfection efficiency of the formulation, and how they can be modulated by varying the lipidic composition or through the introduction of novel lipids, will further enable the development of improved formulations.

Finally, combination with other cancer treatments, including chemotherapy and radiotherapy represents a promising way to further potentiate the therapeutic efficacy of mRNA-based strategies.

AUTHOR CONTRIBUTIONS

SP and MG designed and wrote the manuscript. FP contributed to the writing and to revising the manuscript. All authors contributed to the article and approved the submitted version.

REFERENCES

Arteta, M. Y., Kjellman, T., Bartesaghi, S., Wallin, S., Wu, X., Kvist, A. J., et al. (2018). Successful reprogramming of cellular protein production through mRNA delivered by functionalized lipid nanoparticles. *Proc. Natl. Acad. Sci. U.S.A.* 115, E3351–E3360. doi: 10.1073/pnas.1720542115

Bailey, A. L., and Cullis, P. R. (1994). Modulation of membrane fusion by asymmetric transbilayer distributions of amino lipids. *Biochemistry* 33, 12573–12580. doi: 10.1021/bi00208a007

Baldin, A. V., Savvateeva, L. V., Bazhin, A. V., and Zamyatnin, J.r, A. A. (2020). Dendritic cells in anticancer vaccination: rationale for *ex vivo* loading or *in vivo* targeting. *Cancers* 12:590. doi: 10.3390/cancers12030590

Ball, R. L., Hajj, K. A., Vizelman, J., Bajaj, P., and Whitehead, K. A. (2018). Lipid nanoparticle formulations for enhanced co-delivery of siRNA and mRNA. *Nano Lett.* 18, 3814–3822. doi: 10.1021/acs.nanolett.8b01101

Belliveau, N. M., Huft, J., Lin, P. J. C., Chen, S., Leung, A. K. K., Leaver, T. J., et al. (2012). Microfluidic synthesis of highly potent limit-size lipid nanoparticles for *in vivo* delivery of siRNA. *Mol. Ther. Nucleic Acids* 1:e37. doi: 10.1038/mtna.2012.28

Billingsley, M. M., Singh, N., Ravikumar, P., Zhang, R., June, C. H., and Mitchell, M. J. (2020). Ionizable lipid nanoparticle-mediated mRNA delivery for human CAR T cell engineering. *Nano Lett.* 20, 1578–1589. doi: 10.1021/acs.nanolett.9b04246

Blakney, A. K., McKay, P. F., Yus, B. I., Aldon, Y., and Shattock, R. J. (2019). Inside out: optimization of lipid nanoparticle formulations for exterior complexation and *in vivo* delivery of saRNA. *Gene Ther.* 26, 363–372. doi: 10.1038/s41434-019-0095-2

Blanco, E., Shen, H., and Ferrari, M. (2015). Principles of nanoparticle design for overcoming biological barriers to drug delivery. *Nat. Biotechnol.* 33, 941–951. doi: 10.1038/nbt.3330

Brudno, J. N., and Kochenderfer, J. N. (2016). Toxicities of chimeric antigen receptor T cells: recognition and management. *Blood* 127, 3321–3330. doi: 10.1182/blood-2016-04-703751

Cheng, Q., Wei, T., Farbiak, L., Johnson, L. T., Dilliard, S. A., and Siegwart, D. J. (2020). Selective organ targeting (SORT) nanoparticles for tissue-specific mRNA delivery and CRISPR-Cas gene editing. *Nat. Nanotechnol.* 15, 313–320. doi: 10.1038/s41565-020-0669-6

Crooke, S. N., Ovsyannikova, I. G., Poland, G. A., and Kennedy, R. B. (2019). Immunosenescence and human vaccine immune responses. *Immun. Ageing* 16:25. doi: 10.1186/s12979-019-0164-9

Cullis, P. R., and Hope, M. J. (2017). Lipid nanoparticle systems for enabling gene therapies. *Mol. Ther.* 25, 1467–1475. doi: 10.1016/j.ymthe.2017.03.013

De Beuckelaer, A., Pollard, C., Van Lint, S., Roose, K., Van Hoecke, L., Naessens, T., et al. (2016). Type I interferons interfere with the capacity of mRNA lipoplex vaccines to elicit cytolytic T cell responses. *Mol. Ther.* 24, 2012–2020. doi: 10.1038/mt.2016.161

Eygeris, Y., Patel, S., Jozic, A., and Sahay, G. (2020). Deconvoluting lipid nanoparticle structure for messenger RNA delivery. *Nano Lett.* 20, 4543–4549. doi: 10.1021/acs.nanolett.0c01386

Farkona, S., Diamandis, E. P., and Blasutig, I. M. (2016). Cancer immunotherapy: the beginning of the end of cancer?. *BMC Med.* 14:73. doi: 10.1186/s12916-016-0623-5

Felgner, P. L., and Ringold, G. M. (1989). Cationic liposome-mediated transfection. *Nature* 337, 387–388. doi: 10.1038/337387a0

Fenton, O. S., Kauffman, K. J., McClellan, R. L., Appel, E. A., Dorkin, J. R., Tibbitt, M. W., et al. (2016). Bioinspired alkenyl amino alcohol ionizable lipid materials for highly potent *in vivo* mRNA delivery. *Adv. Mater.* 28, 2939–2943. doi: 10.1002/adma.201505822

Foster, J. B., Barrett, D. M., and Karikó, K. (2019). The emerging role of *in vitro*-transcribed mRNA in adoptive T cell immunotherapy. *Mol Ther.* 27, 747–756. doi: 10.1016/j.ymthe.2019.01.018

Gall, D. (1966). The adjuvant activity of aliphatic nitrogenous bases. *Immunology* 11, 369–386.

Gilleron, J., Querbes, W., Zeigerer, A., Borodovsky, A., Marsico, G., Schubert, U., et al. (2013). Image-based analysis of lipid nanoparticle-mediated siRNA delivery, intracellular trafficking and endosomal escape. *Nat. Biotechnol.* 31, 638–646. doi: 10.1038/nbt.2612

Gómez-Aguado, I., Rodríguez-Castejón, J., Vicente-Pascual, M., Rodríguez-Gascón, A., Solinís, M. A., and Del Pozo-Rodríguez, A. (2020). Nanomedicines to deliver mRNA: state of the art and future perspectives. *Nanomaterials* 10:364. doi: 10.3390/nano10020364

Granot, Y., and Peer, D. (2017). Delivering the right message: challenges and opportunities in lipid nanoparticles-mediated modified mRNA

therapeutics-An innate immune system standpoint. *Semin. Immunol.* 34,68–77. doi: 10.1016/j.smim.2017.08.015

Guan, S., and Rosenecker, J. (2017). Nanotechnologies in delivery of mRNA therapeutics using nonviral vector-based delivery systems. *Gene Ther.* 24, 133–143. doi: 10.1038/gt.2017.5

Guevara, M. L., Jilesen, Z., Stojdl, D., and Persano, S. (2019a). Codelivery of mRNA with α-Galactosylceramide using a new lipopolyplex formulation induces a strong antitumor response upon intravenous administration. *ACS Omega* 4, 13015–13026. doi: 10.1021/acsomega.9b00489

Guevara, M. L., Persano, S., and Persano, F. (2019b). Lipid-based vectors for therapeutic mRNA-based anti-cancer vaccines. *Curr Pharm Des.* 25, 1443–1454. doi: 10.2174/1381612825666190619150221

Haabeth, O. A. W., Blake, T. R., McKinlay, C. J., Tveita, A. A., Sallets, A., Waymouth, R. M., et al. (2019). Local delivery of Ox4Ol, Cd80, and Cd86 mRNA kindles global anticancer immunity. *Cancer Res.* 79, 1624–1634. doi: 10.1158/0008-5472.CAN-18-2867

Hajj, K. A., and Whitehead, K. A. (2017). Tools for translation: non-viral materials for therapeutic mRNA delivery. *Nat. Rev. Mater.* 2:17056. doi: 10.1038/natrevmats.2017.56

Harper, P. E., Mannock, D. A., Lewis, R. N. A. H., McElhaney, R. N., and Gruner,. S. (2001). X-ray diffraction of some phosphatidylethanolamine lamellar and inverted hexagonal phases. *Biophys. J.* 81, 2693–2706. doi: 10.1016/S0006-3495(01)75912-7

Hartmann, J., Schüßler-Lenz, M., Bondanza, A., and Buchholz, C. J. (2017). Clinical development of CAR T cells—challenges and opportunities in translating innovative treatment concepts. *EMBO Mol. Med.* 9, 1183–1197. doi: 10.15252/emmm.201607485

Henriksen-Lacey, M., Christensen, D., Bramwell, V. W., Lindenstrom, T., Agger, E. M., Andersen, P., et al. (2010). Liposomal cationic charge and antigen adsorption are important properties for the efficient deposition of antigen at the injection site and ability of the vaccine to induce a cmi response. *J. Control Release* 145, 102–108. doi: 10.1016/j.jconrel.2010.03.027

Hoecke, L., and Roose, K. (2019). How mRNA therapeutics are entering the monoclonal antibody field. *J Transl Med.* 17:54. doi: 10.1186/s12967-019-1804-8

Holtkamp, S., Kreiter, S., Selmi, A., Simon, P., Koslowski, M., Huber, C., et al. (2006). Modification of antigen-encoding RNA increases stability, translational efficacy, and T-cell stimulatory capacity of dendritic cells. *Blood* 108, 4009–4017. doi: 10.1182/blood-2006-04-015024

Islam, M. A., Xu, Y., Tao, W., Ubellacker, J. M., Lim, M., Aum, D., et al. (2018). Restoration of tumour-growth suppression *in vivo* via systemic nanoparticle-mediated delivery of PTEN mRNA. *Nat. Biomed. Eng.* 2, 850–864. doi: 10.1038/s41551-018-0284-0

Jackson, H. J., Rafiq, S., and Brentjens, R. J. (2016). Driving CAR T-cells forward. *Nat. Rev. Clin. Oncol.* 13, 370–383. doi: 10.1038/nrclinonc.2016.36

Jackson, N. A. C., Kester, K. E., Casimiro, D., Gurunathan, S., and DeRosa, F. (2020). The promise of mRNA vaccines: a biotech and industrial perspective. *NPJ Vaccines* 5:11. doi: 10.1038/s41541-020-0159-8

Judge, A., McClintock, K., Phelps, J. R., and MacLachlan, I. (2006). Hypersensitivity and loss of disease site targeting caused by antibody responses to PEGylated liposomes. *Mol. Ther.* 13, 328–337. doi: 10.1016/j.ymthe.2005.09.014

Kaczmarek, J. C., Kowalski, P. S., and Anderson, D. G. (2017). Advances in the delivery of RNA therapeutics: from concept to clinical reality. *Genome Med.* 9:60. doi: 10.1186/s13073-017-0450-0

Kaczmarek, J. C., Patel, A. K., Kauffman, K. J., Fenton, O. S., Webber, M. J., Heartlein, M. W., et al. (2016). Polymer-lipid nanoparticles for systemic delivery of mRNA to the lungs. *Angew. Chem. Int. Ed. Engl.* 55, 13808–13812. doi: 10.1002/anie.201608450

Karikó, K., Muramatsu, H., Ludwig, J., and Weissman, D. (2011). Generating the optimal mRNA for therapy: HPLC purification eliminates immune activation and improves translation of nucleoside-modified, protein-encoding mRNA. *Nucleic Acids Res.* 39:e142. doi: 10.1093/nar/gkr695

Kon, E., Hazan-Halevy, I., Rosenblum, D., Cohen, N., Chatterjee, S., Veiga, N., et al. (2020). Resveratrol enhances mRNA and siRNA lipid nanoparticles primary CLL cell transfection. *Pharmaceutics* 12:520. doi: 10.3390/pharmaceutics12060520

Korsholm, K. S., Agger, E. M., Foged, C., Christensen, D., Dietrich, J., Andersen, C. S., et al. (2007). The adjuvant mechanism of cationic dimethyldioctadecylammonium liposomes. *Immunology* 121, 216–226. doi: 10.1111/j.1365-2567.2007.02560.x

Kowalski, P. S., Rudra, A., Miao, L., and Anderson, D. G. (2019). Delivering the messenger: advances in technologies for therapeutic mRNA delivery. *Mol. Ther.* 27, 710–728. doi: 10.1016/j.ymthe.2019.02.012

Kranz, L. M., Diken, M., Haas, H., Kreiter, S., Loquai, C., Reuter, K. C., et al. (2016). Systemic RNA delivery to dendritic cells exploits antiviral defence for cancer immunotherapy. *Nature* 534, 396–401. doi: 10.1038/nature18300

Kreiter, S., Selmi, A., Diken, M., Koslowski, M., Britten, C. M., Huber, C., et al. (2010). Intranodal vaccination with naked antigen-encoding RNA elicits potent prophylactic and therapeutic antitumoral immunity. *Cancer Res.* 70, 9031–9040. doi: 10.1158/0008-5472.CAN-10-0699

Li, S., and Huang, L. (1997). *In vivo* gene transfer via intravenous administration of cationic lipid-protamine-DNA (LPD) complexes. *Gene Ther.* 4, 891–900. doi: 10.1038/sj.gt.3300482

Li, S. D., and Huang, L. (2009). Nanoparticles evading the reticuloendothelial system: role of the supported bilayer. *Biochim. Biophys. Acta* 1788, 2259–2266. doi: 10.1016/j.bbamem.2009.06.022

Lonez, C., Bessodes, M., Scherman, D., Vandenbranden, M., Escriou, V., and Ruysschaert, J. M. (2014). Cationic lipid nanocarriers activate Toll-like receptor 2 and NLRP3 inflammasome pathways. *Nanomedicine* 10, 775–782. doi: 10.1016/j.nano.2013.12.003

Malone, R. W., Felgner, P. L., and Verma, I. M. (1989). Cationic liposome-mediated RNA transfection. *Proc. Natl. Acad. Sci. U.S.A.* 86, 6077–6081. doi: 10.1073/pnas.86.16.6077

Matsui, H., Sato, Y., Hatakeyama, H., Akita, H., and Harashima, H. (2015). Size-dependent specific targeting and efficient gene silencing in peritoneal macrophages using a pH-sensitive cationic liposomal siRNA carrier. *Int. J. Pharm.* 495, 171–178. doi: 10.1016/j.ijpharm.2015.08.044

Maugeri, M., Nawaz, M., Papadimitriou, A., Angerfors, A., Camponeschi, A., Na, M., et al. (2019). Linkage between endosomal escape of LNP-mRNA and loading into EVs for transport to other cells. *Nat. Commun.* 10:4333. doi: 10.1038/s41467-019-12275-6

McKinlay, C. J., Benner, N. L., Haabeth, O. A., Waymouth, R. M., and Wender, P. A. (2018). Enhanced mRNA delivery into lymphocytes enabled by lipid-varied libraries of charge-altering releasable transporters. *Proc. Natl. Acad. Sci. U.S.A.* 115, E5859–E5866. doi: 10.1073/pnas.1805358115

McKinlay, C. J., Vargas, J. R., Blake, T. R., Hardy, J. W., Kanada, M., Contag, C. H., et al. (2017). Charge-altering releasable transporters (CARTs) for the delivery and release of mRNA in living animals. *Proc. Natl. Acad. Sci. U.S.A.* 114, E448–E456. doi: 10.1073/pnas.1614193114

Miao, L., Li, L., Huang, Y., Delcassian, D., Chahal, J., Han, J., et al. (2019). Delivery of mRNA vaccines with heterocyclic lipids increases anti-tumor efficacy by STING-mediated immune cell activation. *Nat. Biotechnol.* 37, 1174–1185. doi: 10.1038/s41587-019-0247-3

Miao, L., Lin, J., Huang, Y., Li, L., Delcassian, D., Ge, Y., et al. (2020). Synergistic lipid compositions for albumin receptor mediated delivery of mRNA to the liver. *Nat. Commun.* 11:2424. doi: 10.1038/s41467-020-16248-y

Mohanty, R., Chowdhury, C. R., Arega, S., Sen, P., Ganguly, P., and Ganguly, N. (2019). CAR T cell therapy: a new era for cancer treatment (Review). *Oncol. Rep.* 42, 2183–2195. doi: 10.3892/or.2019.7335

Nabhan,J. F., Wood, K. M., Rao, V. P., Morin, J., and Bhamidipaty, S., LaBranche, T. P., et al. (2016). Intrathecal delivery of frataxin mRNA encapsulated in lipid nanoparticles to dorsal root ganglia as a potential therapeutic for Friedreich's ataxia. *Sci. Rep.* 6:20019. doi: 10.1038/srep20019

Oberli, M. A., Reichmuth, A. M., Dorkin, J. R., Mitchell, M. J., Fenton, O. S., and Jaklenec, A. (2017). Lipid nanoparticle assisted mRNA delivery for potent cancer immunotherapy. *Nano Lett.* 17, 1326–1335. doi: 10.1021/acs.nanolett.6b03329

Pardi, N., Hogan, M. J., Porter, F. W., and Weissman, D. (2018). mRNA vaccines - a new era in vaccinology. *Nat Rev Drug Discov.* 17, 261–279. doi: 10.1038/nrd.2017.243

Pardi, N., Secreto, A. J., Shan, X., Debonera, F., Glover, J., Yi, Y., et al. (2017). Administration of nucleoside-modified mRNA encoding broadly neutralizing antibody protects humanized mice from HIV-1 challenge. *Nat. Commun.* 8:14630. doi: 10.1038/ncomms14630

Parhiz, H., Shuvaev, V. V., Pardi, N., Khoshnejad, M., Kiseleva, R. Y., Brenner, J. S., et al. (2018). PECAM-1 directed re-targeting of exogenous mRNA providing

two orders of magnitude enhancement of vascular delivery and expression in lungs independent of apolipoprotein E-mediated uptake. *J. Control Release* 291, 106–115. doi: 10.1016/j.jconrel.2018.10.015

Park, Y. J., Da-Sol Kuen, D. S., and Chung, Y. (2018). Future prospects of immune checkpoint blockade in cancer: from response prediction to overcoming resistance. *Exp. Mol. Med.* 50:109. doi: 10.1038/s12276-018-0130-1

Pastor, F., Berraondo, P., Etxeberria, I., Frederick, J., Sahin, U., Gilboa, E., et al. (2018). An RNA toolbox for cancer immunotherapy. *Nat Rev Drug Discov.* 17, 751–767. doi: 10.1038/nrd.2018.132

Patel, S., Ashwanikumar, N., Robinson, E., DuRoss, A., Sun, C., Murphy-Benenato, K. E., et al. (2017). Boosting intracellular delivery of lipid nanoparticle-encapsulated messenger RNA. *Nano Lett.* 17, 5711–5718. doi: 10.1021/acs.nanolett.7b02664

Patel, S., Ashwanikumar, N., Robinson, E., Xia, Y., Mihai, C., Griffith, J. P., et al. (2020). Naturally-occurring cholesterol analogues in lipid nanoparticles induce polymorphic shape and enhance intracellular delivery of mRNA. *Nat. Commun.* 11:983. doi: 10.1038/s41467-020-14527-2

Persano, S., Guevara, M. L., Li, Z., Mai, J., Ferrari, M., Pompa, P. P., et al. (2017). Lipopolyplex potentiates anti-tumor immunity of mRNA-based vaccination. *Biomaterials* 125, 81–89. doi: 10.1016/j.biomaterials.2017.02.019

Pozzi, D., Marchini, C., Cardarelli, F., Amenitsch, H., Garulli, C., Bifone, A., et al. (2012). Transfection efficiency boost of cholesterol-containing lipoplexes. *Biochim. Biophys. Acta* 1818, 2335–2343. doi: 10.1016/j.bbamem.2012.05.017

Reichmuth, A. M., Oberli, M. A., Jaklenec, A., Langer, R., and Blankschtein, D. (2016). mRNA vaccine delivery using lipid nanoparticles. *Ther. Deliv.* 7, 319–334. doi: 10.4155/tde-2016-0006

Rybakova, Y., Kowalski, P. S., Huang, Y., Gonzalez, J. T., Heartlein, M. W., DeRosa, F., et al. (2019). mRNA delivery for therapeutic anti-HER2 antibody expression *in vivo. Mol. Ther.* 27, 1415–1423. doi: 10.1016/j.ymthe.2019.05.012

Sahin, U., Karikó, K., and Türeci, Ö. (2014). mRNA-based therapeutics–developing a new class of drugs. *Nat Rev Drug Discov.* 13, 759–780. doi: 10.1038/nrd4278

Sato, Y., Okabe, N., Note, Y., Hashiba, K., Maeki, M., Tokeshi, M., et al. (2020). Hydrophobic scaffolds of pH-sensitive cationic lipids contribute to miscibility with phospholipids and improve the efficiency of delivering short interfering RNA by small-sized lipid nanoparticles. *Acta Biomater.* 102, 341–350. doi: 10.1016/j.actbio.2019.11.022

Schlake, T., Thess, A., Thran, M., and Jordan, I. (2019). mRNA as novel technology for passive immunotherapy. *Cell Mol. Life Sci.* 76, 301–328. doi: 10.1007/s00018-018-2935-4

Stadler, C. R., Bähr-Mahmud, H., Celik, L., Hebich, B., Roth, A. S., Roth, R. P., et al. (2017). Elimination of large tumors in mice by mRNA-encoded bispecific antibodies. *Nat. Med.* 23, 815–817. doi: 10.1038/nm.4356

Suzuki, M., Kato, C., and Kato, A. (2015). Therapeutic antibodies: their mechanisms of action and the pathological findings they induce in toxicity studies. *J. Toxicol. Pathol.* 28, 133–139. doi: 10.1293/tox.2015-0031

Tam, Y. Y. C., Chen, S., and Cullis, P. R. (2013). Advances in lipid nanoparticles for siRNA delivery. *Pharmaceutics* 5, 498–507. doi: 10.3390/pharmaceutics5030498

Thomas, A., Garg, S. M., De Souza, R. A. G., Ouellet, E., Tharmarajah, G., Reichert, D., et al. (2018). Microfluidic production and application of lipid nanoparticles for nucleic acid transfection. *Methods Mol. Biol.* 1792, 193–203. doi: 10.1007/978-1-4939-7865-6_14

Thran, M., Mukherjee, J., Pönisch, M., Fiedler, K., Thess, A., and Mui, B. L. (2017). mRNA mediates passive vaccination against infectious agents, toxins, and tumors. *EMBO Mol. Med.* 9, 1434–1447. doi: 10.15252/emmm.201707678

Tiwari, P. M., Vanover, D., Lindsay, K. E., Bawage, S. S., Kirschman, J. L., Bhosle, S., et al. (2018). Engineered mRNA-expressed antibodies prevent respiratory syncytial virus infection. *Nat. Commun.* 9:3999. doi: 10.1038/s41467-018-06508-3

Turnis, M. E., and Rooney, C. M. (2010). Enhancement of dendritic cells as vaccines for cancer. *Immunotherapy* 2, 847–862. doi: 10.2217/imt.10.56

Van der Jeught, K., De Koker, S., Bialkowski, L., Heirman, C., Joe, P. T., Perche, F., et al. (2018). Dendritic cell targeting mRNA lipopolyplexes combine strong antitumor T-cell immunity with improved inflammatory safety. *ACS Nano* 12, 9815–9829. doi: 10.1021/acsnano.8b00966

Van Lint, S., Goyvaerts, C., Maenhout, S., Goethals, L., Disy, A., Benteyn, D., et al. (2012). Preclinical evaluation of TriMix and antigen mRNA-based antitumor therapy. *Cancer Res.* 72, 1661–1671. doi: 10.1158/0008-5472.CAN-11-2957

Verbeke, R., Lentacker, I., Wayteck, L., Breckpot, K., Van Bockstal, M., Descamps, B., et al. (2017). Co-delivery of nucleoside-modified mRNA and TLR agonists for cancer immunotherapy: restoring the immunogenicity of immunosilent mRNA. *J. Control Release* 266, 287–300. doi: 10.1016/j.jconrel.2017.09.041

Vitale, C., and Strati, P. (2020). CAR T-cell therapy for B-cell non-hodgkin lymphoma and chronic lymphocytic leukemia: clinical trials and real-world experiences. *Front Oncol.* 10:849. doi: 10.3389/fonc.2020.00849

Wadhwa, A., Aljabbari, A., Lokras, A., Foged, C., and Thakur, A. (2020). Opportunities and challenges in the delivery of mRNA-based vaccines. *Pharmaceutics* 12:102. doi: 10.3390/pharmaceutics12020102

Wahane, A., Waghmode, A., Kapphahn, A., Dhuri, K., Gupta, A., and Bahal, R. (2020). Role of lipid-based and polymer-based non-viral vectors in nucleic acid delivery for next-generation gene therapy. *Molecules* 25:2866. doi: 10.3390/molecules25122866

Wang, Y., and Huang, L. (2013). A window onto siRNA delivery. *Nat. Biotechnol.* 31, 611–612. doi: 10.1038/nbt.2634

Wang, Y., Zhang, L., Xu, Z., Miao, L., and Huang, L. (2018). mRNA vaccine with antigen-specific checkpoint blockade induces an enhanced immune response against established melanoma. *Mol. Ther.* 26, 420–434. doi: 10.1016/j.ymthe.2017.11.009

Weissman, D. (2014). mRNA transcript therapy. *Expert Rev. Vaccines* 14, 265–281. doi: 10.1586/14760584.2015.973859

Weng, Y., Li, C., Yang, T., Hu, B., Zhang, M., Guo, S., et al. (2020). The challenge and prospect of mRNA therapeutics landscape. *Biotechnol. Adv.* 40:107534. doi: 10.1016/j.biotechadv.2020.107534

Wiesinger, M., März, J., Kummer, M., Schuler, G., Dörrie, J., Schuler-Thurner, B., et al. (2019). Clinical-scale production of CAR-T cells for the treatment of melanoma patients by mRNA transfection of a CSPG4-specific CAR under full GMP compliance. *Cancers* 11:1198. doi: 10.3390/cancers11081198

Wilk, A. J., Benner, N. L., Vergara, R., Haabeth, O. A. W., Levy, R., Waymouth, R. M., et al. (2020). Charge-altering releasable transporters enable specific phenotypic manipulation of resting primary natural killer cells. *bioRxiv.* doi: 10.1101/2020.02.28.970491

Xue, H. Y., Guo, P., Wen, W. C., and Wong, H. L. (2015). Lipid-based nanocarriers for RNA Delivery. *Curr. Pharm. Des.* 21, 3140–3147. doi: 10.2174/1381612821666150531164540

Zelphati, O., and Szoka, F. C. Jr. (1996). Mechanism of oligonucleotide release from cationic liposomes. *Proc. Natl. Acad. Sci. U.S.A.* 93, 11493–11498. doi: 10.1073/pnas.93.21.11493

Zhang, F., Parayath, N. N., Ene, C. I., Stephan, S. B., Koehne, A. L., Coon, M. E., et al. (2019). Genetic programming of macrophages to perform anti-tumor functions using targeted mRNA nanocarriers. *Nat Commun.* 10:3974. doi: 10.1038/s41467-019-11911-5

Zhao, Z., Chen, Y., Francisco, N. M., Zhang, Y., and Wu, M. (2018). The application of CAR-T cell therapy in hematological malignancies: advantages and challenges. *Acta Pharm. Sin. B* 8, 539–551. doi: 10.1016/j.apsb.2018.03.001

Zhigaltsev, I. V., Belliveau, N., Hafez, I., Leung, A. K. K., Huft, J., Hansen, C., et al. (2012). Bottom-up design and synthesis of limit size lipid nanoparticle systems with aqueous and triglyceride cores using millisecond microfluidic mixing. *Langmuir* 28, 3633–3640. doi: 10.1021/la204833h

Zhong, Z., McCafferty, S., Combes, F., Huysmans, H., De Temmerman, J., Gitsels, A., et al. (2018). mRNA therapeutics deliver a hopeful message. *Nano Today* 23, 16–39. doi: 10.1016/j.nantod.2018.10.005

Zhu, X., Tao, W., Liu, D., Wu, J., Guo, Z., Ji, X., et al. (2017). Surface De-PEGylation controls nanoparticle-mediated siRNA delivery *in vitro* and *in vivo. Theranostics* 7, 1990–2002. doi: 10.7150/thno.18136

Solid Lipid Nanoparticles for Drug Delivery: Pharmacological and Biopharmaceutical Aspects

Sebastián Scioli Montoto[1,2], Giuliana Muraca[1,3] and María Esperanza Ruiz[1,2]*

[1] Laboratorio de Investigación y Desarrollo de Bioactivos, Departamento de Ciencias Biológicas, Facultad de Ciencias Exactas, Universidad Nacional de La Plata, La Plata, Argentina, [2] Consejo Nacional de Investigaciones Científicas y Técnicas, Buenos Aires, Argentina, [3] Instituto Nacional de Medicamentos (INAME, ANMAT), Buenos Aires, Argentina

In the golden age of pharmaceutical nanocarriers, we are witnessing a maturation stage of the original concepts and ideas. There is no doubt that nanoformulations are extremely valuable tools for drug delivery applications; the current challenge is how to optimize them to ensure that they are safe, effective and scalable, so that they can be manufactured at an industrial level and advance to clinical use. In this context, lipid nanoparticles have gained ground, since they are generally regarded as non-toxic, biocompatible and easy-to-produce formulations. Pharmaceutical applications of lipid nanocarriers are a burgeoning field for the transport and delivery of a diversity of therapeutic agents, from biotechnological products to small drug molecules. This review starts with a brief overview of the characteristics of solid lipid nanoparticles and discusses the relevancy of performing systematic preformulation studies. The main applications, as well as the advantages that this type of nanovehicles offers in certain therapeutic scenarios are discussed. Next, pharmacokinetic aspects are described, such as routes of administration, absorption after oral administration, distribution in the organism (including brain penetration) and elimination processes. Safety and toxicity issues are also addressed. Our work presents an original point of view, addressing the biopharmaceutical aspects of these nanovehicles by means of descriptive statistics of the state-of-the-art of solid lipid nanoparticles research. All the presented results, trends, graphs and discussions are based in a systematic (and reproducible) bibliographic search that considered only original papers in the subject, covering a 7 years range (2013-today), a period that accounts for more than 60% of the total number of publications in the topic in the main bibliographic databases and search engines. Focus was placed on the therapeutic fields of application, absorption and distribution processes and current efforts for the translation into the clinical practice of lipid-based nanoparticles. For this, the currently active clinical trials on lipid nanoparticles were reviewed, with a brief discussion on what achievements or milestones are still to be reached, as a way of understanding the reasons for the scarce number of solid lipid nanoparticles undergoing clinical trials.

Keywords: clinical trials, drug delivery, nanostructured lipid carriers, nanotoxicity, pharmacokinetics, pharmacodynamics, routes of administration, solid lipid nanoparticles

INTRODUCTION

For many years, lipid materials that are solid at room temperature have been used in the pharmaceutical industry for the preparation of different types of formulations such as emulsions, lotions, ointments and suppositories, among others (de Blaey and Polderman, 1980). Due to the high affinity of the lipid-rich intercellular space of the stratum corneum for this kind of materials, they have been most commonly used as inert ingredients in topical medications, but lipids (both solid or liquid at room temperature) are also regular constituents of other enteral and parenteral formulations, like soft/hard capsules or parenteral emulsions (Feeney et al., 2016).

Nanoscience, on the other hand, arose initially from the field of physics and electronic engineering, to rapidly impact other scientific areas, such as biology, biochemistry, and medicine, where the size range of nanoparticles (NPs) has historically been associated with the so-called *colloids* (Hauser, 1955). Colloidal systems are dispersion of particles (very large molecules or molecule aggregates) of intermediate size between molecules in solution and particles in coarse suspension, and it has been almost 100 years since a *colloidal* size range of 1–1000 nm was proposed (le Chatelier, 1919), which is still accepted today (McNaught and Wilkinson, 1997).

Hence, the novelty that NPs brought to the biomedical and therapeutic fields was not their size, but a radical change in the prevailing therapeutic paradigm: a designed, tailored, functional or at least protective system, usually carrying a drug, that could reach the systemic circulation of the patient along with the drug. In other words, due to their size, nanovehicles brought down the classical concept that only drugs dissolved in biological fluids can be absorbed and/or distributed through the body.

When back in the 90s Müller et al. (2002) proposed the term *solid lipid nanoparticles* (SLN®), as well as *nanostructured lipid carriers* (NLC®), it seemed like a natural idea: to combine the advantageous characteristics of NPs (mostly metallic and polymeric at that time) with those of lipid-based parenteral emulsions, based on non-toxic and biodegradable lipid components (Schwarz et al., 1994). These lipid NPs were promoted as a safer option compared to other nanosystems; they are constituted of a solid matrix that would allow the controlled release of the drug, but being more stable (and certainly cheaper) than phospholipid-based liposomes developed so far (Martins et al., 2007).

If lipid NPs were up to the expectations, is what remains to be determined. With that in mind, this review presents an overview of the investigations regarding SLN and NLC for drug delivery applications, and a descriptive statistical analysis of the field from 2013 until today. No size restrictions have been imposed on the systems considered, and the nano-classification proposed by the authors is maintained. Consequently, despite that all the reviewed nanovehicles belong to the colloidal size range mentioned before, those closer to the upper limit could be better addressed as microparticles, which have been in the pharmaceutical market for several years now (Siepmann and Siepmann, 2006).

Our work presents an original point of view, by addressing the biopharmaceutical aspects of these nanovehicles by means of trends and descriptive statistics covering the last 7 years of research in the field. In gathering and presenting the information, focus was placed on the therapeutic fields of application, pharmacokinetic aspects, safety issues, toxicological concerns and current efforts for the translation into the clinical practice of lipid-based NPs. We believe it will be a valuable read for all those researchers interested in knowing what therapeutic challenges are being addressed through the use of SLN, and what remains to be done.

Our Bibliographic Search

At present, we are witnessing a huge expansion of scientific knowledge, with countless work groups researching common themes, collaboratively or individually, throughout all countries all over the world. This makes it virtually impossible to review topics in a comprehensive manner, that is, covering everything published to date with respect to a given topic. Limiting the information reviewed is thus imperative, with the inevitable risk of falling into involuntary biases regarding the information sampling.

Therefore, in order to perform a search as objective as possible, the following criteria were set:

- Original publications in English dating from the last 7 years: this meant excluding from the systematic search the review articles and limiting the search to original works published since 2013, inclusive. Although it is true that there is a lot of information prior to that date, the analysis of year-by-year statistics of academic databases and search engines reveals that, of the total number of publications retrieved when searching for the phrase "solid lipid nanoparticles" in the title, more than 60% correspond to the period 2013-2020. In particular, publications from 2013 to date were 1600 out of 2630 in Google Scholar (60.8%), 944 out of 1264 in PubMed (74.7%), and 1300 out of 2111 in Scopus (61.6%), which is remarkable considering that the total SLN/NLC publication period is 25 years [the first references date from Maaßen et al. (1993); Muller et al. (1993)].
- R&D publications focused on the application of lipid nanosystems for the delivery of drugs, excluding merely technological developments without any biological or biorelevant assay. For this, the following keywords were included in the search (with the "OR" connector): drug delivery, in vivo, cell, cells, pharmacokinetic, pharmacokinetics.

Despite Google Scholar retrieved the largest number of publications, Scopus was selected to perform the final search due to its more versatile advanced search interface, and the possibility to download the search results. At the time of the writing of this work, this search yielded 371 scientific articles, which constitute the database on which the descriptive statistics and trends presented in the following sections are based.

The Tiny Big Universe of Lipid Nanoparticles

When firstly developed, SLN were presented as tiny and spherical particles, made of solid lipids at room temperature, that may be thought as perfect crystal lipid matrices, able to accommodate a drug or other molecules between fatty acid chains (Puri et al., 2009). Nowadays, however, it is known that this is not necessarily true in all cases, since disc-like shape or flat ellipsoidal geometry have also been described (Mazuryk et al., 2016; Shah et al., 2019). Moreover, the loaded drug may be attached mostly to the carrier matrix surface instead of being embedded into the solid core (Pink et al., 2019; Shah et al., 2019).

Almost 10 years after SLN introduction, a second generation of lipid NPs, the nanostructured lipid carriers (NLC) appeared (Muller et al., 2002). Considered as an advanced version of SLN, NLC incorporate into their structure small amounts of liquid lipids at room temperature (oils), to produce structural rearrangements of the matrix. By that time, it was observed that the maturation of the crystalline structure that SLN exhibit along the time often results in the expulsion of the incorporated drug to the surrounding medium (Mehnert and Mäder, 2001). The oils in NLC act by reducing the crystalline degree of the lipid core of SLN, thus avoiding the expulsion of the drug from the matrix and increasing the drug loading capacity and physical and chemical long-term stability (Müller et al., 2002). The highly-ordered crystalline structure of the lipids in a SLN has been recently studied by Pink et al. (2019) whose work provides a detailed description of the internal and external structure of SLN.

A detailed description of the materials and methods used for the synthesis of SLN / NLC is beyond the scope of this review, and can be found elsewhere (see, for example, Geszke-Moritz and Moritz, 2016; Gordillo-Galeano and Mora-Huertas, 2018; Jain and Thareja, 2020). However, it is worth highlighting that, being strongly hydrophobic, lipidic NPs in aqueous environments are very low hydrated or no hydrated at all, and thus they are not able to be spontaneously dissolved or dispersed in water. Therefore, the preparation of these dispersions necessarily implies transferring energy to the system, in order to generate very small particles, with very high specific surface area (Troy, 2000). Regardless the details of each synthesis method, they all share the common feature of an energy-providing step, under the form of ultrasonic waves [probe-type sonication (Haque et al., 2018; Pandya et al., 2018; Scioli Montoto et al., 2018) or ultrasonic bath (Rajpoot and Jain, 2018; Rosière et al., 2018; Chirio et al., 2019), high pressures (de Jesus et al., 2013; Küçüktürkmen and Bozkır, 2018; Wang et al., 2018), high speed homogenization (Nakhlband et al., 2018; Sathya et al., 2018; Youssef et al., 2018), or even microwaves (Shah et al., 2016a)]. The comparative performance of the two most commonly applied methods for lipid NPs preparation, hot homogenization and high pressure homogenization, was evaluated in the first studies within the field (Schwarz et al., 1994).

On the other hand, besides the energy that must be transferred to the system to *create* the particles, it is also necessary to implement other technological strategies in order to *maintain* the large surface area exposed by the dispersed NPs. Suspended in aqueous media, lipid NPs constitute a lyophobic dispersion (i.e., NPs have no affinity for the dispersing medium), and thus intrinsically unstable. The most stable state of the lyophobic colloids contains the dispersed phase aggregated in large crystals or droplets, to minimize the specific surface area and, hence, the interfacial free energy (Leite and Ribeiro, 2012). To prevent this aggregation process (*coalescence*), the particles must be electrostatically and/or sterically stabilized (Keck et al., 2014; Kovačević et al., 2014). **Figure 1** shows a schematic representation of a SLN and a NLC sterically stabilized with a neutral surfactant.

The superficial charge of lipid NPs is mostly determined by the materials used for their synthesis, and the pH of the surrounding medium. The Z potential (ζ) is the electric potential at the slipping (or shear) plane, i.e., the potential difference between the stationary double layer of fluid that surrounds a colloidal particle in suspension and any point in the surrounding liquid medium. It is a measure of the surface charge of the particle, and thus it is directly related to the charge exhibited by the lipid or surfactant of the nanosystem, at the pH value of the formulation (Cheng and Lee, 2016).

The ζ required to stabilize the lipid NPs dispersion only by electrostatic repulsion is usually accepted to be ±30 mV or higher, to assure enough repulsion of nearby NPs in the suspension (Kovačević et al., 2014). Negative values of ζ are achieved when particles are formulated with negatively charged components at the pH of the formulation, like stearic acid (Liu et al., 2017), sodium taurocholate (Rosière et al., 2018) or 1-Oleoyl-glycero-3-phosphate sodium salt (Abd-Rabou et al., 2018), among others. On the contrary, positively charged starting materials are needed to produce lipid NPs with ζ values greater than zero, such as stearylamine (Costa et al., 2018), quaternary ammonium lipids (Doktorovova et al., 2018; Küçüktürkmen and Bozkır, 2018; Wu et al., 2018) or chitosan coatings (Liu et al., 2017; Vijayakumar et al., 2017). Nevertheless, the majority of lipid components (as well as surfactants) currently used to formulate SLN/NLC are neutral, with the two most common being ester (e.g., glycerides) and ether (e.g., Tween, Poloxamer, Brij) functions. Lipid NPs based on these materials tend to present ζ values slightly or moderately negative (between -30 and -3 mV).

The small absolute values of ζ are not enough to prevent the coalescence of the NPs, which need to be further stabilized by steric repulsion. To do so, hydrophilic polymers and/or surfactants are included in the formulation. These compounds tend to adsorb onto the particles surface and project their polar residues to the surrounding aqueous medium, thus preventing the NPs to get too close so that the attractive forces predominate (Luo et al., 2015).

It is not easy, however, predicting the effect that the NPs composition and preparation method will have on the ζ, particle size (PS) and entrapment efficiency (%EE). Systematic approaches like the quality by design (QbD) concepts, strongly related to the pharmaceutical industry, are very useful to comprehensively study and characterize the design space of the formulation. From the 371 articles reviewed, only 48 (nearly 13%) applied this type of analysis.

FIGURE 1 | Schematic representation of a SLN and a NLC sterically stabilized with a neutral surfactant (gray). The oxygen atoms in the liquid and solid lipids are shown in orange. Drug molecules are not depicted since they may be located inside the lipid core and/or attached to the outer shell.
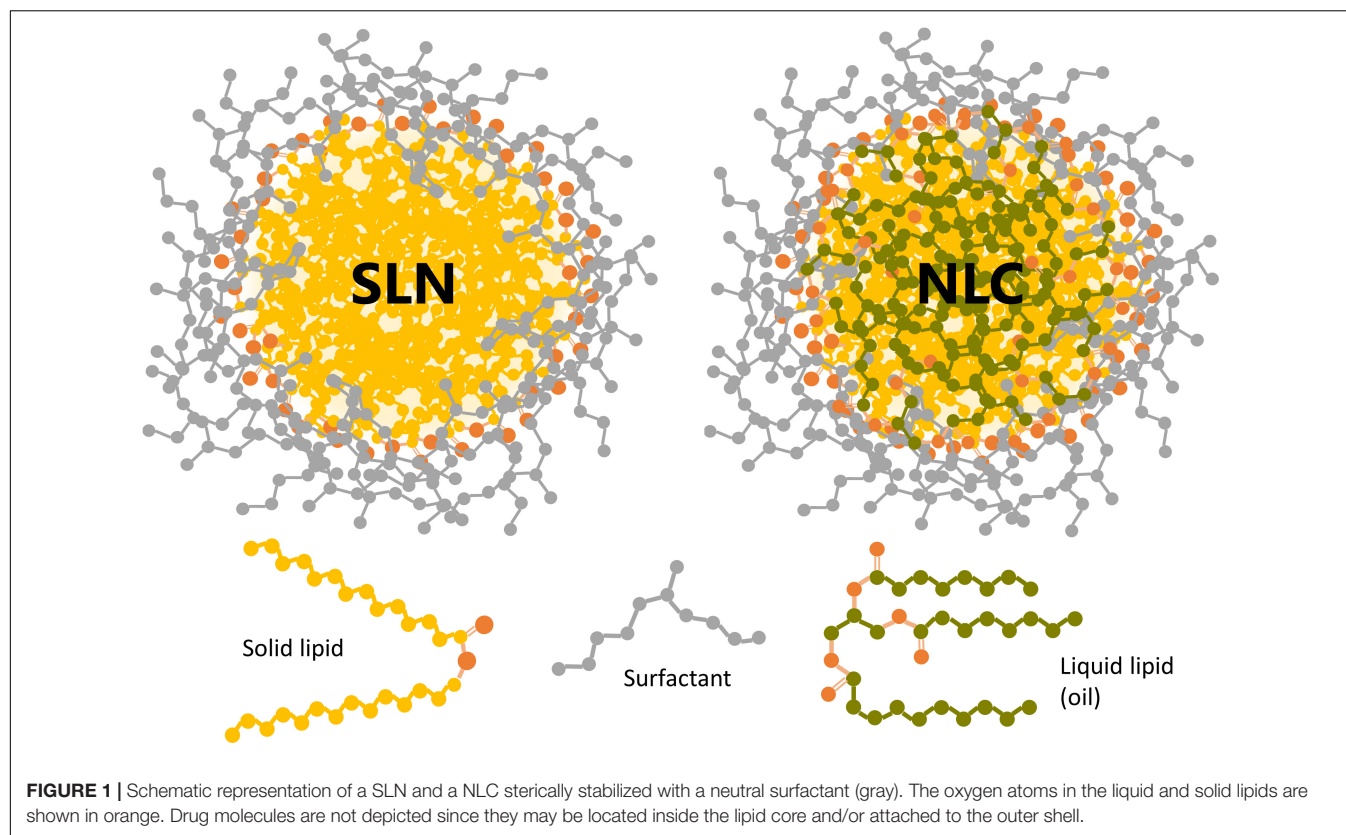
In terms of the product, QbD tools arise from the recognition that in order to guarantee the quality, it is not enough (nor economically efficient) to verify it in the finished product but has to be incorporated from its design. In the nanotechnology area, and more precisely, the development and preparation of SLN/NLC, this idea means to replace the old development empirical approach (i.e., in an artisanal way) by a more systematic one, based on the experimental design and the statistical analysis of the results (ICH, 2009).

To do so, it is usually convenient to start with fractional factorial designs, which allow to study multiple variables at the same time with the smallest number of runs: while a full factorial design requires 2^k experiments or runs to study the effect of k factor at 2 levels (without replicates), the $\frac{1}{4}$ fraction of this design allows estimating main effects with 2^{k-2} runs. The decrease in the number of runs (i.e., in degrees of freedom), inevitably implies a loss of information, but fractional designs are ideal preliminary designs, to study several factors at a time with focus on their main effects, as generally happens during the design of products and processes (Montgomery, 2017).

Once the more relevant factors are identified, a minor number of them are studied with more details [i.e., more levels, so that the "curvature" in the response function can be addressed) in the optimization stage. For this, response surface methodologies (RSM) are usually employed (although other statistical techniques may apply, see for example (Amasya et al., 2019)]. RSM are generated from designs where factors are studied in more than two level (n levels), such as full

factorial (n^k) designs or more efficient ones like the central composite or Box-Behnken designs. This type of designs allows to find functional relationships among studied responses (quality attributes, such as particle size or ζ) and factors, like the amount of lipid, the synthesis time or temperature, among others.

The above mentioned is particularly relevant in SLN/NLC area, since even with the experience accumulated in these years, very few trends are predictable. Perhaps the only example is the positive relationship between the amount of lipid and the particle size, which is verified in almost all the cases and independently of the drug and preparation method: all the review articles that include the study of particle size as a function of the lipid amount found a direct relationship between them, at least in part of the studied range, if not in all. However, these results must be interpreted carefully since the existence of interactions among factors can cause this relationship to be modified according to the levels of the other factors. It is not unusual that at higher surfactant concentrations, the effect of the amount of lipid over the particle size is minor or null (Cacicedo et al., 2019; Rajpoot and Jain, 2019). The presence of interactions among factors and their magnitude can only be studied by means of designs of several crossed factors, such as those mentioned before, being insufficient the individual or univariate optimization of the responses in function of each process attribute or parameter (Montgomery, 2017).

Systematization of the preformulation stage through the aforementioned statistical tools allow not only to gain insights

in a more efficient manner but also to study several response variables at once. As said before, decreasing the amount of lipid incorporated into the formulation frequently helps to reduce particle size, but has a negative effect on the entrapment efficiency (Kurakula et al., 2016; Talluri et al., 2017; Ahmad et al., 2019). Simultaneous optimization of both responses as a function of the formulation components and/or process operational variables allows to find the optimum compromise solution as well as other possible approaches, such as increasing the energy (frequency, speed) during the synthesis to decrease the particle size without sacrificing entrapment efficiency (Nooli et al., 2017; Dara et al., 2019; Khatri et al., 2019; Patel et al., 2019a), or decreasing the surfactant/lipid ratio (Bhalekar et al., 2017; Pandya et al., 2018; Ahmad et al., 2019).

A DESCRIPTIVE ANALYSIS OF THERAPEUTIC APPLICATION FIELDS OF SLN

Figure 2 shows the distribution of publications on SLN/NLC of the last 7 years, grouped by therapeutic fields. It can be

seen that, as for other nanosystems, cancer treatment represents the most relevant field of application (Hare et al., 2017). Of the 371 publications surveyed, 41.8% (155) corresponded to anticancer therapies, 14.3% (53) to antimicrobials, 12.4% (46) to the treatment of central nervous system (CNS) diseases and/or disorders (excluding cancer and infection), 7.3% (27) to site-specific treatments, 7.5% (28) to nanovehicles not intended for any specific therapeutic area (i.e., with no indication, including SLN for diagnostic purposes) and the remaining 16.7% (62) comprises drugs for various conditions or diseases (in gray in **Figure 2**).

In general, the treatment of any disease can be enhanced by the formulation of drugs loaded into lipid-based NPs, mainly due to physicochemical and/or biopharmaceutical aspects, like an improved pharmacokinetic profile, as we will discuss in the next section. However, the distribution displayed in **Figure 2** suggests that lipid-based NPs may possess additional advantages in certain specific therapeutic fields.

The large efforts in nanotechnologies focusing on **cancer treatment** is not surprising. Cancer is one of the major public health concerns and is among the leading causes of death worldwide. According to the National Cancer Institute
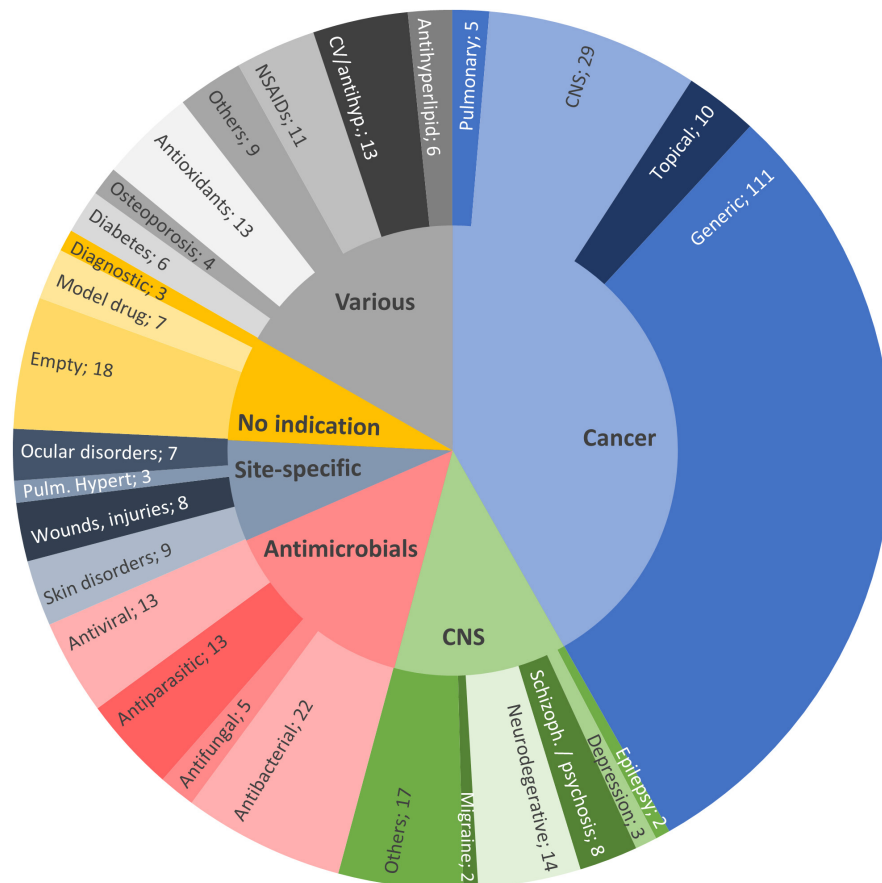

FIGURE 2 | Distribution of the 2013–2020 reviewed publications on SLN/NLC, by therapeutic field: anticancer therapies (41.8%, light blue); antimicrobials (14.3%, pink); CNS diseases, excluding cancer and infection (12.4%, green); site-specific treatments (7.3%, dark blue); various indications (16.7%, gray) and; nanovehicles not intended for any specific therapeutic area (7.5%, yellow).

(NCI, NIH), while in 2012 there were 14.1 million new cases (and 8.2 million cancer-related deaths worldwide), it is expected that the number of new cancer cases per year will reach 23.6 million by 2030[1].

The analysis of the database entries corresponding to SLN/NLC for cancer treatment reveals a great variety of encapsulated drugs, from large lipophilic molecules such as taxanes, to small molecules of higher polarity such as 5-fluorouracil. Even Pt-based chemotherapeutic agents (like the water-soluble drugs cisplatin and oxaliplatin) have been efficiently loaded into SLN, highlighting the versatility of these nanocarriers to encapsulate almost the whole range of chemotherapeutic agents available today.

In addition to the strong reasons for seeking new strategies for cancer therapies, cancerous tissues possess unique characteristics that make the choice of nano-based drug delivery especially interesting. The high rate of tumor growth leads to abnormal angiogenesis, with abundant fenestrations and large gaps between endothelial cells, as well as deficient lymphatic drainage in the area (von Roemeling et al., 2017). Combined, these characteristics lead to the accumulation, only based on the size (i.e., passive targeting), of NPs in the tumor vicinity, a phenomenon known as the Enhanced Permeability and Retention (EPR) effect. Although there is still controversy regarding the lack of uniformity in the observed EPR effect between species, at least in some human tumors the passive targeting of macromolecules and NPs has been demonstrated (Bjö et al., 2017).

On the other hand, a large number of genes (including many cell surface and nuclear receptors genes) are amplified or overexpressed in cancer cells. With the right surface ligands, NPs may be directed (i.e., actively targeted) to specifically bound those receptors (Shi et al., 2017). Among the 155 articles of SLN applicable to cancer, 23 of them involved some active targeting strategy. In contrast to the wide variety of payloads mentioned above, the targeting moieties belong, in the majority of cases, to one of two main classes: peptides and proteins (including antibodies, 70%) or folate residues (26%).

The α-isoform of the folate receptor, which is normally expressed at the apical surface of epithelial tissues and overexpressed in tumor cells of epithelial origin. Hence, it could be used to promote drug uptake by cancer cells via receptor-mediated endocytosis, by attaching folate residues to a nanoparticle surface (Holm and Hansen, 2020). Indeed, this strategy was successfully applied to the design and preparation of folate-grafted SLN loaded with irinotecan (Rajpoot and Jain, 2020) and a combination of resveratrol and ferulic acid (Senthil Kumar et al., 2020) for the treatment of colorectal cancer. Another example is found in integrin αvβ3, an adhesion molecule presented in all cells but overexpressed in several types of tumors. It has been demonstrated that its interaction with the RGD tripeptide (arginine-glycine-aspartic) leads to a number of cell functions that ultimately contributes to angiogenesis and metastasis (Martínez-Jothar et al., 2020). Conjugation of SLN with RGD increased *in vitro* antitumor efficacy and

in vivo cytotoxicity in comparison with non-targeted SLN (Zheng et al., 2019).

On the other hand, targeting ligands may be intended to promote the passage through physiological barriers like the blood brain barrier (BBB), to reach a site of action at CNS. This approach was applied in the formulation of docetaxel-loaded SLN functionalized with angiopep-2 (A-SLN), that specially binds to the low-density lipoprotein receptor related protein 1 (LRP1) overexpressed at the BBB. Higher *in vitro* cytotoxicity and BBB permeability were found for A-SLN, attributable to receptor-mediated endocytic processes (Kadari et al., 2018). Moreover, dual-approaches or combinations are also possible: Kuo and Lee (2016) achieved an increased toxicity on tumor cells by incorporating two antibodies for a two-stage targeting: first to BBB cells (83-14 MAb), and then to glioblastoma cells (AEGFR).

It is worth highlighting that, in order to efficiently conjugate the targeting moiety to the SLN, much more complicated synthesis methods are required. The systems are no longer made of the simple mix lipid/s - surfactant/s - drug/s. Instead, other reagents, solvents and reaction steps must be incorporated to the preparation protocol.

There are several options for attaching a targeting ligand to an SLN, such as linking a fatty acid of the NP with an amino group of the ligand (Siddhartha et al., 2018), an amino group of a phospholipid to an acid group of the ligand (Rajpoot and Jain, 2020), or an amino group of the chitosan coating with an acid group of the ligand (Senthil Kumar et al., 2020), among others. Regardless of the particulars, these examples end in the formation of an amide, which is by far the most widely used bond to attach ligands to the surface of lipid nanoparticles. In order to efficiently form an amide bond, activating reagents are required (carbodiimide, H-hydroxysuccinimide, etc.), and several steps must be performed in potentially toxic organic solvents. Therefore, the improvement in efficacy and/or biodistribution aimed by means of active targeting strategies is achieved by sacrificing what is (possibly) the main advantage of SLN/NLC: their green synthesis and safety profile.

Perhaps a better option is to use other types of chemical bonds instead of covalent bonds. Souto et al. (2019) synthesized extremely positive SLNs (ca. +70 mV, by choosing cetyltrimethylammonium bromide as surfactant) able to electrostatically interact with negatively charged streptavidin (pI = 5). The objective was to bind a biotinylated antibody (CAB51, against human epithelial growth receptor 2, HER2), taking advantage of the strong interaction between streptavidin and biotin. The goal was somehow accomplished, since *in vitro* assays revealed an improved internalization of the targeted NPs on a HER2 positive cell line (BT-474) compared to a HER2 negative cell line (MCF-7). But further optimization will be necessary to reduce the cytotoxicity exhibited by the nanoparticles themselves, which according to the authors was probably due to the cationic surfactant and/or their positive charge (Souto et al., 2019).

Last, but not least, the economic aspect must be mentioned. The costs of taking a novel nanomedicine into the clinic can be a significant obstacle for the introduction of new nanomedicines in the pharmaceutical market (Hare et al., 2017). Histories of success

---

[1]www.cancer.gov

like Abraxane, with sales of nearly \$1 billion by 2015 (van der Meel et al., 2017), and efforts like the Cancer Moonshot Task Force recommendation to enhance public–private partnerships (Jaffee et al., 2017) are expected to encourage drug developers to invest time and resources for cancer R&D.

Another area that could take much advantage from pharmaceutical nanovehicles is the one related to antibacterials, antivirals, antiparasitic and antifungals, grouped as **antimicrobials** in **Figure 2**.

All the reviewed articles corresponding to SLN/NLC applications to antiviral therapies present as main advantage the optimization of the distribution / accumulation of the drug in the site of action, as well as an improved biodistribution and diminished cytotoxicity.

As we will discuss later, drugs whose site of action is at the CNS level always represent a challenge in terms of biodistribution in order to achieve effective concentrations in the brain. Lipid NPs of zidovudine and saquinavir intended for the CNS showed promising results in cell cultures *in vitro* (Kuo and Wang, 2014; Joshy et al., 2016), and SLN-based formulations of efavirez (Gupta et al., 2017) and nevirapine (Lahkar and Kumar Das, 2018) exhibited an improved central *in vivo* bioavailability (BA). In the case of efavirenz, the strategy was to circumvent the BBB by means of the nasal administration of the nanoparticles, while in the nevirapine case the administration was by intravenous (IV) route and the improved biodistribution was attributed to the coating (polysorbate 80), able to enrich the protein crown in ApoE, resulting in a higher passage through the BBB due to the contribution of receptor-mediated transcytosis (Li et al., 2018; Krishna et al., 2019).

Regarding antiviral formulations intended for systemic effect after oral administration (Gaur et al., 2014; Shi et al., 2015; Ravindra Babu et al., 2019), an interesting work by Ravi et al. (2014) evaluated the comparative performance of the protease inhibitor lopinavir (LPV)-SLN with respect to LPV alone and the combination of LPV-Ritonavir (RTV). LPV is co-formulated with subtherapeutic doses of Ritonavir to overcome its poor oral BA due to CYP3A4 metabolism and P-glycoprotein (P-gp) efflux, both inhibited by RTV. The LPV-SLN presented greater oral BA than the LPV-RTV combination, and in vitro metabolic stability and rat everted gut sac studies allowed the authors to conclude that the observed results were due to a combination of a metabolic protection and increased intestinal permeability of the drug encapsulated into the SLN (Ravi et al., 2014).

A very promising aspect, although not still fully addressed, of the use of lipid-based NP to the delivery of antibiotics is the possibility to overcome some of the drug resistance mechanisms acquired by bacteria. Multiple-drug resistance (MDR) may be acquired by either a mutation or the acquisition of new genetic material from an exogenous source, that results in a mutated version of a drug target, membrane protein, transporters or enzymes, as beta-lactamases. In the same manner as NPs may help to optimize the pharmacokinetic (PK) profile of a drug by reducing its metabolism and/or efflux by ABC transporters in humans, it is feasible to apply the same concept to overcome the resistance produced by similar mechanisms in bacteria (Christaki et al., 2020). The possibility to deliver

biotechnological drugs encapsulated into SLN/NLC may also help to overcome MDR by exploring new therapeutic strategies, like interfering with the bacterial transcription process through the delivery of DNA molecules complexed with lipid NP (González-Paredes et al., 2019).

Moreover, lipid-based nanosystems offer several indirect-ways to address drug-resistance issues, by one or more of the following strategies:

- Achieving a sustained release profile of the drug, to maintain steady concentrations within its therapeutic concentration, and thus avoiding suboptimal levels which can promote resistant microbes selection (Nafee et al., 2014; Chetoni et al., 2016).
- Lowering the drug toxicity by encapsulation, allowing higher doses and/or treatment periods (Severino et al., 2015; Chaves et al., 2018).
- Increasing systemic BA (Chetoni et al., 2016; Banerjee et al., 2020) and CNS levels (Abdel Hady et al., 2020).
- Allowing pulmonary administration, with less unspecific distribution (Nafee et al., 2014; Gaspar et al., 2016, 2017; Maretti et al., 2017; Vieira et al., 2018).
- Promoting accumulation in target cells by means of active targeting (Maretti et al., 2017; Costa et al., 2018; Vieira et al., 2018; Hosseini et al., 2019; Banerjee et al., 2020).
- Increasing inhibitory effect (i.e., decreasing MIC) over bacterial strains (Severino et al., 2015; Pignatello et al., 2017; Ghaderkhani et al., 2019; Rodenak-Kladniew et al., 2019).

On the other hand, the very lipophilic groups of antiparasitic and azole antifungal agents highlight another advantageous aspect of lipid-based NPs. Due to its lipid components, SLN/NLC are able to solubilize highly lipophilic (i.e., aqueous insoluble) drugs, and keep them in a stable suspension, avoiding the use of large amounts of surface-active compounds and improving the biopharmaceutical performance after oral (Souza et al., 2014; Aljaeid and Hosny, 2016; Omwoyo et al., 2016; Rehman et al., 2018), ocular (Mohanty et al., 2015; Kumar and Sinha, 2016), and/or parenteral administration (Ahmadnia et al., 2013; Permana et al., 2019).

The hydrophobic constituents of lipid-based nanosystems provide a suitable environment for the entrapment of hydrophobic drugs, positioning SLN/NLC as a promising tool, particularly relevant in the current context where there is a growing trend toward more lipophilic drug candidates. *In silico* drug discovery strategies, high throughput screening methodologies and the more classical lead-optimization programs tend to favor compounds with higher pharmacological potency, in detriment of other properties that may be desirable from a physicochemical or pharmacokinetic point of view. On the contrary, it is a known fact that when the biopharmaceutical characteristics of drug candidates are addressed in early stages of discovery programs the consequence is an increase in failures due to lack of efficacy and, to a lesser extent, for toxicity concerns (Kola and Landis, 2004). Therefore, pharmaceutical chemists will always have to deal with the PK/PD & toxicity balance, and the aqueous solubility will remain to be a

critical factor in drug discovery. Proof of this is that, to date, approximately 39% of the marketed drugs (Benet, 2013) and 60% of the new chemical entities (Kovačević, 2020) belong to the biopharmaceutical categories that group *low solubility* drugs (i.e., BCS classes 2 and 4).

ROUTES OF ADMINISTRATION PROPOSED FOR SLN /NLC

As can be seen in **Figure 3**, the most commonly proposed administration route for lipid-based nanosystems is the parenteral route, closely followed by the oral route. Both administration routes seek to achieve systemic effects of the encapsulated drugs, but the trend described is opposite to the current distribution of pharmaceutical products in the market, where the oral route of administration is the preferred and most widely used route for drug administration.

Parenteral routes, on the other hand, allow the delivery of drugs directly to the systemic circulation with no absorptive barriers to overcome or with minimal restrictions, as in the case of the intramuscular and/or subcutaneous route. More than 50% of the lipid nanosystems assayed by parenteral routes (46 out of 81) corresponds to anticancer drugs, a therapeutic field where IV route remains predominant, in spite of its non-negligible negative aspects, such as invasiveness, associated risks, inability to self-manage and higher technological

requirements to be manufactured with suitable microbiological quality (Ruiz and Scioli Montoto, 2018).

Oral Route

The oral route, being a natural route of entry of substances to the organism, enjoys the greatest acceptability, as well as some technological advantages, since oral pharmaceuticals mostly comprise non-sterile solids dosage forms. For a successful therapy by the oral route, though, a drug must generally fall within certain ranges of lipophilicity, molecular weight, and hydrogen bonding ability, as well as aqueous solubility and permeability, which altogether contribute to its *druglikeness* (Di and Kerns, 2016).

Curcumin, for example, represents a real challenge for its formulation as oral product, due to its very low aqueous solubility, poor absorption, rapid metabolism and pH-dependent degradation rate (Sanidad et al., 2019). Oral BA of curcumin has been reported to be as low as 1% (Ma et al., 2019). On the other hand, successful outcomes of curcumin in both preclinical and clinical trial of different diseases make it a very promising drug, that seems to be able to modulate several cell signaling pathways and, thus, holds a great therapeutic potential against a wide range of human diseases (e.g., cancer, infections, inflammatory, metabolic and neurodegenerative diseases, among others) (Gupta et al., 2013). Furthermore, there is enough evidence to support the hypothesis of dose-dependent pharmacological activity of curcumin, with the anticancer properties corresponding to the highest doses (Doktorovova et al., 2018).

FIGURE 3 | Distribution of the 2013–2020 reviewed publications on SLN/NLC, by the proposed route of administration. Only publications with a PD and/or PK studies were considered (211 of 371).
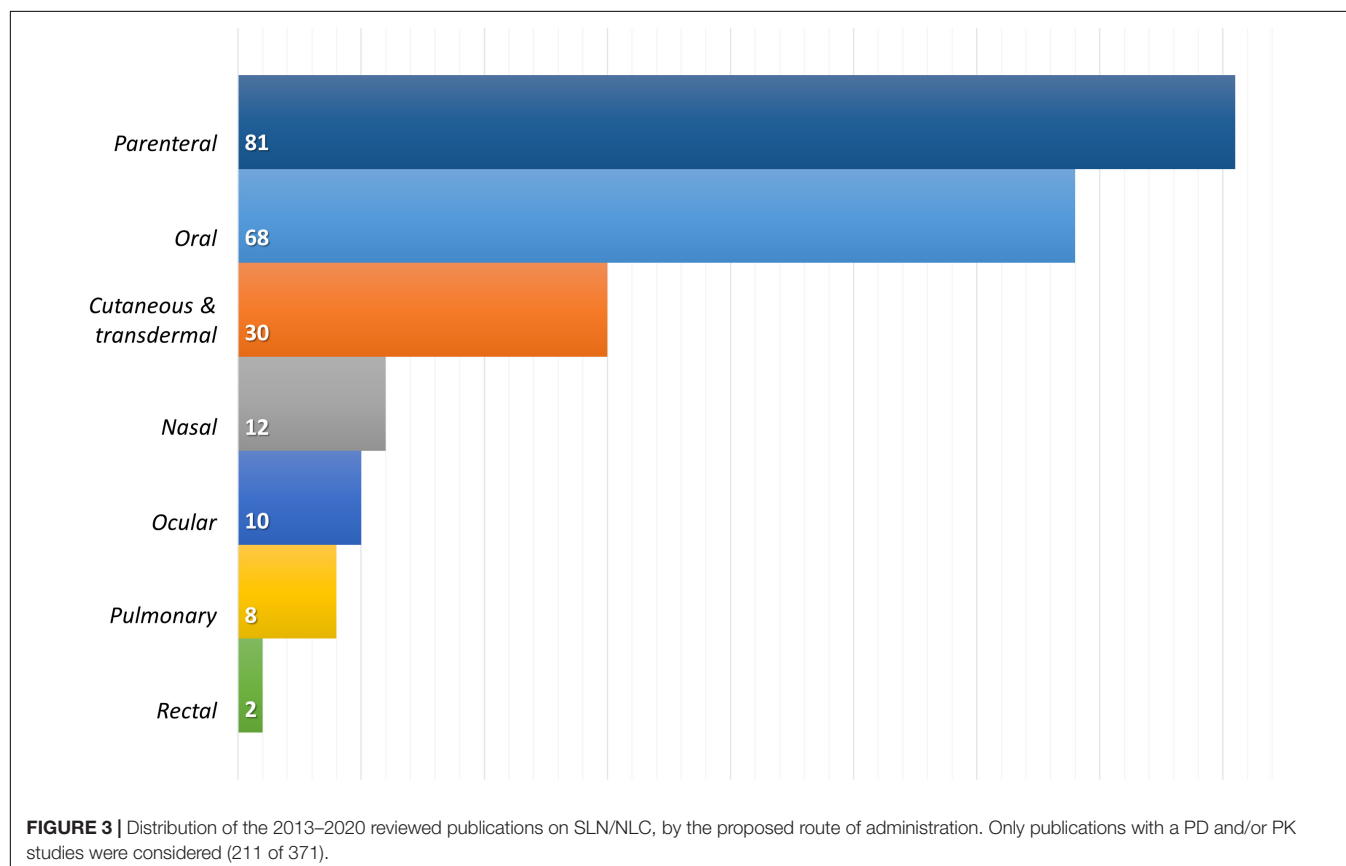
Regardless the somehow inconsistent reports on curcumin oral BA (possible due to variations in experimental conditions), there is agreement on the positive increment in the oral BA of curcumin formulated within nanosystems, with respect to the free drug in solution (Anand et al., 2007). Predictably, the publications reviewed here confirmed that trend, since curcumin oral BA achieved with SLN/NLC was from 2 to more than 10-fold higher than that of the free drug solution (Kakkar et al., 2013; Ramalingam and Ko, 2015; Baek and Cho, 2017). The examination of the PK profiles seems to indicate that the BA improvement of curcumin is related to the combined effect of a higher absorption and a minor elimination of the encapsulated drug, similarly to what was described for LPV-SLN.

Among the reviewed articles, the aforementioned trend is confirmed by many other examples. Administration as SLN/NLC greatly increases the oral BA of drugs with very low aqueous solubility such as aripiprazole (Silki and Sinha, 2018), rhein (Feng et al., 2017), zaleplon (Dudhipala and Janga, 2017), miconazole (Aljaeid and Hosny, 2016), raloxifene (Singh et al., 2013; Tran et al., 2014), efavirenz (Gaur et al., 2014), doxorubicin (Yuan et al., 2013), asenapine (Patel et al., 2019b), linagliptin (Veni and Gupta, 2020), and niclosamide (Rehman et al., 2018), among several others.

The group of calcium channel blockers derived from dihydropyridine, for example, is characterized by its low oral BA due to its low water solubility and high rate of first-pass metabolism. Administered as lipid-based nanosystems, significant increases in the oral relative BA was observed for isradipine [4.5-fold, (Kumar et al., 2018)], nisolpine [2.5-fold, (Dudhipala et al., 2018)], felodipine [3.2-fold, (He et al., 2020)], and cilnidipine [2.4-folds, (Diwan et al., 2020)]. These are very promising results taking into consideration that, when administered as conventional formulations, the oral BA of these four drugs is in the range of 5-20% (Wishart et al., 2018).

These previous examples illustrate the possibilities and advantages offered by lipid NPs for oral pharmacological therapy. Nonetheless, despite the abundance of PK and pharmacological "advantages," the underlying mechanisms are not yet fully understood. Regarding the higher oral BA, evidences suggest a combination of four possible effects:

(1) Drug protection against both chemical and enzymatic degradation. Encapsulation in a nano-sized lipid matrix may reduce or retard a drug pH-dependent hydrolytic degradation (Baek and Cho, 2017), as well as the drug inactivation by the gastrointestinal (GI) tract digestive enzymes, which may be crucial for the oral administration of biological drugs. It has been demonstrated, for example, that whereas free salmon calcitonin was almost completely degraded *in vitro* by pancreatin in 15 min, the drug encapsulated into SLN exhibited a much slower degradation kinetics, and was still detectable in the reaction media up to 12 h (Fan et al., 2014).

(2) Lipid effect on solubility improvement that allows higher effective doses. Shangguan et al. (2015) evaluated the BA of silymarin in Beagle dogs, comparing the administration as intact drug-loaded SLN/NLC and as a lipolysate produced by the enzymatic action of pancreatic lipase over the lipid NP. The lower BA obtained with the lipolysate was in agreement with the loss of drug in the formulation, since the micelles formed in the GI to facilitate the uptake of lipophilic compounds (known as "mixed micelles," and mainly composed by phospholipids, bile salts, and cholesterol, Yao et al., 2017) cannot keep all silymarin in suspension, and drug precipitation occurs. In other words, when the BA values are corrected by a factor that accounts for the true dose administered (i.e., amount of drug remaining in suspension), it may be concluded that the lipolysis pathway is the predominant mechanism underlying the enhanced oral BA of a drug formulated as lipid NPs, whereas the absorption of intact NPs only plays a minor role.

(3) Major retention in the GI tract. When a lipid-based NP reaches the GI tract, its hydrophobic surface tends to adhere to the mucus layer, whose superficial layers are quickly and continuously cleared as protection against particles and pathogens (Maisel et al., 2015). To minimize such effect, "mucus penetrating particles" (MPP) can be formulated. MPP have a smaller size than the mucus layer, and a hydrophilic, non-muco-adhesive surface (generally obtained with PEG cover) (Schneider et al., 2017). In spite of their lipid nature, these particles are capable of getting in contact with the GI epithelium, thus achieving prolonged absorption of the encapsulated drug (Yuan et al., 2013).

(4) Finally, in the same way that NPs protect the drug from degradation by enzymes present in GI lumen, they can also prevent/reduce the degradation by metabolic enzymes, as in the lopinavir example mentioned in the previous section (Ravi et al., 2014). Reduction in pre-systemic *in vivo* metabolism may occur due to less hepatic metabolism (e.g., NP accessing portal circulation as such, see the next section) and/or increased lymphatic uptake of the NPs by the lymphatic vessels in the gut (Baek and Cho, 2017; Bernier-Latmani and Petrova, 2017). Working with a chylomicron production blocking agent, Patel et al. found that the lymphatic uptake represented nearly 30% of the drug oral BA (asenapine maleate, administered as a SLN suspension) (Patel et al., 2019b).

Additionally, we can mention one more effect, common to all orally administrable pharmaceutical forms: the presence of excipients that may affect the rate and extent of drug absorption (FDA/CDER, 2015). Tensioactives and surfactants belong to this group and are usually present at high concentrations in SLN/NLC.

It is likely that the combination or synergistic action of all these effects is the cause of the large increase in oral BA associated with lipid nanovehicles and, in turn, of the increasing trend in the selection of this route of administration for SLN/NLC (see **Figure 4**). Furthermore, due to all the previously described effects, lipid-based NP have been examined for the oral delivery of peptide therapeutics, such as salmon calcitonin (Chen et al., 2013; Fan et al., 2014) and insulin (Hecq et al., 2016; Xu et al., 2018; Alsulays et al., 2019).
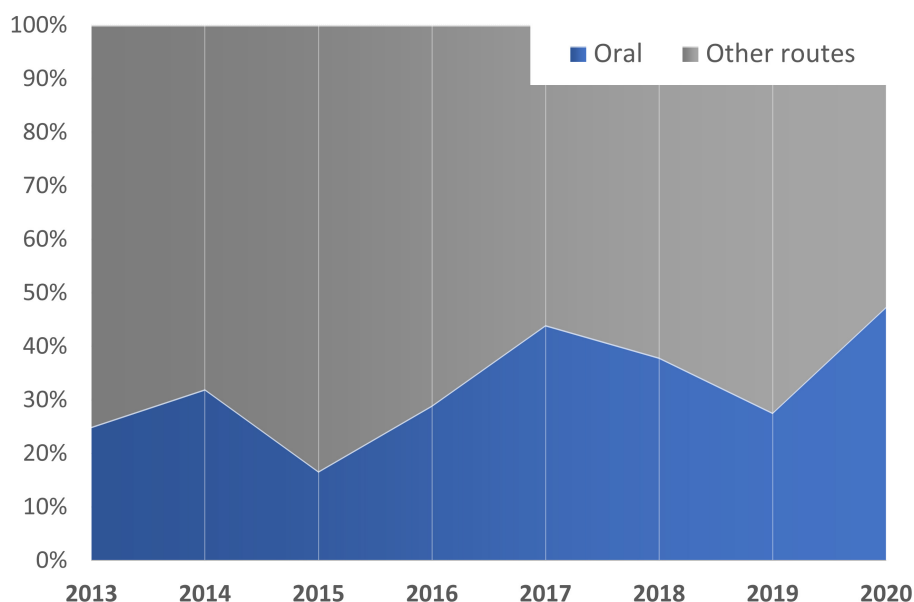
FIGURE 4 | Time-trend of the SLN/NLC intended for oral administration. Only publications with *in vivo* (PD and/or PK) studies are considered (211 of 371).

Percutaneous Route

According to the FDA classification, the percutaneous route of administration consists in the administration of drugs through the skin (FDA, 2017), and it comprises two groups of pharmaceutical products: those intended to exert a local action, at some level of the skin, and those that seek a systemic action of the drug, also known as transdermal formulations. Of the 30 reviewed publications corresponding to preparations to be administered onto the skin, only 3 of them (10%) seek systemic action of the drug: metformin for diabetes (Sharma et al., 2013), avanafil for erectile dysfunction (Kurakula et al., 2016) and piperine for rheumatic arthritis (Bhalekar et al., 2017), while the remaining 90% consists of formulations for local action.

The skin is composed of two main histological layers, the epidermis at the surface, and the dermis below. In turn, the outermost layer of the epidermis is the stratum corneum or the *horny layer*, which is the real barrier that prevents the entry of foreign (and potentially harmful) substances into the body. The stratum corneum is formed by cells named corneocytes or keratinized cells, surrounded by shallow valleys that comprise the intercellular regions filled with lipid multilamellae, rich in ceramides, fatty acids and cholesterol.

The ability of a drug to penetrate the skin depends on its physicochemical properties (mainly its size, molecular weight, pKa and partition coefficient) as well as the vehicle in which it is formulated. There are substances known as "permeation enhancers" which are capable of reversibly disorganizing the stratum corneum, facilitating the drug entry (e.g., fatty acids and alcohols with long carbon chains, surfactants, terpenes and fatty esters, Gupta et al., 2019). These excipients are commonly used in classic semi-solids preparations like emulsions, lotions and ointments, as well as of their more recent relatives' lipid-based nanoformulations. Hence, it is logical that these

formulations are, among other nanosystems, the first choice for percutaneous/transdermal applications.

The most studied nanoparticulate systems for percutaneous application are, by far, liposomes. And although it has been shown that the constituent lipids of liposomes are capable of reaching the deeper layers of the skin (i.e., the dermis), it still remains unclear if they can act as carriers, penetrating through the skin, or if they only act as penetration enhancers, changing the skin physical properties in a way that facilitates the (free) drug penetration through it (Peralta et al., 2018).

Nevertheless, pharmaceutical formulations of SLN/NLC have proven to be useful for percutaneous administration of drugs, to treat diseases or alterations at every level of the skin: the epidermis, like fungal infections (Vaghasiya et al., 2013), hyperpigmentation (Ghanbarzadeh et al., 2015), skin cancer (Taveira et al., 2014; Geetha et al., 2015; Khallaf et al., 2016; Tupal et al., 2016) and atopic dermatitis (Kang et al., 2019); the dermis, as in the case of anti-inflammatory drugs (Dasgupta et al., 2013; Gaur et al., 2013; Raj et al., 2016; Daneshmand et al., 2018; Shinde et al., 2019) and local anesthetics (You et al., 2017); both dermis and epidermis, like psoriasis (Sonawane et al., 2014) and infections by herpes virus (Gide et al., 2013; El-Assal, 2017) and; the appendices, like hair follicles (Hamishehkar et al., 2016).

DISPOSITION IN THE BODY AND PENETRATION TO THE CNS

Studying the distribution of these drug delivery nanosystems within the body is one of the main research challenges in the field. Although the advances that so far have been achieved in terms of the development of SLN/NLC are relevant, only a few works are dedicated to a detailed study of the fate of this type

of NPs once they enter the organism. This section is intended to describe the main mechanisms involved in the uptake, transport and distribution of NPs into the body, as well as how these structures face the natural barrier that protects the CNS.

Gastrointestinal Absorption of Lipid Nanoparticles

As mentioned in previous sections, SLN and NLC proved to be particularly promising for the enhancement of drugs oral BA, by avoiding their degradation in the GI tract, improving their solubility and dissolution rate, increasing their contact with the epithelium and/or minimizing their efflux by P-gp and other drug transporters. Either by one or by several of these mechanisms, orally administered lipid NPs can effectively increase the area under the plasmatic concentration curve of the encapsulated drug, as described by the curcumin examples. In the same manner, Wang and co-workers managed to improve the oral BA of [6]-shogaol, an alkylphenol extracted from ginger roots, of great interest for its antitumor, antioxidative and antirheumatic properties, as demonstrated by the greater AUC exhibited by the drug incorporated into SLN, but also by a significant decrease of serum uric acid, IL-1β and TNF-α levels with respect to free [6]-shogaol tests (Wang et al., 2018).

NPs constituents could have an effect on the intestinal absorption enhancement: lipids are able to increase the intestinal mucosa permeability (Talegaonkar and Bhattacharyya, 2019) and, although some controversy exists (Ball et al., 2018), modulation of the tight junctions (Beguin et al., 2013). On the other hand, tensioactives, surfactants and hydrophilic coatings like chitosan have also been proposed to enhance BA by the opening of tight junctions (Han et al., 2019; McCartney et al., 2019).

Overall, when it comes to the demonstration of the GI absorption of intact NPs, evidence is much scarcer. Regarding cellular uptake of the NPs, endocytosis is considered the predominant pathway (Wang et al., 2011; Patel et al., 2019b). There are two principal endocytosis mechanisms: pinocytosis and phagocytosis. Cellular uptake by macrophages (phagocytic cells) is reserved for those particles larger than 0.5-10 μm (Zhao et al., 2011). Pinocytosis, on the other hand, occurs in all types of cells and is responsible of the uptake of smaller particles (50 nm–5 μm). It may be further classified into clathrin-dependent (or clathrin-mediated endocytosis, CME) and clathrin-independent, the latter comprising caveolae-mediated and clathrin/caveolae-independent endocytosis, and macropinocytosis (also clathrin/caveolae independent, but for the internalization of larger particles, similar to phagocytosis) (Sahay et al., 2010).

This classification is based on the proteins (*clathrin* and *caveolin*) involved in the endocytic process, and thus it may overlap with other classifications based on different criteria, like *receptor mediated* or *adsorptive* endocytosis. For example, it was proposed that folate grafted NPs may be internalized by clathrin-mediated, clathrin/caveolae-independent (Sahay et al., 2010) and/or caveolae−mediated endocytosis (Wang et al., 2011). Rajpoot and Jain (2018, 2019) employed folic acid (FA) as targeting ligand of SLN containing oxaliplatin and irinotecan

for the treatment of colorectal cancer, finding a slightly higher uptake (and higher toxicity) of the FA-SLN compared with the non-targeted SLN in HT 29 cells.

Cellular uptake via the LDL receptor, on the other hand, occurs by CME (Sahay et al., 2010; Wang et al., 2011). This pathway has been explored for the active targeting of rosuvastatin loaded SLN (Beg et al., 2017). To mimic the outer layer of LDL particles, rosuvastatin-SLN were coated with phospholipids (phospholipon 90G and/or PEGylated DSPE), and the endocytosis process was studied in Caco-2 cells by using filipin and sucrose as specific blockers of caveolae and clathrin-mediated endocytosis, respectively. A significant reduction in the cellular uptake of the drug in the presence of sucrose was found, providing indirect evidence of the lipid NPs internalization via the LDL receptor by CME (Beg et al., 2017). CME was also the predominant pathway responsible for the internalization of stearic acid based-SLN in human epithelial cells (lung A549 and cervical HeLa cells) (Shah et al., 2016b).

It is worth mentioning, however, that the successful endocytosis of a NP does not guarantee its absorption: once in the intracellular space of an epithelial cell, the NP should be further exocytosed on the basolateral side to reach the capillary vessels, in a process known as transcytosis. A comprehensive work by Chai et al. (2014) showed that SLN (60-100 nm) with no targeting ligand were internalized mostly by caveolae and clathrin-mediated endocytosis in MDCK cells. Once inside the cells, lysosomes were the main destination of the endocytic vesicles, whereas the transcytosis to the basolateral side account for only about 2.5% of the total NPs (Chai et al., 2014). This result is in line with those of Hu et al. (2016), who concluded that orally administered SLN exhibit significant cellular uptake but fail to penetrate cell monolayers. The authors studied the *in vivo* distribution of SLN and their interaction with biomembranes by water-quenching fluorescence, and could not find evidence of penetration of integral nanocarriers (Hu et al., 2016).

In a follow-up article, however, the same authors found some evidence of intact uptake of the SLN from the GI lumen to the circulation, apparently through the lymphatic route, but representing only a minor contribution to the oral BA of a drug (Ma et al., 2017). Regarding the lymphatic uptake, lipid NPs may access the lymphatic system through the intestinal lipid transport system (O'Driscoll, 2002) as well as by *transcellular* passage, by the association with chylomicrons after the digestion of the lipid nanosystems, and by *specific passage* through the M-cells in the Peyer's patches (Salah et al., 2020). In the last case, NPs size is a relevant variable, since particles larger than 100 nm will be retained longer in the Peyer's patches, while smaller ones will be transported to the thoracic duct (Bummer, 2004). Surface charge is also a key feature that affects this process, with anionic particles being more rapidly absorbed by the lymphatic route (Yu et al., 2019).

Systemic Circulation and Protein Corona Formation

Due to their small size and, thus, their large surface area, NPs are characterized by a high free energy. Accordingly, the interaction

with different macromolecules, when they are in contact with biological fluids, will be favored. Once NPs have reached systemic circulation, another inconvenience is presented: a biological macromolecules-cover known as *protein corona* (PC) begins to form upon their surface.

This corona is composed of two layers formed in a time dependent manner. During a first stage, a loose layer named *soft corona* starts to settle. This corona is composed by low-affinity proteins with a high relative abundancy, which are in constant exchange with the biological medium and NPs surface, in a process known as "Vroman effect" (Vroman, 1962). Then, in a second stage, low-affinity proteins begin to be replaced by those with lower relative abundance, but with a higher surface affinity, staying close to it for a longer period. Is in this stage where the formation of the *hard corona* is evidenced (Baimanov et al., 2019). It follows that the "chemical identity" of the NP is not equal to its "biological identity:" the formation of the PC (both soft and hard) substantially changes the nanosystems properties, being able to impact in their size, shape, and final surface composition (Lima et al., 2020), turning them into a new biological identity.

Gessner et al. (2002) studied the influence of surface charge density on protein adsorption on polymeric NPs, concluding that the higher the surface charge density, the higher the amount of proteins adsorbed. The authors observed no qualitative change in the pattern of adsorbed proteins.

As expected in a complex biological process, the pattern of protein adsorption does not only depend on the protein capacity to access the particles surface, but also on the characteristics of the surface itself (Göppert and Müller, 2003). As it was previously described for polysorbate 80 coatings, the use of different Poloxamer in the formulation of SLN facilitates the adsorption of different proteins *in vitro*: the MW Poloxamer 184 and Poloxamer 235 showed a high ApoE absorption, which mediates the uptake through the BBB. Even more interesting, these lipid NPs showed a high adsorption of ApoA-IV (involved in the promotion of brain uptake) and a low adsorption of ApoC-II (responsible for the inhibition of receptor mediated binding and uptake of lipoproteins) (Goppert and Muller, 2005).

During the formation of the PC, the incorporation of proteins of the complement system also known as *opsonins* occur. The complement system is part of the innate immune system and facilitates the recognition of NPs by the mononuclear phagocytic system (MPS), which in turn leads to an increase of NPs clearance and a reduction of their systemic residence time.

A study by Fang et al. (2006) confirmed the dependency of phagocytosis by murine macrophages with the particle size of the NPs, as well as with the molecular weight of methoxy polyethylene glycol (MePEG) used for coating. The authors observed that those NPs coated with MePEG of the same molecular weight, showed a higher distribution half-life as the size decreased. On the other hand, the uptake by macrophages was decreased by increasing the coating molecular weight (Fang et al., 2006).

Previously, Müller et al. (1996a) had studied the dependence of the uptake by macrophages with hydrophilicity and steric hindrance given by different types of emulsifiers (e.g., poloxamine 908 and poloxamer 407), demonstrating that an increase in hydrophilicity and steric hindrance diminished the uptake by macrophages. Xiao et al. (2011) worked with different types of D-aspartic acids and D-lysines-derivatized telodendrimers which possessed different surface charges. Those dendrimers composed by D-aspartic acids (negatively charged) and the acetylated derivatized NPs (neutral charge) showed a lower macrophage uptake in comparison with the cationic D-lysines (positively charged) (Xiao et al., 2011).

To achieve distribution beyond the liver, NPs need to avoid rapid opsonization and clearance by the MPS (Müller et al., 1996a). A great deal of work has been devoted to developing the so-called stealth NPs, which are "invisible" to macrophages (Brigger et al., 2012; Rudhrabatla et al., 2019, 2020), due to the PEG chains on their surface (*PEGylated* NPs) (Hadjesfandiari, 2018). This coating prevents or delays the formation of the PC and, thus, NPs exhibit a prolonged half-life in the blood compartment (Pelaz et al., 2015). However, a number of limitations to the use of PEG have also been described, such as the production of anti-PEG antibodies or the impairment of cellular internalization by the stealth coating (Baimanov et al., 2019). Depending on the nature of the nanovehicle, different approaches have been explored to circumvent these limitations, e.g., stimuli-responsive PEG-derivatized nanocarriers (Fang et al., 2017).

Passage Through the Blood Brain Barrier (BBB)

The BBB is a semipermeable structure composed mainly of the microvasculature of the CNS. This barrier is formed by a continuous layer of endothelial cells integrated to a complex systems that regulates the bloodstream-to-CNS movement of molecules, ions and cells, also responsible for the homeostasis regulation (Ayloo and Gu, 2019). Unlike the peripheral endothelium, BBB endothelial cells present a high content of mitochondria, lack of fenestrations and pinocytic activity and, as a salient characteristic, particularly occlusive tight junctions formed by several transmembrane proteins (such as claudins, occludins, and junctional adhesion molecules or JAM, among others Stamatovic et al., 2008), that efficiently limit the paracellular diffusion pathway. Another characteristic of the BBB is the expression of efflux transporters of the ABC (ATP-binding cassette) superfamily, transmembrane proteins responsible for pumping xenobiotics or toxic substrates out of the intracellular space, avoiding their access to the CNS since they are localized almost exclusively at the luminal membrane of the endothelial cells (Pardridge, 2020). These transporters are one of the main causes of multi-drug resistance phenomena, which is why they are also known as multidrug resistance (MDR) proteins (the most representative one being P-gp). It has been proposed that encapsulating a drug into a NP may help to bypass these transporters (Cavaco et al., 2017; Sadegh Malvajerd et al., 2019).

The transport of substances through the BBB may occur by four main mechanisms (Xie et al., 2019): *paracellular diffusion,* reserved for small water soluble substances; *transcellular diffusion,* which is more relevant for molecules with an appreciable lipophilicity and a molecular weight smaller than 450 kDa; *carrier-facilitated diffusion and active transport,*

responsible for the passage of specific molecules like small peptides, sugars, monocarboxylic acids, amino acids, organic anions and cations, neurotransmitters and nucleosides; and *endocytosis*, this pathway has been reported for the passage of peptides and proteins through the BBB, such as insulin and the insulin-like growing factor (IGF-I and IGF-II) (Patel et al., 2013).

Although it has been suggested that NPs can enter the CNS by the paracellular pathway (through the transient opening of the tight junctions, as in the case of chitosan-coated NPs, Yu et al., 2013; Zhang et al., 2014), there is now evidence suggesting that the predominant mechanism is the NPs endocytosis. Once inside the endothelial cell, NPs can be exocytosed to the other side (*transcytocis* of the NP) or released in the intracellular space, promoting their access to the CNS (Saraiva et al., 2016).
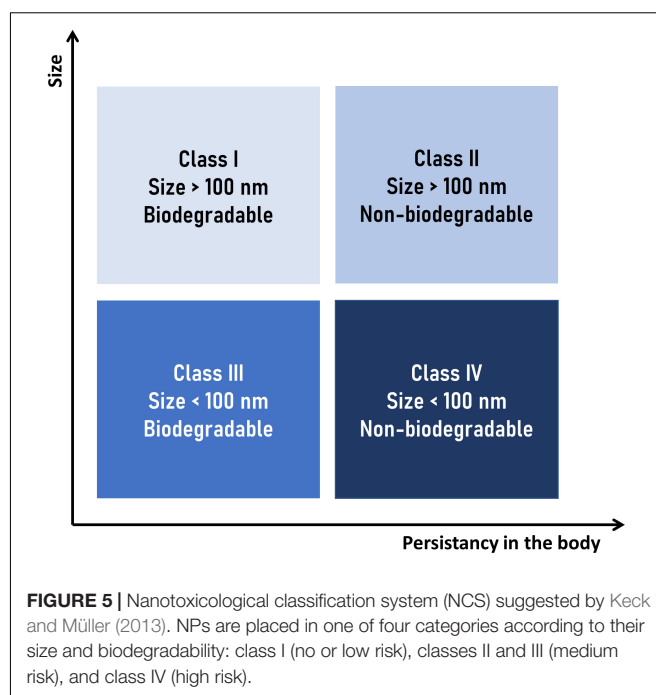
Since endocytosis of NPs by the BBB endothelial cells seems to be predominantly mediated by receptors, many efforts have been made with SLN surface functionalization to enhance their CNS availability (Ceña and Játiva, 2018; Kuo et al., 2019; Wang et al., 2019), as discussed in Section 2 for the functionalized angiopep-2 NPs to treat glioblastoma multiforme (Kadari et al., 2018).

As another example, functionalized ApoE NPs appear to be particularly promising in such way. ApoE possess high affinity receptors along the BBB, a characteristic that has been exploited for the delivery of drugs in functionalized nanosystems with this protein (Zensi et al., 2009). In a series of studies, Neves *et al.* investigated the cellular uptake of ApoE-grafted SLN by hCMEC/D3 cells, as a model of human BBB, and found that functionalized NPs were better internalized than non-functionalized ones, due to the specific recognition of the targeting ligand by the highly expressed LDL receptors (Neves et al., 2015, 2016, 2017). Moreover, by the use of specific inhibitors, CME was identified as the preferential endocytic pathway for ApoE-SLN (Neves et al., 2017).

CLEARANCE MECHANISMS AND TOXICOLOGICAL ASPECTS

Achieving nanocarriers with low or no toxicity for the organism and the environment is one of the biggest challenges in designing drug delivery nanosystems. Ideally, the drug carrier should be rapidly removed from the body after the drug has been released. Lipid-based NPs sizes are far over the renal filtration threshold (Yang et al., 2019), for what, once in the bloodstream, they have to be opsonized by serum proteins and subsequently uptaken by the MPS in specialized organs (i.e., liver, kidney, spleen, lungs, and lymph nodes) for their efficient elimination from the body (Di Ianni et al., 2017). Despite the fact that fenestrations in the spleen may filter out particles larger than 200 nm, particle deformability can allow large particles to squeeze through them and remain in the bloodstream (Park et al., 2017).

Considering the clearance mechanism described above, Keck and Müller (2013), a "nanotoxicological classification system" (NCS), as a rational approach to assess the potential risks of toxicity of a given nanocarrier. According to that system, a nanocarrier is placed in one of four categories according to their size and biodegradability (**Figure 5**):

FIGURE 5 | Nanotoxicological classification system (NCS) suggested by Keck and Müller (2013). NPs are placed in one of four categories according to their size and biodegradability: class I (no or low risk), classes II and III (medium risk), and class IV (high risk).

- Class I (no or low risk), for nanosystems of size above of 100 nm and made of biodegradable materials.
- Class II (medium risk), for nanosystems of size above 100 nm but made of non-biodegradable materials.
- Class III (medium risk), for nanosystems of size below 100 nm, made of biodegradable materials.
- Class IV (high risk), for nanosystems of size below 100 nm and made of non-biodegradable materials.

The size limit between classes of 100 nm was adopted considering the greater distribution in the organism of smaller particles (e.g., ease of access to the CNS), as well as the greater probability of non-specific endocytosis in off-target cells. However, when applying the NCS, it should be taken into consideration that larger particles can also be internalized by the cells through other mechanisms (Zhao et al., 2011; Danaei et al., 2018).

With regard to the biodegradability of the nanocarrier materials, SLN and NLC are generally considered as members of the NCS classes I or III, since they are composed of physiologically compatible lipids (fatty acids, glycerides or other fatty acid esters, sterols, sterol esters, waxes, etc.).

As stated before, a NP in the bloodstream will be taken up by the MPS. After the opsonization and phagocytosis has occurred, the resulting phagosome needs to "mature" to a phagolysosome [by a series of fusion and fission interactions with endosomes and lysosomes (Rosales and Uribe-Querol, 2017)]. The phagolysosome possesses a unique membrane composition to resist a very acidic and degradative environment, necessary to the final digestion of its content. Internalized non-biodegradable materials may however exert several cytotoxic effects, contributing to chronic inflammation and progressive tissue injury (Gordon, 2016; Azarnezhad et al., 2020).

It must be noted that toxicological outcomes are strongly dependent on the administration route: for instance, orally administered SLN/NLC can be eroded and degraded by bile salts and pancreatic lipase in the body (Müller et al., 1996b; Agrawal et al., 2014).

Although the previously described classification system may seem an excessively reductionist approach to the matter of nanotoxicology, it is a valuable tool in the current state of research of pharmaceutical nanovehicles. A huge number of different nanosystems are being proposed for drug delivery applications based on promising results in terms of their PK and/or PD performance, but for which the multiple aspects that could generate adverse events or toxicity in patients are still to be studied in detail.

One of the aspects not directly addressed by the NCS is the effect that the surface charge of the particles may exhibit on the toxicity or clearance mechanisms. In order to enhance cellular uptake, NPs are sometimes formulated with a positively charged surface, to facilitate electrostatic interaction with the negatively charged plasma membranes of cells, hence promoting internalization by non-selective, adsorptive mediated endocytosis (Ayloo and Gu, 2019). An example of this strategy is found in lipoplexes (a combination of negatively charged nucleic acids and positively charged lipids), which have demonstrated their ability to effectively deliver their load to target cells (Kowalski et al., 2019; Pardridge, 2020). Positively charged lipid NPs were also proposed for carrying nucleic acids (Kong et al., 2013; Fàbregas et al., 2014; Shi et al., 2014; Kotmakçı et al., 2017; Küçüktürkmen and Bozkır, 2018; González-Paredes et al., 2019). Despite these advantages, positively charged NPs have been associated with several toxic effects (Azarnezhad et al., 2020). Based on cell cultures experiments, some authors reported higher cytotoxicity values for cationic (vs. neutral and anionic) SLN (Karn-orachai et al., 2016), while others postulate that cell cultures are able to tolerate high concentrations of cationic SLN/NLC without appreciable toxicity (Doktorovová et al., 2016). These apparently inconsistent results may be explained by the fact that surface charge is not the only toxicity determinant of a NPs, and that other covariables (such as the chemical composition of the NP) may also be considered.

Nevertheless, caution should be taken when working with cationic SLN/NLC, as also some *in vivo* toxicity reports may be found. For example, Wu et al. (2018) demonstrated that SLN with different surface charges and PEG densities resulted toxic to platelets (and, to a lesser extent, to red blood cells), and that the toxic effects were dependent of the surface charge (the higher positive charge, the worst) and PEG densities (the lower, the worst).

TRANSLATION INTO THE CLINIC OF LIPID (BUT NOT SOLID) NANOPARTICLES

At the time of writing this review, a search was made on the website www.clinicaltrials.gov, finding 13 relevant results corresponding to the keywords "lipid" and "nanoparticles" (see **Table 1**). However, of those studies, only one comprise what can be regarded as *classical* SLN: oxiconazole-loaded stearic acid NPs, further included in a carbopol gel formulation for the topical treatment of topical tinea infections (Mahmoud et al., 2020).

TABLE 1 | Lipid Nanoparticle Drug Delivery Systems (LNDDS) on currently active clinical trials (terminated or withdrawn studies were excluded).

Track number	Status	Drug	Disease	Route of administration
siRNA therapy				
NCT01960348	Phase III	Patisiran (ALN-TTR02)	hTTR - mediated amyloidosis	IV infusion
NCT01858935	Phase I	ND-L02-s0201	Hepatic fibrosis	IV infusion
NCT02227459	Phase I	ND-L02-s0201	Hepatic fibrosis	IV infusion
NCT01437007	Phase I	TKM-080301	Primary liver carcinoma or metastatic liver cancer	Hepatic arterial infusion
mRNA therapy				
NCT04416126	Phase I	ARCT-810	OTC deficiency	IV infusion
NCT04442347	Phase I	ARCT-810	OTC deficiency	IV infusion
NCT03323398	Phase I Phase II	mRNA-2416	Solid tumors / Lymphoma / Ovarian Cancer	Intratumoural
NCT03739931	Phase I	mRNA-2752	Solid tumor malignancies / Lymphoma	Intratumoural
NCT04283461	Phase I	mRNA-1273	COVID-19	IM injection
Others				
NCT02971007	Phase II	CAMB	Vulvovaginal candidiasis	Oral
NCT02629419	Phase II	CAMB	Mucocutaneous candidiasis	Oral
NCT04148833	Phase II Phase III	Paclitaxel	Aortic and coronary atherosclerotic disease	IV injection
NCT03823040	Phase I	Oxiconazole	Tinea pedis / Tinea versicolor/Tinea circinate	SLNs loaded gel for topical application

CAMB, encochleated amphotericin B; HSP47, Heat Shock Protein; IM, intramuscular; IV, intravenous; OTC, ornithine transcarbamylase; PLK1, polo-like kinase-1; TTR, Transthyretin.

Two studies correspond to phase II trials of oral encochleated amphotericin B (CAMB). Cochleates are constituted by several layers of continuous lipid bilayers that self-assemble by spiral wrapping, resulting in relatively rigid cylindrical structures with the drug.

Among the remaining clinical trials retrieved, two are undergoing phase III: a cholesterol-rich, protein-free nanoemulsion of paclitaxel, that resemble low-density lipoproteins and can be IV administered for the treatment of atherosclerosis, and lipid NP with *patisiran* (ALN-TTR02), a siRNA to treat hereditary transthyretin (TTR) induced amyloidosis, made with an optimized ionizable cationic lipid, DLin-MC3-DMA (Kulkarni et al., 2018).

Short interfering RNAs (siRNAs) are 19-23 base pairs double stranded RNAs that are part of the family of small non-coding regulatory RNAs (sncRNA). In Fire et al. (1998) described the gene silencing regulation mechanism of siRNA in *Caenorhabditis elegans*, unveiling what later would become a major change in human therapy approaches. This suppression mechanism, named RNA interference (RNAi), is a normal mechanism of gene expression control involving regulation of mRNA translation and degradation via the binding of short strands of homologous RNA generated by the Dicer enzyme (Reynolds et al., 2004).

Therefore, siRNA presents as an appealing therapeutic tool to suppress gene expression, that can be used to silence aberrant endogenous genes (as in cancer diseases) or to knockdown genes that are essential to the proliferation of infectious organisms (Whitehead et al., 2009). However, in order to become a successful tool for human therapy, siRNA might be administered as an exogenous RNA product, thus representing a drug delivery challenge (McManus and Sharp, 2002). Despite the use of cationic lipids is the natural approach to encapsulate negatively charged biomolecules like nucleic acids, lipids with a *permanent* positive charge tend to form complexes with nucleic acid polymers with limited or no *in vivo* utility due to their size (*ca.* 1 μm of diameter), instability, positive surface charge, and toxic side effects (Cullis and Hope, 2017). Ionizable cationic lipids, on the other hand, allow achieving high loading efficiencies for RNA/DNA molecules in small (<100 nm) vesicular systems, with low surface charge (almost neutral) and less toxicity issues compared with cationic NPs, as discussed in the previous section.

In general, these lipids present an amine group with a pKa value less than 7, a characteristic that allows them to be positively charged at low pH values, thus achieving efficient encapsulation of negatively charged polymers at acidic pH, but also to exhibit a relatively neutral surface at physiological pH values (Kulkarni et al., 2018). As mentioned earlier, a recent research breakthrough on lipid NPs encapsulating siRNA was the 21 base pairs siRNA drug *patisiran* to treat TTR amyloidosis, a multisystemic disease causes by misfolded TTR, that affects nerves, heart, and the gastrointestinal tract (Adams et al., 2017). *Patisiran* lipid NPs reduced amyloidogenic protein expression of the mutated TTR: previous phase II results (NCT01617967) showed an 80% decrease on TTR levels in serum. The efficacy results of patisiran constitute a milestone in the field and led to the approval of the first targeted RNA-lipid NP- based therapy in August Pastor et al. (2018).
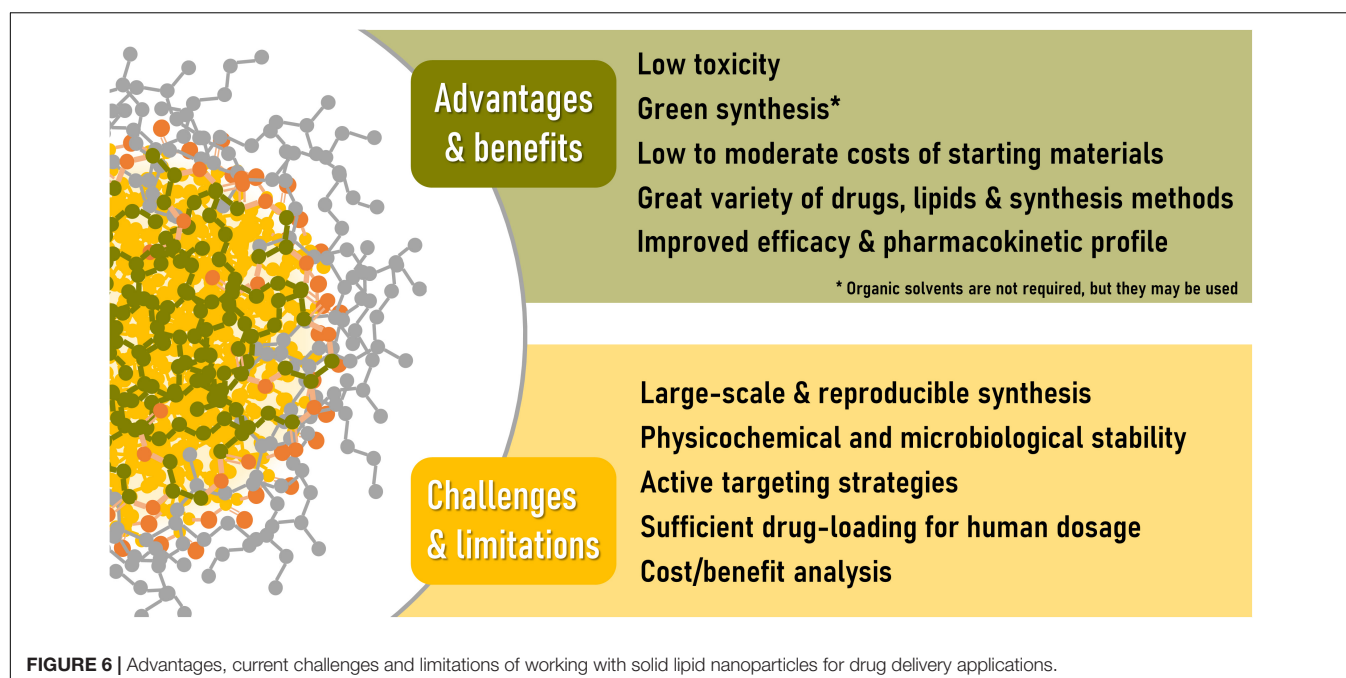
Another kind of RNA therapy is not directed to *silence* a given gene but rather to *express* its product, a therapeutic protein. Dimitriadis was the first to achieve expression of rabbit globin on mouse spleen lymphocytes through the delivery of rabbit reticulocyte 9S mRNA through liposomes (Dimitriadis, 1978). This RNA therapy involves much larger mRNA molecules than siRNA (1–15 kb, 300-5000 kDA vs. 14 kDa). Therapeutic approaches may include immunotherapy through mRNA of antibodies, protein expression to supply the product of a defective or missing gene, and *cellular reprogramming* through growth or transcription factors that modulate cellular metabolism. These kinds of treatment can be considered improvements over direct protein administration which face numerous problems like enzyme degradation or misfolding (Kowalski et al., 2019).

The phase I clinical trial of the biological product named mRNA-2416, which encodes for OX40L, the ligand of the T cells co-stimulator tumor necrosis factor receptor superfamily member 4 (TNFRSF4; OX40). According to the NCI drug dictionary, expressed on the cancer cells membrane, OX40L binds to its receptor on T cells to activate a signaling pathway that leads to an increased cytokine production, thus inducing proliferation of lymphocytes and subsequent death of surrounding cancer cells. As in the siRNA systems, this mRNA is formulated in an ionizable lipid-based NP for intratumoural injection to patients with relapsed/refractory solid tumor malignancies or lymphoma.

Another clinical trial (NCT03739931) on lipid nanoparticles for mRNA delivery to solid tumor malignancies or lymphoma is currently recruiting patients. In this case, NPs are used for the intratumoral administration of mRNA-2752, that encodes OX40L, IL-23 and IL-36G. The co-administration of interleukins is thought to potentiate the anticancer effect by activating an inflammatory response at the tumor site (Bauer et al., 2019).

In June 2020, started two phase I clinical trials of ARCT-810, a mRNA therapy for Ornithine Transcarbamylase (OTC) deficiency, a genetic disorder produced by a mutation on the X chromosome. OTC enzyme is involved in the nitrogen metabolism, and the lack of this protein results in high blood ammonia levels that might lead to seizure and coma state in untreated patients. The current treatment is a low protein diet and ammonia scavenging medication, with future insights on liver transplantation (Peng et al., 2020). ARCT-810 is formulated in a novel pH-responsive lipid delivery system named LUNAR®, that aims at superseding the lack of native OTC providing a complete copy of its mRNA, thus restoring enzyme levels to establish a regular urea cycle. Preclinical data on a murine model showed full expression of the protein (Perez-Garcia et al., 2019).

In view of the current situation regarding the SARS-CoV-2 pandemic scenario, a recent clinical study respecting a mRNA-based vaccine has been initiated. The vaccine consists of a lipid nanoparticle encapsulating mRNA-1273 which encodes for the full length prefusion stabilized spike protein of the virus (SARS-CoV-2 spike glycoprotein). After intramuscular administration, mRNA-1273 translates in the myocytes' cytoplasm. Spike protein is released from the cell and captured by macrophages, dendritic cells, and other immune cells initiating the immune response (Wang et al., 2020).

FIGURE 6 | Advantages, current challenges and limitations of working with solid lipid nanoparticles for drug delivery applications.

Leaving aside the CAMB and Oxiconazole formulations, the described nanovehicles share several common characteristics. They are non-viral delivery systems derived from classic liposomes, where the introduction of (permanent or transient) positively charged lipids that have strong electrostatic associations with RNA polymers provides larger payloads of this biomolecules (Cullis and Hope, 2017). Furthermore, most of them are intended for parenteral administration, with the liver as target organ. The fact that siRNA therapy is confined to the liver is a consequence of the tendency of these smaller and more homogeneous analogs of lipoplexes to accumulate in the liver (Wittrup and Lieberman, 2015; Kulkarni et al., 2018).

CURRENT CHALLENGES AND LIMITATIONS OF SOLID LIPID NANOPARTICLES

The information presented in the previous section reveals that, aside from cosmetic/dermatological applications (Müller et al., 2014), there are currently no *classical* SLN/NLCs in clinical evaluation stages, so their early entry into the market would not be expected. Liposomes that have entered the market in recent years are the result of more than 50 years of research. Similarly, we could think that there are still years to come before SLN/NLC enter the pharmaceutical market. A proof that they are still in their initial stages of research can be seen in the publications reviewed here, a large percentage of which are technological (and not disease) focused research, and usually lacking of a rationale cost/benefit analysis, a characteristic of the initial stages of any research.

A great number of SLN/NLC reports are based on experimental drugs with no approved therapeutic indications,

like curcumin, rhein or quercetin, while many others encapsulate pharmaceutical ingredients for which formulations with good therapeutic performance are currently available with low associated costs, such as famotidine, carvedilol, metformin, ibuprofen, dexamethasone, aliconazole, and many others. But it is not all bad news. In the case of RNA or DNA therapies, the use of nanovehicles results essential, since parenterally administered "naked" nucleic acids fail to reach therapeutic levels in target cells. They are rapidly degraded in biological fluids (and excreted by the kidneys) and, if they get to the target tissue, cannot penetrate into the cells (Cullis and Hope, 2017). Therefore, whatever the associated cost, it is compensated by the possibility of having this type of therapies in the market.

Taken altogether, current results on pharmacological application of SLN/NLC show good perspectives. They have proven to be safe and versatile drug delivery systems capable of improving the efficacy and pharmacokinetic profile of the encapsulated drugs and, as discussed in the previous sections, many are the therapeutic fields that can be benefited from the use of these nanocarriers. Large-scale manufacturing processes, sterilization, tailoring strategies and stability issues are some of the challenges that need to be overcome before lipid nanoparticles may become commercially available products, with approved therapeutic indications (**Figure 6**).

CONCLUSION AND FINAL REMARKS

In the last decade, SLNs and nanostructured lipid carriers have attracted much attention as potential drug delivery (nano)systems. Their major advantage is possibly the use of biocompatible, environmental-friendly constituents and preparation methods. Based on their size and biodegradable

nature, most of the nanocarriers in this category fall within the low risk class (class I) from the nanotoxicological classification system suggested by Keck and Müller. It should be noted, though, that careful clinical and environmental safety assessment should be performed before advancing these systems to massive production and commercialization. Development of standardized procedures to assess potential risks of exposure to nanomaterials are urgently needed, as well as the correspondent regulatory framework.

As for other nanosized drug delivery systems, cancer therapy is the most frequent area of research where SLNs are applied, which may reflect both the vast levels of funding in the area but also the suitability of nanocarriers for the delivery of antineoplastic agents, mainly due to the passive and active targeting posed by cancerous cells and tissues. Nevertheless, there are many therapeutic fields that can benefit from the application of lipid NPs, as discussed for the case of antibiotics and CNS drugs.

Given that the oral administration route is the most convenient and accepted one for conventional medications, the fact that nanocarriers (including SLNs) administered through the oral route are not absorbed extensively, it may seem a daunting scenario for the advancement of this technology. However, this may not be true for the particular case of lipid NPs, since they have demonstrated their ability to increase the BA of drugs administered orally, a critical point when it comes to (the increasingly numerous) drugs with very low solubility in water.

Unfortunately, more time and financial resources are needed for SLN/NLC to prove its therapeutic value in real scenarios. For now, the scarcity of SLNs that have reached clinical trials indicates that at least some years will go by before these technologies land to the pharmaceutical market.

AUTHOR CONTRIBUTIONS

MR conceived the structure of the manuscript and the search criteria and completed, revised, and approved the manuscript. SM performed the bibliographic search and generated the database. SM and GM analyzed the database and wrote parts of the manuscript. All authors contributed to the article and approved the submitted version.

FUNDING

REFERENCES

Abdel Hady, M., Sayed, O. M., and Akl, M. A. (2020). Brain uptake and accumulation of new levofloxacin-doxycycline combination through the use of solid lipid nanoparticles: formulation; Optimization and *in-vivo* evaluation. *Colloids Surf. B Biointerfaces* 193:111076. doi: 10.1016/j.colsurfb.2020.111076

Abd-Rabou, A. A., Bharali, D. J., and Mousa, S. A. (2018). Taribavirin and 5-Fluorouracil-Loaded Pegylated-Lipid Nanoparticle Synthesis, p38 Docking, and Antiproliferative Effects on MCF-7 Breast Cancer. *Pharm. Res.* 35:76. doi: 10.1007/s11095-017-2283-3

Adams, D., Suhr, O. B., Dyck, P. J., Litchy, W. J., Leahy, R. G., Chen, J., et al. (2017). Trial design and rationale for APOLLO, a Phase 3, placebo-controlled study of patisiran in patients with hereditary ATTR amyloidosis with polyneuropathy. *BMC Neurol.* 17:181. doi: 10.1186/s12883-017-0948-5

Agrawal, U., Sharma, R., Gupta, M., and Vyas, S. P. (2014). Is nanotechnology a boon for oral drug delivery? *Drug Discov. Today* 19, 1530–1546. doi: 10.1016/J.DRUDIS.2014.04.011

Ahmad, I., Pandit, J., Sultana, Y., Mishra, A. K., Hazari, P. P., and Aqil, M. (2019). Optimization by design of etoposide loaded solid lipid nanoparticles for ocular delivery: characterization, pharmacokinetic and deposition study. *Mater. Sci. Eng. C Mater. Biol. Appl.* 100, 959–970. doi: 10.1016/j.msec.2019.03.060

Ahmadnia, S., Moazeni, M., Mohammadi-Samani, S., and Oryan, A. (2013). *In vivo* evaluation of the efficacy of albendazole sulfoxide and albendazole sulfoxide loaded solid lipid nanoparticles against hydatid cyst. *Exp. Parasitol.* 135, 314–319. doi: 10.1016/j.exppara.2013.07.017

Aljaeid, B. M., and Hosny, K. M. (2016). Miconazole-loaded solid lipid nanoparticles: formulation and evaluation of a novel formula with high bioavailability and antifungal activity. *Int. J. Nanomed.* 11, 441–447. doi: 10.2147/IJN.S100625

Alsulays, B. B., Anwer, M. K., Soliman, G. A., Alshehri, S. M., and Khafagy, E.-S. (2019). Impact of penetratin stereochemistry on the oral bioavailability of insulin-loaded solid lipid nanoparticles. *Int. J. Nanomed.* 14, 9127–9138. doi: 10.2147/IJN.S225086

Amasya, G., Aksu, B., Badilli, U., Onay-Besikci, A., and Tarimci, N. (2019). QbD guided early pharmaceutical development study: Production of lipid nanoparticles by high pressure homogenization for skin cancer treatment. *Int. J. Pharm.* 563, 110–121. doi: 10.1016/j.ijpharm.2019.03.056

Anand, P., Kunnumakkara, A. B., Newman, R. A., and Aggarwal, B. B. (2007). Bioavailability of curcumin: problems and promises. *Mol. Pharm.* 4, 807–818. doi: 10.1021/mp700113r

Ayloo, S., and Gu, C. (2019). Transcytosis at the blood-brain barrier. *Curr. Opin. Neurobiol.* 57, 32–38. doi: 10.1016/j.conb.2018.12.014

Azarnezhad, A., Samadian, H., Jaymand, M., Sobhani, M., and Ahmadi, A. (2020). Toxicological profile of lipid-based nanostructures: are they considered as completely safe nanocarriers? *Crit. Rev. Toxicol.* 50, 148–176. doi: 10.1080/10408444.2020.1719974

Baek, J.-S., and Cho, C.-W. (2017). Surface modification of solid lipid nanoparticles for oral delivery of curcumin: improvement of bioavailability through enhanced cellular uptake, and lymphatic uptake. *Eur. J. Pharm. Biopharm.* 117, 132–140. doi: 10.1016/j.ejpb.2017.04.013

Baimanov, D., Cai, R., and Chen, C. (2019). Understanding the chemical nature of nanoparticle-protein interactions. *Bioconjug. Chem.* 30, 1923–1937. doi: 10.1021/acs.bioconjchem.9b00348

Ball, R. L., Bajaj, P., and Whitehead, K. A. (2018). Oral delivery of siRNA lipid nanoparticles: fate in the GI tract. *Sci. Rep.* 8:2178. doi: 10.1038/s41598-018-20632-6

Banerjee, S., Roy, S., Bhaumik, K. N., and Pillai, J. (2020). Mechanisms of the effectiveness of lipid nanoparticle formulations loaded with anti-tubercular drugs combinations toward overcoming drug bioavailability in tuberculosis. *J. Drug Target.* 28, 55–69. doi: 10.1080/1061186X.2019.1613409

Bauer, T., Patel, M., Jimeno, A., Wang, D., McDermott, J., Zacharek, S., et al. (2019). Abstract CT210: A Phase I, open-label, multicenter, dose escalation study of mRNA-2752, a lipid nanoparticle encapsulating mRNAs encoding human OX40L, IL-23, and IL-36γ, for intratumoral injection alone and in combination with immune checkpoint blockade. *Cancer Res.* 79:CT210. doi: 10.1158/1538-7445.am2019-ct210

Beg, S., Jain, S., Kushwah, V., Bhatti, G. K., Sandhu, P. S., Katare, O., et al. (2017). Novel surface-engineered solid lipid nanoparticles of rosuvastatin calcium for low-density lipoprotein-receptor targeting: a quality by design-driven perspective. *Nanomedicine* 12, 333–356. doi: 10.2217/nnm-2016-0336

Beguin, P., Errachid, A., Larondelle, Y., and Schneider, Y.-J. (2013). Effect of polyunsaturated fatty acids on tight junctions in a model of the human intestinal epithelium under normal and inflammatory conditions. *Food Funct.* 4, 923–931. doi: 10.1039/c3fo60036j

Benet, L. Z. (2013). The role of BCS (biopharmaceutics classification system) and BDDCS (biopharmaceutics drug disposition classification system) in drug development. *J. Pharm. Sci.* 102, 34–42. doi: 10.1002/jps.23359

Bernier-Latmani, J., and Petrova, T. V. (2017). Intestinal lymphatic vasculature: structure, mechanisms and functions. *Nat. Rev. Gastroenterol. Hepatol.* 14, 510–526. doi: 10.1038/nrgastro.2017.79

Bhalekar, M. R., Madgulkar, A. R., Desale, P. S., and Marium, G. (2017). Formulation of piperine solid lipid nanoparticles (SLN) for treatment of rheumatoid arthritis. *Drug Dev. Ind. Pharm.* 43, 1003–1010. doi: 10.1080/03639045.2017.1291666

Bjö, M., Thurecht, K. J., Michael, M., Scott, A. M., and Caruso, F. (2017). Bridging bio-nano science and cancer nanomedicine. *ACS Nano* 11, 9594–9613. doi: 10.1021/acsnano.7b04855

Brigger, I., Dubernet, C., and Couvreur, P. (2012). Nanoparticles in cancer therapy and diagnosis. *Adv. Drug Deliv. Rev.* 64, 24–36. doi: 10.1016/j.addr.2012.09.006

Bummer, P. M. (2004). Physical chemical considerations of lipid-based oral drug delivery–solid lipid nanoparticles. *Crit. Rev. Ther. Drug Carrier Syst.* 21, 1–20. doi: 10.1002/chin.200502271

Cacicedo, M. L., Ruiz, M. C., Scioli-Montoto, S., Ruiz, M. E., Fernández, M. A., Torres-Sanchez, R. M., et al. (2019). Lipid nanoparticles-Metvan: revealing a novel way to deliver a vanadium compound to bone cancer cells. *New J. Chem.* 43, 17726–17734. doi: 10.1039/c9nj01634a

Cavaco, M. C., Pereira, C., Kreutzer, B., Gouveia, L. F., Silva-Lima, B., Brito, A. M., et al. (2017). Evading P-glycoprotein mediated-efflux chemoresistance using Solid Lipid Nanoparticles. *Eur. J. Pharm. Biopharm.* 110, 76–84. doi: 10.1016/J.EJPB.2016.10.024

Ceña, V., and Játiva, P. (2018). Nanoparticle crossing of blood–brain barrier: a road to new therapeutic approaches to central nervous system diseases. *Nanomedicine* 13, 1513–1516. doi: 10.2217/nnm-2018-0139

Chai, G.-H., Hu, F.-Q., Sun, J., Du, Y.-Z., You, J., and Yuan, H. (2014). Transport pathways of solid lipid nanoparticles across Madin–Darby canine kidney epithelial cell monolayer. *Mol. Pharm.* 11, 3716–3726. doi: 10.1021/mp5004674

Chaves, L. L., Lima, S., Vieira, A. C. C., Ferreira, D., Sarmento, B., and Reis, S. (2018). Overcoming clofazimine intrinsic toxicity: statistical modelling and characterization of solid lipid nanoparticles. *J. R. Soc. Interface* 15:20170932. doi: 10.1098/rsif.2017.0932

Chen, C., Fan, T., Jin, Y., Zhou, Z., Yang, Y., Zhu, X., et al. (2013). Orally delivered salmon calcitonin-loaded solid lipid nanoparticles prepared by micelle-double emulsion method via the combined use of different solid lipids. *Nanomedicine* 8, 1085–1100. doi: 10.2217/nnm.12.141

Cheng, X., and Lee, R. J. (2016). The role of helper lipids in lipid nanoparticles (LNPs) designed for oligonucleotide delivery. *Adv. Drug Deliv. Rev.* 99(Pt A), 129–137. doi: 10.1016/J.ADDR.2016.01.022

Chetoni, P., Burgalassi, S., Monti, D., Tampucci, S., Tullio, V., Cuffini, A. M., et al. (2016). Solid lipid nanoparticles as promising tool for intraocular tobramycin delivery: pharmacokinetic studies on rabbits. *Eur. J. Pharm. Biopharm.* 109, 214–223. doi: 10.1016/j.ejpb.2016.10.006

Chirio, D., Peira, E., Dianzani, C., Muntoni, E., Gigliotti, C. L., Ferrara, B., et al. (2019). Development of solid lipid nanoparticles by cold dilution of microemulsions: curcumin loading, preliminary *in vitro* studies, and biodistribution. *Nanomaterials* 9:230. doi: 10.3390/nano9020230

Christaki, E., Marcou, M., and Tofarides, A. (2020). Antimicrobial resistance in bacteria: mechanisms, evolution, and persistence. *J. Mol. Evol.* 88, 26–40. doi: 10.1007/s00239-019-09914-3

Costa, A., Sarmento, B., and Seabra, V. (2018). Mannose-functionalized solid lipid nanoparticles are effective in targeting alveolar macrophages. *Eur. J. Pharm. Sci.* 114, 103–113. doi: 10.1016/j.ejps.2017.12.006

Cullis, P. R., and Hope, M. J. (2017). Lipid nanoparticle systems for enabling gene therapies. *Mol. Ther.* 25, 1467–1475. doi: 10.1016/J.YMTHE.2017.03.013

Danaei, M., Dehghankhold, M., Ataei, S., Hasanzadeh Davarani, F., Javanmard, R., Dokhani, A., et al. (2018). Impact of particle size and polydispersity index on the clinical applications of lipidic nanocarrier systems. *Pharmaceutics* 10:57. doi: 10.3390/pharmaceutics10020057

Daneshmand, S., Jaafari, M. R., Movaffagh, J., Malaekeh-Nikouei, B., Iranshahi, M., Seyedian Moghaddam, A., et al. (2018). Preparation, characterization, and optimization of auraptene-loaded solid lipid nanoparticles as a natural anti-inflammatory agent: *in vivo* and *in vitro* evaluations. *Colloids Surf. B Biointerfaces* 164, 332–339. doi: 10.1016/j.colsurfb.2018.01.054

Dara, T., Vatanara, A., Nabi Meybodi, M., Vakilinezhad, M. A., Malvajerd, S. S., Vakhshiteh, F., et al. (2019). Erythropoietin-loaded solid lipid nanoparticles: preparation, optimization, and *in vivo* evaluation. *Colloids Surf. B Biointerfaces* 178, 307–316. doi: 10.1016/j.colsurfb.2019.01.027

Dasgupta, S., Ghosh, S. K., Ray, S., and Mazumder, B. (2013). Solid lipid nanoparticles (SLNs) gels for topical delivery of aceclofenac *in vitro* and *in vivo* evaluation. *Curr. Drug Deliv.* 10, 656–666. doi: 10.2174/15672018100631125150023

de Blaey, C. J., and Polderman, J. (1980). "Rationales in the design of rectal and vaginal delivery forms of drugs," in *Medicinal Chemistry*, ed. E. J. Ariens (London: Academic Press), 237. doi: 10.1016/B978-0-12-060309-1.50011-2

de Jesus, M. B., Radaic, A., Zuhorn, I. S., and de Paula, E. (2013). Microemulsion extrusion technique: a new method to produce lipid nanoparticles. *J. Nanopart. Res.* 15:1960. doi: 10.1007/s11051-013-1960-3

Di, L., and Kerns, E. H. (2016). *Drug-Like Properties.* Amsterdam: Elsevier. doi: 10.1016/B978-0-12-801076-1.00023-X

Di Ianni, M. E., Islan, G. A., Chain, C. Y., Castro, G. R., Talevi, A., and Vela, M. E. (2017). Interaction of solid lipid nanoparticles and specific proteins of the Corona studied by surface plasmon resonance. *J. Nanomater.* 2017:6509184. doi: 10.1155/2017/6509184

Dimitriadis, G. J. (1978). Translation of rabbit globin mRNA introduced by liposomes into mouse lymphocytes. *Nature* 274, 923–924. doi: 10.1038/274923a0

Diwan, R., Ravi, P. R., Pathare, N. S., and Aggarwal, V. (2020). Pharmacodynamic, pharmacokinetic and physical characterization of cilnidipine loaded solid lipid nanoparticles for oral delivery optimized using the principles of design of experiments. *Colloids Surf. B Biointerfaces* 193:111073. doi: 10.1016/j.colsurfb.2020.111073

Doktorovová, S., Kovačević, A. B., Garcia, M. L., and Souto, E. B. (2016). Preclinical safety of solid lipid nanoparticles and nanostructured lipid carriers: current evidence from *in vitro* and *in vivo* evaluation. *Eur. J. Pharm. Biopharm.* 108, 235–252. doi: 10.1016/j.ejpb.2016.08.001

Doktorovova, S., Souto, E. B., and Silva, A. M. (2018). Hansen solubility parameters (HSP) for prescreening formulation of solid lipid nanoparticles (SLN): *in vitro* testing of curcumin-loaded SLN in MCF-7 and BT-474 cell lines. *Pharm. Dev. Technol.* 23, 96–105. doi: 10.1080/10837450.2017.1384491

Dudhipala, N., and Janga, K. Y. (2017). Lipid nanoparticles of zaleplon for improved oral delivery by Box–Behnken design: optimization, *in vitro* and *in vivo* evaluation. *Drug Dev. Ind. Pharm.* 43, 1205–1214. doi: 10.1080/03639045.2017.1304957

Dudhipala, N., Janga, K. Y., and Gorre, T. (2018). Comparative study of nisoldipine-loaded nanostructured lipid carriers and solid lipid nanoparticles for oral delivery: preparation, characterization, permeation and pharmacokinetic evaluation. *Artif. Cells Nanomed. Biotechnol.* 46, 616–625. doi: 10.1080/21691401.2018.1465068

El-Assal, M. I. A. (2017). Acyclovir loaded solid lipid nanoparticle based cream: a novel drug delivery system. *Int. J. Drug Deliv. Technol.* 7, 52–62. doi: 10.25258/ijddt.v7i1.8917

Fàbregas, A., Sánchez-Hernández, N., Ticó, J. R., García-Montoya, E., Pérez-Lozano, P., Suñé-Negre, J. M., et al. (2014). A new optimized formulation of cationic solid lipid nanoparticles intended for gene delivery: development, characterization and DNA binding efficiency of TCERG1 expression plasmid. *Int. J. Pharm.* 473, 270–279. doi: 10.1016/j.ijpharm.2014.06.022

Fan, T., Chen, C., Guo, H., Xu, J., Zhang, J., Zhu, X., et al. (2014). Design and evaluation of solid lipid nanoparticles modified with peptide ligand for oral delivery of protein drugs. *Eur. J. Pharm. Biopharm.* 88, 518–528. doi: 10.1016/j.ejpb.2014.06.011

Fang, C., Shi, B., Pei, Y.-Y., Hong, M.-H., Wu, J., and Chen, H.-Z. (2006). *In vivo* tumor targeting of tumor necrosis factor-α-loaded stealth nanoparticles: effect of MePEG molecular weight and particle size. *Eur. J. Pharm. Sci.* 27, 27–36. doi: 10.1016/j.ejps.2005.08.002

Fang, Y., Xue, J., Gao, S., Lu, A., Yang, D., Jiang, H., et al. (2017). Cleavable PEGylation: a strategy for overcoming the "PEG dilemma" in efficient drug delivery. *Drug Deliv.* 24, 22–32. doi: 10.1080/10717544.2017.1388451

FDA (2017). *Route of Administration*. Available at: https://www.fda.gov/drugs/developmentapprovalprocess/formssubmissionrequirements/electronicsubmissions/datastandardsmanualmonographs/ucm071667.htm (accessed August 15, 2020).

FDA/CDER (2015). *Guidance for Industry: Waiver of In Vivo Bioavailability and Bioequivalence Studies for Immediate-Release Solid Oral Dosage Forms Based on a BCS*. Available at: http://www.fda.gov/downloads/Drugs/GuidanceComplianceRegulatoryInformation/Guidances/UCM456594.pdf.3 (accessed December 3, 2015).

Feeney, O. M., Crum, M. F., McEvoy, C. L., Trevaskis, N. L., Williams, H. D., Pouton, C. W., et al. (2016). 50 years of oral lipid-based formulations: provenance, progress and future perspectives. *Adv. Drug Deliv. Rev.* 101, 167–194. doi: 10.1016/J.ADDR.2016.04.007

Feng, H., Zhu, Y., Fu, Z., and Li, D. (2017). Preparation, characterization, and in vivo study of rhein solid lipid nanoparticles for oral delivery. *Chem. Biol. Drug Des.* 90, 867–872. doi: 10.1111/cbdd.13007

Fire, A., Xu, S., Montgomery, M. K., Kostas, S. A., Driver, S. E., and Mello, C. C. (1998). Potent and specific genetic interference by double-stranded RNA in *Caenorhabditis elegans*. *Nature* 391, 806–811. doi: 10.1038/35888

Gaspar, D. P., Faria, V., Gonçalves, L. M. D., Taboada, P., Remuñán-López, C., and Almeida, A. J. (2016). Rifabutin-loaded solid lipid nanoparticles for inhaled antitubercular therapy: physicochemical and *in vitro* studies. *Int. J. Pharm.* 497, 199–209. doi: 10.1016/j.ijpharm.2015.11.050

Gaspar, D. P., Gaspar, M. M., Eleutério, C. V., Grenha, A., Blanco, M., Gonçalves, L. M. D., et al. (2017). Microencapsulated solid lipid nanoparticles as a hybrid platform for pulmonary antibiotic delivery. *Mol. Pharm.* 14, 2977–2990. doi: 10.1021/acs.molpharmaceut.7b00169

Gaur, P. K., Mishra, S., Bajpai, M., and Mishra, A. (2014). Enhanced oral bioavailability of Efavirenz by solid lipid nanoparticles: *in vitro* drug release and pharmacokinetics studies. *Biomed Res. Int.* 2014:363404. doi: 10.1155/2014/363404

Gaur, P. K., Mishra, S., and Purohit, S. (2013). Solid lipid nanoparticles of guggul lipid as drug carrier for transdermal drug delivery. *Biomed Res. Int.* 2013:750690. doi: 10.1155/2013/750690

Geetha, T., Kapila, M., Prakash, O., Deol, P. K., Kakkar, V., and Kaur, I. P. (2015). Sesamol-loaded solid lipid nanoparticles for treatment of skin cancer. *J. Drug Target.* 23, 159–169. doi: 10.3109/1061186X.2014.965717

Gessner, A., Lieske, A., Paulke, B. R., and Müller, R. H. (2002). Influence of surface charge density on protein adsorption on polymeric nanoparticles: analysis by two-dimensional electrophoresis. *Eur. J. Pharm. Biopharm.* 54, 165–170. doi: 10.1016/S0939-6411(02)00081-4

Geszke-Moritz, M., and Moritz, M. (2016). Solid lipid nanoparticles as attractive drug vehicles: composition, properties and therapeutic strategies. *Mater. Sci. Eng. C Mater. Biol. Appl.* 68, 982–994. doi: 10.1016/J.MSEC.2016.05.119

Ghaderkhani, J., Yousefimashouf, R., Arabestani, M., Roshanaei, G., Asl, S. S., and Abbasalipourkabir, R. (2019). Improved antibacterial function of Rifampicin-loaded solid lipid nanoparticles on *Brucella abortus*. *Artif. Cells Nanomed. Biotechnol.* 47, 1181–1193. doi: 10.1080/21691401.2019.1593858

Ghanbarzadeh, S., Hariri, R., Kouhsoltani, M., Shokri, J., Javadzadeh, Y., and Hamishehkar, H. (2015). Enhanced stability and dermal delivery of hydroquinone using solid lipid nanoparticles. *Colloids Surf. B Biointerfaces* 136, 1004–1010. doi: 10.1016/j.colsurfb.2015.10.041

Gide, P. S., Gidwani, S. K., and Kothule, K. U. (2013). Enhancement of transdermal penetration and bioavailability of poorly soluble acyclovir using solid lipid nanoparticles incorporated in gel cream. *Indian J. Pharm. Sci.* 75, 138–142. doi: 10.4103/0250-474X.115457

González-Paredes, A., Sitia, L., Ruyra, A., Morris, C. J., Wheeler, G. N., McArthur, M., et al. (2019). Solid lipid nanoparticles for the delivery of anti-microbial oligonucleotides. *Eur. J. Pharm. Biopharm.* 134, 166–177. doi: 10.1016/j.ejpb.2018.11.017

Goppert, T., and Muller, R. (2005). Protein adsorption patterns on poloxamer- and poloxamine-stabilized solid lipid nanoparticles (SLN). *Eur. J. Pharm. Biopharm.* 60, 361–372. doi: 10.1016/j.ejpb.2005.02.006

Göppert, T. M., and Müller, R. H. (2003). Plasma protein adsorption of Tween 80- and poloxamer 188-stabilized solid lipid nanoparticles. *J. Drug Target.* 11, 225–231. doi: 10.1080/10611860310001615956

Gordillo-Galeano, A., and Mora-Huertas, C. E. (2018). Solid lipid nanoparticles and nanostructured lipid carriers: a review emphasizing on particle structure and drug release. *Eur. J. Pharm. Biopharm.* 133, 285–308. doi: 10.1016/j.ejpb.2018.10.017

Gordon, S. (2016). Phagocytosis: an immunobiologic process. *Immunity* 44, 463–475. doi: 10.1016/J.IMMUNI.2016.02.026

Gupta, R., Dwadasi, B. S., Rai, B., and Mitragotri, S. (2019). Effect of chemical permeation enhancers on skin permeability: *in silico* screening using molecular dynamics simulations. *Sci. Rep.* 9:1456. doi: 10.1038/s41598-018-37900-0

Gupta, S., Kesarla, R., Chotai, N., Misra, A., and Omri, A. (2017). Systematic approach for the formulation and optimization of solid lipid nanoparticles of Efavirenz by high pressure homogenization using design of experiments for brain targeting and enhanced bioavailability. *Biomed Res. Int.* 2017:5984014. doi: 10.1155/2017/5984014

Gupta, S. C., Patchva, S., and Aggarwal, B. B. (2013). Therapeutic roles of curcumin: lessons learned from clinical trials. *AAPS J.* 15, 195–218. doi: 10.1208/s12248-012-9432-8

Hadjesfandiari, N. (2018). "Stealth coatings for nanoparticles: Polyethylene glycol alternatives," in *Engineering of Biomaterials for Drug Delivery Systems: Beyond Polyethylene Glycol*, ed. A. Parambath (Cambridge: Woodhead Publishing), 345–361. doi: 10.1016/B978-0-08-101750-0.00013-1

Hamishehkar, H., Ghanbarzadeh, S., Sepehran, S., Javadzadeh, Y., Adib, Z. M., and Kouhsoltani, M. (2016). Histological assessment of follicular delivery of flutamide by solid lipid nanoparticles: potential tool for the treatment of androgenic alopecia. *Drug Dev. Ind. Pharm.* 42, 846–853. doi: 10.3109/03639045.2015.1062896

Han, X., Zhang, E., Shi, Y., Song, B., Du, H., and Cao, Z. (2019). Biomaterial-tight junction interaction and potential impacts. *J. Mater. Chem. B* 7, 6310–6320. doi: 10.1039/c9tb01081e

Haque, S., Whittaker, M., McIntosh, M. P., Pouton, C. W., Phipps, S., and Kaminskas, L. M. (2018). A comparison of the lung clearance kinetics of solid lipid nanoparticles and liposomes by following the 3H-labelled structural lipids after pulmonary delivery in rats. *Eur. J. Pharm. Biopharm.* 125, 1–12. doi: 10.1016/j.ejpb.2018.01.001

Hare, J. I., Lammers, T., Ashford, M. B., Puri, S., Storm, G., and Barry, S. T. (2017). Challenges and strategies in anti-cancer nanomedicine development: an industry perspective. *Adv. Drug Deliv. Rev.* 108, 25–38. doi: 10.1016/J.ADDR.2016.04.025

Hauser, E. A. (1955). The history of colloid science: in memory of Wolfgang Ostwald. *J. Chem. Educ.* 32:2. doi: 10.1021/ed032p2

He, Y., Zhan, C., Pi, C., Zuo, Y., Yang, S., Hu, M., et al. (2020). Enhanced oral bioavailability of felodipine from solid lipid nanoparticles prepared through effervescent dispersion technique. *AAPS PharmSciTech* 21:170. doi: 10.1208/s12249-020-01711-2

Hecq, J., Amighi, K., and Goole, J. (2016). Development and evaluation of insulin-loaded cationic solid lipid nanoparticles for oral delivery. *J. Drug Deliv. Sci. Technol.* 36, 192–200. doi: 10.1016/j.jddst.2016.10.012

Holm, J., and Hansen, S. I. (2020). Characterization of soluble folate receptors (folate binding proteins) in humans. Biological roles and clinical potentials in infection and malignancy. *Biochim. Biophys. Acta Proteins Proteom.* 1868:140466. doi: 10.1016/j.bbapap.2020.140466

Hosseini, S. M., Abbasalipourkabir, R., Jalilian, F. A., Asl, S. S., Farmany, A., Roshanaei, G., et al. (2019). Doxycycline-encapsulated solid lipid nanoparticles as promising tool against *Brucella melitensis* enclosed in macrophage: a pharmacodynamics study on J774A.1 cell line. *Antimicrob. Resist. Infect. Control* 8:62. doi: 10.1186/s13756-019-0504-8

Hu, X., Fan, W., Yu, Z., Lu, Y., Qi, J., Zhang, J., et al. (2016). Evidence does not support absorption of intact solid lipid nanoparticles via oral delivery. *Nanoscale* 8, 7024–7035. doi: 10.1039/c5nr07474f

ICH (2009). *Pharmaceutical Development Q8-R2. ICH Harmonized Tripartite Guideline*. Available online at: https://database.ich.org/sites/default/files/Q8_R2_Guideline.pdf (accessed September 17, 2020).

Jaffee, E. M., Dang, C., Van, Agus, D. B., Alexander, B. M., Anderson, K. C., et al. (2017). Future cancer research priorities in the USA: a Lancet Oncology

Commission. *Lancet Oncol.* 18, e653–e706. doi: 10.1016/S1470-2045(17)30698-8

Jain, A. K., and Thareja, S. (2020). "Solid lipid nanoparticles," in *Nanomaterials and Environmental Biotechnology*, eds I. Bhushan, V. Singh, and D. Tripathi (Cham: Springer), 221–249. doi: 10.1007/978-3-030-34544-0_13

Joshy, K. S., Sharma, C. P., Kalarikkal, N., Sandeep, K., Thomas, S., and Pothen, L. A. (2016). Evaluation of in-vitro cytotoxicity and cellular uptake efficiency of zidovudine-loaded solid lipid nanoparticles modified with Aloe Vera in glioma cells. *Mater. Sci. Eng. C* 66, 40–50. doi: 10.1016/j.msec.2016.03.031

Kadari, A., Pooja, D., Gora, R. H., Gudem, S., Kolapalli, V. R. M., Kulhari, H., et al. (2018). Design of multifunctional peptide collaborated and docetaxel loaded lipid nanoparticles for antiglioma therapy. *Eur. J. Pharm. Biopharm.* 132, 168–179. doi: 10.1016/j.ejpb.2018.09.012

Kakkar, V., Muppu, S. K., Chopra, K., and Kaur, I. P. (2013). Curcumin loaded solid lipid nanoparticles: an efficient formulation approach for cerebral ischemic reperfusion injury in rats. *Eur. J. Pharm. Biopharm* 85(3 Pt A), 339–345. doi: 10.1016/J.EJPB.2013.02.005

Kang, J. H., Chon, J., Kim, Y., Il, Lee, H. J., Oh, D. W., et al. (2019). Preparation and evaluation of tacrolimus-loaded thermosensitive solid lipid nanoparticles for improved dermal distribution. *Int. J. Nanomed.* 14, 5381–5396. doi: 10.2147/IJN.S215153

Karn-orachai, K., Smith, S. M., Saesoo, S., Treethong, A., Puttipipatkhachorn, S., Pratontep, S., et al. (2016). Surfactant effect on the physicochemical characteristics of γ-oryanol-containing solid lipid nanoparticles. *Colloids Surf. A Physicochem. Eng. Asp.* 488, 118–128. doi: 10.1016/j.colsurfa.2015.10.011

Keck, C. M., Kovačević, A., Müller, R. H., Savić, S., Vuleta, G., and Miliæ, J. (2014). Formulation of solid lipid nanoparticles (SLN): The value of different alkyl polyglucoside surfactants. *Int. J. Pharm.* 474, 33–41. doi: 10.1016/J.IJPHARM.2014.08.008

Keck, C. M., and Müller, R. H. (2013). Nanotoxicological classification system (NCS) - a guide for the risk-benefit assessment of nanoparticulate drug delivery systems. *Eur. J. Pharm. Biopharm.* 84, 445–448. doi: 10.1016/j.ejpb.2013.01.001

Khallaf, R. A., Salem, H. F., and Abdelbary, A. (2016). 5-Fluorouracil shell-enriched solid lipid nanoparticles (SLN) for effective skin carcinoma treatment. *Drug Deliv.* 23, 3452–3460. doi: 10.1080/10717544.2016.1194498

Khatri, H., Chokshi, N., Rawal, S., and Patel, M. M. (2019). Fabrication, characterization and optimization of artemether loaded PEGylated solid lipid nanoparticles for the treatment of lung cancer. *Mater. Res. Express* 6:045014. doi: 10.1088/2053-1591/aaf8a3

Kola, I., and Landis, J. (2004). Can the pharmaceutical industry reduce attrition rates? *Nat. Rev. Drug Discov.* 3, 711–715. doi: 10.1038/nrd1470

Kong, W. H., Park, K., Lee, M.-Y., Lee, H., Sung, D. K., and Hahn, S. K. (2013). Cationic solid lipid nanoparticles derived from apolipoprotein-free LDLs for target specific systemic treatment of liver fibrosis. *Biomaterials* 34, 542–551. doi: 10.1016/j.biomaterials.2012.09.067

Kotmakçı, M., Çetintaş, V. B., and Kantarcı, A. G. (2017). Preparation and characterization of lipid nanoparticle/pDNA complexes for STAT3 downregulation and overcoming chemotherapy resistance in lung cancer cells. *Int. J. Pharm.* 525, 101–111. doi: 10.1016/j.ijpharm.2017.04.034

Kovačević, A. B. (2020). "Lipid nanocarriers for delivery of poorly soluble and poorly permeable drugs," in *Nanopharmaceuticals*, ed. R. Shegokar (Amsterdam: Elsevier), 151–174. doi: 10.1016/b978-0-12-817778-5.00008-7

Kovačević, A. B., Müller, R. H., Saviæ, S. D., Vuleta, G. M., and Keck, C. M. (2014). Solid lipid nanoparticles (SLN) stabilized with polyhydroxy surfactants: preparation, characterization and physical stability investigation. *Colloids Surf. A Physicochem. Eng. Asp.* 444, 15–25. doi: 10.1016/J.COLSURFA.2013.12.023

Kowalski, P. S., Rudra, A., Miao, L., and Anderson, D. G. (2019). Delivering the messenger: advances in technologies for therapeutic mRNA delivery. *Mol. Ther.* 27, 710–728. doi: 10.1016/j.ymthe.2019.02.012

Krishna, K. V., Wadhwa, G., Alexander, A., Kanojia, N., Saha, R. N., Kukreti, R., et al. (2019). Design and biological evaluation of lipoprotein-based donepezil nanocarrier for enhanced Brain uptake through oral delivery. *ACS Chem. Neurosci.* 10, 4124–4135. doi: 10.1021/acschemneuro.9b00343

Küçüktürkmen, B., and Bozkır, A. (2018). Development and characterization of cationic solid lipid nanoparticles for co-delivery of pemetrexed and miR-21 antisense oligonucleotide to glioblastoma cells. *Drug Dev. Ind. Pharm.* 44, 306–315. doi: 10.1080/03639045.2017.1391835

Kulkarni, J. A., Cullis, P. R., and van der Meel, R. (2018). Lipid nanoparticles enabling gene therapies: from concepts to clinical utility. *Nucleic Acid Ther.* 28, 146–157. doi: 10.1089/nat.2018.0721

Kumar, R., and Sinha, V. R. (2016). Solid lipid nanoparticle: an efficient carrier for improved ocular permeation of voriconazole. *Drug Dev. Ind. Pharm.* 42, 1956–1967. doi: 10.1080/03639045.2016.1185437

Kumar, V., Chaudhary, H., and Kamboj, A. (2018). Development and evaluation of isradipine via rutin-loaded coated solid–lipid nanoparticles. *Interv. Med. Appl. Sci.* 10, 236–246. doi: 10.1556/1646.10.2018.45

Kuo, Y.-C., and Lee, C.-H. (2016). Dual targeting of solid lipid nanoparticles grafted with 83-14 MAb and anti-EGF receptor for malignant brain tumor therapy. *Life Sci.* 146, 222–231. doi: 10.1016/j.lfs.2016.01.025

Kuo, Y. C., Rajesh, R., and Hsu, J. P. (2019). Electrophoretic mobility of neuron-like cells regenerated from iPSCs with induction of retinoic acid- and nerve growth factor-loaded solid lipid nanoparticles. *J. Taiwan Inst. Chem. Eng.* 103, 167–176. doi: 10.1016/j.jtice.2019.07.010

Kuo, Y.-C., and Wang, C.-C. (2014). Cationic solid lipid nanoparticles with cholesterol-mediated surface layer for transporting saquinavir to the brain. *Biotechnol. Prog.* 30, 198–206. doi: 10.1002/btpr.1834

Kurakula, M., Ahmed, O. A. A., Fahmy, U. A., and Ahmed, T. A. (2016). Solid lipid nanoparticles for transdermal delivery of avanafil: optimization, formulation, in-vitro and ex-vivo studies. *J. Liposome Res.* 26, 288–296. doi: 10.3109/08982104.2015.1117490

Lahkar, S., and Kumar Das, M. (2018). Surface modified kokum butter lipid nanoparticles for the brain targeted delivery of nevirapine. *J. Microencapsul.* 35, 680–694. doi: 10.1080/02652048.2019.1573857

le Chatelier, H. (1919). Crystalloids against colloids in the theory of cements. *Trans. Faraday Soc.* 14, 8–11. doi: 10.1039/tf9191400008

Leite, E. R., and Ribeiro, C. (2012). "Basic principles: thermodynamics and colloidal chemistry," in *Crystallization and Growth of Colloidal Nanocrystals*, eds E. R. Leite and C. Ribeiro (New York, NY: Springer), 7–17. doi: 10.1007/978-1-4614-1308-0_2

Li, Y., Wu, M., Zhang, N., Tang, C., Jiang, P., Liu, X., et al. (2018). Mechanisms of enhanced antiglioma efficacy of polysorbate 80-modified paclitaxel-loaded PLGA nanoparticles by focused ultrasound. *J. Cell. Mol. Med.* 22, 4171–4182. doi: 10.1111/jcmm.13695

Lima, T., Bernfur, K., Vilanova, M., and Cedervall, T. (2020). Understanding the lipid and protein corona formation on different sized polymeric nanoparticles. *Sci. Rep.* 10:1129. doi: 10.1038/s41598-020-57943-6

Liu, J.-L., Li, J., Zhang, L.-Y., Zhang, P.-L., Zhou, J.-L., and Liu, B. (2017). Preparation of N, N, N-trimethyl chitosan-functionalized retinoic acid-loaded lipid nanoparticles for enhanced drug delivery to glioblastoma. *Trop. J. Pharm. Res.* 16, 1765–1772. doi: 10.4314/tjpr.v16i8.3

Luo, Y., Teng, Z., Li, Y., and Wang, Q. (2015). Solid lipid nanoparticles for oral drug delivery: chitosan coating improves stability, controlled delivery, mucoadhesion and cellular uptake. *Carbohydr. Polym.* 122, 221–229. doi: 10.1016/J.CARBPOL.2014.12.084

Ma, Y., He, H., Xia, F., Li, Y., Lu, Y., Chen, D., et al. (2017). *In vivo* fate of lipid-silybin conjugate nanoparticles: implications on enhanced oral bioavailability. *Nanomedicine* 13, 2643–2654. doi: 10.1016/j.nano.2017.07.014

Ma, Z., Wang, N., He, H., and Tang, X. (2019). Pharmaceutical strategies of improving oral systemic bioavailability of curcumin for clinical application. *J. Control. Release* 316, 359–380. doi: 10.1016/j.jconrel.2019.10.053

Maaßen, S., Schwarz, C., Mehnert, W., Lucks, J. S., Yunis-Specht, F., Muller, B. W., et al. (1993). Comparison of cytotoxicity between polyester nanoparticles and solid lipid nanoparticles (SLN). *Proc. Int. Symp. Control. Rel. Bioact. Mater.* 20, 490–491.

Mahmoud, R. A., Hussein, A. K., Nasef, G. A., and Mansour, H. F. (2020). Oxiconazole nitrate solid lipid nanoparticles: formulation, in-vitro characterization and clinical assessment of an analogous loaded carbopol gel. *Drug Dev. Ind. Pharm.* 46, 706–716. doi: 10.1080/03639045.2020.1752707

Maisel, K., Ensign, L., Reddy, M., Cone, R., and Hanes, J. (2015). Effect of surface chemistry on nanoparticle interaction with gastrointestinal mucus and distribution in the gastrointestinal tract following oral and rectal administration in the mouse. *J. Control. Release* 197, 48–57. doi: 10.1016/J.JCONREL.2014.10.026

Maretti, E., Costantino, L., Rustichelli, C., Leo, E., Croce, M. A., Buttini, F., et al. (2017). Surface engineering of Solid Lipid Nanoparticle assemblies by

methyl α-D-mannopyranoside for the active targeting to macrophages in anti-tuberculosis inhalation therapy. *Int. J. Pharm.* 528, 440–451. doi: 10.1016/j.ijpharm.2017.06.045

Martínez-Jothar, L., Barendrecht, A. D., de Graaff, A. M., Oliveira, S., van Nostrum, C. F., Schiffelers, R. M., et al. (2020). Endothelial cell targeting by crgd-functionalized polymeric nanoparticles under static and flow conditions. *Nanomaterials* 10:1353. doi: 10.3390/nano10071353

Martins, S., Sarmento, B., Ferreira, D. C., and Souto, E. B. (2007). Lipid-based colloidal carriers for peptide and protein delivery–liposomes versus lipid nanoparticles. *Int. J. Nanomed.* 2, 595–607.

Mazuryk, J., Deptuła, T., Polchi, A., Gapiński, J., Giovagnoli, S., Magini, A., et al. (2016). Rapamycin-loaded solid lipid nanoparticles: morphology and impact of the drug loading on the phase transition between lipid polymorphs. *Colloids Surf. A Physicochem. Eng. Asp.* 502, 54–65. doi: 10.1016/j.colsurfa.2016.05.017

McCartney, F., Rosa, M., and Brayden, D. J. (2019). Evaluation of sucrose laurate as an intestinal permeation enhancer for macromolecules: *ex vivo* and *in vivo* studies. *Pharmaceutics* 11:565. doi: 10.3390/pharmaceutics11110565

McManus, M. T., and Sharp, P. A. (2002). Gene silencing in mammals by small interfering RNAs. *Nat. Rev. Genet.* 3, 737–747. doi: 10.1038/nrg908

McNaught, A. D., and Wilkinson, A. (eds) (1997). *Colloidal*. Oxford: Blackwell Scientific Publications. doi: 10.1351/goldbook.C01172

Mehnert, W., and Mäder, K. (2001). Solid lipid nanoparticles: production, characterization and applications. *Adv. Drug Deliv. Rev.* 47, 165–196. doi: 10.1016/s0169-409x(01)00105-3

Mohanty, B., Majumdar, D. K., Mishra, S. K., Panda, A. K., and Patnaik, S. (2015). Development and characterization of itraconazole-loaded solid lipid nanoparticles for ocular delivery. *Pharm. Dev. Technol.* 20, 458–464. doi: 10.3109/10837450.2014.882935

Montgomery, D. C. (2017). *Design and Analysis of Experiments.* Hoboken, NJ: John Wiley & Sons, Inc.

Müller, R. H., Maaben, S., Weyhers, H., and Mehnert, W. (1996a). Phagocytic uptake and cytotoxicity of solid lipid nanoparticles (SLN) sterically stabilized with poloxamine 908 and poloxamer 407. *J. Drug Target.* 4, 161–170. doi: 10.3109/10611869609015973

Müller, R. H., Radtke, M., and Wissing, S. A. (2002). Solid lipid nanoparticles (SLN) and nanostructured lipid carriers (NLC) in cosmetic and dermatological preparations. *Adv. Drug Deliv. Rev.* 54, S131–S155. doi: 10.1016/S0169-409X(02)00118-7

Muller, R. H., Radtke, M., and Wissing, S. A. (2002). Nanostructured lipid matrices for improved microencapsulation of drugs. *Int. J. Pharm.* 242, 121–128. doi: 10.1016/s0378-5173(02)00180-1

Müller, R. H., Rühl, D., and Runge, S. A. (1996b). Biodegradation of solid lipid nanoparticles as a function of lipase incubation time. *Int. J. Pharm.* 144, 115–121. doi: 10.1016/S0378-5173(96)04731-X

Muller, R. H., Schwarz, C., Mehnert, W., and Lucks, J. S. (1993). Production of solid lipid nanoparticles (SLN) for controlled drug delivery. *Proc. Control. Release Soc.* 20, 480–481.

Müller, R. H., Staufenbiel, S., and Keck, C. M. (2014). Lipid Nanoparticles (SLN, NLC) for innovative consumer care & household products. *Househ. Pers. Care Today* 9, 18–25.

Nafee, N., Husari, A., Maurer, C. K., Lu, C., De Rossi, C., Steinbach, A., et al. (2014). Antibiotic-free nanotherapeutics: ultra-small, mucus-penetrating solid lipid nanoparticles enhance the pulmonary delivery and anti-virulence efficacy of novel quorum sensing inhibitors. *J. Control. Release* 192, 131–140. doi: 10.1016/j.jconrel.2014.06.055

Nakhlband, A., Eskandani, M., Saeedi, N., Ghafari, S., Omidi, Y., Barar, J., et al. (2018). Marrubiin-loaded solid lipid nanoparticles' impact on TNF-α treated umbilical vein endothelial cells: a study for cardioprotective effect. *Colloids Surf. B Biointerfaces* 164, 299–307. doi: 10.1016/j.colsurfb.2018.01.046

Neves, A. R., Queiroz, J. F., Lima, S. A. C., and Reis, S. (2017). Apo E-functionalization of Solid Lipid Nanoparticles enhances brain drug delivery: uptake mechanism and transport pathways. *Bioconjug. Chem.* 28, 995–1004. doi: 10.1021/acs.bioconjchem.6b00705

Neves, A. R., Queiroz, J. F., and Reis, S. (2016). Brain-targeted delivery of resveratrol using solid lipid nanoparticles functionalized with apolipoprotein E. *J. Nanobiotechnology* 14:27. doi: 10.1186/s12951-016-0177-x

Neves, A. R., Queiroz, J. F., Weksler, B., Romero, I. A., Couraud, P.-O., and Reis, S. (2015). Solid lipid nanoparticles as a vehicle for brain-targeted drug delivery: two new strategies of functionalization with apolipoprotein E. *Nanotechnology* 26:495103. doi: 10.1088/0957-4484/26/49/495103

Nooli, M., Chella, N., Kulhari, H., Shastri, N. R., and Sistla, R. (2017). Solid lipid nanoparticles as vesicles for oral delivery of olmesartan medoxomil: formulation, optimization and *in vivo* evaluation. *Drug Dev. Ind. Pharm.* 43, 611–617. doi: 10.1080/03639045.2016.1275666

O'Driscoll, C. M. (2002). Lipid-based formulations for intestinal lymphatic delivery. *Eur. J. Pharm. Sci.* 15, 405–415. doi: 10.1016/S0928-0987(02)00051-9

Omwoyo, W. N., Melariri, P., Gathirwa, J. W., Oloo, F., Mahanga, G. M., Kalombo, L., et al. (2016). Development, characterization and antimalarial efficacy of dihydroartemisinin loaded solid lipid nanoparticles. *Nanomedicine* 12, 801–809. doi: 10.1016/j.nano.2015.11.017

Pandya, N. T., Jani, P., Vanza, J., and Tandel, H. (2018). Solid lipid nanoparticles as an efficient drug delivery system of olmesartan medoxomil for the treatment of hypertension. *Colloids Surf. B Biointerfaces* 165, 37–44. doi: 10.1016/j.colsurfb.2018.02.011

Pardridge, W. M. (2020). Blood-brain barrier and delivery of protein and gene therapeutics to brain. *Front. Aging Neurosci.* 11:373. doi: 10.3389/fnagi.2019.00373

Park, S., Aalipour, A., Vermesh, O., Yu, J. H., and Gambhir, S. S. (2017). Towards clinically translatable *in vivo* nanodiagnostics. *Nat. Rev. Mater.* 2:17014. doi: 10.1038/natrevmats.2017.14

Pastor, F., Berraondo, P., Etxeberria, I., Frederick, J., Sahin, U., Gilboa, E., et al. (2018). An RNA toolbox for cancer immunotherapy. *Nat. Rev. Drug Discov.* 17, 751–767. doi: 10.1038/nrd.2018.132

Patel, M. H., Mundada, V. P., and Sawant, K. K. (2019a). Fabrication of solid lipid nanoparticles of lurasidone HCl for oral delivery: optimization, *in vitro* characterization, cell line studies and *in vivo* efficacy in schizophrenia. *Drug Dev. Ind. Pharm.* 45, 1242–1257. doi: 10.1080/03639045.2019.1593434

Patel, M. H., Mundada, V. P., and Sawant, K. K. (2019b). Enhanced intestinal absorption of asenapine maleate by fabricating solid lipid nanoparticles using TPGS: elucidation of transport mechanism, permeability across Caco-2 cell line and in vivo pharmacokinetic studies. *Artif. Cells Nanomed. Biotechnol.* 47, 144–153. doi: 10.1080/21691401.2018.1546186

Patel, M., Souto, E. B., and Singh, K. K. (2013). Advances in brain drug targeting and delivery: limitations and challenges of solid lipid nanoparticles. *Expert Opin. Drug Deliv.* 10, 889–905. doi: 10.1517/17425247.2013.784742

Pelaz, B., del Pino, P., Maffre, P., Hartmann, R., Gallego, M., Rivera-Fernández, S., et al. (2015). Surface functionalization of nanoparticles with polyethylene glycol: effects on protein adsorption and cellular uptake. *ACS Nano* 9, 6996–7008. doi: 10.1021/acsnano.5b01326

Peng, M.-Z., Li, X.-Z., Mei, H.-F., Sheng, H.-Y., Yin, X., Jiang, M.-Y., et al. (2020). Clinical and biochemical characteristics of patients with ornithine transcarbamylase deficiency. *Clin. Biochem.* 84, 63–72. doi: 10.1016/j.clinbiochem.2020.06.011

Peralta, M. F., Guzmán, M. L., Pérez, A. P., Apezteguia, G. A., Fórmica, M. L., Romero, E. L., et al. (2018). Liposomes can both enhance or reduce drugs penetration through the skin. *Sci. Rep.* 8, 13253. doi: 10.1038/s41598-018-31693-y

Perez-Garcia, C. G., Tachikawa, K., Matsuda, D., and Chivukula, P. (2019). Compositions and methods for treating ornithine transcarbamylase deficiency. U.S. Patent No. US20200181584A1. Washington, DC: U.S. Patent and Trademark Office.

Permana, A. D., Tekko, I. A., McCrudden, M. T. C., Anjani, Q. K., Ramadon, D., McCarthy, H. O., et al. (2019). Solid lipid nanoparticle-based dissolving microneedles: a promising intradermal lymph targeting drug delivery system with potential for enhanced treatment of lymphatic filariasis. *J. Control. Release* 316, 34–52. doi: 10.1016/j.jconrel.2019.10.004

Pignatello, R., Fuochi, V., Petronio, G. P., Greco, A. S., and Furneri, P. M. (2017). Formulation and characterization of erythromycin–loaded solid lipid nanoparticles. *Biointerface Res. Appl. Chem.* 7, 2145–2150.

Pink, D. L., Loruthai, O., Ziolek, R. M., Wasutrasawat, P., Terry, A. E., Lawrence, M. J., et al. (2019). On the structure of solid lipid nanoparticles. *Small* 15:e1903156. doi: 10.1002/smll.201903156

Puri, A., Loomis, K., Smith, B., Lee, J.-H. H., Yavlovich, A., Heldman, E., et al. (2009). Lipid-based nanoparticles as pharmaceutical drug carriers: from concepts to clinic. *Crit. Rev. Ther. Drug Carrier Syst.* 26, 523–580. doi: 10.1615/CritRevTherDrugCarrierSyst.v26.i6.10

Raj, R., Mongia, P., Ram, A., and Jain, N. K. (2016). Enhanced skin delivery of aceclofenac via hydrogel-based solid lipid nanoparticles. *Artif. Cells Nanomed. Biotechnol.* 44, 1434–1439. doi: 10.3109/21691401.2015.1036997

Rajpoot, K., and Jain, S. K. (2018). Colorectal cancer-targeted delivery of oxaliplatin via folic acid-grafted solid lipid nanoparticles: preparation, optimization, and *in vitro* evaluation. *Artif. Cells Nanomed. Biotechnol.* 46, 1236–1247. doi: 10.1080/21691401.2017.1366338

Rajpoot, K., and Jain, S. K. (2019a). Irinotecan hydrochloride trihydrate loaded folic acid-tailored solid lipid nanoparticles for targeting colorectal cancer: development, characterization, and *in vitro* cytotoxicity study using HT-29 cells. *J. Microencapsul.* 36, 659–676. doi: 10.1080/02652048.2019.1665723

Rajpoot, K., and Jain, S. K. (2020). Oral delivery of pH-responsive alginate microbeads incorporating folic acid-grafted solid lipid nanoparticles exhibits enhanced targeting effect against colorectal cancer: a dual-targeted approach. *Int. J. Biol. Macromol.* 151, 830–844. doi: 10.1016/j.ijbiomac.2020.02.132

Ramalingam, P., and Ko, Y. T. (2015). Enhanced oral delivery of curcumin from N-trimethyl chitosan surface-modified solid lipid nanoparticles: pharmacokinetic and brain distribution evaluations. *Pharm. Res.* 32, 389–402. doi: 10.1007/s11095-014-1469-1

Ravi, P. R., Vats, R., Dalal, V., and Murthy, A. N. (2014). A hybrid design to optimize preparation of lopinavir loaded solid lipid nanoparticles and comparative pharmacokinetic evaluation with marketed lopinavir/ritonavir coformulation. *J. Pharm. Pharmacol.* 66, 912–926. doi: 10.1111/jphp.12217

Ravindra Babu, M., Ravi Prakash, P., and Devanna, N. (2019). Absorption enhancement effect of piperine and chitosan on ganciclovir sol-id lipid nanoparticles: formulation, optimization and invivo pharmacoki-netics. *Int. J. Res. Pharm. Sci.* 10, 1143–1151. doi: 10.26452/ijrps.v10i2.395

Rehman, M. U., Khan, M. A., Khan, W. S., Shafique, M., and Khan, M. (2018). Fabrication of Niclosamide loaded solid lipid nanoparticles: *in vitro* characterization and comparative in vivo evaluation. *Artif. Cells Nanomed. Biotechnol.* 46, 1926–1934. doi: 10.1080/21691401.2017.1396996

Reynolds, A., Leake, D., Boese, Q., Scaringe, S., Marshall, W. S., and Khvorova, A. (2004). Rational siRNA design for RNA interference. *Nat. Biotechnol.* 22, 326–330. doi: 10.1038/nbt936

Rodenak-Kladniew, B., Scioli Montoto, S., Sbaraglini, M. L., Di Ianni, M., Ruiz, M. E., Talevi, A., et al. (2019). Hybrid Ofloxacin/eugenol co-loaded solid lipid nanoparticles with enhanced and targetable antimicrobial properties. *Int. J. Pharm.* 569:118575. doi: 10.1016/j.ijpharm.2019.118575

Rosales, C., and Uribe-Querol, E. (2017). Phagocytosis: a fundamental process in immunity. *Biomed Res. Int.* 2017:9042851. doi: 10.1155/2017/9042851

Rosière, R., Van Woensel, M., Gelbcke, M., Mathieu, V., Hecq, J., Mathivet, T., et al. (2018). New folate-grafted chitosan derivative to improve delivery of paclitaxel-loaded solid lipid nanoparticles for lung tumor therapy by inhalation. *Mol. Pharm.* 15, 899–910. doi: 10.1021/acs.molpharmaceut.7b00846

Rudhrabatla, V. S. A., Sudhakar, B., and Reddy, K. V. N. (2019). Ritonavir loaded surface modified stealth solid lipid nanoparticles: full factorial design and pharmacokinetic studies. *Int. J. Res. Pharm. Sci.* 10, 77–89. doi: 10.26452/ijrps.v10i1.1783

Rudhrabatla, V. S. A. P., Sudhakar, B., and Reddy, K. V. N. S. (2020). *In vitro* and *in vivo* assessment of designed melphalan loaded stealth solid lipid nanoparticles for parenteral delivery. *Bionanoscience* 10, 168–190. doi: 10.1007/s12668-019-00680-6

Ruiz, M. E., and Scioli Montoto, S. (2018). "Routes of drug administration," in *ADME Processes in Pharmaceutical Sciences*, eds A. Talevi and P. A. Quiroga (Cham: Springer), 97–133. doi: 10.1007/978-3-319-99593-9_6

Sadegh Malvajerd, S., Azadi, A., Izadi, Z., Kurd, M., Dara, T., Dibaei, M., et al. (2019). Brain delivery of curcumin using solid lipid nanoparticles and nanostructured lipid carriers: preparation, optimization, and pharmacokinetic evaluation. *ACS Chem. Neurosci.* 10, 728–739. doi: 10.1021/acschemneuro.8b00510

Sahay, G., Alakhova, D. Y., and Kabanov, A. V. (2010). Endocytosis of nanomedicines. *J. Control. Release* 145, 182–195. doi: 10.1016/J.JCONREL.2010.01.036

Salah, E., Abouelfetouh, M. M., Pan, Y., Chen, D., and Xie, S. (2020). Solid lipid nanoparticles for enhanced oral absorption: a review. *Colloids Surf. B Biointerfaces* 196:111305. doi: 10.1016/j.colsurfb.2020.111305

Sanidad, K. Z., Sukamtoh, E., Xiao, H., McClements, D. J., and Zhang, G. (2019). Curcumin: recent advances in the development of strategies to improve oral bioavailability. *Annu. Rev. Food Sci. Technol.* 10, 597–617. doi: 10.1146/annurev-food-032818-121738

Saraiva, C., Praça, C., Ferreira, R., Santos, T., Ferreira, L., and Bernardino, L. (2016). Nanoparticle-mediated brain drug delivery: overcoming blood–brain barrier to treat neurodegenerative diseases. *J. Control. Release* 235, 34–47. doi: 10.1016/J.JCONREL.2016.05.044

Sathya, S., Shanmuganathan, B., Manirathinam, G., Ruckmani, K., and Devi, K. P. (2018). α-Bisabolol loaded solid lipid nanoparticles attenuates Aβ aggregation and protects Neuro-2a cells from Aβ induced neurotoxicity. *J. Mol. Liq.* 264, 431–441. doi: 10.1016/j.molliq.2018.05.075

Schneider, C. S., Xu, Q., Boylan, N. J., Chisholm, J., Tang, B. C., Schuster, B. S., et al. (2017). Nanoparticles that do not adhere to mucus provide uniform and long-lasting drug delivery to airways following inhalation. *Sci. Adv.* 3, e1601556. doi: 10.1126/sciadv.1601556

Schwarz, C., Mehnert, W., Lucks, J. S., and Müller, R. H. (1994). Solid lipid nanoparticles (SLN) for controlled drug delivery I. Production, characterization and sterilization. *J. Control. Release* 30, 83–96. doi: 10.1016/0168-3659(94)90047-7

Scioli Montoto, S., Sbaraglini, M. L. L., Talevi, A., Couyoupetrou, M., Di Ianni, M., Pesce, G. O. O., et al. (2018). Carbamazepine-loaded solid lipid nanoparticles and nanostructured lipid carriers: physicochemical characterization and *in vitro/in vivo* evaluation. *Colloids Surf. B Biointerfaces* 167, 73–81. doi: 10.1016/j.colsurfb.2018.03.052

Senthil Kumar, C., Thangam, R., Mary, S. A., Kannan, P. R., Arun, G., and Madhan, B. (2020). Targeted delivery and apoptosis induction of trans-resveratrol-ferulic acid loaded chitosan coated folic acid conjugate solid lipid nanoparticles in colon cancer cells. *Carbohydr. Polym.* 231:115682. doi: 10.1016/j.carbpol.2019.115682

Severino, P., Chaud, M. V., Shimojo, A., Antonini, D., Lancelloti, M., Santana, M. H. A., et al. (2015). Sodium alginate-cross-linked polymyxin B sulphate-loaded solid lipid nanoparticles: antibiotic resistance tests and HaCat and NIH/3T3 cell viability studies. *Colloids Surf. B Biointerfaces* 129, 191–197. doi: 10.1016/j.colsurfb.2015.03.049

Shah, R. M., Eldridge, D. S., Palombo, E. A., and Harding, I. H. (2016a). Microwave-assisted formulation of solid lipid nanoparticles loaded with non-steroidal anti-inflammatory drugs. *Int. J. Pharm.* 515, 543–554. doi: 10.1016/j.ijpharm.2016.10.054

Shah, R. M., Mata, J. P., Bryant, G., de Campo, L., Ife, A., Karpe, A. V., et al. (2019). Structure analysis of solid lipid nanoparticles for drug delivery: a combined USANS/SANS study. *Part. Part. Syst. Charact.* 36:1800359. doi: 10.1002/ppsc.201800359

Shah, R. M., Rajasekaran, D., Ludford-Menting, M., Eldridge, D. S., Palombo, E. A., and Harding, I. H. (2016b). Transport of stearic acid-based solid lipid nanoparticles (SLNs) into human epithelial cells. *Colloids Surf. B Biointerfaces* 140, 204–212. doi: 10.1016/j.colsurfb.2015.12.029

Shangguan, M., Qi, J., Lu, Y., and Wu, W. (2015). Comparison of the oral bioavailability of silymarin-loaded lipid nanoparticles with their artificial lipolysate counterparts: implications on the contribution of integral structure. *Int. J. Pharm.* 489, 195–202. doi: 10.1016/j.ijpharm.2015.05.005

Sharma, R. K., Sharma, N., Rana, S., and Shivkumar, H. G. (2013). Solid lipid nanoparticles as a carrier of metformin for transdermal delivery. *Int. J. Drug Deliv.* 5, 137–145.

Shi, J., Kantoff, P. W., Wooster, R., and Farokhzad, O. C. (2017). Cancer nanomedicine: progress, challenges and opportunities. *Nat. Rev. Cancer* 17, 20–37. doi: 10.1038/nrc.2016.108

Shi, L.-L., Cao, Y., Zhu, X.-Y., Cui, J.-H., and Cao, Q.-R. (2015). Optimization of process variables of zanamivir-loaded solid lipid nanoparticles and the prediction of their cellular transport in Caco-2 cell model. *Int. J. Pharm.* 478, 60–69. doi: 10.1016/j.ijpharm.2014.11.017

Shi, S., Han, L., Deng, L., Zhang, Y., Shen, H., Gong, T., et al. (2014). Dual drugs (microRNA-34a and paclitaxel)-loaded functional solid lipid nanoparticles for synergistic cancer cell suppression. *J. Control. Release* 194, 228–237. doi: 10.1016/j.jconrel.2014.09.005

Shinde, S. V., Nikam, S., Raut, P., and Ghag, M. K. (2019). Lipid nanoparticles for transdermal delivery of celecoxib: an *in vitro* and *in vivo* investigation. *Indian Drugs* 56, 38–48.

Siddhartha, V. T., Pindiprolu, S. K. S. S., Chintamaneni, P. K., Tummala, S., and Nandha Kumar, S. (2018). RAGE receptor targeted bioconjuguate lipid

nanoparticles of diallyl disulfide for improved apoptotic activity in triple negative breast cancer: in vitro studies. *Artif. Cells Nanomed. Biotechnol.* 46, 387–397. doi: 10.1080/21691401.2017.1313267

Siepmann, J., and Siepmann, F. (2006). "Microparticles used as drug delivery systems," in *Smart Colloidal Materials*, ed. W. Richtering (Berlin: Springer), 15–21. doi: 10.1007/3-540-32702-9_3

Silki, and Sinha, V. R. (2018). Enhancement of in vivo efficacy and oral bioavailability of aripiprazole with solid lipid nanoparticles. *AAPS PharmSciTech* 19, 1264–1273. doi: 10.1208/s12249-017-0944-5

Singh, S. K., Kushwaha, A. K., Vuddanda, P. R., Karunanidhi, P., and Singh, S. K. (2013). Development and evaluation of solid lipid nanoparticles of raloxifene hydrochloride for enhanced bioavailability. *Biomed. Res. Int.* 2013:584549. doi: 10.1155/2013/584549

Sonawane, R., Harde, H., Katariya, M., Agrawal, S., and Jain, S. (2014). Solid lipid nanoparticles-loaded topical gel containing combination drugs: an approach to offset psoriasis. *Expert Opin. Drug Deliv.* 11, 1833–1847. doi: 10.1517/17425247.2014.938634

Souto, E. B., Doktorovova, S., Campos, J. R., Martins-Lopes, P., and Silva, A. M. (2019). Surface-tailored anti-HER2/neu-solid lipid nanoparticles for site-specific targeting MCF-7 and BT-474 breast cancer cells. *Eur. J. Pharm. Sci.* 128, 27–35. doi: 10.1016/j.ejps.2018.11.022

Souza, A. L. R. D., Andreani, T., De Oliveira, R. N., Kiill, C. P., Santos, F. K. D., Allegretti, S. M., et al. (2014). In vitro evaluation of permeation, toxicity and effect of praziquantel-loaded solid lipid nanoparticles against Schistosoma mansoni as a strategy to improve efficacy of the schistosomiasis treatment. *Int. J. Pharm.* 463, 31–37. doi: 10.1016/j.ijpharm.2013.12.022

Stamatovic, S. M., Keep, R. F., and Andjelkovic, A. V. (2008). Brain endothelial cell-cell junctions: how to "open" the blood brain barrier. *Curr. Neuropharmacol.* 6, 179–192. doi: 10.2174/157015908785777210

Talegaonkar, S., and Bhattacharyya, A. (2019). Potential of lipid nanoparticles (SLNs and NLCs) in enhancing oral bioavailability of drugs with poor intestinal permeability. *AAPS PharmSciTech* 20:121. doi: 10.1208/s12249-019-1337-8

Talluri, S. V., Kuppusamy, G., Karri, V. V. S. R., Yamjala, K., Wadhwani, A., Madhunapantula, S. V., et al. (2017). Application of quality-by-design approach to optimize diallyl disulfide-loaded solid lipid nanoparticles. *Artif. Cells Nanomed. Biotechnol.* 45, 474–488. doi: 10.3109/21691401.2016.1173046

Taveira, S. F., De Santana, D. C. A. S., Araújo, L. M. P. C., Marquele-Oliveira, F., Nomizo, A., and Lopez, R. F. V. (2014). Effect of iontophoresis on topical delivery of doxorubicin-loaded solid lipid nanoparticles. *J. Biomed. Nanotechnol.* 10, 1382–1390. doi: 10.1166/jbn.2014.1834

Tran, T. H., Ramasamy, T., Cho, H. J., Kim, Y. I., Poudel, B. K., Choi, H.-G., et al. (2014). Formulation and optimization of raloxifene-loaded solid lipid nanoparticles to enhance oral bioavailability. *J. Nanosci. Nanotechnol.* 14, 4820–4831. doi: 10.1166/jnn.2014.8722

Troy, D. B. (ed.) (2000). *Remington: The Science and Practice of Pharmacy*. Philadelphia, PA: Lippincott Williams & Wilkins. doi: 10.1016/S0165-6147(96)90065-6

Tupal, A., Sabzichi, M., Ramezani, F., Kouhsoltani, M., and Hamishehkar, H. (2016). Dermal delivery of doxorubicin-loaded solid lipid nanoparticles for the treatment of skin cancer. *J. Microencapsul.* 33, 372–380. doi: 10.1080/02652048.2016.1200150

Vaghasiya, H., Kumar, A., and Sawant, K. (2013). Development of solid lipid nanoparticles based controlled release system for topical delivery of terbinafine hydrochloride. *Eur. J. Pharm. Sci.* 49, 311–322. doi: 10.1016/j.ejps.2013.03.013

van der Meel, R., Lammers, T., and Hennink, W. E. (2017). Cancer nanomedicines: oversold or underappreciated? *Expert Opin. Drug Deliv.* 14, 1–5. doi: 10.1080/17425247.2017.1262346

Veni, D. K., and Gupta, N. V. (2020). Development and evaluation of Eudragit coated environmental sensitive solid lipid nanoparticles using central composite design module for enhancement of oral bioavailability of linagliptin. *Int. J. Polym. Mater. Polym. Biomater.* 69, 407–418. doi: 10.1080/00914037.2019.1570513

Vieira, A. C. C., Chaves, L. L., Pinheiro, M., Lima, S. A. C., Ferreira, D., Sarmento, B., et al. (2018). Mannosylated solid lipid nanoparticles for the selective delivery of rifampicin to macrophages. *Artif. Cells Nanomed. Biotechnol.* 46, 653–663. doi: 10.1080/21691401.2018.1434186

Vijayakumar, A., Baskaran, R., Jang, Y. S., Oh, S. H., and Yoo, B. K. (2017). Quercetin-loaded solid lipid nanoparticle dispersion with improved physicochemical properties and cellular uptake. *AAPS PharmSciTech* 18, 875–883. doi: 10.1208/s12249-016-0573-4

von Roemeling, C., Jiang, W., Chan, C. K., Weissman, I. L., and Kim, B. Y. S. (2017). Breaking down the barriers to precision cancer nanomedicine. *Trends Biotechnol.* 35, 159–171. doi: 10.1016/J.TIBTECH.2016.07.006

Vroman, L. (1962). Effect of absorbed proteins on the wettability of hydrophilic and hydrophobic solids. *Nature* 196, 476–477. doi: 10.1038/196476a0

Wang, F., Kream, R. M., and Stefano, G. B. (2020). An evidence based perspective on mRNA-SARS-CoV-2 vaccine development. *Med. Sci. Monit.* 26:e924700. doi: 10.12659/MSM.924700

Wang, J., Byrne, J. D., Napier, M. E., and DeSimone, J. M. (2011). More effective nanomedicines through particle design. *Small* 7, 1919–1931. doi: 10.1002/smll.201100442

Wang, L., Zhao, X., Du, J., Liu, M., Feng, J., and Hu, K. (2019). Improved brain delivery of pueraria flavones via intranasal administration of borneol-modified solid lipid nanoparticles. *Nanomedicine* 14, 2105–2119. doi: 10.2217/nnm-2018-0417

Wang, Q., Yang, Q., Cao, X., Wei, Q., Firempong, C. K., Guo, M., et al. (2018). Enhanced oral bioavailability and anti-gout activity of [6]-shogaol-loaded solid lipid nanoparticles. *Int. J. Pharm.* 550, 24–34. doi: 10.1016/j.ijpharm.2018.08.028

Whitehead, K. A., Langer, R., and Anderson, D. G. (2009). Knocking down barriers: advances in siRNA delivery. *Nat. Rev. Drug Discov.* 8, 129–138. doi: 10.1038/nrd2742

Wishart, D. S., Feunang, Y. D., Guo, A. C., Lo, E. J., Marcu, A., Grant, J. R., et al. (2018). DrugBank 5.0: a major update to the DrugBank database for 2018. *Nucleic Acids Res.* 46, D1074–D1082. doi: 10.1093/nar/gkx1037

Wittrup, A., and Lieberman, J. (2015). Knocking down disease: a progress report on siRNA therapeutics. *Nat. Rev. Genet.* 16, 543–552. doi: 10.1038/nrg3978

Wu, X., Chen, H., Wu, C., Wang, J., Zhang, S., Gao, J., et al. (2018). Inhibition of intrinsic coagulation improves safety and tumor-targeted drug delivery of cationic solid lipid nanoparticles. *Biomaterials* 156, 77–87. doi: 10.1016/j.biomaterials.2017.11.040

Xiao, K., Li, Y., Luo, J., Lee, J. S., Xiao, W., Gonik, A. M., et al. (2011). The effect of surface charge on in vivo biodistribution of PEG-oligocholic acid based micellar nanoparticles. *Biomaterials* 32, 3435–3446. doi: 10.1016/j.biomaterials.2011.01.021

Xie, J., Shen, Z., Anraku, Y., Kataoka, K., and Chen, X. (2019). Nanomaterial-based blood-brain-barrier (BBB) crossing strategies. *Biomaterials* 224:119491. doi: 10.1016/j.biomaterials.2019.119491

Xu, Y., Zheng, Y., Wu, L., Zhu, X., Zhang, Z., and Huang, Y. (2018). Novel solid lipid nanoparticle with endosomal escape function for oral delivery of insulin. *ACS Appl. Mater. Interfaces* 10, 9315–9324. doi: 10.1021/acsami.8b00507

Yang, G., Phua, S. Z. F., Bindra, A. K., and Zhao, Y. (2019). Degradability and clearance of inorganic nanoparticles for biomedical applications. *Adv. Mater.* 31:e1805730. doi: 10.1002/adma.201805730

Yao, M., McClements, D. J., Zhao, F., Craig, R. W., and Xiao, H. (2017). Controlling the gastrointestinal fate of nutraceutical and pharmaceutical-enriched lipid nanoparticles: from mixed micelles to chylomicrons. *Nanoimpact* 5, 13–21. doi: 10.1016/J.IMPACT.2016.12.001

You, P., Yuan, R., and Chen, C. (2017). Design and evaluation of lidocaine- and prilocaine-coloaded nanoparticulate drug delivery systems for topical anesthetic analgesic therapy: a comparison between solid lipid nanoparticles and nanostructured lipid carriers. *Drug Des. Devel. Ther.* 11, 2743–2752. doi: 10.2147/DDDT.S141031

Youssef, N. A. H. A., Kassem, A. A., Farid, R. M., Ismail, F. A., El-Massik, M. A. E., and Boraie, N. A. (2018). A novel nasal almotriptan loaded solid lipid nanoparticles in mucoadhesive in situ gel formulation for brain targeting: preparation, characterization and in vivo evaluation. *Int. J. Pharm.* 548, 609–624. doi: 10.1016/j.ijpharm.2018.07.014

Yu, S.-H., Tang, D.-W., Hsieh, H.-Y., Wu, W.-S., Lin, B.-X., Chuang, E.-Y., et al. (2013). Nanoparticle-induced tight-junction opening for the transport of an anti-angiogenic sulfated polysaccharide across Caco-2 cell monolayers. *Acta Biomater.* 9, 7449–7459. doi: 10.1016/J.ACTBIO.2013.04.009

Yu, Z., Fan, W., Wang, L., Qi, J., Lu, Y., and Wu, W. (2019). Effect of surface charges on oral absorption of intact solid lipid nanoparticles. *Mol. Pharm.* 16, 5013–5024. doi: 10.1021/acs.molpharmaceut.9b00861

Yuan, H., Chen, C.-Y., Chai, G.-H., Du, Y.-Z., and Hu, F.-Q. (2013). Improved transport and absorption through gastrointestinal tract by pegylated solid lipid nanoparticles. *Mol. Pharm.* 10, 1865–1873. doi: 10.1021/mp300649z

Zensi, A., Begley, D., Pontikis, C., Legros, C., Mihoreanu, L., Wagner, S., et al. (2009). Albumin nanoparticles targeted with Apo E enter the CNS by transcytosis and are delivered to neurones. *J. Control. Release* 137, 78–86. doi: 10.1016/j.jconrel.2009.03.002

Zhang, J., Zhu, X., Jin, Y., Shan, W., and Huang, Y. (2014). Mechanism study of cellular uptake and tight junction opening mediated by goblet cell-specific trimethyl chitosan nanoparticles. *Mol. Pharm.* 11, 1520–1532. doi: 10.1021/mp400685v

Zhao, F., Zhao, Y., Liu, Y., Chang, X., Chen, C., and Zhao, Y. (2011). Cellular uptake, intracellular trafficking, and cytotoxicity of nanomaterials. *Small* 7, 1322–1337. doi: 10.1002/smll.201100001

Zheng, G., Zheng, M., Yang, B., Fu, H., and Li, Y. (2019). Improving breast cancer therapy using doxorubicin loaded solid lipid nanoparticles: Synthesis of a novel arginine-glycine-aspartic tripeptide conjugated, pH sensitive lipid and evaluation of the nanomedicine *in vitro* and in vivo. *Biomed. Pharmacother.* 116:109006. doi: 10.1016/j.biopha.2019.109006

Conflict of Interest: The authors declare that the research was conducted in the absence of any commercial or financial relationships that could be construed as a potential conflict of interest.

Functional Hybrid Nanoemulsions for Sumatriptan Intranasal Delivery

Lígia N. M. Ribeiro[1], Gustavo H. Rodrigues da Silva[1], Verônica M. Couto[1],
Simone R. Castro[1], Márcia C. Breitkreitz[2], Carolina S. Martinez[3], Daniela E. Igartúa[3],
Maria J. Prieto[3] and Eneida de Paula[1]*

[1] Department of Biochemistry and Tissue Biology, Institute of Biology, University of Campinas (UNICAMP), Campinas, Brazil,
[2] Department of Analytical Chemistry, Institute of Chemistry, University of Campinas, Campinas, Brazil, [3] Department of
Science and Technology, National University of Quilmes, Bernal, Argentina

In recent years, advanced nanohybrid materials processed as pharmaceuticals have
proved to be very advantageous. Triptans, such as the commercially available intranasal
sumatriptan (SMT), are drugs employed in the treatment of painful migraine symptoms.
However, SMT effectiveness by the intranasal route is limited by its high hydrophilicity
and poor mucoadhesion. Therefore, we designed hybrid nanoemulsions (NE) composed
of copaiba oil as the organic component plus biopolymers (xanthan, pectin, alginate)
solubilized in the continuous aqueous phase, aiming at the intranasal release of SMT
(2% w/v). Firstly, drug-biopolymer complexes were optimized in order to decrease the
hydrophilicity of SMT. The resultant complexes were further encapsulated in copaiba oil-
based nanoparticles, forming NE formulations. Characterization by FTIR-ATR, DSC, and
TEM techniques exposed details of the molecular arrangement of the hybrid systems.
Long-term stability of the hybrid NE at 25°C was confirmed over a year, regarding
size ($\sim$ 120 nm), polydispersity ($\sim$ 0.2), zeta potential ($\sim$ −25 mV), and nanoparticle
concentration ($\sim$ 2.10^{14} particles/mL). SMT encapsulation efficiency in the formulations
ranged between 41–69%, extending the *in vitro* release time of SMT from 5 h (free drug)
to more than 24 h. The alginate-based NE was selected as the most desirable system
and its *in vivo* nanotoxicity was evaluated in a zebrafish model. Hybrid NE treatment did
not affect spontaneous movement or induce morphological changes in zebrafish larvae,
and there was no evidence of mortality or cardiotoxicity after 48 h of treatment. With
these results, we propose alginate-based nanoemulsions as a potential treatment for
migraine pain.

Keywords: sumatriptan, hybrid nanoemulsions, vegetable oil, intranasal administration, biopolymers, nanotoxicity

INTRODUCTION

Migraines are one of the top 10 causes of work disability in the world (Natoli et al., 2010;
Vos et al., 2015). It is a painful and limiting disease with a prevalence above 20% (Yeh et al.,
2018), characterized by periodic headache outbreaks, often associated with gastric problems
and photo/phonophobia.

Although the disease mechanism is not fully understood, serotonin (5-hydroxytryptamine) is
the probable trigger of migraine crises (Deen et al., 2019). In the late 1980s, some serotonin
agonists, known as triptans, were developed for the treatment of migraine. Intranasal sumatriptan
(SMT) is the gold standard treatment for severe migraines (Muzzi et al., 2020). However, SMT
is a hydrophilic molecule, which limits its permeation through the nasal mucosa and makes it

difficult to cross the blood-brain barrier (BBB), despite SMT action on the central nervous system (Pascual and Muñoz, 2005; Tfelt-Hansen, 2010). So far, there are no effective drugs available for treating migraines.

Nanoemulsions (NE) are drug delivery systems (DDS) in which at least 2 immiscible liquids are kinetically stabilized. They are mainly composed of aqueous and oily phases, with a huge loading capacity for hydrophobic molecules (Singh et al., 2017). They are able to prolong the drug release profile of several classes of drugs, improving their bioavailability (Rai et al., 2018). Moreover, NE with particle sizes smaller than 200 nm are especially promising to overcome the BBB. Indeed, NE have proved to be excellent DDS for the sustained release of drugs with neurological action (Islam et al., 2020; Nirale et al., 2020).

Additionally, NE composed of vegetable oils can take advantage of several therapeutic properties of these natural compounds (Badea et al., 2015; Ribeiro et al., 2017b). Copaiba oil is found in Central and Western Amazonia. It is composed of a mixture of triglycerides and fat acids (Ribeiro et al., 2017b), among which copalic acid is the major compound (Souza et al., 2020). The literature shows many reports on functional copaiba oil-based NE with remarkable anti-Leishmania (Dhorm Pimentel de Moraes et al., 2018), larvicidal (Rodrigues et al., 2014), anti-inflammatory (Lucca et al., 2018) and antimicrobial (Vaucher et al., 2015) activities. Moreover, the *in vivo* biocompatibility of copaiba oil was already reported in mice and rats (Alvarenga et al., 2020; Souza et al., 2020).

Biopolymers are natural materials that have been used in biomedical applications as DDS and biosensors, and in tissue engineering and diagnoses for at least 75 years (George et al., 2020; Qureshi et al., 2020). Due to their available carboxyl groups, hydrophilic biopolymers such as dextran, pectin (PCT), alginate (ALG), pullulan and xanthan (XAN) provide systems with mucoadhesive properties, favoring the permeation of drugs across the mucous tissue (Ribeiro et al., 2018b, 2020). Polymer-lipid DDS is one of the best combinations of pharmaceutical excipients, resulting in several optimized properties (Siepmann et al., 2019). In addition, biopolymers can be added to oily phases (Shinde et al., 2011) or complexed with hydrophilic molecules (Neupane et al., 2013), improving drug upload and *in vivo* efficacy, as noticed for other alginate-based lipid nanoformulations (Severino et al., 2015; Rodrigues da Silva et al., 2020).

In this work, we prepared different functional NE composed of copaiba oil and biopolymers complexed with SMT (2%) for intranasal administration. The long-term stability of NE was monitored for a year at room temperature. The most suitable formulation was structurally characterized and tested through *in vivo* nanotoxicity assays in a zebrafish model. The promising results evinced the potential of the hybrid alginate-nanoemulsion system for future clinical applications in the treatment of acute migraine crises.

MATERIALS AND METHODS

Materials
Copaiba oil (*Copaifera langsdorffi*), Tween 20[®] (T-20), Tween 80[®] (T-80), xanthan gum from *Xanthomonas campestris* (XAN), alginate from brown algae (ALG), pectin from apple (PCT), and sumatriptan succinate (SMT) were purchased from Sigma-Aldrich (St Louis, MO, USA). Deionized water (18 mΩ) was obtained from an Elga ultrapure water purifier (Merck KGaA, Darmstadt, Germany). All other reagents were of analytical or pharmaceutical grade.

Preparation of Biopolymer-SMT Complexes
Different biopolymer-SMT (1:4; w/w) complexes were obtained by homogenization of the excipients under magnetic stirring, at 25°C for 2 h. Then, such complexes were lyophilized, resulting in XAN-SMT, ALG-SMT, and PCT-SMT powder complexes, that were subsequently used as the active molecules in the hybrid nanoemulsion preparation.

Preparation of Hybrid Nanoemulsions
Control NE were prepared as follows: the aqueous phase was obtained by adding 0.4 g T-80 plus, in which 0.05 g biopolymer (XAN, ALG or PCT) was solubilized in 10 mL of deionized water, under magnetic stirring (500 rpm), at 70°C for 10 min. The organic phase was simultaneously prepared, mixing 0.4 g T-20 and 1 g of copaiba oil, also under magnetic stirring at 70°C for 10 min. Then, the organic phase was dropped into the aqueous phase under constant agitation at the same temperature, for 10 min. The resultant copaiba oil-based emulsion was homogenized at 10,000 rpm for 3 min, using an Ultra-turrax machine (IKA® T18 basic). Finally, the microemulsion was ultrasonicated with a titanium micro-tip in a Vibracell machine (Sonics & Mat. Inc Danbury, USA) in cycles of 30 s (on/off) for 25 min (Dhorm Pimentel de Moraes et al., 2018). Finally, to prepare hybrid nanoemulsions with SMT (2%, w/v), the previously prepared, freeze-dried biopolymer-SMT complexes were added to the aqueous phase of NE, resulting in the NE/XAN-SMT, NE/ALG-SMT, and NE/PCT-SMT formulations.

Long-Term Stability Study
The long-term stability of NE formulations with and without drug was monitored by following the parameters: particle size (nm), polydispersity index (PDI), Zeta potential (mV)—measured by Dynamic Light Scattering in a ZetaSizer Nano ZS 90 (Malvern Instruments, Malvern, Worcestershire, UK), and number of nanoparticles/mL—by Nanoparticle Tracking Analysis in a *NanoSight* NS300 instrument (Malvern Instruments, Malvern, Worcestershire, UK). The samples were diluted 1:2,000 and 1:250,000 for DLS and NTA measurements, respectively, and analyzed at predetermined time intervals for 1 year at 25°C ($n = 3$).

Sumatriptan Encapsulation Efficiency (%EE)
SMT encapsulation efficiency (%EE) in the NE formulations was determined by the ultrafiltration-centrifugation method, followed by UV-vis quantification at $\lambda = 227$ nm (Agrawal et al., 2010). The concentration of SMT in the NE was determined by the difference between the non-encapsulated SMT quantified in the ultrafiltrate (free SMT) and the total amount

of added sumatriptan (SMT initial concentration). The %EE was calculated according to the following equation:

$$\%EE = A/B \, x \, 100 \tag{1}$$

where: A is the amount of encapsulated SMT, and B is the SMT initial concentration; A = B – (free SMT).

Sumatriptan *in vitro* Release Kinetics

The *in vitro* release of SMT (2%) was performed using Franz-type diffusion cells. The polycarbonate membrane was horizontally placed between the donor and acceptor compartments (area 1.77 cm^2). The donor compartment was filled with 400 µL of each sample (free SMT, NE/ALG-SMT, and NE/PCT-SMT). The acceptor compartment (4 mL) was filled with 10 mM PBS solution to ensure the sink condition and kept at 37°C, under magnetic stirring (350 rpm). At predefined time intervals and up to 24 h, aliquots of 200 µL were removed from the acceptor compartment and immediately replaced with PBS. The concentration of SMT released during the experiment was photometrically determined at 227 nm ($n = 5$) and expressed as percent SMT released.

Modeling of the kinetic curves was carried out using KinetDS 3.0 software (Mendyk and Jachowicz, 2007). Among all the tested models (zero order, first order, Higuchi, Korsmeyer-Peppas, and Weibull), the Weibull model (Equation 2) showed the highest coefficient of determination (R^2) values, for all the NE-based formulations:

$$m = 1 - exp\left[\frac{-(t)^b}{a}\right] \tag{2}$$

where: m is the concentration of SMT released at the time t, b is the release exponent, and a is the time scale of release.

Structural Characterization

FTIR-ATR, DSC, and TEM techniques were employed in the structural characterization of the excipients in nature, and the lyophilized ALG-SMT complex, NE, and NE-ALG/SMT samples.

FTIR-ATR spectra were collected by an infrared spectrometer equipped with ATR (Bruker IFS, Bruker, Billerica, MA, USA). The analyses were performed in transmittance mode, in the range of 4500–500 cm^{-1} with 2 cm^{-1} resolution. DSC thermal profiles were obtained with a TA Q20 calorimeter (TA Instruments, New Castle, DE, USA) equipped with a cooling system. Calibration was carried out using indium. The samples (5 mg) were added in aluminum pans and the spectra were detected from 0 to 200°C, at a 10°C/min heating rate, under nitrogen flow. The morphology of hybrid nanoemulsions, with and without drug, by TEM analyses was performed in a Leo 906 (Carl Zeiss, Oberkochen, Germany) transmission electron microscope, operating at 60 kV. Briefly, the samples were previously diluted (50 x) and a drop of the sample was added to the grid; after 1 min the excess was removed and a 2% uranyl solution (w/v) was added, providing contrast to the

images. After 1 min the excess volume was removed, and a drop of deionized water was added to the sample that was dried at ambient temperature. Then, micrographs of the samples were obtained at different magnifications and the ImageJ software (US Nat. Institute of Health, Bethesda, USA) was employed to calculate the nanoparticle size from the micrographs.

In vivo Zebrafish Tests

Maintenance and Spawning

Wild-type zebrafish (*Danio rerio*) were kept in tanks at a temperature of 28°C, with 14/10 light/dark cycles (Prieto et al., 2012). All embryos were collected by natural spawning and kept in Petri dishes with an E3 solution (5 mM NaCl, 0.17 mM KCl, 0.33 mM CaCl$_2$, 0.33 mM MgSO$_4$ at pH 7.0) (Kimmel et al., 1995). After 1-day post-fertilization (*dpf*), they were transferred to a 96-well-plate with an E3 medium, three eggs per well, and maintained at 28 ± 0.5°C in a 14/10 h light/dark cycle, until 5 *dpf*. The procedures performed were approved by the ethics committees of the National University of Quilmes (CE-UNQ 2/2014, CICUAL-UNQ 013-15 e 014-15).

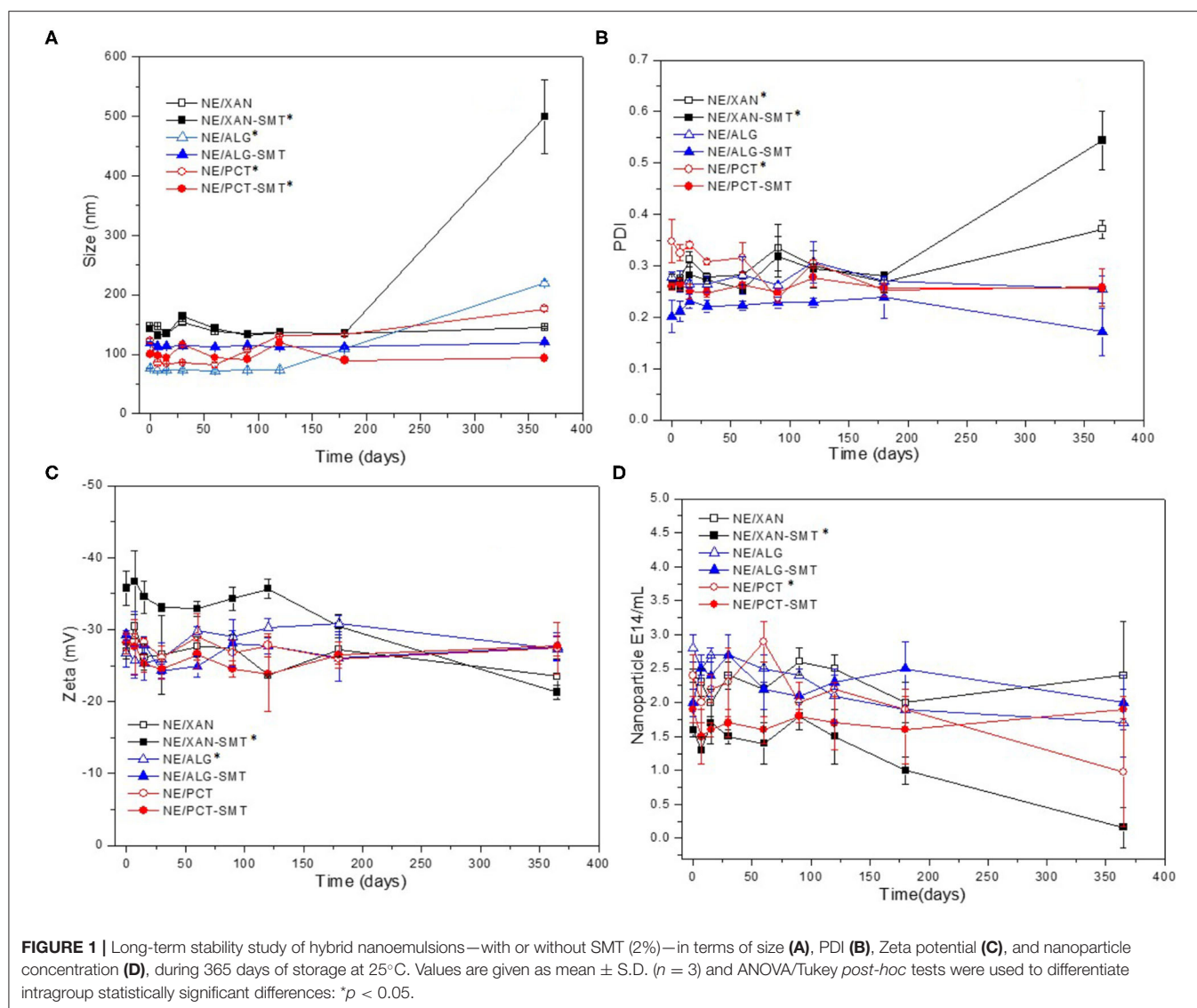### Viability and Determination of the Lethal Dose (LD$_{50}$)

Five dpf larvae were exposed to SMT, NE/ALG-SMT, and NE/ALG, all diluted in an E3 medium. As a negative control, larvae were kept only in E3. The concentrations of SMT, free or encapsulated in NE/ALG-SMT, ranged from 2×10^{-6} to 2×10^4 µg/mL. Controls prepared without SMT (NE/ALG) were used in the same particle concentrations of the NE/ALG-SMT formulation. For each assay, eight technical replicates and three biological replicates were used for each condition ($n = 24$). At 24 h post-incubation (hpi), larvae viability was observed in the stereomicroscope. Larvae were considered dead when they had no heartbeat and viability was expressed as the percentage of live larvae in relation to the control (larvae in the E3 medium). LD50 was determined as the drug concentration capable of causing the death of 50% of larvae (Martinez et al., 2019).

Heart Rate and Spontaneous Movement

For these tests, larvae were incubated at a sublethal concentration of 0.02 µg/mL SMT (SMT, NE/ALG-SMT) and NE/ALG for 24 h. Heart rate was determined by visually counting the larvae's heartbeats. The animals were immobilized on slides, placed under a stereomicroscope, and recorded in parasagittal orientation. The counting results were expressed as the percentage of beats per minute in relation to the control (larvae in the E3 medium). Spontaneous movement was analyzed in a multichannel ADC system (WMicrotracker, Designplus SRL) with infrared rays that are interrupted by the larvae's swimming activity ($n = 24$) (Igartúa et al., 2020). Spontaneous movement was expressed as the percentage of locomotor activity in relation to the control. Statistical analyses were performed with GraphPad Prism v.6.

Toxicity Analysis: Morphological Changes

For the study of morphological changes, after 24 *hpi* with the samples containing 2×10^{-6}-2×10^{-2} µg/mL µg/mL SMT, the larvae were photographed in parasagittal orientation, with 60× magnification. The photomicrographs were analyzed for

FIGURE 1 | Long-term stability study of hybrid nanoemulsions—with or without SMT (2%)—in terms of size **(A)**, PDI **(B)**, Zeta potential **(C)**, and nanoparticle concentration **(D)**, during 365 days of storage at 25°C. Values are given as mean ± S.D. ($n = 3$) and ANOVA/Tukey *post-hoc* tests were used to differentiate intragroup statistically significant differences: *$p < 0.05$.

the following morphological changes: curvature of the body, malformation of the jaw, opacity of the head, opaque liver, opacity in the yolk sac, non-depletion of the yolk sac, uninflated swimming bladder, edema, and malformation of the tail. A score was assigned to each larva based on the degree of morphological anomalies: 0 = no anomalies; 1 = one to two morphological anomalies; 2 = three to four anomalies; 3 = more than four anomalies; and 4 = dead (Martinez et al., 2019). The average toxicity score for each treatment was determined by the score of the individual larvae.

Statistical Analyses

One-way ANOVA followed by Tukey *post-hoc* multiple comparison tests were used to analyze significant differences over time of NE samples, in terms of nanoparticle size, PDI, Zeta potential and nanoparticle concentration, performed with R (version 4.0.1) analytical software. In addition, the same tests were employed to determine statistically significant differences

between free sumatriptan and hybrid nanoemulsion, in the *in vivo* zebrafish model, regarding different parameters: viability, heart rate, spontaneous movement, and morphological changes. The significance level was defined as 5% ($p < 0.05$).

RESULTS

As a first approach, different complexes of biopolymer-SMT (1:4 w/w) were prepared in order to improve drug loading in copaiba oil-based nanoparticles. Then, copaiba oil-based NE formulations, containing or not the biopolymer-SMT complexes, were successfully prepared and stored for a year at room temperature.

Long-Term Stability Study

Hybrid NE formulations either containing or not containing SMT (2%) were monitored in the long-term stability study. The parameters analyzed for a year (25°C) were: size (nm), PDI,

TABLE 1 | Sumatriptan (2%) encapsulation efficiency (%EE) in NE (without biopolymer in the composition) and in the hybrid biopolymer-NE formulations.

Formulations	%EE
NE/SMT	10.30 ± 4.52
NE/XAN-SMT	69.08 ± 7.92
NE/ALG-SMT	42.65 ± 1.04
NE/PCT-SMT	41.63 ± 12.20

Values as mean ± S.D. (n = 3).

XAN, 0.5% xanthan; ALG, 0.5 % alginate; PCT, 0.5% pectin.

Zeta potential (mV), and nanoparticle concentration/mL (**Figure 1**). In general, initial particle size ranged from 76 to 148 nm (**Figure 1A**), with PDI values around 0.25 (**Figure 1B**), zeta potential from -26 to -35 mV (**Figure 1C**), and number of particles of 1.6–2.9 10^{14}/mL (**Figure 1D**), for all NE.

NE/XAN-SMT exhibited statistically significant differences ($p < 0.05$) in all parameters tested after a year. NE/ALG-SMT was the only system that did not show any statistically significant difference ($p > 0.05$) after 365 days of storage, in any of the analyzed parameters. NE/PCT-SMT showed a significant increase in particle size ($p < 0.05$) at the end of the experiment. Taking into account such results, NE-XAN/SMT was excluded from subsequent (kinetic release and *in vivo*) experiments.

Encapsulation Efficiency Test

SMT encapsulation efficiency (%EE) in the formulations is listed in **Table 1**. The hybrid NE formulations showed %EE values in the range of 41–69%, while NE/SMT encapsulated only *ca.* 10% of the drug.

Figure 2 shows the *in vitro* release profiles of SMT, free (control) or encapsulated in NE/ALG-SMT or NE/PCT-SMT. In the second hour of testing, SMT and NE samples discharged around 98 and 60%, respectively. After 5 h, SMT reached 100% of release in the acceptor compartment, while both hybrid NE released around 80% only after 24 h.

Mathematical modeling of NE kinetics was carried out using KinetDS 3.0 software. The best model was selected based on the highest coefficient of determination (R^2). For SMT in solution, Higuchi was the best-fitted model, while the release kinetics of SMT in NE/ALG-SMT and NE/PCT-SMT was better described by the Weibull model (**Table 2**). The shape of the release curve (b-values) in the Weibull equation describes the mechanism of drug release. Here, the $b < 1$ values revealed a biphasic SMT release profile for both hybrid NE formulations (Papadopoulou et al., 2006).

Taking into account the long-term stability study, %EE and *in vitro* SMT release results, NE/ALG-SMT was selected as the most desirable formulation. Therefore, the structural characterization and *in vivo* nanotoxicity assays (zebrafish larvae model) were performed for NE/ALG-SMT, NE/ALG, and free SMT samples.
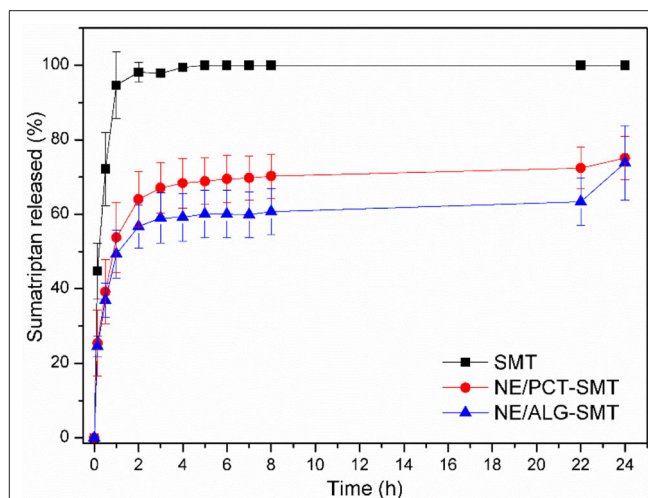
FIGURE 2 | *In vitro* release kinetics of SMT, in solution or encapsulated in hybrid NE formulations, at 37°C, for 24 h. Data expressed as mean ± S.D. ($n = 5$).

TABLE 2 | Mathematical modeling of release kinetic curves by the Weibull model.

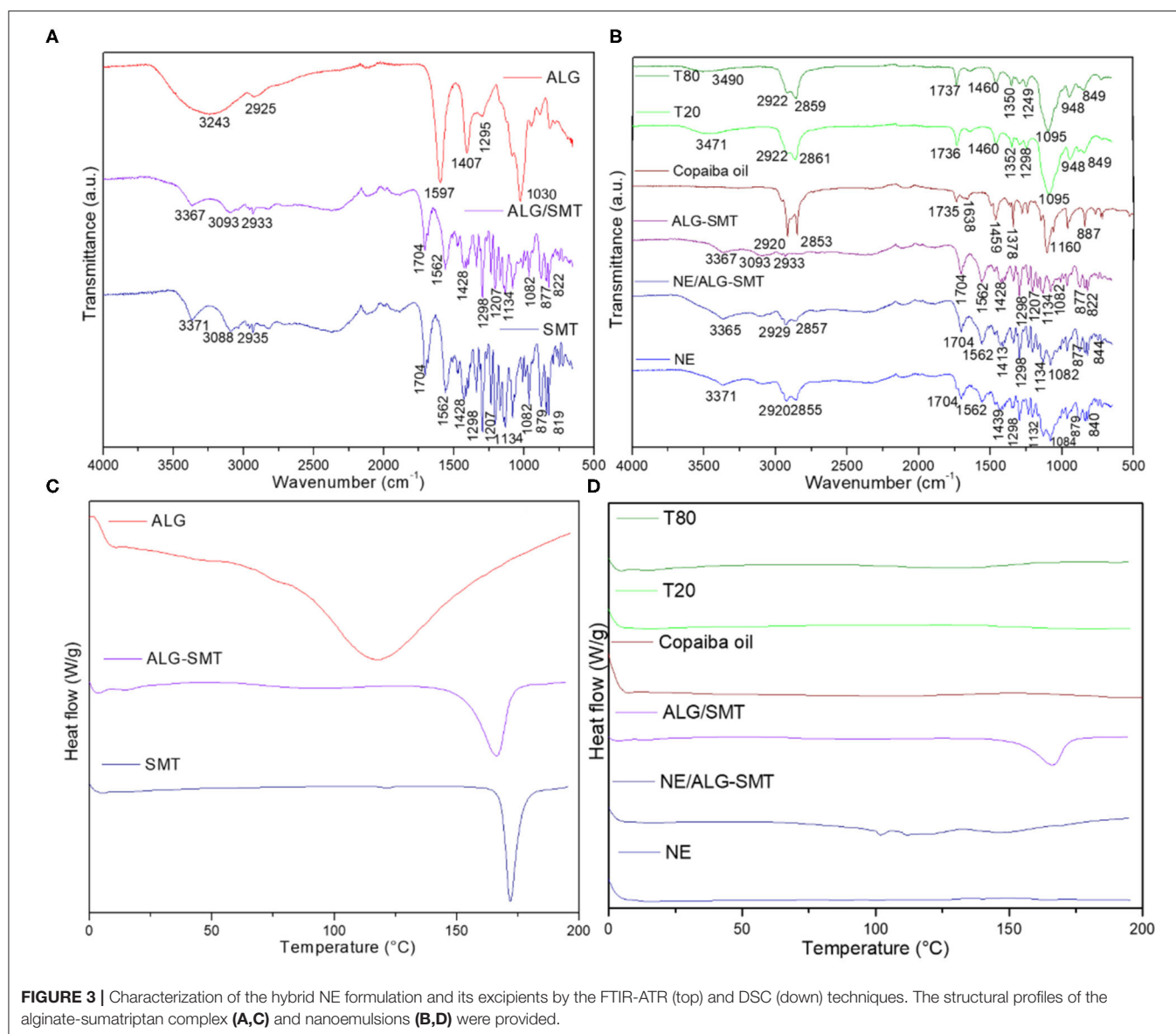| Nanoemulsion	Weibull	
	R^2	b
NE/PCT-SMT	0.92	0.22
NE/ALG-SMT	0.96	0.27

R^2, coefficient of determination; b, shape of release curve.

Structural Characterization

The hybrid alginate-based NE containing or not SMT (NE/ALG-SMT and NE/ALG, respectively) were characterized using FTIR-ATR, DSC, and TEM techniques.

Figure 3A shows the spectroscopic profile of the pure ALG, SMT, and ALG-SMT complex. Typical SMT bands were observed at 3371, 3088, 1298, 1207, and 1134 cm^{-1}, ascribed to the stretching of -NH, C-H, sulfonamide, tertiary amine, and O-H (Galgatte et al., 2014), respectively, in the SMT spectrum. The spectrum of pure ALG displayed bands centered at 3243, 1587, 1407, and 1030 cm^{-1} assigned to O-H, -COO, -COO, and C-O-C stretching, respectively (Ribeiro et al., 2014). The ALG-SMT complex exhibited a spectroscopic profile similar to that of the SMT spectrum, where the SMT amine band (3371 cm^{-1}) was shifted to 3367 cm^{-1}. In addition, the broad band stretching band of -OH (3243 cm^{-1}) from alginate was not detected in the complexed ALG-SMT spectrum.

Figure 3B features the FTIR-ATR spectra of the excipients, NE and NE/ALG-SMT formulations. NE (with and without SMT) spectra revealed bands in the regions of 2920–2929, 2855–2857, and 1132–1134 cm^{-1}, corresponding to the stretching of CH, O-CH$_2$, and C=O (Ribeiro et al., 2014), respectively. The spectrum of copaiba oil revealed bands centered at 2920, 2853, 1735, and 1160 cm^{-1}, corresponding to CH, O-CH$_2$, C=O, and C=O stretching, respectively (Ribeiro et al., 2017b). In addition, the

FIGURE 3 | Characterization of the hybrid NE formulation and its excipients by the FTIR-ATR (top) and DSC (down) techniques. The structural profiles of the alginate-sumatriptan complex **(A,C)** and nanoemulsions **(B,D)** were provided.

bands observed between 3365 and 3371 cm^{-1} in both NE and NE/ALG-SMT spectra are attributed to the interaction of copaiba oil with the hydroxyl groups of surfactants and biopolymer (Yu et al., 2012; Norcino et al., 2020).

Figure 3C features the thermodynamic transitions of the ALG-SMT complex, ALG, and SMT. It can be observed that the ALG-SMT complex showed an endothermic peak centered at 166°C, slightly lower than the melting point of pure SMT (172°C) (Galgatte et al., 2014) (**Figure 3C**). The melting point of the alginate (117°C) (Rodrigues da Silva et al., 2020) was not detected in the DSC analysis of the biopolymer-drug complex. **Figure 3D** shows the thermal profile of the excipients, NE, and NE/ALG, with or without SMT. All excipients (T-80, T-20, copaiba oil) were liquid at room temperature, and therefore did not show any thermodynamic transition in the analysis. Furthermore, there is no evidence of any peak of sample degradation up to 200°C.

The micrographs of **Figure 4** confirmed the spherical morphology of the nanoparticles and their narrow size distribution, as expected for this system (Kelmann et al., 2007). The incorporation of the ALG-SMT complex in NE did not interfere with the integrity and morphology of the nanoparticles. The particle sizes (around 94 and 123 nm for NE/ALG and NE/ALG-SMT, respectively) calculated from the micrographies using the ImageJ software were also in agreement with DLS data (**Figure 1A**).

In vivo Zebrafish Tests

The first test performed on a zebrafish model was the determination of the dose capable of causing the death of 50% of larvae (LD$_{50}$). The results found after 24 h post-incubation are given in **Figure 5A**. While free SMT showed LD$_{50}$ = 3288 μg/mL, the NE-ALG/SMT formulation decreased

DISCUSSION

The development of innovative nanostructured formulations aiming at the sustained release of active molecules requires satisfactory physicochemical properties, long-term stability, and biocompatibility (de Araújo et al., 2019; de Paula et al., 2020). Therefore, such features were pursued here.

It is essential to monitor some structural parameters of nanoparticles, such as particle size homogeneity and Zeta potential values to ensure quality control of pharmaceutical products (Attama et al., 2012). Nanoparticle disruption, coalescence, or degradation in colloids directly affect their potential as DDS. Thus, a novel *in vitro* biophysical method, called Nanoparticle Tracking Analysis (NTA), has been useful as an analytical method for nanoparticles (Filipe et al., 2010). In addition to the easy, fast, and reliable determination of particle size and polydispersity (Span index) of samples, this technique provides a unique piece of information, the number of nanoparticles in a known volume, without being affected by sample polydispersity or particle morphology (Ribeiro et al., 2018a).

NE-based XAN loading SMT was stable for only 6 months. After this period, average particle size (measured by DLS) increased significantly, followed by an abrupt decrease in the number of particles (measured by NTA). The strong negative correlation between these two parameters over time and measured by distinct techniques was already proposed by us as an instability indicator of colloids (Ribeiro et al., 2018a). NE/ALG-SMT was the only formulation that did not show significant changes in any of the analyzed parameters during long-term (365 days) storage. In addition, considering that the zeta potential is a parameter related with the non-colloidal stability, the highly negative values observed in here (−36 mV) confirmed the shelf-time of hybrid nanoemulsion (Honary and Zahir, 2013). In fact, ALG is the most successful biopolymer used as a carrier, absorption enhancer or adjuvant for DDS (Guo et al., 2020; Kuznetsova et al., 2020), as well as the polymer counterpart of organic-organic DDS (Ribeiro et al., 2017a; Siepmann et al., 2019).

The complexation of SMT with different biopolymers prior to NE preparation aimed to improve loading in copaiba oil nanoparticles. Such strategy has been previously described for modulating the hydrophilicity of other drugs encapsulated in lipid nanoparticles (Olbrich et al., 2004; Severino et al., 2015). In fact, all drug-biopolymer complexes were satisfactorily solubilized in the organic (nanoemulsion) phase, resulting in a DDS of higher SMT upload capacity than oily nanoparticles. Synergistically, such biopolymers impart an additional property to the system: mucoadhesion (Ribeiro et al., 2018b, 2020; Rodrigues da Silva et al., 2020), which is highly desirable for intranasal formulations.

Moreover, prolonged *in vitro* SMT release was observed for both NE/ALG-SMT and NE/PCT-SMT in comparison to free SMT. In addition, a burst release effect was observed for both NE in the first 2 h of analysis, which is desirable for pain management drugs (Franz-Montan et al., 2017a). The non-encapsulated fraction of SMT ensured the immediate onset
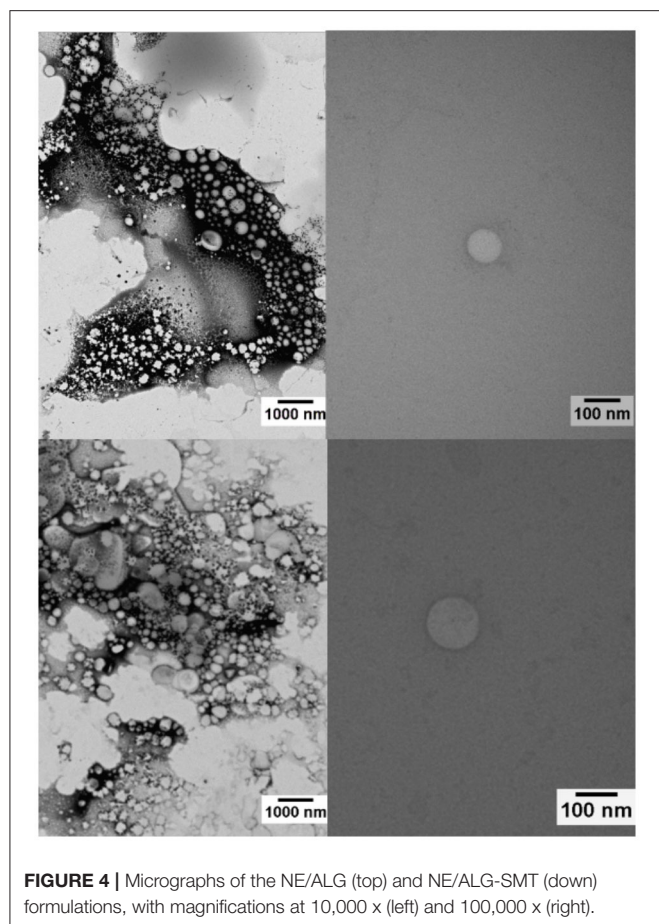

FIGURE 4 | Micrographs of the NE/ALG (top) and NE/ALG-SMT (down) formulations, with magnifications at 10,000 x (left) and 100,000 x (right).

this concentration to 0.2 μg/mL. A sublethal dose was then chosen in order to evaluate the action of the formulations on the target tissues (cardiac and neuronal). It is important to consider that the hybrid system without SMT (NE-ALG) also showed LD_{50} at a concentration equivalent to 0.6 μg/mL of SMT in the NE-ALG/SMT, or 3×10^{-4} mg/mL of copaiba oil or 6×10^8 particles/mL.

Thus, heart rate (**Figure 5B**) and spontaneous movement (**Figure 5C**) were determined. Heart rate did not change in relation to the control when the larvae were incubated with free SMT. However, NE-ALG and NE-ALG/SMT decreased heart rate by 10 and 20%, respectively. Regarding the spontaneous movement of zebrafish larvae, a slight increase of 8% and >20% was observed for NE-ALG and NE-ALG/SMT, respectively, in relation to free SMT. In addition, to identify any possible systemic toxicity in larvae, several morphological parameters (as described in methods) were analyzed, and the mean score of each formulation is shown in **Figure 5D**, with representative images of the analyzed larvae in **Figure 5E**. The results show that in the tested concentrations, none of the formulations showed significant toxic effects, not reaching the score of 1. That is, <1 change was registered per larva, indicating systemic non-toxicity of the formulations.
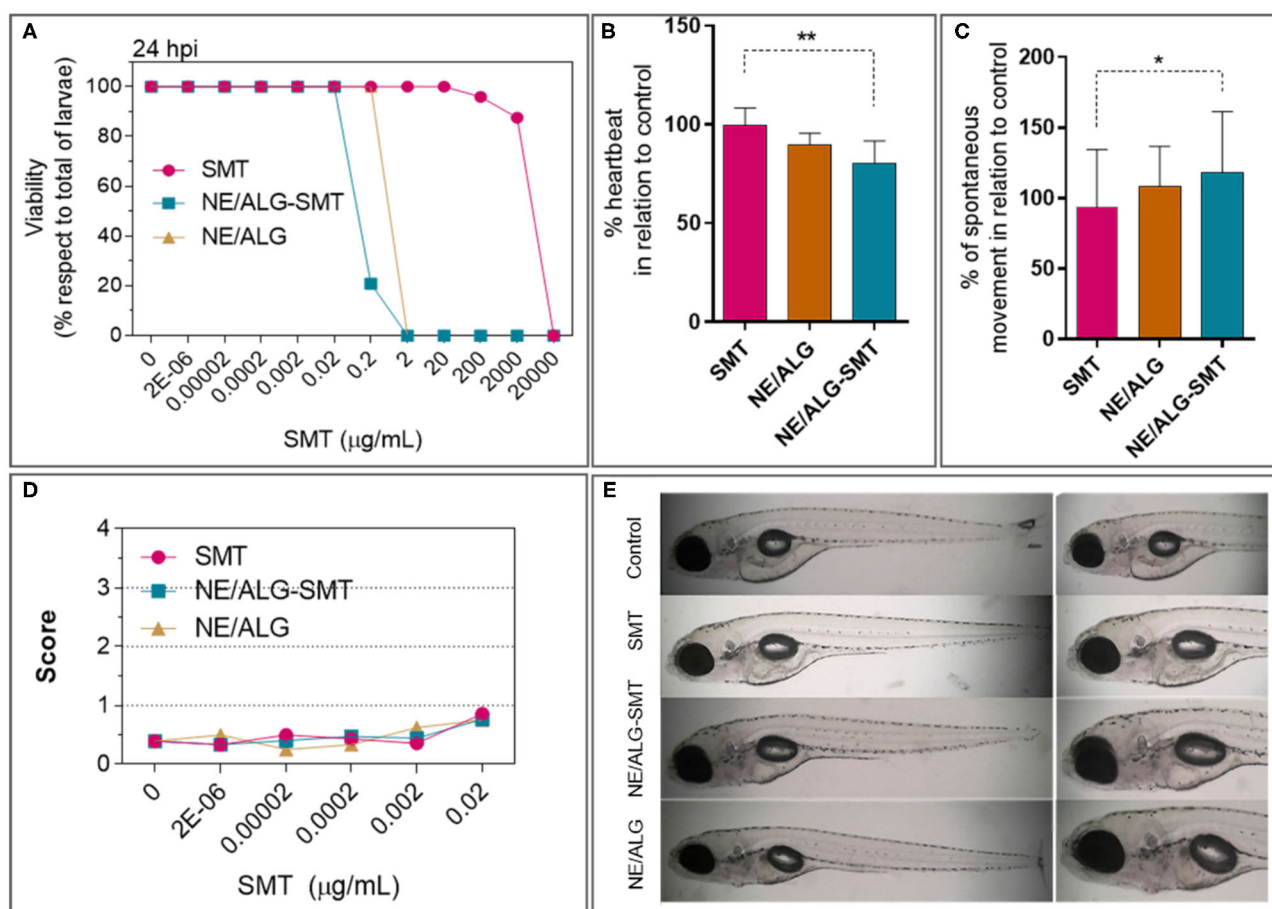
FIGURE 5 | (A) Viability of zebrafish larvae after 24 h of exposure (*hpi*) to: sumatriptan in an aqueous solution (SMT), sumatriptan incorporated in the hybrid system (NE/ALG-SMT); control nanoemulsion without sumatriptan (NE/ALG). **(B)** Percentual variation of heart rate, in relation to control. **(C)** Percentual variation of spontaneous movement, compared to control. **(D)** Toxicological test: score of morphological changes after 24 *hpi*. **(E)** Representative images of the analyzed larvae after 24 *hpi*. Score: 0 = no changes; 1 = one to two morphological anomalies; 2 = three to four anomalies; 3 = more than four anomalies; and 4 = dead. Anova *post-hoc* Tukey test: *p <0.05; **p <0.01.

of analgesia, followed by a sustained release of SMT loaded by copaiba oil nanoparticles. This biphasic release profile of NE is a consequence of its complex composition and unique supramolecular organization.

In this sense, the structural characterization of pharmaceutical products provided information of their molecular arrangement, as well as the possible interactions between the carriers and the drugs (Muniz et al., 2018). Here, FTIR-ATR, DSC, and TEM analyses evidenced the compatibility among all the components of the hybrid system. As expected, the ALG-SMT complex exhibited a similar spectroscopic profile to pure SMT, since there was 4 times more SMT than the biopolymer in the complex. In addition, the absence of the broad hydroxyl band from alginate and the shift of the SMT amine band to smaller wavenumbers in the ALG-SMT spectrum is indicative of electrostatic interactions taking place between the free amine of SMT and alginate carboxylic groups. Evidence of such interactions was also observed by DSC analyses, from the slight decrease of the SMT melting point in the ALG-SMT complex.

On the other hand, all NE spectra showed the typical spectroscopic profile of the lipid nanocarrier, reflecting the major contribution of copaiba oil to the NE structure (Ribeiro et al., 2017b). Thermal analyses also confirmed the compatibility of the excipients in NE/ALG-SMT. There was no evidence of a degradation peak in the NE/ALG-SMT thermal profile, suggesting interaction between the complex and NE with thermal stability to at least 200°C. Considering the physiological temperature range, around 35–37°C, these results indicated that NE can be applied as DDS without unexpected calorimetric transitions (Franz-Montan et al., 2017b).

The zebrafish model has emerged as an important preclinical tool to evaluate drugs and DDS (Berghmans et al., 2008; Fako and Furgeson, 2009; Haque and Ward, 2018; Jia et al., 2019). Practicality, low cost, quick testing of various parameters and good predictability with humans (>75%) are some of the factors that evidenced the importance of this model for nanotoxicity tests (Parng et al., 2002). Moreover, zebrafish larvae are transparent, which allows *in vivo* temporal imaging. In

addition, the cardiovascular, nervous, and digestive systems are physiologically similar to mammals (Martinez et al., 2017). Specifically regarding the nervous system, it has been reported that the physiology of serotonergic neurotransmitters in zebrafish is similar to that of humans (Nowicki et al., 2014), with the development of BBB after 3 *dpf* (Eliceiri et al., 2011), thus being a coherent model for testing SMT (5HT1B and 5HT1D serotonin receptor agonist).

A particularity of the zebrafish model in relation to other models is the route of administration. In zebrafish, the larvae are exposed directly to the formulations in the bath solution. Thus, different pathways (gastrointestinal, dermal, etc.) can occur simultaneously in the larvae (van Pomeren et al., 2017). The viability results obtained revealed that high doses of free SMT are required to induce any effect on the larvae, as expected from its limited bioavailability. Conversely, NE/ALG-SMT showed the highest effect on larvae, which can be explained by the improvement of SMT bioavailability, as proposed in a recent review (Jia et al., 2019). This review showed that use of the zebrafish model to evaluate nanomaterials resulted in improved effectiveness of the encapsulated drug. Thus, the decrease in LD_{50} values of NE/ALG-SMT compared to free SMT is a strong indication of enhanced SMT delivery from NE/ALG-SMT. Moreover, it was no surprise that NE/ALG, composed of copaiba oil, had an effect on the larvae. Copaiba oil has exhibited several intrinsic therapeutic properties, such as analgesia (Gomes et al., 2007). However, when SMT is loaded in NE (despite only %EE 40%), the effect on viability is enhanced, indicating that encapsulated SMT had a higher impact on larval physiology.

In order to validate such a hypothesis, heart rate and spontaneous movement (reflecting the effects on the cardiac and nervous system, respectively) were analyzed. In both tests, SMT encapsulation potentiated the decrease of heart rate or the increase of spontaneous movement. These results confirmed the efficient delivery of SMT from NE/ALG-SMT, reaching these targets more efficiently. The changes in heart rate observed after treatment with free SMT should be correlated with its action in blood vessels (Caekebeke et al., 1992; Hack, 2004). In addition, copaiba oil was responsible for a decrease in larval heartbeat in NE/ALG by acting on opioid receptors (Leandro et al., 2012). Similar to the spontaneous movement results, the increase in larval movement when treated with encapsulated SMT should be a result of somatosensory discomfort, as already reported, e.g., discomfort to touch (Krämer et al., 2007).

Although these results indicated higher SMT bioavailability and synergy with copaiba oil effects in NE/ALG-SMT, no other systemic change was noticed in the tested doses, confirming the low toxicity of NE/ALG-SMT. Even though the zebrafish model does not reproduce the intended administration route (intranasal), it provided relevant insights into the bioavailability of SMT loading in NE, confirming the promising strategy to improve antimigraine triptan delivery.

CONCLUSIONS

This work aimed at the development of hybrid nanoemulsions composed of copaiba oil and biopolymers for the loading of sumatriptan (2%) for intranasal administration. Firstly, the drug was complexed with different biopolymers to decrease its hydrophilicity and increase its upload by the copaiba oil-based nanoparticles. Then, those complexes were used as active molecules in NE. The NE/ALG-SMT formulation was stable for a year and prolonged *in vitro* SMT release for more than 24 h. Structural characterization revealed the singular supramolecular arrangement of NE, with electrostatic interactions detected between the biopolymer and SMT, plus hydrogen bonds between the complex and copaiba oil-nanoparticles. Finally, the *in vivo* nanotoxicity assays showed that NE/ALG-SMT was not toxic to zebrafish larvae in any of the analyzed parameters. Therefore, the nanoemulsion composed of copaiba oil plus alginate (0.5%) and sumatriptan (2%) is ready to be tested for *in vivo* efficacy in humans and subsequent clinical trials, aiming at migraine pain management.

DATA AVAILABILITY STATEMENT

The raw data supporting the conclusions of this article will be made available by the authors, without undue reservation.

ETHICS STATEMENT

The animal study was reviewed and approved by Ethics committees of the National University of Quilmes, Argentina.

AUTHOR CONTRIBUTIONS

FUNDING

ACKNOWLEDGMENTS

REFERENCES

Agrawal, V., Gupta, V., Ramteke, S., and Trivedi, P. (2010). Preparation and evaluation of tubular micelles of pluronic lecithin organogel for transdermal delivery of sumatriptan. *AAPS PharmSciTech* 11, 1718–1725. doi: 10.1208/s12249-010-9540-7

Alvarenga, M. O. P., Bittencourt, L. O., Mendes, P. F. S., Ribeiro, J. T., Lameira, O. A., Monteiro, M. C., et al. (2020). Safety and effectiveness of copaiba oleo resin

(*C. reticulata* Ducke) on inflammation and tissue repair of oral wounds in rats. *Int. J. Mol. Sci.* 21:3568. doi: 10.3390/ijms21103568

Attama, A. A., Momoh, M. A., and Builders, P. F. (2012). "Lipid nanoparticulate drug delivery systems: a revolution in dosage form design and development," in *Recent Advances in Drug Delivery Systems*, eds J. M. Anderson and S. W. Kim (London: Plenum Press). p. 106–140.

Badea, G., Lacatusu, I., Badea, N., Ott, C., and Meghea, A. (2015). Use of various vegetable oils in designing photoprotective nanostructured formulations for UV protection and antioxidant activity. *Ind. Crops Prod.* 67, 18–24. doi: 10.1016/j.indcrop.2014.12.049

Berghmans, S., Butler, P., Goldsmith, P., Waldron, G., Gardner, I., Golder, Z., et al. (2008). Zebrafish based assays for the assessment of cardiac, visual and gut function — potential safety screens for early drug discovery. *J. Pharmacol. Toxicol. Methods* 58, 59–68. doi: 10.1016/j.vascn.2008.05.130

Caekebeke, J. F. V., Ferrari, M. D., Zwetsloot, C. P., Jansen, J., and Saxena, P. R. (1992). Antimigraine drug sumatriptan increases blood flow velocity in large cerebral arteries during migraine attacks. *Neurology* 42, 1522–1526. doi: 10.1212/WNL.42.8.1522

de Araújo, D. R., Ribeiro, L. N. M., and de Paula, E. (2019). Lipid-based carriers for the delivery of local anesthetics. *Expert Opin. Drug Deliv.* 16, 1–14. doi: 10.1080/17425247.2019.1629415

de Paula, E., Lima, F. F., Oliveira, J. D., and Ribeiro, L. N. M. (2020). "Liposome-based delivery of therapeutic agents," in *Controlled Drug Delivery Systems*, ed E. C. Opara (Boca Raton, FL: CRC press Taylor & Francis), 297–323. Available online at: https://bookshelf.vitalsource.com/books/9780429582752. doi: 10.1201/9780429197833-16

Deen, M., Hougaard, A., Hansen, H. D., Schain, M., Dyssegaard, A., Knudsen, G. M., et al. (2019). Association between sumatriptan treatment during a migraine attack and central 5-HT 1B receptor binding. *JAMA Neurol.* 76, 834–840. doi: 10.1001/jamaneurol.2019.0755

Dhorm Pimentel de Moraes, A. R., Tavares, G. D., Soares Rocha, F. J., de Paula, E., and Giorgio, S. (2018). Effects of nanoemulsions prepared with essential oils of copaiba- and andiroba against Leishmania infantum and leishmania amazonensis infections. *Exp. Parasitol.* 187, 12–21. doi: 10.1016/j.exppara.2018.03.005

Eliceiri, B. P., Gonzalez, A. M., and Baird, A. (2011). Zebrafish model of the blood-brain barrier: morphological and permeability studies. *Methods Mol. Biol.* 686, 371–378. doi: 10.1007/978-1-60761-938-3_18

Fako, V. E., and Furgeson, D. Y. (2009). Zebrafish as a correlative and predictive model for assessing biomaterial nanotoxicity. *Adv. Drug Deliv. Rev.* 61, 478–486. doi: 10.1016/j.addr.2009.03.008

Filipe, V., Hawe, A., and Jiskoot, W. (2010). Critical evaluation of nanoparticle tracking analysis (NTA) by nanosight for the measurement of nanoparticles and protein aggregates. *Pharm. Res.* 27, 796–810. doi: 10.1007/s11095-010-0073-2

Franz-Montan, M., de Araújo, D. R., Ribeiro, L. N. M., de Melo, N. F. S., and de Paula, E. (2017a). "Nanostructured systems for transbuccal drug delivery," in *Nanostructures for Oral Medicine*, eds. E. Andronescu and A. Grumezescu (Amsterdam: Elsevier), 87–114. doi: 10.1016/B978-0-323-47720-8.00005-5

Franz-Montan, M., Ribeiro, L. N. M., Volpato, M. C., Cereda, C. M., Groppo, F. C., Tofoli, G. R., et al. (2017b). Recent advances and perspectives in topical oral anesthesia. *Expert Opin. Drug Deliv.* 14, 673–684. doi: 10.1080/17425247.2016.1227784

Galgatte, U. C., Kumbhar, A. B., and Chaudhari, P. D. (2014). Development of *in situ* gel for nasal delivery: Design, optimization, *in vitro* and *in vivo* evaluation. *Drug Deliv.* 21, 62–73. doi: 10.3109/10717544.2013.849778

George, A., Sanjay, M. R., Srisuk, R., Parameswaranpillai, J., and Siengchin, S. (2020). A comprehensive review on chemical properties and applications of biopolymers and their composites. *Int. J. Biol. Macromol.* 154, 329–338. doi: 10.1016/j.ijbiomac.2020.03.120

Gomes, N. M., Rezende, C. M., Fontes, S. P., Matheus, M. E., and Fernandes, P. D. (2007). Antinociceptive activity of amazonian copaiba oils. *J. Ethnopharmacol.* 109, 486–492. doi: 10.1016/j.jep.2006.08.018

Guo, X., Wang, Y., Qin, Y., Shen, P., and Peng, Q. (2020). Structures, properties and application of alginic acid: a review. *Int. J. Biol. Macromol.* 162, 618–628. doi: 10.1016/j.ijbiomac.2020.06.180

Hack, J. B. (2004). Oral sumatriptan-induced myocardial infarction. *J. Toxicol. Clin. Toxicol.* 42, 309–311. doi: 10.1081/CLT-120037434

Haque, E., and Ward, A. C. (2018). Zebrafish as a model to evaluate nanoparticle toxicity. *Nanomaterials* 8:561. doi: 10.3390/nano8070561

Honary, S., and Zahir, F. (2013). Effect of zeta potential on the properties of nano-drug delivery systems - a review (Part 2). *Trop. J. Pharm. Res.* 12:265. doi: 10.4314/tjpr.v12i2.19

Igartúa, D. E., Martinez, C. S., Alonso, S. V., and Prieto, M. J. (2020). Combined therapy for alzheimer's disease: tacrine and PAMAM dendrimers co-administration reduces the side effects of the drug without modifying its activity. *AAPS PharmSciTech* 21:110. doi: 10.1208/s12249-020-01652-w

Islam, S. U., Shehzad, A., Ahmed, M. B., and Lee, Y. S. (2020). Intranasal delivery of nanoformulations: a potential way of treatment for neurological disorders. *Molecules* 25:1929. doi: 10.3390/molecules25081929

Jia, H. R., Zhu, Y. X., Duan, Q. Y., Chen, Z., and Wu, F. G. (2019). Nanomaterials meet zebrafish: toxicity evaluation and drug delivery applications. *J. Control. Release* 311–312, 301–318. doi: 10.1016/j.jconrel.2019.08.022

Kelmann, R. G., Kuminek, G., Teixeira, H. F., and Koester, L. S. (2007). Carbamazepine parenteral nanoemulsions prepared by spontaneous emulsification process. *Int. J. Pharm.* 342, 231–239. doi: 10.1016/j.ijpharm.2007.05.004

Kimmel, C. B., Ballard, W. W., Kimmel, S. R., Ullmann, B., and Schilling, T. F. (1995). Stages of embryonic development of the zebrafish. *Dev. Dyn.* 203, 253–310. doi: 10.1002/aja.1002030302

Krämer, H. H., Lundblad, L., Birklein, F., Linde, M., Karlsson, T., Elam, M., et al. (2007). Activation of the cortical pain network by soft tactile stimulation after injection of sumatriptan. *Pain* 133, 72–78. doi: 10.1016/j.pain.2007.03.001

Kuznetsova, T. A., Andryukov, B. G., Besednova, N. N., Zaporozhets, T. S., and Kalinin, A. V. (2020). Marine algae polysaccharides as basis for wound dressings, drug delivery, and tissue engineering: a review. *J. Mar. Sci. Eng.* 8:481. doi: 10.3390/jmse8070481

Leandro, L. M., de Sousa Vargas, F., Barbosa, P. C. S., Neves, J. K. O., da Silva, J. A., and da Veiga-Junior, V. F. (2012). Chemistry and biological activities of terpenoids from copaiba (copaifera spp.) oleoresins. *Molecules* 17, 3866–3889. doi: 10.3390/molecules17043866

Lucca, L. G., de Matos, S. P., Kreutz, T., Teixeira, H. F., Veiga, V. F., de Araújo, B. V., et al. (2018). Anti-inflammatory effect from a hydrogel containing nanoemulsified copaiba oil (copaifera multijuga hayne). *AAPS PharmSciTech* 19, 522–530. doi: 10.1208/s12249-017-0862-6

Martinez, C. S., Igartúa, D. E., Calienni, M. N., Feas, D. A., Siri, M., Montanari, J., et al. (2017). Relation between biophysical properties of nanostructures and their toxicity on zebrafish. *Biophys. Rev.* 9, 775–791. doi: 10.1007/s12551-017-0294-2

Martinez, C. S., Igartúa, D. E., Czarnowski, I., Feas, D. A., Alonso, S. V., and Prieto, M. J. (2019). Biological response and developmental toxicity of zebrafish embryo and larvae exposed to multi-walled carbon nanotubes with different dimension. *Heliyon* 5:e02308. doi: 10.1016/j.heliyon.2019.e02308

Mendyk, A., and Jachowicz, R. (2007). Unified methodology of neural analysis in decision support systems built for pharmaceutical technology. *Expert Syst. Appl.* 32, 1124–1131. doi: 10.1016/j.eswa.2006.02.019

Muniz, B. V., Baratelli, D., Di Carla, S., Serpe, L., da Silva, C. B., Guilherme, V. A., et al. (2018). Hybrid hydrogel composed of polymeric nanocapsules co-loading lidocaine and prilocaine for topical intraoral anesthesia. *Sci. Rep.* 8:17972. doi: 10.1038/s41598-018-36382-4

Muzzi, M., Zecchi, R., Ranieri, G., Urru, M., Tofani, L., De Cesaris, F., et al. (2020). Ultra-rapid brain uptake of subcutaneous sumatriptan in the rat: implication for cluster headache treatment. *Cephalalgia* 40, 330–336. doi: 10.1177/0333102419896370

Natoli, J., Manack, A., Dean, B., Butler, Q., Turkel, C., Stovner, L., et al. (2010). Global prevalence of chronic migraine: a systematic review. *Cephalalgia* 30, 599–609. doi: 10.1111/j.1468-2982.2009.01941.x

Neupane, Y. R., Sabir, M. D., Ahmad, N., Ali, M., and Kohli, K. (2013). Lipid drug conjugate nanoparticle as a novel lipid nanocarrier for the oral delivery of decitabine: *ex vivo* gut permeation studies. *Nanotechnology* 24:415102. doi: 10.1088/0957-4484/24/41/415102

Nirale, P., Paul, A., and Yadav, K. S. (2020). Nanoemulsions for targeting the neurodegenerative diseases: alzheimer's, parkinson's and prion's. *Life Sci.* 245:117394. doi: 10.1016/j.lfs.2020.117394

Norcino, L. B., Mendes, J. F., Natarelli, C. V. L., Manrich, A., Oliveira, J. E., and Mattoso, L. H. C. (2020). Pectin films loaded with copaiba oil nanoemulsions

for potential use as bio-based active packaging. *Food Hydrocoll.* 106:105862. doi: 10.1016/j.foodhyd.2020.105862

Nowicki, M., Tran, S., Muraleetharan, A., Markovic, S., and Gerlai, R. (2014). Serotonin antagonists induce anxiolytic and anxiogenic-like behavior in zebrafish in a receptor-subtype dependent manner. *Pharmacol. Biochem. Behav.* 126, 170–180. doi: 10.1016/j.pbb.2014.09.022

Olbrich, C., Gessner, A., Schröder, W., Kayser, O., and Müller, R. H. (2004). Lipid-drug conjugate nanoparticles of the hydrophilic drug diminazene - cytotoxicity testing and mouse serum adsorption. *J. Control. Release* 96, 425–435. doi: 10.1016/j.jconrel.2004.02.024

Papadopoulou, V., Kosmidis, K., Vlachou, M., and Macheras, P. (2006). On the use of the weibull function for the discernment of drug release mechanisms. *Int. J. Pharm.* 309, 44–50. doi: 10.1016/j.ijpharm.2005.10.044

Parng, C., Seng, W. L., Semino, C., and McGrath, P. (2002). Zebrafish: a preclinical model for drug screening. *Assay Drug Dev. Technol.* 1, 41–48. doi: 10.1089/154065802761001293

Pascual, J., and Muñoz, P. (2005). Correlation between lipophilicity and triptan outcomes. *Headache J. Head Face Pain* 45, 3–6. doi: 10.1111/j.1526-4610.2005.05003.x

Prieto, M. J., Gutierrez, H. C., Arévalo, R. A., Chiaramoni, N. S., and Alonso, S. V. (2012). Effect of risperidone and fluoxetine on the movement and neurochemical changes of zebrafish. *Open J. Med. Chem.* 02, 129–138. doi: 10.4236/ojmc.2012.24016

Qureshi, D., Nayak, S. K., Anis, A., Ray, S. S., Kim, D., Hanh Nguyen, T. T., et al. (2020). "Introduction of biopolymers," in *Biopolymer-Based Formulations*, eds K. Pal, I. Banerjee, P. Sarkar, D. Kim, W.-P. Deng, N. K. Dubey, and K. Majumder (Amsterdam: Elsevier), 1–45. doi: 10.1016/B978-0-12-816897-4.00001-1

Rai, V. K., Mishra, N., Yadav, K. S., and Yadav, N. P. (2018). Nanoemulsion as pharmaceutical carrier for dermal and transdermal drug delivery: formulation development, stability issues, basic considerations and applications. *J. Control. Release* 270, 203–225. doi: 10.1016/j.jconrel.2017.11.049

Ribeiro, L. N. M., Alcântara, A. C. S., Darder, M., Aranda, P., Herrmann, P. S. P., Araújo-Moreira, F. M., et al. (2014). Bionanocomposites containing magnetic graphite as potential systems for drug delivery. *Int. J. Pharm.* 477, 553–563. doi: 10.1016/j.ijpharm.2014.10.033

Ribeiro, L. N. M., Alcântara, A. C. S., Rodrigues da Silva, G. H., Franz-Montan, M., Nista, S. V. G., Castro, S. R., et al. (2017a). Advances in hybrid polymer-based materials for sustained drug release. *Int. J. Polym. Sci.* 2017, 1–16. doi: 10.1155/2017/1231464

Ribeiro, L. N. M., Breitkreitz, M. C., Guilherme, V. A., Rodrigues da Silva, G. H., Couto, V. M., Castro, S. R., et al. (2017b). Natural lipids-based NLC containing lidocaine: from pre-formulation to *in vivo* studies. *Eur. J. Pharm. Sci.* 106, 102–112. doi: 10.1016/j.ejps.2017.05.060

Ribeiro, L. N. M., Couto, V. M., Fraceto, L. F., and de Paula, E. (2018a). Use of nanoparticle concentration as a tool to understand the structural properties of colloids. *Sci. Rep.* 8:982. doi: 10.1038/s41598-017-18573-7

Ribeiro, L. N. M., Franz-Montan, M., Alcântara, A. C. S., Breitkreitz, M. C., Castro, S. R., Guilherme, V. A., et al. (2020). Hybrid nanofilms as topical anesthetics for pain - free procedures in dentistry. *Sci. Rep.* 10:11341. doi: 10.1038/s41598-020-68247-0

Ribeiro, L. N. M., Franz-Montan, M., Breitkreitz, M. C., Rodrigues da Silva, G., Castro, S., Guilherme, V., et al. (2018b). Nanohybrid hydrogels designed for transbuccal anesthesia. *Int. J. Nanomed.* 13, 6453–6463. doi: 10.2147/IJN.S180080

Rodrigues da Silva, G. H., Geronimo, G., Ribeiro, L. N. M., Guilherme, V. A., de Moura, L. D., Bombeiro, A. L., et al. (2020). Injectable *in situ* forming nanogel: a hybrid Alginate-NLC formulation extends bupivacaine anesthetic effect. *Mater. Sci. Eng. C* 109:110608. doi: 10.1016/j.msec.2019.110608

Rodrigues, E. R. C., Ferreira, A. M., Vilhena, J. C. E., Almeida, F. B., Cruz, R. A. S., Florentino, A. C., et al. (2014). Development of a larvicidal nanoemulsion with copaiba (Copaifera duckei) oleoresin. *Rev. Bras. Farmacogn.* 24, 699–705. doi: 10.1016/j.bjp.2014.10.013

Severino, P., Chaud, M. V., Shimojo, A., Antonini, D., Lancelloti, M., Santana, M. H. A., et al. (2015). Sodium alginate-cross-linked polymyxin B sulphate-loaded solid lipid nanoparticles: antibiotic resistance tests and HaCat and NIH/3T3 cell viability studies. *Colloids Surf. B Biointerfaces* 129, 191–197. doi: 10.1016/j.colsurfb.2015.03.049

Shinde, R. L., Jindal, A. B., and Devarajan, P.V. (2011). Microemulsions and nanoemulsions for targeted drug delivery to the brain. *Curr. Nanosci.* 7, 119–133. doi: 10.2174/157341311794480282

Siepmann, J., Faham, A., Clas, S. D., Boyd, B. J., Jannin, V., Bernkop-Schnürch, A., et al. (2019). Lipids and polymers in pharmaceutical technology: lifelong companions. *Int. J. Pharm.* 558, 128–142. doi: 10.1016/j.ijpharm.2018.12.080

Singh, Y., Meher, J. G., Raval, K., Khan, F. A., Chaurasia, M., Jain, N. K., et al. (2017). Nanoemulsion: concepts, development and applications in drug delivery. *J. Control. Release* 252, 28–49. doi: 10.1016/j.jconrel.2017.03.008

Souza, F. C., Brito, L. F., Silva, M. T., Sugimoto, M. A., Pinto, A. C., Almeida, P. D. O., et al. (2020). Synthesis, characterization and *in vitro*, *in vivo* and *in silico* anti-inflammatory studies of the novel hybrid based on ibuprofen and 3-hydroxy-copalic acid isolated from copaiba oil (Copaifera multijuga). *J. Braz. Chem. Soc.* 31, 1335–1344. doi: 10.21577/0103-5053.20190266

Tfelt-Hansen, P. C. (2010). Does sumatriptan cross the blood–brain barrier in animals and man? *J. Headache Pain* 11, 5–12. doi: 10.1007/s10194-009-0170-y

van Pomeren, M., Brun, N. R., Peijnenburg, W. J. G. M., and Vijver, M. G. (2017). Exploring uptake and biodistribution of polystyrene (nano)particles in zebrafish embryos at different developmental stages. *Aquat. Toxicol.* 190, 40–45. doi: 10.1016/j.aquatox.2017.06.017

Vaucher, R. A., Giongo, J. L., Bolzan, L. P., Côrrea, M. S., Fausto, V. P., dos Santos Alves, C. F., et al. (2015). Antimicrobial activity of nanostructured amazonian oils against *Paenibacillus* species and their toxicity on larvae and adult worker bees. *J. Asia. Pac. Entomol.* 18, 205–210. doi: 10.1016/j.aspen.2015.01.004

Vos, T., Barber, R. M., Bell, B., Bertozzi-Villa, A., Biryukov, S., Bolliger, I., et al. (2015). Global, regional, and national incidence, prevalence, and years lived with disability for 301 acute and chronic diseases and injuries in 188 countries, 1990–2013: a systematic analysis for the global burden of disease study 2013. *Lancet* 386, 743–800. doi: 10.1016/S0140-6736(15)60692-4

Yeh, W. Z., Blizzard, L., and Taylor, B. V. (2018). What is the actual prevalence of migraine? *Brain Behav.* 8:e00950. doi: 10.1002/brb3.950

Yu, M. R., Suyambrakasam, G., Wu, R. J., and Chavali, M. (2012). Preparation of organic-inorganic (SWCNT/TWEEN-TEOS) nano hybrids and their NO gas sensing properties. *Sens. Actuators B Chem.* 161, 938–947. doi: 10.1016/j.snb.2011.11.068

Trypanosomatid-Caused Conditions: State of the Art of Therapeutics and Potential Applications of Lipid-Based Nanocarriers

Giuliana Muraca[1,2], Ignacio Rivero Berti[3], María L. Sbaraglini[1], Wagner J. Fávaro[4], Nelson Durán[4,5], Guillermo R. Castro[3] and Alan Talevi[1]*

[1] Laboratory of Bioactive Research and Development (LIDeB), Department of Biological Sciences, Faculty of Exact Sciences, University of La Plata (UNLP), La Plata, Argentina, [2] Administración Nacional de Medicamentos, Alimentos y Tecnología Médica (ANMAT), Buenos Aires, Argentina, [3] Laboratorio de Nanobiomateriales, Centro de Investigación y Desarrollo en Fermentaciones Industriales (CINDEFI), Departamento de Química, Facultad de Ciencias Exactas, Universidad Nacional de La Plata (UNLP) -CONICET (CCT La Plata), La Plata, Argentina, [4] Laboratory of Urogenital Carcinogenesis and Immunotherapy, Department of Structural and Functional Biology, Institute of Biology, University of Campinas (UNICAMP), Campinas, Brazil, [5] Nanomedicine Research Unit (Nanomed), Federal University of ABC (UFABC), Santo André, Brazil

Trypanosomatid-caused conditions (African trypanosomiasis, Chagas disease, and leishmaniasis) are neglected tropical infectious diseases that mainly affect socioeconomically vulnerable populations. The available therapeutics display substantial limitations, among them limited efficacy, safety issues, drug resistance, and, in some cases, inconvenient routes of administration, which made the scenarios with insufficient health infrastructure settings inconvenient. Pharmaceutical nanocarriers may provide solutions to some of these obstacles, improving the efficacy–safety balance and tolerability to therapeutic interventions. Here, we overview the state of the art of therapeutics for trypanosomatid-caused diseases (including approved drugs and drugs undergoing clinical trials) and the literature on nanolipid pharmaceutical carriers encapsulating approved and non-approved drugs for these diseases. Numerous studies have focused on the obtention and preclinical assessment of lipid nanocarriers, particularly those addressing the two currently most challenging trypanosomatid-caused diseases, Chagas disease, and leishmaniasis. In general, *in vitro* and *in vivo* studies suggest that delivering the drugs using such type of nanocarriers could improve the efficacy–safety balance, diminishing cytotoxicity and organ toxicity, especially in leishmaniasis. This constitutes a very relevant outcome, as it opens the possibility to extended treatment regimens and improved compliance. Despite these advances, last-generation nanosystems, such as targeted nanocarriers and hybrid systems, have still not been extensively explored in the field of trypanosomatid-caused conditions and represent promising opportunities for future developments. The potential use of nanotechnology in extended, well-tolerated drug regimens is particularly interesting in the light of recent descriptions of quiescent/dormant stages of *Leishmania* and *Trypanosoma cruzi*, which have been linked to therapeutic failure.

Keywords: Chagas, leishmaniasis, human African trypanosomiasis, lipid nanoparticles, liposomes, solid lipid nano particles, nanoestructed lipid carrier, nanoparticle

INTRODUCTION

Since the first description of liposomes in the mid-1960s, lipid-based pharmaceutical nanocarriers have made their way to the market and have undergone substantial evolution (Puri et al., 2009; Akbarzadeh et al., 2013). Their applications in the medical field include drug delivery, imaging molecules, decoration with ligands for site-specific targeting, and formulation with destabilizing lipid systems that allow for on-demand drug release. A relevant parameter of an ideal drug vehicle is the absence of toxicity (both for the patient and the environment) of the carrier itself or its by-products. Among the wide array of nanomaterials, lipid-based systems are undoubtedly among the safest ones (Puri et al., 2009). Later generations of lipid-based drug delivery systems include solid lipid nanoparticle (SLN), nanostructured-lipid carriers (NLCs), and, more recently, lipid–polymer hybrid systems (Puri et al., 2009; Mukherjee et al., 2019; Liu et al., 2020) and quatsomes (Ferrer-Tasies et al., 2013). It is expected that such drug carriers will allow for higher control over drug release, enhanced stability, and increased circulation times. Some general advantages of lipid nanosystems are schematically summarized in **Figure 1**.

Trypanosomatid-caused human conditions, namely, Chagas disease, leishmaniasis, and human African trypanosomiasis (HAT), are considered as neglected infectious diseases that have been listed as high-priority diseases by the World Health Organization (WHO), needing innovative and increased disease management (Parthasarathy and Kalesh, 2020). The real amount of infected people is possibly miscalculated as available figures are often extrapolation of data from incomplete epidemiological surveys. Also, the situation worsened by social and military conflicts and because of undiagnosed or unreported patients living in rural areas with limited access to health system facilities

(Malvy and Chappuis, 2011). In 2010, it was estimated that these conditions affected about 27 million people worldwide and caused ∼150,000 annual deaths (Nussbaum et al., 2010). Since then, depending on the case, advance and retreats have been registered. For instance, a 90% drop in the number of African trypanosomiasis cases has been realized between 2009 and 2018 (World Health Organization, 2020a), and the first all-oral medication for such condition has recently been launched (Deeks, 2019). On the other hand, a jump of 26.9% in leishmaniasis prevalence was observed between 2006 and 2016 (GBD 2016 Disease Injury Incidence Prevalence Collaborators, 2017). As no vaccine is available, treatment solely depends on chemotherapy. Specifically, in the case of Chagas disease and leishmaniasis, available treatment options are dramatically limited. Among disadvantages of much of the available therapeutic arsenal, we might mention toxicity, emerging drug-resistance issues, high costs, limited efficacy, and inconvenient routes of administration (Patterson and Wyllie, 2014). Therefore, novel therapeutic options are urgently required to improve both accessibility and therapeutic output and control potential resistance issues. Interestingly, the existence of quiescent and dormant stages (characterized by low or no replication and diminished metabolic activity) has been described, respectively, in *Leishmania* and *Trypanosoma cruzi* (Berg et al., 2013; Kloehn et al., 2015; Jara et al., 2017, 2019; Sánchez-Valdez et al., 2018). Depending on the case, such forms may emerge spontaneously (Sánchez-Valdez et al., 2018) or as an adaptive response to stress conditions (e.g., drug pressure) (Berg et al., 2013; Jara et al., 2019), contributing to treatment failure. It has been suggested that these new resistance mechanisms, which add to classical genetic-based drug resistance, may be treated using current drugs in extended therapeutic regimens that extend beyond the dormancy potential (Sánchez-Valdez et al., 2018).

FIGURE 1 | General advantages of lipid-based nanosystems.
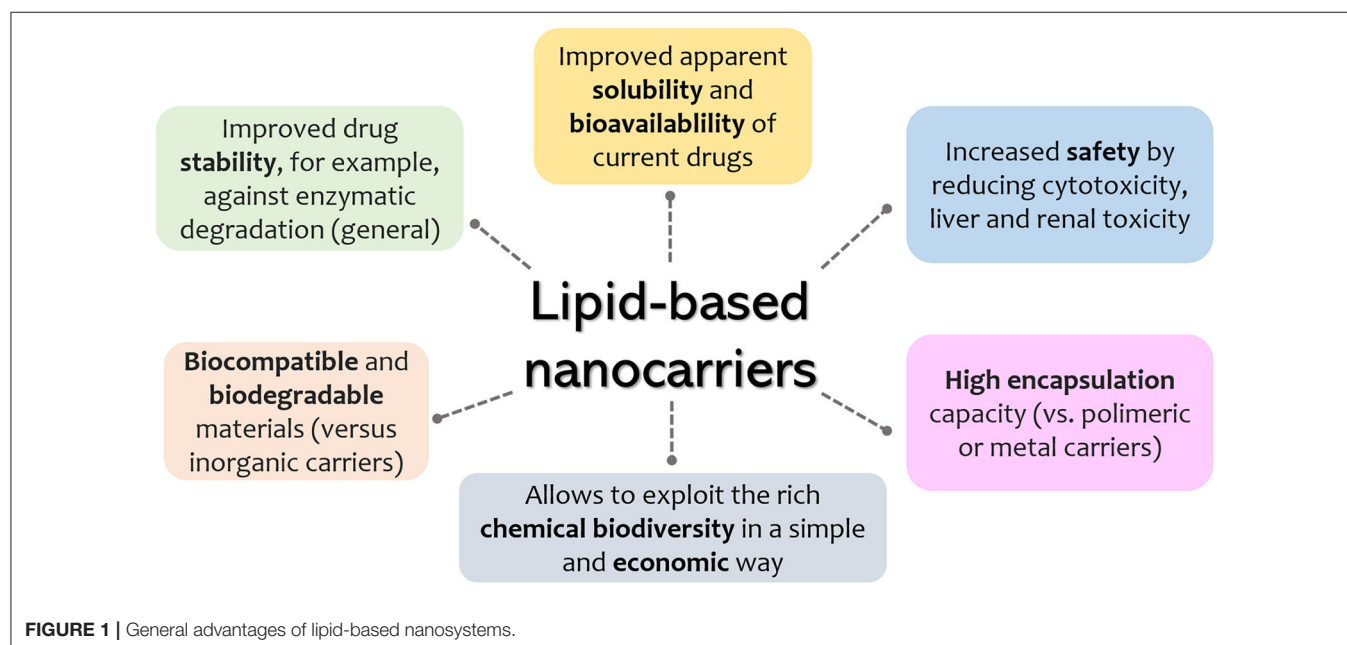
Here, we will briefly overview the trypanosomatid-caused human diseases, along with the strengths and limitations known chemotherapies to treat such conditions and recent or ongoing clinical trials. Later, we will review the recent advances on lipid nanocarriers encapsulating available and potential pharmacological agents against Chagas disease, sleeping sickness, and leishmaniasis. Noteworthy, other types of nanomaterials (e.g., polymeric systems and metal nanoparticles) have also been investigated (see, for instance, Ahmad et al., 2020; Nafari et al., 2020), although they fall outside the scope of the present review and article collection. Finally, some concluding remarks including possible future directions in the field will be included.

Other recent reviews on the topic have been published, including a comprehensive review on drug nanocarriers of different materials targeting trypanosomatid-caused diseases (Volpedo et al., 2019) and reviews exclusively focused on a given condition (Quezada et al., 2019; Saleem et al., 2019) or in specific drugs encapsulated in a diversity of nanocarriers (Arrúa et al., 2019).

LITERATURE SURVEY

We initially search in Scopus all the combinations of one of the following terms "Chagas disease," "leishmaniasis," "human African trypanosomiasis," "Trypanosoma cruzi," "*Trypanosoma brucei*," "Leishmania" with one of the following terms "nanocarrier," "nanolipid," "solid lipid nanoparticles," "nanostructured lipid carrier," "nanosystem," "drug delivery." Two of the authors (GM and MLS) scrutinized the abstracts of the resulting articles and selected those related to the review scope. The search was conducted in Google Scholar and Scopus.

HUMAN AFRICAN TRYPANOSOMIASIS

HAT is transmitted by the tsetse fly *Glossina* spp.; the etiologic agents are two subspecies of *Trypanosoma brucei* (World Health Organization, 2020a). The disease presents a first stage (also called hemolymphatic, or early stage), taking place when the parasite invades the bloodstream, and a second stage (meningoencephalitic, or late stage) linked to invasion of the patient's central nervous system (CNS) by the parasite. In humans, the disease presents in two forms, depending on the parasite subspecies involved. When the etiological agent is *T. brucei gambiense* (gHAT), the disease usually evolves without major signs or symptoms. Nevertheless, when symptoms emerge, the patient has often reached the advanced stage of the disease, compromising the CNS and narrowing treatment options. On the other hand, when the infection is caused by *T. brucei rhodesiense* (rHAT), the disease develops rapidly, with the first signs/symptoms being observed as soon as a few weeks after infection, also compromising the CNS (World Health Organization, 2020a).

Human African Trypanosomiasis Treatment
Today, WHO recommends a diversity of treatment options against HAT, depending on the parasite subspecies involved

and the evolution stage of the disease, including pentamidine, suramin, melarsoprol, eflornithine, nifurtimox, and fexinidazole.

Pentamidine appeared in 1940 and has since then been employed for the treatment of the early phase of gHAT. It is an aromatic diamidine that has numerous undesirable side effects such as disturbances of glucose homeostasis, leukopenia, and hypotension, as well as an inconvenient route of administration (intramuscular) (Yang et al., 2014; Sbaraglini et al., 2016). Besides, it has low brain–blood barrier (BBB) permeability, which means that is not effective for the treatment of late-stage HAT.
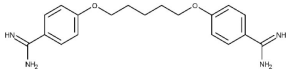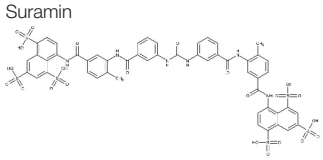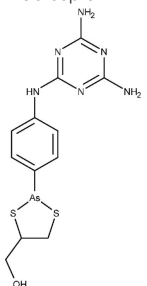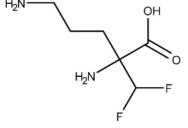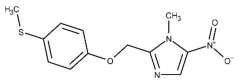
Suramin reached the market in 1920 and is still one of the treatment options for the first stage of rHAT. Its most frequent side effect is urticarial rash (which affects around 90% of the patients). Other adverse events include reversible nephrotoxicity, pyrexia, and nausea (Nagle et al., 2014).

For the treatment of second stage of HAT, an arsenic derivate has been recommended for years: the melarsoprol. It was employed from 1949 (Nok, 2003), but its toxicity is extremely high, causing severe encephalopathic syndrome in some cases, which is associated to high mortality rate (Kennedy, 2004).

Another approved drug for the treatment of HAT is eflornithine, a repurposed drug first explored as anticancer agent (Nwaka and Hudson, 2006). Eflornithine has been used as an alternative to melarsoprol, and its mode of action involves the inhibition of the enzyme ornithine decarboxylase (O'Shea et al., 2016). Its side effects are less severe than those of melarsoprol, but it requires intravenous administration because of its low oral bioavailability. This is an important drawback if one considers that most patients with HAT have limited access to adequate health facilities, complicating the follow-up. Furthermore, it is active only against *T. b. gambiense*. The outcome is significantly improved when eflornithine is combined with nifurtimox. As monotherapy in *T. b. gambiense* infections, nifurtimox is effective against both the early and late stages, but it has a very variable cure rate (30–80%) and high toxicity upon long-term administration (Bouteille et al., 2003). Nifurtimox combined with eflornithine (Nagle et al., 2014), though, is an interesting therapeutic choice, and it was incorporated to the WHO List of Essential Medicines for the treatment of gHAT (World Health Organization, 2020a).
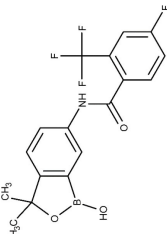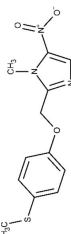
In 1983, Raether and Seidenath reported fexinidazole as a highly active new antiparasitic drug effective against trichomonads, *Entamoeba histolytica* and *T. cruzi*, but the project was abandoned by the pharmaceutical company Hoechst when its tropical disease program was shut down (Raether and Seidenath, 1983). Thanks to the non-profit Drugs for Neglected Diseases initiative (DNDi) organization and the pharmaceutical company Sanofi joint efforts, this drug finalized preclinical stage and underwent clinical trials (Fairlamb, 2019). It has been approved as the first all oral medication against both hemolymphatic and meningoenchepalitic gHAT, and it is undergoing a 5-year clinical trial to prove its efficacy against rHAT (ClinicalTrials.gov NCT03974178, 2020; Drugs for Neglected Diseases initiative, 2020e). After oral administration, fexinidazole is readily distributed throughout the body, including the brain (Tarral et al., 2014).

TABLE 1 | Drugs approved or under clinical trials for the treatment of human African trypanosomiasis (HAT).

Drugs	Stage of the disease	Administration via	Adverse reactions	References
WHO-recommended drug treatments				
Pentamidine	First stage	Intramuscular	Hyperglycemia or hypoglycemia, prolongation of the QT interval on electrocardiogram, hypotension, and gastrointestinal features	(Nok, 2003)
Suramin	First stage	Intravenous	Renal failure, skin lesions, anaphylactic shock, bone marrow toxicity, and neurological complications such as peripheral neuropathy	(Nok, 2003)
Melarsoprol	Second Stage	Intravenous	Reactive arsenical encephalopathy (RAE) has been attributed to the toxic effect of melarsoprol, peripheral neuropathy, cutaneous reactions, renal or hepatic dysfunction, allergic or hypersensitivity reactions	(Nok, 2003; Eperon et al., 2014)
Eflornithine	Second stage. Only useful against *T. b. gambiense*	Intravenous	Generally, are reversible after the end of treatment. Convulsions, gastrointestinal symptoms such as nausea, vomiting, and diarrhea; bone marrow toxicity leading to anemia, leukopenia, and thrombocytopenia	(Burri, 2010; Alirol et al., 2013)
Nifurtimox & Eflornithine	First and second stage	Intravenous (eflornithine) Oral (nifurtimox)	Convulsions, gastrointestinal symptoms such as nausea, vomiting, and diarrhea; Genotoxicity, neurotoxicity	(Burri, 2010; Yun et al., 2010; Kuemmerle et al., 2020)
Fexinidazole	First and second stage of *T. b. gambiense* infection	Oral	Headache and vomiting	(Tarral et al., 2014; Fairlamb, 2019; ClinicalTrials.gov NCT01685827, 2020; ClinicalTrials.gov NCT03025789, 2020)

(Continued)

61

TABLE 1 | Continued

Drugs	Stage of the disease	Administration via	Adverse reactions	References
Undergoing clinical trials				
Acoziborole (SCYX-7158)	First stage Second stage	Oral	Diarrhea, constipation, nausea, vomiting, abdominal pain, headaches	(ClinicalTrials.gov NCT01533961, 2020; ClinicalTrials.gov NCT03087955, 2020; Dickie et al., 2020)
Fexinidazole	First and second stage of *T. b. rhodesiense* infection	Oral	Results have not been disclosed yet	(ClinicalTrials.gov NCT03974178, 2020)

Currently, the oxaborole SCYX-7158 is undergoing clinical trials for the treatment of HAT. Encouraging results of SCYX-7158 in animal models made the responsible researchers suspect that it might be a good treatment option for late-stage HAT (Jacobs et al., 2011). Two other oxaborole compounds, SCYX-1608210 and SCYX-1330682, have shown good performance in animal models of the disease (Drugs for Neglected Diseases initiative, 2020c). In 2015, a placebo-controlled, randomized, double-blind study was completed, which assessed the tolerability and pharmacokinetic parameters of SCYX-7158 (ClinicalTrials.gov NCT01533961, 2020). The study confirmed that the drug readily crosses the BBB, thus being a promising candidate to treat late-stage HAT, although some adverse effects such as gastrointestinal reactions and headaches were observed (Drugs for Neglected Diseases initiative, 2020c). Based on these results, a phase II/III trial started in 2017, to evaluate the effectiveness and safety of SCYX-7158 as an oral treatment for adult patients with gHAT (ClinicalTrials.gov NCT03087955, 2020). The chosen dosage regimen involved a single administration of 960 mg. Phase II/III results are awaited in the next years (Dickie et al., 2020).

Table 1 summarizes the therapeutic scenario for HAT.

Lipid Nanosystems Encapsulating Approved Drugs

Limited permeability across the blood–brain barrier by therapeutic agents is one of the main limitations that an efficacious trypanocidal agent may present to be considered a valid option to treat late-stage HAT. For instance, pentamidine is mostly ineffective once the parasite has invaded the CNS, and such lack of efficacy is thought to respond to its inability to enter the brain. The limited bioavailability of pentamidine in the brain has been demonstrated in mice by Sanderson et al. (2009), whose results suggested that the drug distribution to the brain is conditioned by active efflux mediated by P-glycoprotein and multidrug resistance–associated proteins. Different approaches have been used for the delivery of drugs to the brain, such as intracerebroventricular administration or intranasal delivery. Among them, vector-mediated brain delivery, involving enhanced brain bioavailability through drug-carrier conjugates, seems particularly promising because of its versatility and reduced side effects compared to other delivery options (Li et al., 2017; Gondim et al., 2019). Omarch et al. (2019) investigated the permeability of polycaprolactone nanoparticles and liposomes containing both pentamidine across a monolayer of immortalized mouse brain endothelioma cells. Pentamidine-loaded polycaprolactone nanoparticles showed a mean diameter of 267.6 nm and zeta potential of −28.1 mV, whereas liposomes had a mean diameter of 119.6 nm and zeta potential of 11.78. Both systems displayed low dispersity and similar loading capacity. After 24 h, liposomes and polycaprolactone nanoparticles transported 87 and 66% of the doses, respectively. Besides, free pentamidine penetration was only 63% of the dose. The data suggested that lipid structures can be promising nanocarriers to increase brain bioavailability of pentamidine.

Lipid Nanosystems Encapsulating Non-approved Drugs

Like pentamidine, diminazene aceturate is a trypanocidal aromatic diamidine of veterinary use. Its mode of action involves the irreversible inhibition of S-adenosyl-L-methionine decarboxylase of the trypanosome (Pépin and Milord, 1994). In the past, diminazene aceturate has been used off-label by national control programs and clinicians in many HAT endemic regions of the world, with the consequent ethical controversy (Pépin and Milord, 1994). Diminazene presents limited stability and brain bioavailability (Kroubi et al., 2010).

Kroubi et al. (2010) obtained cationic polysaccharide nanoparticles with a lipid core (anionic phospholipids). It was previously observed that these types of nanocarrier could be endocytosed by the blood–brain barrier endothelial cells and did not activate the complement system, which strongly suggests a stealth behavior (Jallouli et al., 2007; Paillard et al., 2010). The authors tested two drug loading approaches, in process (at 80°C) and post-loading (at room temperature), although poor stability was observed in the former approach. The hydrodynamic diameter of the prepared nanoparticles was 74 nm, with low dispersion and a zeta potential +29 mV. Possibly because of the porous nature of the nanosystem, the mean size was not changed by the drug load. The loading capacity and stability of the hybrid nanoparticles greatly depended on the drug to phospholipid ratio: formulations with a drug-to-phospholipid ratio <5% were stable in terms of size, charge, and drug loading for at least 6 months (4°C). It was also observed that the encapsulation of the drug protected it against oxidation, being stable for at least 6 months at 4°C. Furthermore, *in vitro* assays on *T. brucei* showed an increased efficacy of the loaded nanoparticles compared with the free drug.

CHAGAS DISEASE (AMERICAN TRYPANOSOMIASIS)

Chagas disease, caused by the protozoan *T. cruzi*, is endemic to Latin America, but it has also spread to non-endemic countries because of human migration. It is transmitted mainly through an insect vector commonly known as "kissing bug" or *vinchuca* (*Triatoma infestans*), but other transmission ways have become increasingly relevant, including congenital transmission, blood transfusion, and organ transplant (Pereira and Navarro, 2013; World Health Organization, 2020b). It presents itself in two or three stages (acute and chronic, or acute, latent/undetermined, and chronic), depending on bibliographic sources. The acute stage is associated with a high parasite load in blood and displays absent or mild and unspecific symptoms. In the chronic stage, the parasite predominates in other tissues (mainly in the heart and digestive muscles), with up to 30% of patients experiencing cardiac disease and around 10% displaying digestive complications. The chronic stage often leads to sudden death due to cardiac cardiomyopathy (World Health Organization, 2020b).

Chagas Disease Treatment

Only two trypanocidal drugs are available to treat Chagas disease: benznidazole and nifurtimox, with both being discovered around 1970 (World Health Organization, 2020a). The mode of action of benznidazole involves the covalent modification of biomolecules, due to the generation of reactive intermediates emerging from reduction of the nitro group (Mecca et al., 2008). It is highly efficacious in the acute stage; however, as the disease progresses, the efficacy decreases, and the cure rate in the chronic phase is estimated around 10–20% (Prata, 2001). The BENEFIT was a multicenter, prospective, randomized study including patients with Chagas' cardiomyopathy who received benznidazole or placebo for up to an 80-day period (Morillo et al., 2015). Two thousand eight hundred fifty-four patients were followed up for more than 5 years after the intervention. Sixty-six percent of the patients treated with benznidazole reverted positive polymerase chain reaction (PCR) results in comparison to 33.5% of patients in the placebo arm. This positive outcome, nonetheless, was overshadowed by the fact that cardiac deterioration was not prevented in the active arm. It is worth mentioning that benznidazole is often poorly tolerated, presenting adverse reactions/side effects such as rashes, peripheral neuropathy, hypersensitivity syndromes with fever, lymphadenopathy, exfoliative dermatitis, anorexia, nausea, vomiting, and insomnia (World Health Organization, 2020a), which often lead to treatment interruption.

Nifurtimox, the second-line treatment, is prescribed in cases where benznidazole is not well-tolerated. Its mode of action, again, relates to the reduction of the nitro group, leading to the formation of reactive oxygen species (Urbina and Docampo, 2003, Maya et al., 2007). As previously discussed, nifurtimox is also associated to several complications, including anorexia, psychic disorders, irritability, insomnia, nausea, and diarrhea (Bern et al., 2007).

Regarding recent and ongoing clinical trials, disappointing results were obtained with the repurposed antifungal posaconazole. Docampo et al. (1981) were the first to suggest the use of azole compounds against *T. cruzi*. In 2010, posaconazole was included in a clinical trial to assess its efficacy against chronic Chagas disease. It did show trypanosomal activity, but more posaconazole patients (compared with benznidazole treatment) showed failure throughout the follow-up of the treatment (Molina et al., 2014; ClinicalTrials.gov NCT01162967, 2020). Later, a second trial was started to study the efficacy of oral posaconazole for the treatment of asymptomatic Chagas disease (ClinicalTrials.gov NCT01377480, 2020), but once again, the investigators found better performance in the control arm (Morillo et al., 2017). Highly sensitive bioluminescence studies were later performed with bioluminescent *T. cruzi* to assess parasite survival in mice, after treatment with either posaconazole or benznidazole; cyclophosphamide-induced immunosuppression was used to facilitate the detection of relapse (Fortes Francisco et al., 2015). While 20-day treatment with benznidazole was successful to achieve sterile cure, posaconazole failed in almost all cases. In the acute phase, the adipose tissue appears to be the major reservoir of recurrence in

mice under posaconazole therapy. Inadequate choice of the dose at clinical trials and emergence of azole-resistant parasites should also be considered as possible explanations to the failure at the clinical studies (Campos et al., 2017; Villalta and Rachakonda, 2019).

E-1224 (a prodrug of ravuconazole) is another azole being investigated as potential therapy for Chagas (Diniz et al., 2018). In 2011, a proof-of-concept study was started in individuals with chronic indeterminate Chagas disease (ClinicalTrials.gov NCT01489228, 2020) but the outcome did not cover the expectations, as the control group showed better results after 1-year treatment (Torrico et al., 2018). More recent studies are focusing on the evaluation of improved treatment regimens of benznidazole in monotherapy and in combination with E1224 (ClinicalTrials.gov NCT03378661, 2020).

After Bahia et al. (2012) demonstrated the *in vitro* an *in vivo* effects over *T cruzi*, fexinidazole entered a phase II trial to determine its efficacy in adults with chronic indeterminate disease, finding that the drug was highly effective at the lowest dose (ClinicalTrials.gov NCT02498782, 2020; Drugs for Neglected Diseases initiative, 2020j). A second study started a few years later in which 3, 7, and 10 days of treatment with low doses of the drugs are being evaluated, to establish the minimal effective and safe dose to treat adult patients undergoing chronic indeterminate Chagas disease (ClinicalTrials.gov NCT03587766, 2020). Results are expected in 2020.

A second study started a few years later for adult patients' therapy having chronic indeterminate Chagas sickness for which they received 3, 7, and 10 days of treatment with low drug doses.

As cardiac deterioration is the major complication in chronic Chagas disease, there are also some undergoing trials focused on ameliorating Chagas cardiomyopathy. In 2009, a clinical trial started to estimate the effect of selenium treatment on prevention of heart disease progression in cardiac patients with Chagas (ClinicalTrials.gov NCT00875173, 2020). Selenium has prevented myocardial lesions in acute and chronic models (Souza et al., 2010). In 2018, there were protocol modifications (Holanda et al., 2018), and recruitment of patients has been reestablished. Results should be expected soon, and if the hypothesis of the trial is confirmed, the inclusion of this micronutrient in the daily diet could have a therapeutic effect on Chagas myocardiopathy.

Another example of a repurposed drug that could be used to treat the Chagas-associated cardiomyopathy is the antigout agent colchicine, which has demonstrated cardioprotective effects (reduced fibrosis and diminished inflammation in the cardiac tissue) (Fernandes et al., 2012). Positive effects on myocardial remodeling, linked to interference in the synthesis of collagen, were also reported. Currently, a clinical study is in the recruiting phase, with the first results being expected by 2021 (ClinicalTrials.gov NCT03704181, 2020).

Finally, amiodarone is a class III antiarrhythmic agent and was first found as an antimycotic (Courchesne, 2002; Hejchman et al., 2012). Later, Benaim et al. (2006) reported its trypanocidal effects against *T. cruzi* (Bellera et al., 2013). The potential benefits on both its cardiovascular activity and the intracellular Ca^{2+} regulation of the parasite make this compound particularly attractive. An ongoing phase III clinical

trial (ATTACH) was designed to test the effect of amiodarone, administered over 6 months, in subjects with mild to moderate Chagas cardiomyopathy; secondarily, potential trypanocidal effects associated with beneficial clinical effects will be explored (ClinicalTrials.gov NCT03193749, 2020).

Table 2 presents a summary of the therapeutic scenario for Chagas disease, including approved drugs and drugs that have or are undergoing clinical trials.
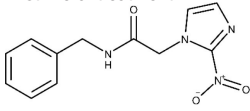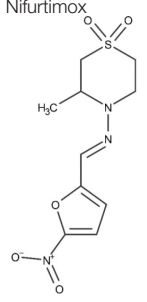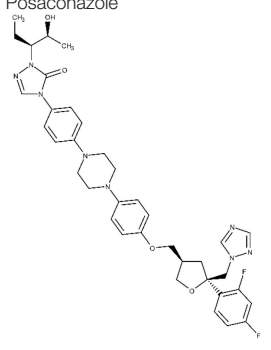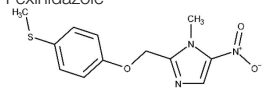
Lipid Nanosystems Encapsulating Approved Drugs

Although much of the efforts toward encapsulation of benznidazole and nifurtimox has focused on polymeric nanosystems, a considerable number of studies have also been published reporting the use of lipid-based nanocarriers, especially in the case of the first-line therapy benznidazole (Arrúa et al., 2019).

Morilla et al. (2002) reported the obtention of benznidazole multilamellar liposomal formulations; they proposed that such strategy would compensate benznidazole low solubility and improve its biodistribution. Among many tested formulations, the highest drug load was observed in hydrogenated phosphatidylcholine from soybean: cholesterol: distearoyl-phosphatidylglycerol in a molar ratio of 2:2:1. Drug loading of 2 g of the drug per 100 g of lipids was achieved. A 450-fold dilution in buffer at 37°C led to a reduction in the quantity of drug associated to liposomes from 2 g to 0.25 g/100 g of total lipids at 65% of drug lost per minute since the first minute and by severe decrease of drug release (0.4% of drug lost per minute) in the next hour. The low efficiency of the drug carrier concomitantly with high amount of drug loss can be attributed to the liposomal thermodynamic instability under physiological conditions (Cacicedo et al., 2016). Subsequently, the same authors investigated the ability of such liposomes to enhance the delivery of benznidazole to the liver in rats (Morilla et al., 2004). Three-fold raise in benznidazole was accumulated in the liver, together with 1.1 μg/mL BNZ in blood, which is 30% lower than the blood BNZ concentration achieved upon intravenous administration of free drug happened 4 h post-ijnjection. Besides, the increase of BNZ liver uptake had no effect on parasitemia levels of mice infected with the RA *T. cruzi* strain.
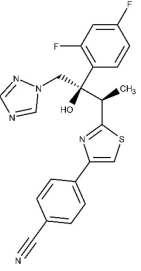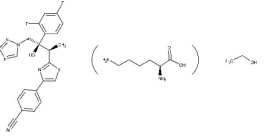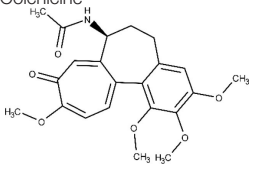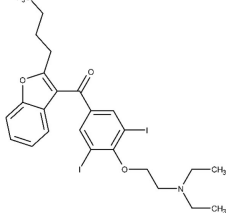
A diversity of nanocarriers encapsulating benznidazole (among them, several lipid-based systems) were studied by the BERENICE consortium (BEnznidazol and triazol REsearch group for Nanomedicine and Innovation on Chagas disease, a project originally conceived to develop low-cost therapeutic interventions for Chagas disease using nanotechnology to reduce the final dose of the drug) (Vinuesa et al., 2017). The drug delivery systems tested included different cyclodextrins, quatsomes, liposomes, SLN, and NLC formulations. Liposomal formulations sedimented in time, although this behavior was prevented through PEGylation. The release profiles of the SLN and NLC showed a considerable initial burst release. In the case of SLN, those with the higher benznidazole load (20%) released 18% of the load at 1.5 h. Subsequently, the release rate was much slower (the maximum drug release was 19.5%). The

TABLE 2 | Summary of the therapeutic scenario for Chagas disease, including WHO-recommended therapies, and recent/undergoing clinical trials.

Drugs	Stage of the disease	Administration via	Adverse reactions	References
Drugs used to treat Chagas disease recommended by WHO				
Benznidazole First line of treatment	Acute phase Chronic phase	Oral	Rashes, peripheral neuropathy, hypersensitivity syndromes with fever, lymphadenopathy, exfoliative dermatitis, anorexia, nausea, vomiting, weight loss, and insomnia	(Bern et al., 2007; Mecca et al., 2008; Crespillo-Andújar et al., 2020; ClinicalTrials.gov NCT03191162, 2020; ClinicalTrials.gov NCT03981523, 2020)
Nifurtimox	Acute phase (for those patients who do not tolerate benznidazole)	Oral	Anorexia, weight loss, psychic disorders, irritability, insomnia, nausea, diarrhea	(Urbina and Docampo, 2003; Bern et al., 2007; Maya et al., 2007; Boiani et al., 2010; Hall et al., 2011; ClinicalTrials.gov NCT03981523, 2020)
Undergoing clinical trials				
Posaconazole	Acute phase Chronic phase	Oral	Drug interactions related to CYP3A4 inhibition. Caution must be taken when coadministered with other CYP3A4 substrates. Care must be taken when administered to a patient with arrhythmic disorders or taking proarrhythmic drugs	(Molina et al., 2014; Morillo et al., 2017; Urbina, 2017; ClinicalTrials.gov NCT01377480, 2020; Echeverría et al., 2020)
Fexinidazole	Acute phase Chronic phase	Oral	Headache and vomiting of acceptable intensity	(Neal and van Bueren, 1988; Bustamante and Tarleton, 2014; ClinicalTrials.gov NCT02498782, 2020; ClinicalTrials.gov NCT03587766, 2020)

(Continued)

65

TABLE 2 | Continued

Drugs	Stage of the disease	Administration via	Adverse reactions	References
Ravuconazole and E-1224	Acute phase	Oral	Not informed	(Urbina et al., 2003; ClinicalTrials.gov NCT01489228, 2020; ClinicalTrials.gov NCT03378661, 2020; ClinicalTrials.gov NCT03892213, 2020)
Ravuconazole E-1224	Chronic phase			
Selenium	For prevent Chagas cardiomyopathy	Oral	Not reported	(Holanda et al., 2018; ClinicalTrials.gov NCT00875173, 2020)
Colchicine	For prevent Chagas cardiomyopathy	Oral	Not reported	(ClinicalTrials.gov NCT03704181, 2020)
Amiodarone		Oral	Not reported	(Bellera et al., 2013; Carmo et al., 2015; ClinicalTrials.gov NCT03193749, 2020)

maximum release achieved with the NLC was higher than that of SLN (up to 55% of the load for the highest drug load, i.e., 30%), and the initial burst was reached only 5 h later. Regarding cytotoxicity of the empty carriers, quatsomes resulted to be highly cytotoxic at high concentrations. Liposomal preparations were much less cytotoxic, with some of them displaying negligible toxicity. NLC showed dose-dependent (but low) cytotoxicity: empty NLC showed at most 10% toxicity (at 100 μg/mL) on mice fibroblasts. A paradoxical (unexplained) behavior was registered, since the higher the benznidazole load, the smaller the toxicity detected. Similarly, CD had low cytotoxicity. None of the formulations tested provided substantial improvement on the trypanocidal effect of benznidazole, and only cyclodextrin complexes achieved some improvement in the selectivity index. These discouraging results possibly led the BERENICE team to discard the nanotechnology approach.

Another recent study investigated the ability of oil-in-water nanoemulsions to modify benznidazole release and their impact on the parasite viability (Streck et al., 2019). Dispersions of medium-chain triglycerides were stabilized by using phosphatidylcholine and sodium oleate. The nanoemulsion increased benznidazole apparent aqueous solubility and led to a slower drug release. Cell viability studies revealed that the nanoformulation enhanced the cytotoxicity at high concentrations (200 μg mL^{-1}). The tested formulations also induced a remarkable increment of efficacy against epimastigotes and trypomastigotes, in comparison with the free drug.

Lipid Nanosystems Encapsulating Non-approved Drugs

In 1999, the performance of three marketed lipid amphotericin B formulations (i.e., the liposomal AmBisome^{TM}, the lipid complex Abelcett^{TM}, and Amphocil^{TM}, a colloidal dispersion) was challenged *in vitro* and *in vivo* against amphotericin B deoxycholate (Fungizone^{TM}). Amphocil and Fungizone showed 42- and 7-fold more activity than Abelcet and AmBisome against amastigotes of *T. cruzi* in macrophages, respectively. However, the tested formulations showed similar performance against *T. cruzi* amastigotes in cultures of Vero cells. Interestingly, administration of a single 25 mg/kg dose of AmBisome inhibited acute infections of *T. cruzi* in mice, whereas at the same dose the other lipid formulations enhanced the survival rate, but the infections were not eliminated in all animals (Yardley and Croft, 1999). These results clearly evidence the absence of *in vitro*–*in vivo* correlation. In good agreement with these findings, Cencig et al. (2011) proved that the increase in survival and parasitemia decreases in the course of acute or chronic phases of *T. cruzi* of infected mice by six intraperitoneal AmBisome injections. Analysis by quantitative PCR of infected mice showed significant parasite load reductions in heart, spleen, skeletal muscle, liver, and adipose tissues in both phases. Noteworthy, earlier administration of the amphotericin B formulation led to increased efficacy in parasite load decreases in spleen and liver, and recurrent drug administration also had beneficial effects in the parasite load in heart and liver during the chronic phase. Unfortunately, immunosuppression

with cyclophosphamide boosted the infection to parasite levels equivalent to untreated animals acutely infected. These results strongly suggest that, at least in the assayed dosing schedule, the liposomal formulation failed to fully cure the infection.

Morilla et al. (2005) encapsulated the trypanocidal drug etanidazole in pH-sensitive liposomes made of dioleoyl-phosphatidylethanolamine and cholesteryl hemisuccinate 6:4. The liposomes were also loaded with a fluorescent probe. Their mean diameter was around 380 nm. The mean size drastically changed (5-fold increase) when the pH of the external media dropped from 8.7 to 3 (it would have been interesting, though, to study the behavior at intermediate, physiologically relevant pH values). It was demonstrated that they were phagocytosed by uninfected and *T. cruzi*–infected macrophages, eliciting an appreciable trypanocidal effect, while control with free drug did not show any therapeutic effect. Intravenous administration of the encapsulated drug to infected mice also decreased parasitemia levels, whereas administration of a 180-fold higher dose of the free drug had no positive effect.

Carneiro et al. (2014) developed SLN containing the potential trypanocidal drug lead 5-hydroxy-3-methyl-5-phenyl-pyrazoline-1-(S-benzyldithiocarbazate). The mean diameter of the loaded SLN was 127 nm with low dispersity; the zeta potential revealed a considerably negative surface charge (-56.1 mV). A high entrapment efficiency was also demonstrated. The *in vitro* and *in vivo* performances of the encapsulated drug, the free drug, and benznidazole were compared. The SLN system outperformed the other treatments in a mice model of infection, both in terms of parasitemia reduction. Liver inflammation and damage were also diminished by the drug-loaded nanocarrier.

More recently, Spósito et al. (2017) resorted to a self-emulsifying formulation to efficiently deliver ravuconazole, a low-solubility drug pertaining to class II of the Biopharmaceutical Classification System. The emulsifying system considerably enhanced the *in vitro* drug dissolution extent and rate in comparison with the free drug (20 vs. 3% at 6 h). The formulation clearly improved the *in vitro* activity of the drug against the intracellular stage of *T. cruzi*. Cruz-Bustos et al. (2012) used *Quillaja* saponin (an immunostimulant agent used as vaccine adjuvant, which forms nanometer pentagonal dodecahedral balls known as immunostimulant complexes) in the design of targeted nanocapsules loaded with actinomycin D and functionalized with anti–*T. cruzi* antibodies. Confronted with *T. cruzi* epimastigotes, the encapsulated drug elicited trypanocidal effects in a dose-dependent manner, at much lower concentrations than the free drug control. Remarkably, this is to our best knowledge the first reported targeted lipid nanocarrier against Chagas disease.

De Morais et al. (2019) reported the obtention of polymeric micelles and phospholipid 2-dipalmitoyl-sn-glycero-3-phosphocholine liposomes containing the photosensitizer drug hypericin. The mean size, polydispersity index, or zeta potential were not informed. Confronted with *T. cruzi* trypomastigotes, pluronic micelles showed efficacious even in the absence of light, with their EC$_{50}$ around 7 μmol L^{-1}. Under light, the best result was achieved by the liposomal system, with EC$_{50}$ around 0.31 μmol L^{-1}. Although free hypericin showed a

very similar potency, authors underlined that the encapsulated drug would be protected against blood components, which constitutes and additional advantage of the loaded liposomes. At last, Parra et al. (2020) reported the obtention of double targeted imiquimod-containing nanovesicles prepared from lipids from the archaebacterium *Halorubrum tebenquichense*, to induce protection against *T. cruzi* infection. The therapeutic efficacy of the vesicles was assessed in a mice model of acute infection, and it was shown that it prevented mortality, reduced parasitemia levels (although not as much as benznidazole), and reduced myocardial and skeletal muscle damage (even more than benznidazole).

Violacein, a natural colorant produced by some Gram-negative bacteria, showed a predominantly apoptotic effect in developmental forms of *T. cruzi* (Y strain) and selectivity index of 9 (Canuto et al., 2019). However, the poor aqueous solubility of violacein is a serious obstacle for development pharmaceutical formulations. In the present year, Rivero Berti et al. (2020) developed a novel SLN formulation of violacein containing surface-active ionic liquids (SAILs) of the cation 1-alkylimidazolium and a fluorescent tracer $DiOC_{18}$. The results indicate 6-fold incorporation of the SLN in mammalian cell cultures with high apoptotic activity (Rivero Berti et al., 2020).

LEISHMANIASIS

Leishmaniasis is caused by more than 20 different species of the *Leishmania* genre, and it is spread to mammalians through the bite of female phlebotomine infected sandflies. The disease presents itself in three forms (mainly): cutaneous (the most common), visceral (the most severe form, also known as kala-azar), and mucocutaneous. The epidemiology of leishmaniasis involves many aspects such as type of sandfly species, parasite, ecological features of the transmission places, and human behavior (World Health Organization, 2020c,d).

Leishmaniasis Treatment

Alike the already described HAT treatment scenario, there is a wide range of treatments that may or may not be applicable, depending on the cost, stage of the disease, parasite species, geographic location, and tolerability. It is difficult to develop a single drug capable of universally treating the disease, because of the huge variability of strains and clinical manifestations. According to the report of a meeting of the WHO Expert Committee on the Control of Leishmaniases, the recommended drugs are amphotericin B (traditional and liposomal formulation), pentavalent antimonial, paromomycin, miltefosine, and pentamidine.

Amphotericin B (AmBD) is an aminoglycoside with biostatic or biocidal properties that binds to sterols (ergosterol) in the cell membrane of microorganisms, thus creating a transmembrane channel and disrupting the membrane integrity (Wortmann et al., 2010). Its disadvantages include cost, the route of administration (slow intravenous infusion), and systemic and renal toxicity (Stone et al., 2016). In 1997, a liposomal formulation of AmBD—LAMBD—was authorized by the Food and Drug Administration (FDA). LAMBD diminishes the incidence of the severe side effects, thus improving tolerability. However, the production cost of the liposomal formulation is still a key barrier to accessibility in endemic countries.

Pentavalent antimonials, mainly meglumine antimoniate and sodium stibogluconate, are the first-line drugs to treat leishmaniasis (Frézard et al., 2009; Miranda-Verastegui et al., 2009). They have been the treatment of choice since 1940. It has been proposed that sodium stibogluconate may act as a prodrug that is later reduced *in vivo*, disrupting the cell thiol redox potential. It was also shown that these compounds bind to DNA I topoisomerase inhibiting plasmid DNA unwinding. Among their many side effects are nausea, vomiting, skin rashes, abdominal colic, and cardiotoxicity (Frézard et al., 2009). After all those years as the main clinical choice, the alarming growing rate of antimonial resistance is not surprising (Arevalo et al., 2001).

Discovered in 1950, paromomycin is an aminoglycoside antibiotic originally isolated from *Streptomyces rimosus* (Wiwanitkit, 2012). It binds to 16S rRNA and consequently inhibits protein synthesis by increasing the error rate in the translation process. It also disrupts the pathogen membrane fluidity and lipid metabolism. In 2006, paromomycin was approved by the FDA as an antileishmanial medication against the visceral presentation of the disease. Although it produces several undesirable side effects such as abdominal cramps and diarrhea (Wiwanitkit, 2012), it is still considered as one of the most cost-effective treatments. It is still considered as one of the most cost-effective treatments. The combination of puromycin with sodium stibogluconate (SSG&PM) has been demonstrated safe and effective, with the advantages of being a shorter and less expensive treatment. SSG&PM has been recommended by WHO as first-line treatment for visceral leishmaniasis (Kimutai et al., 2017; Drugs for Neglected Diseases initiative, 2020i).

The alkyl phospholipid miltefosine was the first oral drug registered to treat visceral leishmaniasis. Its mechanism of actions is not still fully understood but it is related to programmed cell death triggered by alkyl phospholipids. Miltefosine was first considered as potential treatment in breast cancer and other solid tumors, but it was discontinued after signs of severe gastrointestinal toxicity (Sundar and Olliaro, 2007). Later, it demonstrated high efficacy against *Leishmania* both *in vitro* and *in vivo* (Croft et al., 1987). In 2014, it was approved as the first oral treatment of leishmaniasis by the FDA. Its disadvantages include the already mentioned gastrointestinal toxicity, hand in hand with high cost and teratogenicity potential (Soto and Soto, 2006). It did not take long to show the synergy effects *in vitro* between miltefosine and liposomal amphotericin B (Seifert and Croft, 2006). Moreover, a retrospective study demonstrated a good cure rate (>80%) in human immunodeficiency virus patients coinfected with visceral leishmaniasis treated with that combination (Abongomera et al., 2018; Drugs for Neglected Diseases initiative, 2020a). Currently in the recruiting phase (phase III), this is a randomized study to test the effectiveness of oral miltefosine in combination with intravenous liposomal amphotericin and intramuscular paromomycin in patients with post Kala Azar dermal leishmaniasis (PKDL) (ClinicalTrials.gov NCT03399955, 2020; Drugs for Neglected Diseases initiative, 2020g,h). The combination of miltefosine with paromomycin

was found successful over the intracellular amastigote stage and in diminishing parasite loads in the liver, spleen, and bone marrow of an *in vivo* model (Hendrickx et al., 2017). In 2017, a randomized trial (phase III) was developed to compare the effect of miltefosine in combination with paromomycin for the treatment of visceral leishmaniasis in adults and children (ClinicalTrials.gov NCT03129646, 2020; Drugs for Neglected Diseases initiative, 2020g). Results of the study are expected by the end of 2020.

Pentamidine isethionate has already been discussed for the treatment of HAT. Pentamidine is a broad-spectrum anti-infective agent active against several parasitic worms, protozoa, and fungi with relatively toxic effects, thus requiring careful monitoring during therapy (Hafiz and Kyriakopoulos Pentamidine, 2020; World Health Organization, 2020d). It has been used as monotherapy or in combination to treat cutaneous and visceral leishmaniasis. However, the adverse effects of the drug are severe, and consequently, it is preferably averted.

There are some new chemical entities that are undergoing clinical studies (phase I). DNDI-0690 is a nitroimidazole that displays very promising (*in vitro*) activity against laboratory strains of *Leishmania infantum* and *in vivo* in the early curative hamster model (Van den Kerkhof et al., 2018). Furthermore, based on *in vivo* bioluminescence imaging, only two administrations of this compound were enough to lower the *Leishmania mexicana* parasite load by 100-fold in a murine model of cutaneous leishmaniasis (Wijnant et al., 2019). In 2015, DNDi-0690 was nominated as a preclinical candidate, intended to be used as oral treatment for visceral and cutaneous leishmaniasis. Last year, the first trial in humans was started to evaluate the safety and tolerability of a single administration of this compound (ClinicalTrials.gov NCT03929016, 2020).

Other compound under phase I is the DNDI-6148, from the oxaborole class (Drugs for Neglected Diseases initiative, 2020d). At the preclinical phase, it proved highly active against many *Leishmania* species known to produce both visceral (Van den Kerkhof et al., 2018) and cutaneous leishmaniasis (Van Bocxlaer et al., 2019). In 2018, a phase I, blinded, randomized, single-dose trial was started to study the pharmacokinetics and tolerability of a single oral dose of DNDI-6148 in healthy male subjects (ISRCTN registry, 2020). The publication of the study results are expected in 2020.

The association between the University of Dundee, GlaxoSmithKline (GSK) and DNDi led to identification of GSK3186899/DDD853651 and GSK3494245/DDD1305143 as potential candidates to treat visceral leishmaniasis (Drugs for Neglected Diseases initiative, 2020f). Both compounds show a favorable pharmacokinetic profile and similar activity to the frontline drug miltefosine in animal models of visceral leishmaniasis (Wyllie et al., 2018, 2019; Thomas et al., 2019). *In vitro* studies indicate that GSK3186899/DDD853651 main mechanism can be attributed to the inhibition of the cdc-2-related kinase 12 (CRK12) of the parasite (Wyllie et al., 2018). Further studies confirmed that GSK3494245 inhibit the chymotrypsin-like activity in the *Leishmania donovani* proteasome (Wyllie et al., 2019). In 2019, GSK3186899 entered a double-blind study started to assess its safety, tolerability, and

pharmacokinetic profile in healthy humans (ClinicalTrial.gov NCT03874234, 2020), but the study was recently suspended by GSK. By the end of this year, a phase I trial will be developed to assess the efficacy and safety of GSK3494245 (ClinicalTrials.gov NCT04504435, 2020).

Novartis and the University of Dundee have reported a selective proteasome inhibitor with efficacy in murine models of visceral and cutaneous leishmaniasis, LXE408 (Nagle et al., 2020), which is currently undergoing phase I human clinical trials (Drugs for Neglected Diseases initiative, 2020b).
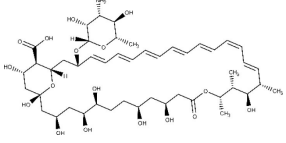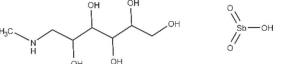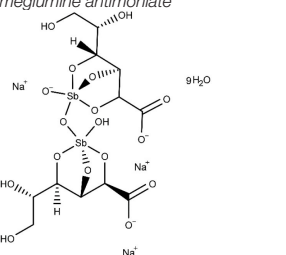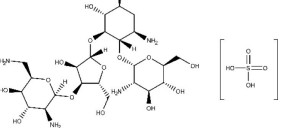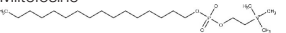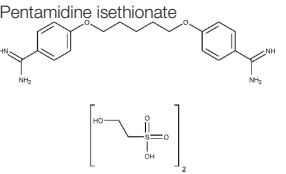
Table 3 summarizes the current therapeutic options for leishmaniasis, as well drugs that have or are undergoing clinical trials.

Lipid Nanosystems Encapsulating Approved Drugs

Leishmaniasis is so far the trypanosomatid-caused condition that has received more attention in the field of pharmaceutical lipid nanocarriers, probably due to the facts that one of the approved drugs against leishmaniasis (amphotericin B) is already available in liposomal formulation, and what is more, cutaneous leishmaniasis may at least be partially treated with topical medications. On the other hand, the predominant role of macrophages in the sequestration of circulating nanocarriers (Baboci et al., 2020) coupled with their importance on *Leishmania* infection establishment and the persistence of the parasite inside the host (De Menezes et al., 2017; Soulat and Bogdan, 2017; Holzmuller et al., 2018) may have contributed to the development of drug nanodelivery systems for this disease. Predictably, then, a substantial fraction of the reported nanosystems correspond to amphotericin B drug delivery systems. Noteworthy, leishmaniasis is also the trypanosomatid-caused infection for which the widest diversity of lipid nanocarriers has been investigated.
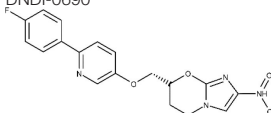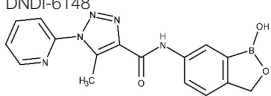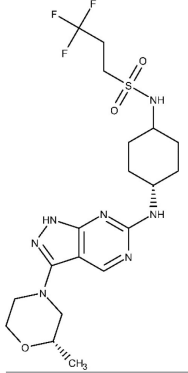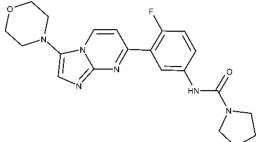
Because macrophages play a crucial role in leishmaniasis (they take part of the immune response against the parasite, but they also constitute the final host cells for its proliferation) (Tomiotto-Pellissier et al., 2018), many researchers have designed macrophage-directed antileishmanial drug delivery systems. Gupta et al. (2007) formulated amphotericin B in trilaurin emulsomes stabilized by soy phosphatidylcholine and targeted with O-palmitoyl mannan, a macrophage-specific ligand. The antileishmanial performance was tested. The antileishmanial activity was tested both *in vitro* and *in vivo*, demonstrating that the decorated emulsomes outperformed both non-decorated drug-loaded emulsomes and the free drug. Similar results were later observed in mice by Veerareddy et al. (2009) using mannose-decorated lipid nanospheres, comparing their efficacy with Fungizone. The decorated nanosystem achieved better performance than Fungizone or the non-decorated formulation. Additionally, mice treated with the encapsulated drug show no elevation in serum glutamate pyruvate transaminase, alkaline phosphatase, urea, and creatinine levels and increased bioavailability in comparison with Fungizone. Remarkably, the targeted system was found to distribute more rapidly to the liver and the spleen. Rathore et al. (2011) proposed a formulation of

TABLE 3 | The therapeutic scenario for leishmaniasis, including WHO-recommended drugs, and current clinical trials.

Drugs	Stage of the disease	Administration via	Adverse reactions	References
Drugs used to treat cutaneous and visceral leishmaniasis recommended by WHO				
Amphotericin B, AmBD and liposomal amphotericin B, amphotericin B lipid complex, and amphotericin B colloidal dispersion	Visceral leishmaniasis	IV	Nephrotoxicity, also myocarditis and death. The liposomal, lipid and colloidal formulations show fewer side effects (rigors and chills)	(Freitas-Junior et al., 2012; ClinicalTrials.gov NCT0265679, 2020; World Health Organization, 2020d)
Pentavalent antimonials meglumine antimoniate and sodium stibogluconate *meglumine antimoniate* *sodium stibogluconate*	Visceral leishmaniasis and cutaneous leishmaniasis	Intravenous Intramuscular	Common side effects are anorexia, vomiting, nausea, abdominal pain, malaise, myalgia, arthralgia, headache, metallic taste and lethargy. High cardiotoxicity, pancreatitis, nephrotoxicity, hepatotoxicity; high treatment failure (up to 65% in major epidemic areas)	(Sundar et al., 2000; World Health Organization, 2020d)
Paromomycin sulfate	Visceral and cutaneous leishmaniasis	Intravenous Intramuscular Topical	Gastrointestinal symptoms including nausea, vomiting, diarrhea, and abdominal discomfort. Nephrotoxicity and ototoxicity are rarely produced	(Ben Salah et al., 2013; ClinicalTrials.gov NCT01140191, 2020; World Health Organization, 2020d)
Miltefosine	Visceral and cutaneous leishmaniasis	Oral	Gastrointestinal symptoms, nephrotoxicity, hepatotoxicity, teratogenicity	(Dorlo et al., 2012; ClinicalTrials.gov NCT03129646, 2020; World Health Organization, 2020d)
Pentamidine isethionate	Visceral and cutaneous leishmaniasis	Intravenous Intramuscular	Diabetes mellitus, severe hypoglycemia, shock, myocarditis, and renal toxicity; limit its use	(ClinicalTrials.gov NCT02919605, 2020; World Health Organization, 2020d)

(Continued)

70

TABLE 3 | Continued

Drugs	Stage of the disease	Administration via	Adverse reactions	References
Undergoing clinical trials				
Miltefosine + liposomal amphotericin B + paromomycin	Post Kala Azar Dermal Leishmanioid	Oral (miltefosine) Intravenous (liposomal amphotericin) Intramuscular (paromomycin)	Not reported yet	(ClinicalTrials.gov NCT03399955, 2020; Drugs for Neglected Diseases initiative, 2020g)
Miltefosine + paromomycin	Visceral leishmaniasis	Oral	Not reported yet	(ClinicalTrials.gov NCT03129646, 2020)
Miltefosine + paromomycin	Cutaneous leishmaniasis	Oral (miltefosine) Topical (paromomycin)		(ClinicalTrials.gov NCT03829917, 2020)
DNDI-0690	Visceral and cutaneous leishmaniasis	Oral	Not reported yet	(ClinicalTrials.gov NCT03929016, 2020)
DNDI-6148	Visceral and cutaneous leishmaniasis	Oral	Not reported yet	(ISRCTN registry, 2020)
GSK3186899/DDD853651 (suspended)	Visceral leishmaniasis	Oral	Not reported yet	(ClinicalTrials.gov NCT03874234, 2020)
GSK3494245/DDD1305143	Visceral leishmaniasis	Oral	Not reported yet	ClinicalTrials.gov Identifier: NCT04504435
	Visceral and cutaneous leishmaniasis	Oral	Not reported	https://dndi.org/wp-content/uploads/2020/06/DNDi-June2020-RDPortfolio.pdf

amphotericin B mannosylated liposomes for the active targeting to the reticular endothelial system. They compared the drug release and biodistribution (in a hamster model of infection) of the free drug, undecorated liposomes, and mannosylated liposomes. At 24 h, comparable but slightly lower percentage of drug release were observed for mannose-coupled liposomes, an expected behavior having in mind the additional diffusional layer present in the decorated carriers. The mannosylated formulation displayed the highest reduction in parasite load, and it was confirmed that the active targeting strategy led to a comparative reduction of circulating liposomes with the concomitant rise in drug increase in liver and spleen. Mannosylated nanomicelles have also been proposed to deliver combination therapy of amphotericin B and doxorubicin for visceral leishmaniasis (Wei et al., 2020).

Using nanoprecipitation followed by sonication, Patel and Patravale (2011) obtained amphotericin B SLN conceived for oral administration (AmbiOnp). The effects of several processes (probe sonication, dialysis cycles, freeze drying, and reconstitution) on the physicochemical features of the nanoparticles (such as particle size, dispersion and entrapment efficiency) were examined. Untreated SLN displayed a relatively high mean diameter (about 350 nm) and considerable dispersion; both were substantially reduced by sonication and dialysis. Drug loading significantly increased the mean diameter of the SLN. A single-dose acute toxicity study suggested the (acute) safety of AmbiOnp orally. Pharmacokinetic studies in rat using a non-compartmental approach suggested and enhanced relative bioavailability of AmbiOnp in comparison to a free drug solution (including a substantial increment in the elimination half-life, the time to reach the concentration peak in plasma, and the total area under the plasma concentration–time curve), although additional time points in the terminal phase of the concentration–time curve should have been obtained for a more accurate estimation of most of the estimated pharmacokinetic parameters. A subsequent study with the same formulation and an improved sampling schedule confirmed, however, that oral AmbiOnp presented increased half-life and total area under the concentration–time curve in comparison to intravenous Fungizone (Chaudhari et al., 2016).

Singodia et al. (2011) reported the obtention of alginate-coated amphotericin B–loaded lipid nanoparticles, hypothesizing that activation of macrophages by alginate would synergize the antileishmanial effects of the drug. The lipid nanoparticles without coating presented a mean particle size of 108 nm, whereas alginate coating increased the mean size to 134 nm and reversed the zeta potential from +28.4 to −19.8 mV. Moderate entrapment efficiency was observed. Inhibition of intramacrophage amastigotes was significantly higher compared to non-coated drug-loaded lipid nanoparticles. Very similar results were documented by Jain et al. (2014) who prepared chitosan-coated SLN loaded with amphotericin B for immunoadjuvant chemotherapy of leishmaniasis. Besides enhanced efficacy in comparison to Fungizone and AmBisome, the authors demonstrated the improved safety profile of the developed formulation in acute toxicity studies.

Lipid–polymer antileishmanial hybrid nanoparticles were designed by Asthana et al. (2015) composed of a poly(D,L-lactide-co-glycolide) core and a stearylamine shell and loaded with amphotericin B. Stearylamine was selected as the lipid component because of its immunostimulant activity and because it acts as a ligand for stearylamine pattern recognition receptors present on the macrophage surface. The stearylamine shell increased the size of the nanoparticles and reverted their charge from negative to positive. The particles used for subsequent studies were about 175 nm. The reported system displayed a very attractive profile, including sustained drug release, reduced erythrocyte and macrophage toxicity, enhanced macrophage uptake, higher accumulation in the spleen and the liver, minima distribution in kidneys, considerable antileishmanial efficacy *in vitro* and *in vivo* against visceral leishmaniasis, and low levels of nephrotoxicity markers. The authors indicated that macrophage pattern recognition receptors were involved in the uptake of the nanoparticles and that the positive charge of the lipid shell allows them to bind to the negatively charged macrophage surface, favoring adsorption mediated endocytosis. Another recently reported hybrid system loaded with both amphotericin B and paromomycin consisted of SLN modified with 2-hydroxypropyl-β-cyclodextrin as an oral matrix system against visceral leishmaniasis (Parvez et al., 2020). The reported formulation possesses a sustained drug release profile. *In vitro* studies verified the total cellular internalization of the modified SLNs with low cytotoxicity in macrophage cells within 24 h of incubation. Moreover, the nanosystem did not elicit hepatic or renal toxicity in mice. *In vitro* and *in vivo* studies showed improved efficacy on *L. donovani* intracellular amastigotes and significantly reduced the liver parasite burden in comparison to miltefosine.

A very interesting, novel approach for the targeted delivery of amphotericin B was devised by Kumar and Bose (2019), who implemented a "ghost cell" (nanoghost) strategy utilizing macrophage membrane-derived nanovesicles as a specific carrier for the drug. The nanoghost delivered the drug specifically to infected macrophages driven by antigenic identification of infected tissues associated to low toxicity toward healthy cells.

Less frequently, other approved drugs against leishmaniasis, besides amphotericin B, have been formulated in colloidal lipid systems. For instance, paromomycin SLN with good entrapment efficiency was reported by Ghadiri et al. (2011). Sometime later, Gaspar et al. (2015) reported the development of six paromomycin liposomal formulations whose biodistribution profiles revealed preferential targeting of the antibiotic to the spleen, liver, and lungs, relative to the free drug. Such observation translated into an augmented therapeutic effect in murine models of infection with *L. infantum* and improved safety profile. Positive results were also observed by Heidari-Kharaji et al. (2016), who prepared paromomycin-loaded SLN and tested their efficacy *in vivo* against *L. major*–infected mice. The parasite load in the footpad swelling was analyzed by real-time PCR, and the level of cytokines was also assessed. The study showed that the developed formulation was efficacious in killing the parasite and switching toward T_H1 response.

da Gama Bitencourt reported the obtention of miltefosine-loaded lipid nanoparticles that enhanced the drug stability with reduced cytotoxicity in macrophages and diminished hemolytic potential, but also retaining the antiparasitic activity (da Gama Bitencourt et al., 2016). Interestingly, because of the amphiphilic nature of the drug, it acted as a powerful surfactant, and addition of increasing amounts of miltefosine reduced the mean particle size, from 144 nm (unloaded nanoparticles) to 40 to 65 nm.

Moosavian et al. (2019) obtained meglumine antimoniate-loaded liposomes containing stearylamine. Liposomal formulations enhanced the drug permeation compared with meglumine antimoniate cream. The liposomal formulation containing stearylamine proved more efficacious than drug-loaded liposomes without stearylamine. In a mice model of cutaneous leishmaniasis, liposomal groups presented smaller lesions compared to control.

Lipid Nanosystems Encapsulating Non-approved Drugs

Lopes et al. (2012) obtained tripalmitin SLN encapsulating the potential antileishmanial dinitroaniline oryzalin. The nanoparticles were stabilized by mixed emulsifier molecules such as soy lecithin, sodium deoxycholate, and Tween 20. The cell viability experiments proved that the nanoencapsulation of the drug diminished its cytotoxicity. A subsequent study by the same group compared the safety and efficacy of oryzalin-loaded SLN and liposomes with those of the free drug (Lopes et al., 2014). As observed in other reviewed articles of the current section, the nanoformulations revealed diminished cytotoxicity and hemolytic activity in comparison with the free drug and without losing *in vitro* efficacy. Superiority of both nanocarriers on the reduction of parasitic burden in spleen and liver (compared with free oryzalin) was demonstrated in a mice model of visceral leishmaniasis. Kupetz et al. (2013) screened a number of colloidal systems to develop parental formulations of the poorly soluble paullon chalcone derivative KuRei300, including micelles stabilized with lecithin/bile salts, liposomes, supercooled smectic liquid crystal of cholesterol myristate nanoparticles, a triglyceride emulsion, and cubic phase nanoparticles.

Other lipid nanosystems have been proposed to exploit the antileishmanial activity of lipophilic compounds and mixtures of natural origin. Marquele-Oliveira et al. (2016) reported a nanodelivery system based on stearic acid SLN encapsulating the liposoluble lignan fraction of the South American plant *Ocotea duckei* Vattimo, which targets the *Leishmania* lysosome of macrophages. Physicochemical analysis revealed that the delivery system presented a core-shell architecture, and the correspondent dissolution studies revealed that the active components are released by a matrix diffusion-based kinetic mechanism. The loaded SLN displayed no toxicity to murine macrophages with an *in vitro* antileishmanial effect. Comparable results were reported by Want et al. (2017), who developed a liposomal artemisinin formulation. Nanoliposomal artemisinin proved superior performance compared to free artemisinin in a mice model of visceral leishmaniasis, with modulation of cell-mediated immunity toward protective T_H1 type. Similarly, Kar et al.

(2017) prepared NLC loaded with cedrol, one of the major sesquiterpenes obtained from the genus Cupressus). *In vivo* studies revealed that the antileishmanial effects of the orally administered nanoformulation were increased (in comparison with free cedrol and miltefosine) against wild type but also to drug-resistant strains of *L. donovani*. Sousa-Batista et al. (2017) reported the obtention of lipid-core nanoparticles made of capric/caprylic triglyceride, sorbitan monostearate (i.e., Span 60^{TM}), and poly(ε-caprolactone), for the oral delivery of quercetin and quercetin penta-acetate; the quercetin-loaded nanoparticles enhanced the oral efficacy of the drug in a model of cutaneous leishmaniasis (mice). Noteworthy, aspartate aminotransferase, alanine aminotransferase, or creatinine serum levels were not modified by the treatments, suggesting they had no liver or renal toxicity. Das et al. (2017) prepared ursolic acid–loaded NLC coated with chitosan oligosaccharides for the visceral leishmaniasis therapy, intended to deliver such active ingredient to macrophages following oral administration. The formulated NLC had nano sizes ranging from 104 to 143 nm, with high drug loading capacity and relatively good entrapment efficiency. The nanoformulation was highly efficient than the free drug against cellular amastigotes from a diversity of strains. It could also substantially suppress the parasite burden *in vivo*. Very recently, NLC containing the monoterpene carvacrol (which, despite promising antileishmanial activity, displays low water solubility, high volatility, and stability issues) has been described (Galvão et al., 2020). The highest encapsulation efficiency was achieved by using beeswax as solid lipid. The drug release from the NLC fitted to the Korsmeyer and Peppas, and Weibull models, suggesting a Fickian release mechanism. Carvacrol incorporation to the NLC resulted in diminished cytotoxicity in comparison to the free drug, also increasing its *in vitro* antileishmanial efficacy (amastigotes). The encapsulation also led to increased elimination half-life in rats.

Recently, Smith et al. (2018) described high-loading self-nanoemulsifying systems for the oral delivery of the poorly soluble antiprotozoal hydroxynaphthoquinone buparvaquone. This self-emulsifying system showed an improved oral bioavailability compared to aqueous dispersions, which translated into an increase area under the plasma concentration–time curve. It demonstrated potent *in vitro* efficacy, and it almost completely suppressed parasite replication in the spleen, whereas it also inhibited the parasite replication in the liver. Mazur et al. (2019) devised beeswax nanoparticles containing copaiba oil to encapsulate diethyldithiocarbamate, which has previously shown excellent leishmanicidal effect. The nanoformulation decreased the cytotoxic effects of the drug against macrophages, which led to an almost 2-fold increase in the selectivity index.

CONCLUSIONS

The reviewed literature shows that the state of the art of lipid nanodelivery systems in the field of human trypanosomatid-caused diseases greatly varies, depending on the disease. Limited efforts have still been made in relation to drug nanocarriers for HAT or Chagas. In the case of HAT, the limited interest in

pharmaceutical nanocarriers possibly responds to the favorable evolution of the epidemiological data in the last decade and the incorporation of novel, efficacious, convenient, and bioavailable options to the therapeutic arsenal. Regarding Chagas disease, there are still not enough or convincing data that suggest that the use of nanodevices could help overcoming the limitations of the currently (and extremely limited) available medications. In any case, the reviewed articles show that most of the reported lipid nanosystems for HAT or Chagas correspond to delivery systems from previous generations (prominently, non-targeted liposomes and SLN). In other words, the potential contribution of state-of-the-art lipid nanocarriers, including functionalized and hybrid systems, has still to be explored. The most relevant challenges here might be the delivery of effective levels of the drugs to poorly irrigated/accessible tissues, targeted delivery to the most affected organs (which could contribute to improved safety and tolerability), and the enhanced effect on dormant parasites.

The scenario is substantially different in the case of leishmaniasis, where a large variety of lipid systems with distinctive architectures and functionalities have been successfully tested at the preclinical level, including macrophage-targeted systems with enhanced parasiticidal effects in affected organs such as liver or spleen and immunostimulant hybrid systems. Either nanoencapsulating already approved or experimental drugs, the outcome of those studies with a focus on lipid nanosystems consistently includes sustained drug release, reduced cytotoxicity and liver and renal toxicity, increased safety and efficacy, and improved bioavailability.

Multiple factors can possibly explain the different scenarios described across diseases, including historical and pathophysiological aspects. Colloidal drug delivery systems (liposomal amphotericin B) are already available to treat leishmaniasis. The disease includes cutaneous presentations that can be treated systemically, but also in combination with topical formulations. Particularly, the macrophages have a relevant role in the establishment and evolution of the infection, and as we know, they are likely to be targeted by pharmaceutical nanocarriers. A considerable proportion of the studies linked to lipid systems in leishmaniasis focus on the oral delivery of poorly soluble/poorly bioavailable drugs, which includes a diversity of lipophilic natural products. Lipid nanocarriers thus constitute a valid alternative to exploit the rich chemical biodiversity and expand the therapeutic options for neglected conditions.

Besides their already discussed advantages (e.g., biocompatibility and biodegradability), other possible reasons might explain the relative abundance of studies linked to the development of lipid nanocarriers for the treatment of trypanosomatid-caused conditions. Among them is the suitability of these delivery systems to load comparatively high amounts of lipophilic agents. It should be considered that, in the case of parasitic diseases, the therapeutic agents must often access to the parasite intracellular space. Furthermore, some parasite reservoirs might be found in deep tissues (poorly irrigated tissues such as adipose tissue or tissues separated from circulation by specialized barriers, e.g., the brain). In any case, lipophilic chemotherapies would be often required to provide an extensive

drug distribution and circumvent the correspondent biological barriers. These facts explain why many therapeutic agents for parasitic diseases do display a significant lipophilicity (in fact, they are one of the therapeutic categories whose members often violate Lipinski rules).

The route of administration and the costs are almost key factors when formulating active ingredients, but that is especially true when dealing with therapeutics for neglected conditions, as the convenience of the dosing forms and the cost of the therapeutic intervention are particularly relevant. Enhancing the efficacy–safety balance of already known drugs by encapsulating them within state-of-the-art nanovehicles could provide affordable solutions for the treatment of neglected conditions. Furthermore, the recent reports on quiescent or dormant stages of the parasite that cause the (today) most challenging human trypanosomatid-caused disorders (leishmaniasis and Chagas disease) may at least partially explain drug failure. It has been suggested that therapeutic benefits might thus be achieved with extended treatments; if so, pharmaceutical carriers enhancing tolerability could be more advantageous than ever. All things considered, improved safety could contribute to treatment adherence (a fundamental aspect in the field of infectious diseases, both from individual and public health perspective) and to the design of well-tolerated extensive dosing plans.

Despite its continuous and vertiginous progress, nanobiotechnology is still an emerging field, and many technological and regulatory challenges are to be faced before massive adoption within the pharmaceutical industry. Individual and environmental toxicological aspects and accurate and standardized evaluation of their pharmacokinetic profile are also to be solved. Lipid-based systems, because of their biocompatible nature, appear as a reasonable option to address some of these issues, whereas stability and scaling-up cost are possibly among their major disadvantages.

Finally, we would like to underline the need to explore last-generation pharmaceutical nanocarriers as vehicles for the treatment of trypanosomatid-caused diseases, disorders that in most cases have been only addressed preclinically using early generations of lipid-based systems. Unfortunately, for the time being, the development of therapeutic options involving last-generation technologies possibly collides with the necessity to achieve affordable solutions for neglected conditions.

AUTHOR CONTRIBUTIONS

All authors listed have made a substantial, direct and intellectual contribution to the work, and approved it for publication.

ACKNOWLEDGMENTS

REFERENCES

Abongomera, C., Diro, E., Pereira, A., de, L., Buyze, J., Stille, K., et al. (2018). The initial effectiveness of liposomal amphotericin B (AmBisome) and miltefosine combination for treatment of visceral leishmaniasis in HIV co-infected patients in Ethiopia: a retrospective cohort study. *PLoS Negl. Trop. Dis.* 12:e0006527. doi: 10.1371/journal.pntd.0006527

Ahmad, A., Ullah, S., Syed, F., Tahir, K., Khan, A. U., and Yuan, Q. (2020). Biogenic metal nanoparticles as a potential class of antileishmanial agents: mechanisms and molecular targets. *Nanomedicine* 15, 809–828. doi: 10.2217/nnm-2019-0413

Akbarzadeh, A., Rezaei-Sadabady, R., Davaran, S., Joo, S. W., Zarghami, N., Hanifehpour, Y., et al. (2013). Liposome: classification, preparation, and applications. *Nanoscale Res. Lett.* 8:102. doi: 10.1186/1556-276X-8-102

Alirol, E., Schrumpf, D., Amici Heradi, J., Riedel, A., de Patoul, C., Quere, M., et al. (2013). Nifurtimox-eflornithine combination therapy for second-stage gambiense human African trypanosomiasis: médecins sans frontières experience in the democratic republic of the congo. *Clin. Infect. Dis.* 56, 195–203. doi: 10.1093/cid/cis886

Arevalo, I., Ward, B., Miller, R., Meng, T. C., Najar, E., Alvarez, E., et al. (2001). Successful treatment of drug-resistant cutaneous leishmaniasis in humans by use of imiquimod, an immunomodulator. *Clin. Infect. Dis.* 33, 1847–1851. doi: 10.1086/324161

Arrúa, E. C., Seremeta, K. P., Bedogni, G. R., Okulik, N. B., and Salomon, C. J. (2019). Nanocarriers for effective delivery of benznidazole and nifurtimox in the treatment of chagas disease: a review. *Acta Trop.* 198:105080. doi: 10.1016/j.actatropica.2019.105080

Asthana, S., Jaiswal, A. K., Gupta, P. K., Dube, A., and Chourasia, M. K. (2015). Th-1 biased immunomodulation and synergistic antileishmanial activity of stable cationic lipid-polymer hybrid nanoparticle: biodistribution and toxicity assessment of encapsulated amphotericin B. *Eur. J. Pharm. Biopharm.* 89, 62–73. doi: 10.1016/j.ejpb.2014.11.019

Baboci, L., Capolla, S., Di Cintio, F., Colombo, F., Mauro, P., Dal Bo, M., et al. (2020). The dual role of the liver in nanomedicine as an actor in the elimination of nanostructures or a therapeutic target. *J. Oncol.* 2020:4638192. doi: 10.1155/2020/4638192

Bahia, M. T., Andrade, I. M., de Martins, T. A. F., Nascimento, Á. F., da Silva do Nascimento, A. F., de Figueiredo Diniz, L., et al. (2012). Fexinidazole: a potential new drug candidate for chagas disease. *PLoS Negl. Trop. Dis.* 6:e1870. doi: 10.1371/journal.pntd.0001870

Bellera, C. L., Balcazar, D. E., Alberca, L., Labriola, C. A., Talevi, A., and Carrillo, C. (2013). Application of computer-aided drug repurposing in the search of new cruzipain inhibitors: discovery of amiodarone and bromocriptine inhibitory effects. *J. Chem. Inf. Model.* 53, 2402–2408. doi: 10.1021/ci400284v

Ben Salah, A., Ben Messaoud, N., Guedri, E., Zaatour, A., Ben Alaya, N., Bettaieb, J., et al. (2013). Topical paromomycin with or without gentamicin for cutaneous leishmaniasis. *N. Engl. J. Med.* 368, 524–532. doi: 10.1056/NEJMoa1202657

Benaim, G., Sanders, J. M., Garcia-Marchán, Y., Colina, C., Lira, R., Caldera, A. R., et al. (2006). Amiodarone has intrinsic anti-*Trypanosoma cruzi* activity and acts synergistically with posaconazole. *J. Med. Chem.* 49, 892–899. doi: 10.1021/jm050691f

Berg, M., Vanaerschot, M., Jankevics, A., Cuypers, B., Maes, I., Mukherjee, S., et al. (2013). Metabolic adaptations of *Leishmania donovani* in relation to differentiation, drug resistance, and drug pressure. *Mol. Microbiol.* 90, 428–442. doi: 10.1111/mmi.12374

Bern, C., Montgomery, S. P., Herwaldt, B. L., Rassi, A., Marin-Neto, J. A., Dantas, R. O., et al. (2007). Evaluation and treatment of chagas disease in the United States: a systematic review. *JAMA.* 298, 2171–2181. doi: 10.1001/jama.298.18.2171

Boiani, M., Piacenza, L., Hernández, P., Boiani, L., Cerecetto, H., González, M., et al. (2010). Mode of action of nifurtimox and N-oxide-containing heterocycles against *Trypanosoma cruzi*: is oxidative stress involved? *Biochem. Pharmacol.* 79, 1736–1745. doi: 10.1016/j.bcp.2010.02.009

Bouteille, B., Oukem, O., Bisser, S., and Dumas, M. (2003). Treatment perspectives for human African trypanosomiasis. *Fundam. Clin. Pharmaco.* 17, 171–181. doi: 10.1046/j.1472-8206.2003.00167.x

Burri, C. (2010). Chemotherapy against human African trypanosomiasis: is there a road to success? *Parasitology* 137, 1987–1994. doi: 10.1017/S0031182010001137

Bustamante, J. M., and Tarleton, R. L. (2014). Potential new clinical therapies for chagas disease. *Expert Rev. Clin. Pharmacol.* 7, 317–325. doi: 10.1586/17512433.2014.909282

Cacicedo, M. L., Islan, G. A., Gurman, P., and Castro, G. R. (2016). *Drug Delivery Devices for Infectious Diseases. Drug Delivery: An Integrated Clinical and Engineering Approach.* Boca Raton, FL: CRC Press. 349–372. doi: 10.1201/9781315117584-13

Campos, M. C., Phelan, J., Francisco, A. F., Taylor, M. C., Lewis, M. D., Pain, A., et al. (2017). Genome-wide mutagenesis and multi-drug resistance in American trypanosomes induced by the front-line drug benznidazole. *Sci. Rep.* 7:14407. doi: 10.1038/s41598-017-14986-6

Canuto, J. A., Lima, D. B., de Menezes, R. R. P. P. B., Batista, A. H. M., Nogueira, P. C. D. N., Silveira, E. R., et al. (2019). Antichagasic effect of violacein from chromobacterium violaceum. *J. Appl. Microbiol.* 127, 1373–1380. doi: 10.1111/jam.14391

Carmo, A. A. L., Rocha, M. O. C., Silva, J. L. P., Ianni, B. M., Fernandes, F., Sabino, E. C., et al. (2015). Amiodarone and *Trypanosoma cruzi* parasitemia in patients with chagas disease. *Int. J. Cardiol.* 189, 182–184. doi: 10.1016/j.ijcard.2015.04.061

Carneiro, Z. A., Maia, P. I., Sesti-Costa, R., Lopes, C. D., Pereira, T. A., Milanezi, C. M., et al. (2014). *In vitro* and *in vivo* trypanocidal activity of H2bdtc-loaded solid lipid nanoparticles. *PLoS Negl. Trop. Dis.* 8:e2847. doi: 10.1371/journal.pntd.0002847

Cencig, S., Coltel, N., Truyens, C., and Carlier, Y. (2011). Parasitic loads in tissues of mice infected with *Trypanosoma cruzi* and treated with AmBisome. *PLoS Negl. Trop. Dis.* 5:e1216. doi: 10.1371/journal.pntd.0001216

Chaudhari, M. B., Desai, P. P., Patel, P. A., and Patravale, V. B. (2016). Solid lipid nanoparticles of amphotericin B (AmbiOnp): *in vitro* and *in vivo* assessment towards safe and effective oral treatment module. *Drug Deliv. Transl. Res.* 6, 354–364. doi: 10.1007/s13346-015-0267-6

ClinicalTrial.gov NCT03874234 (2020). *Safety, Tolerability and Pharmacokinetics (PKs) Investigation of GSK3186899 in Healthy Subjects.* Available online at: https://clinicaltrials.gov/ct2/show/NCT03874234 (accessed August, 2020).

ClinicalTrials.gov NCT00875173 (2020). *Selenium Treatment and Chagasic Cardiopathy (STCC) (STCC).* Available online at: https://clinicaltrials.gov/ct2/show/NCT00875173 (accessed August, 2020).

ClinicalTrials.gov NCT01140191 (2020). *Safety, Efficacy, and PK of Topical Paromomycin/Gentamicin Cream for Treatment of Cutaneous Leishmaniasis (WRNMMC).* Available online at: https://clinicaltrials.gov/ct2/show/NCT01140191 (accessed August, 2020).

ClinicalTrials.gov NCT01162967 (2020). *Clinical Trial for The Treatment of Chronic Chagas Disease With Posaconazole And Benznidazole (CHAGASAZOL).* Available online at: https://clinicaltrials.gov/ct2/show/NCT01162967 (accessed August, 2020).

ClinicalTrials.gov NCT01377480 (2020). *A Study of the Use of Oral Posaconazole (POS) in the Treatment of Asymptomatic Chronic Chagas Disease (P05267) (STOP CHAGAS).* Available online at: https://clinicaltrials.gov/ct2/show/NCT01377480 (accessed August, 2020).

ClinicalTrials.gov NCT01489228 (2020). *Proof-of-Concept Study of E1224 to Treat Adult Patients With Chagas Disease.* Available online at: https://clinicaltrials.gov/ct2/show/NCT01489228 (accessed August, 2020).

ClinicalTrials.gov NCT01533961 (2020). *Human African Trypanosomiasis: First in Man of a Clinical Trail of New Medicinal Product, the SCYX-7158.* Available online at: https://clinicaltrials.gov/ct2/show/study/NCT01533961 (accessed August, 2020).

ClinicalTrials.gov NCT01685827 (2020). *Pivotal Study of Fexinidazole for Human African Trypanosomiasis in Stage 2.* Available online at: https://clinicaltrials.gov/ct2/show/NCT01685827 (accessed August, 2020).

ClinicalTrials.gov NCT02498782 (2020). *Study to Evaluate Fexinidazole Dosing Regimens for the Treatment of Adult Patients With Chagas Disease.* Available online at: https://clinicaltrials.gov/ct2/show/study/NCT02498782 (accessed August, 2020).

ClinicalTrials.gov NCT0265679 (2020). *Topical Liposomal Amphotericin B Gel Treatment for Cutaneous Leishmaniasis.* Available online at: https://clinicaltrials.gov/ct2/show/NCT0265679 (accessed August, 2020).

ClinicalTrials.gov NCT02919605 (2020). *Efficacy and Safety of Pentamidine (7mg/kg) for Patients With Cutaneous Leishmaniasis Caused by L. Guyanensis.*

Available online at: https://clinicaltrials.gov/ct2/show/NCT02919605 (accessed August, 2020).

ClinicalTrials.gov NCT03025789 (2020). *Fexinidazole in Human African Trypanosomiasis Due to T. b. Gambiense at Any Stage.* Available online at: https://clinicaltrials.gov/ct2/show/NCT03025789 (accessed August, 2020).

ClinicalTrials.gov NCT03087955 (2020). *Prospective Study on Efficacy and Safety of Acoziborole (SCYX-7158) in Patients Infected by Human African Trypanosomiasis Due to T.b. Gambiense (OXA002).* Available online at: https://clinicaltrials.gov/ct2/show/NCT03087955 (accessed August, 2020).

ClinicalTrials.gov NCT03129646 (2020). *Miltefosine/Paromomycin Phase III Trial for Treatment of Primary Visceral Leishmaniasis (VL) Patients in Eastern Africa.* Available online at: https://clinicaltrials.gov/ct2/show/NCT03129646 (accessed August, 2020).

ClinicalTrials.gov NCT03191162 (2020). Evaluation of Different Benznidazole Regimens for the Treatment of Chronic Chagas Disease. (MULTIBENZ). Available online at: https://clinicaltrials.gov/ct2/show/NCT03191162 (accessed August, 2020).

ClinicalTrials.gov NCT03193749 (2020). *A Trial Testing Amiodarone in Chagas Cardiomyopathy (ATTACH).* Available online at: https://clinicaltrials.gov/ct2/show/NCT03193749 (accessed August, 2020).

ClinicalTrials.gov NCT03378661 (2020). *BEnznidazole New Doses Improved Treatment and Associations (BENDITA).* Available online at: https://clinicaltrials.gov/ct2/show/NCT03378661 (accessed August, 2020).

ClinicalTrials.gov NCT03399955 (2020). *Short Course Regimens for Treatment of PKDL (Sudan).* Available online at: https://clinicaltrials.gov/ct2/show/NCT03399955?recrs=abd&cond=Leishmaniasis&draw=2&rank=23 (accessed August, 2020).

ClinicalTrials.gov NCT03587766 (2020). *Oral Fexinidazole Dosing Regimens for the Treatment of Adults With Chronic Indeterminate Chagas Disease (FEXI12) Trial.* Available online at: https://clinicaltrials.gov/ct2/show/NCT03587766 (accessed August, 2020).

ClinicalTrials.gov NCT03704181 (2020). *Colchicine for Patients With Chagas' Disease (B1 Stage) (COACH).* Available online at: https://clinicaltrials.gov/ct2/show/NCT03704181 (accessed August, 2020).

ClinicalTrials.gov NCT03829917 (2020). *Oral Miltefosine Plus Topical Paromomycin In American Cutaneous Leishmaniasis.* Available online at: https://clinicaltrials.gov/ct2/show/NCT03829917

ClinicalTrials.gov NCT03874234 (2020). *Safety, Tolerability and Pharmacokinetics (PKs) Investigation of GSK3186899 in Healthy Subjects.* Available online at: https://clinicaltrials.gov/ct2/show/NCT03874234

ClinicalTrials.gov NCT03892213 (2020). *Pharmacokinetic Drug-Drug Interaction Study.* Available online at: https://clinicaltrials.gov/ct2/show/NCT03892213 (accessed August, 2020).

ClinicalTrials.gov NCT03929016 (2020). *Single Oral Dose Escalation Study of DNDI-0690 in Healthy Male Subjects.* Available online at: https://clinicaltrials.gov/ct2/show/NCT03929016 (accessed August, 2020).

ClinicalTrials.gov NCT03974178 (2020). *Efficacy and Safety of Fexinidazole in Patients With Human African Trypanosomiasis (HAT) Due to Trypanosoma Brucei Rhodesiense.* Available online at: https://clinicaltrials.gov/ct2/show/NCT03974178 (accessed August, 2020).

ClinicalTrials.gov NCT03981523 (2020). *New Therapies and Biomarkers for Chagas Infection (TESEO).* Available online at: https://clinicaltrials.gov/ct2/show/NCT03981523 (accessed August, 2020).

ClinicalTrials.gov NCT04504435 (2020). *Safety, Tolerability and Pharmacokinetics (PK) Investigation of GSK3494245 in Healthy Participants.* Available online at: https://clinicaltrials.gov/ct2/show/NCT04504435?recrs=abd&cond=Leishmaniasis&draw=2&rank=22 (accessed August, 2020).

Courchesne, W. E. (2002). Characterization of a novel, broad-based fungicidal activity for the antiarrhythmic drug amiodarone. *J. Pharmacol. Exp. Ther.* 300, 195–199. doi: 10.1124/jpet.300.1.195

Crespillo-Andújar, C., López-Vélez, R., Trigo, E., Norman, F., Díaz-Menéndez, M., Monge-Maillo, B., et al. (2020). Comparison of the toxicity of two treatment schemes with benznidazole for chronic chagas disease: a prospective cohort study in two spanish referral centres. *Clin. Microbiol. Infect.* 26, 384.e1–e4. doi: 10.1016/j.cmi.2019.10.030

Croft, S., Neal, A., Pendergast, W., and Chan, J. (1987). The activity of alkyl phosphorylcholines and related derivatives against *Leishmania*

donovani. Biochem. Pharmaco. 36, 2633–2636. doi: 10.1016/0006-2952(87)90543-0

Cruz-Bustos, T., González-González, G., Morales-Sanfrutos, J., Megía-Fernández, A., Santoyo-González, F., and Osuna, A. (2012). Functionalization of immunostimulating complexes (ISCOMs) with lipid vinyl sulfones and their application in immunological techniques and therapy. *Int. J. Nanomed.* 7, 5941–5956. doi: 10.2147/IJN.S35556

da Gama Bitencourt, J. J., Pazin, W. M., Ito, A. S., Barioni, M. B., de Paula Pinto, C., Santos, M. A., et al. (2016). Miltefosine-loaded lipid nanoparticles: improving miltefosine stability and reducing its hemolytic potential toward erythtocytes and its cytotoxic effect on macrophages. *Biophys. Chem.* 217, 20–31. doi: 10.1016/j.bpc.2016.07.005

Das, S., Ghosh, S., De, A. K., and Bera, T. (2017). Oral delivery of ursolic acid-loaded nanostructured lipid carrier coated with chitosan oligosaccharides: development, characterization, *in vitro* and *in vivo* assessment for the therapy of leishmaniasis. *Int. J. Biol. Macromol.* 102, 996–1008. doi: 10.1016/j.ijbiomac.2017.04.098

De Menezes, J. P., Saraiva, E. M., and da Rocha-Azevedo, B. (2017). The site of the bite: Leishmania interaction with macrophages, neutrophils and the extracellular matrix in the dermis. *Parasit. Vectors* 9:264. doi: 10.1186/s13071-016-1540-3

De Morais, F., Enumo, A., Gonçalves, R. S., Cesar, G. B., Miranda, N., Vilsinski, B. H., et al. (2019). Hypericin photodynamic activity. Part III: *in vitro* evaluation in different nanocarriers against trypomastigotes of *Trypanosoma cruzi. Photochem. Photobiol. Sci.* 18, 487–494. doi: 10.1039/C8PP00444G

Deeks, E. D. (2019). Fexinidazole: first global approval. *Drugs* 79, 215–220. doi: 10.1007/s40265-019-1051-6

Dickie, E. A., Giordani, F., Gould, M. K., Mäser, P., Burri, C., Mottram, J. C., et al. (2020). New drugs for human African trypanosomiasis: a twenty first century success story. *Trop. Med. Infect. Dis.* 5:29. doi: 10.3390/tropicalmed5010029

Diniz, L., de, F., Mazzeti, A. L., Caldas, I. S., Ribeiro, I., and Bahia, M. T. (2018). Outcome of E1224-benznidazole combination treatment for infection with a multidrug-resistant *Trypanosoma cruzi* strain in mice. *Antimicrob. Agents Chem.* 62, e00401–18. doi: 10.1128/AAC.00401-18

Docampo, R., Moreno, S., Turrens, J. F., Katzin, A. F., Gonzalez-Cappa, S. M., and Stoppani, A. O. M. (1981). Biochemical and ultrastructural alterations produced by miconazole and econazole in *Trypanosoma cruzi. Mol. Biochem. Parasitol.* 3, 169–180. doi: 10.1016/0166-6851(81)90047-5

Dorlo, T. P. C., Balasegaram, M., Beijnen, J. H., and de Vries, P. J. (2012). Miltefosine: a review of its pharmacology and therapeutic efficacy in the treatment of leishmaniasis. *J. Antimicrob. Chemother.* 67, 2576–2597. doi: 10.1093/jac/dks275

Drugs for Neglected Diseases initiative (2020a). *Portfolio. New Treatments for HIV/Visceral Leishmaniasis.* Available online at: https://dndi.org/research-development/portfolio/hivvl/ (accessed August, 2020).

Drugs for Neglected Diseases Initiative (2020b). *Portfolio. Novartis LXE408 for the Treatment of Visceral leishmaniasis.* Available online at: https://dndi.org/in-the-media/2020/pharmaceutical-business-review-novartis-dndi-to-jointly-develop-lxe408-for-visceral-leishmaniasis/ (accessed August, 2020).

Drugs for Neglected Diseases initiative (2020c). *Portfolio. Acoziborole for Sleeping Sickness.* Available online at: https://dndi.org/research-development/portfolio/acoziborole/ (accessed August, 2020).

Drugs for Neglected Diseases initiative (2020d). *Portfolio. DNDi-6148 for leishmaniasis.* Available online at: https://dndi.org/research-development/portfolio/dndi-6148/ (accessed August, 2020).

Drugs for Neglected Diseases initiative (2020e). *Portfolio. Fexinidazole for T.b. Rhodesiense.* Available online at: https://dndi.org/research-development/portfolio/fexinidazole-tb-rhodesiense/ (accessed August, 2020).

Drugs for Neglected Diseases initiative (2020f). *Portfolio. GSK3186899 and GSK3494245 for leishmaniasis.* Available online at: https://dndi.org/research-development/portfolio/gsk3186899-ddd853651-gsk3494245-ddd1305143/ (accessed August, 2020).

Drugs for Neglected Diseases Initiative (2020g). *Portfolio. Miltefosine and Paromomycin Combo.* Available online at: https://dndi.org/researchdevelopment/portfolio/miltefosine-paromomycin-combo/

Drugs for Neglected Diseases initiative (2020h). *Portfolio. New treatments for Post-kala-azar dermal leishmaniasis (PKDL).* Available online at: https://dndi.org/research-development/portfolio/new-treatments-pkdl/ (accessed 2020).

Drugs for Neglected Diseases initiative (2020i). *Portfolio. SSGandPM (East Africa). Visceral leishmaniasis*. Available online at: https://dndi.org/research-development/portfolio/ssg-pm/ (accessed August, 2020).

Drugs for Neglected Diseases initiative (2020j). *Portfolio. Fexindazole for Chagas*. Available online at: https://dndi.org/research-development/portfolio/fexinidazole-chagas/

Echeverría, L. E., González, C. I., Hernandez, J. C. M., Díaz, M. L., Eduardo Nieto, J., López-Romero, L. A., et al. (2020). Efficacy of the benznidazole + posaconazole combination therapy in parasitemia reduction: an experimental murine model of acute chagas. *Rev. Soc. Bras. Med. Trop.* 53:e20190477. doi: 10.1590/0037-8682-0477-2019

Eperon, G., Balasegaram, M., Potet, J., Mowbray, C., Valverde, O., and Chappuis, F. (2014). Treatment options for second stage gambiense human African trypanosomiasis. *Expert Rev. Anti. Infect. Ther.* 12, 1407–1417. doi: 10.1586/14787210.2014.959496

Fairlamb, A. H. (2019). Fexinidazole for the treatment of human African trypanosomiasis. *Drugs Today.* 55, 705–712. doi: 10.1358/dot.2019.55.11.3068795

Fernandes, F., Ramires, F. J. A., Ianni, B. M., Salemi, V. M. C., Oliveira, A. M., Pessoa, F. G., et al. (2012). Effect of colchicine on myocardial injury induced by *Trypanosoma cruzi* in experimental chagas disease. *J. Card. Fail.* 18, 654–659. doi: 10.1016/j.cardfail.2012.06.419

Ferrer-Tasies, L., Moreno-Calvo, E., Cano-Sarabia, M., Aguilella-Arzo, M., Angelova, A., Lesieur, S., et al. (2013). Quatsomes: vesicles formed by self-assembly of sterols and quaternary ammonium surfactants. *Langmuir* 29, 6519–6528. doi: 10.1021/la4003803

Fortes Francisco, A., Lewis, M. D., Jayawardhana, S., Taylor, M. C., Chatelain, E., and Kelly, J. M. (2015). Limited ability of posaconazole to cure both ccute and chronic *Trypanosoma cruzi* infections revealed by highly sensitive *in vivo* imaging. *Antimicrob. Agents Chemother.* 59, 4653–4661. doi: 10.1128/AAC.00520-15

Freitas-Junior, L. H., Chatelain, E., Kim, H. A., and Siqueira-Neto, J. L. (2012). Visceral leishmaniasis treatment: what do we have, what do we need and how to deliver it? *Int. J. Parasitol. Drug.* 2, 11–19. doi: 10.1016/j.ijpddr.2012.01.003

Frézard, F., Demicheli, C., and Ribeiro, R. R. (2009). Pentavalent antimonials: new perspectives for old drugs. *Molecules* 14, 2317–2336. doi: 10.3390/molecules14072317

Galvão, J. G., Santos, R. L., Silva, A. R. S. T., Santos, J. S., Costa, A. M. B., Chandasana, H., et al. (2020). Carvacrol loaded nanostructured lipid carriers as a promising parenteral formulation for leishmaniasis treatment. *Eur. J. Pharm. Sci.* 150:105335. doi: 10.1016/j.ejps.2020.105335

Gaspar, M. M., Calado, S., Pereira, J., Ferronha, H., Correia, I., Castro, H., et al. (2015). Targeted delivery of paromomycin in murine infectious diseases through association to nano lipid systems. *Nanomedicine* 11, 1851–1860. doi: 10.1016/j.nano.2015.06.008

GBD 2016 Disease and Injury Incidence and Prevalence Collaborators (2017). Global, regional, and national incidence, prevalence, and years lived with disability for 328 diseases and injuries for 195 countries, 1990–2016: a systematic analysis for the global burden of disease study 2016. *Lancet* 390, 1211–1259. doi: 10.1016/S0140-6736(17)32154-2

Ghadiri, M., Vatanara, A., Doroud, D., and Najafabadi, A. R. (2011). Paromomycin loaded solid lipid nanoparticles: characterization of production parameters. *Biotechnol. Bioproc.* 16, 617–623. doi: 10.1007/s12257-010-0331-5

Gondim, B. L. C., da Silva Catarino, J., de Sousa, M. A. D., de Oliveira Silva, M., Lemes, M. R., de Carvalho-Costa, T. M., et al. (2019). Nanoparticle-mediated drug delivery: blood-brain barrier as the main obstacle to treating infectious diseases in CNS. *Curr. Pharm. Des.* 25, 3983–3996. doi: 10.2174/1381612825666191014171354

Gupta, S., Dube, A., and Vyas, S. P. (2007). Antileishmanial efficacy of amphotericin B bearing emulsomes against experimental visceral leishmaniasis. *J. Drug Target.* 15, 437–444. doi: 10.1080/10611860701453836

Hafiz, S., and Kyriakopoulos, C. Pentamidine (2020) *In: StatPearls*. Treasure Island (FL): StatPearls Publishing. Available online at: https://www.ncbi.nlm.nih.gov/books/NBK557586/ (accessed May 21, 2020).

Hall, B. S., Bot, C., and Wilkinson, S. R. (2011). Nifurtimox activation by trypanosomal type I nitroreductases generates cytotoxic nitrile metabolites. *J. Biol. Chem.* 286, 13088–13095. doi: 10.1074/jbc.M111.230847

Heidari-Kharaji, M., Taheri, T., Doroud, D., Habibzadeh, S., Badirzadeh, A., and Rafati, S. (2016). Enhanced paromomycin efficacy by solid lipid nanoparticle formulation against *Leishmania* in mice model. *Parasite Immunol.* 38, 599–608. doi: 10.1111/pim.12340

Hejchman, E., Ostrowska, K., Maciejewska, D., Kossakowski, J., and Courchesne, W. (2012). Synthesis and antifungal activity of derivatives of 2- and 3-benzofurancarboxylic acids. *J. Pharmacol. Exp. Ther.* 343, 380–388. doi: 10.1124/jpet.112.196980

Hendrickx, S., Kerkhof, M. V., den Mabille, D., Cos, P., Delputte, P., Maes, L., et al. (2017). Combined treatment of miltefosine and paromomycin delays the onset of experimental drug resistance in *Leishmania infantum*. *PLoS Neglect. Trop. Dis.* 11:e0005620. doi: 10.1371/journal.pntd.0005620

Holanda, M. T., Mediano, M. F. F., Hasslocher-Moreno, A. M., Xavier, S. S., Saraiva, R. M., Sousa, A. S., et al. (2018). A protocol update for the selenium treatment and chagasic cardiomyopathy (STCC) trial. *Trials* 19:507. doi: 10.1186/s13063-018-2889-8

Holzmuller, P., Geiger, A., Nzoumbou-Boko, R., Pissarra, J., Hamrouni, S., Rodrigues, V., et al. (2018). Trypanosomatid infections: how do parasites and their excreted–secreted factors modulate the inducible metabolism of l-arginine in macrophages? *Front. Immunol.* 9:778. doi: 10.3389/fimmu.2018.00778

ISRCTN registry. (2020). Available online at: http://www.isrctn.com/ISRCTN54981564 (accessed August 2020).

Jacobs, R. T., Nare, B., Wring, S. A., Orr, M. D., Chen, D., Sligar, J. M., et al. (2011). SCYX-7158, an orally -active benzoxaborole for the treatment of stage 2 human African trypanosomiasis. *PLoS Negl. Trop. Dis.* 5:e1151. doi: 10.1371/journal.pntd.0001151

Jain, V., Gupta, A., Pawar, V. K., Asthana, S., Jaiswal, A. K., Dube, A., et al. (2014). Chitosan-assisted immunotherapy for intervention of experimental leishmaniasis via amphotericin B-loaded solid lipid nanoparticles. *Appl. Biochem. Biotechnol.* 174, 1309–1330. doi: 10.1007/s12010-014-1084-y

Jallouli, Y., Paillard, A., Chang, J., Sevin, E., and Betbeder, D. (2007). Influence of surface charge and inner composition of porous nanoparticles to cross blood-brain barrier *in vitro*. *Int. J. Pharm.* 344, 103–109. doi: 10.1016/j.ijpharm.2007.06.023

Jara, M., Berg, G., Caljon, G., de Muylder, B., Denis, C., Castillo, I., et al. (2017). Macromolecular biosynthetic parameters and metabolic profile in different life stages of *Leishmania braziliensis*: amastigotes as a functionally less active stage. *PLoS ONE* 12:e0180532. doi: 10.1371/journal.pone.0180532

Jara, M., Maes, I., Imamura, H., Domagalska, M. A., Dujardin, J. C., and Arevalo, J. (2019). Tracking of quiescence in leishmania by quantifying the expression of GFP in the ribosomal DNA locus. *Sci. Rep.* 9:18951. doi: 10.1038/s41598-019-55486-z

Kar, N., Chakraborty, S., De, A. K., Ghosh, S., and Bera, T. (2017). Development and evaluation of a cedrol-loaded nanostructured lipid carrier system for *in vitro* and *in vivo* susceptibilities of wild and drug resistant *Leishmania donovani* amastigotes. *Eur. J. Pharm. Sci.* 104, 196–211. doi: 10.1016/j.ejps.2017.03.046

Kennedy, P. G. E. (2004). Human African trypanosomiasis of the CNS: current issues and challenges. *J. Clin. Invest.* 113, 496–504. doi: 10.1172/JCI200421052

Kimutai, R., Musa, A. M., Njoroge, S., Omollo, R., Alves, F., Hailu, A., et al. (2017). Safety and effectiveness of sodium stibogluconate and paromomycin combination for the treatment of visceral leishmaniasis in eastern Africa: results from a pharmacovigilance program. *Clin. Drug Investig.* 37, 259–272. doi: 10.1007/s40261-016-0481-0

Kloehn, J., Saunders, E. C., O'Callaghan, S., Dagley, M. J., and McConville, M. J. (2015). Characterization of metabolically quiescent leishmania parasites in murine lesions using heavy water labeling. *PLoS Pathog.* 11:e1004683. doi: 10.1371/journal.ppat.1004683

Kroubi, M., Daulouede, S., Karembe, H., Jallouli, Y., Howsam, M., Mossalayi, D., et al. (2010). Development of a nanoparticulate formulation of diminazene to treat African trypanosomiasis. *Nanotechnology* 21:505102. doi: 10.1088/0957-4484/21/50/505102

Kuemmerle, A., Schmid, C., Kande, V., Mutombo, W., Ilunga, M., Lumpungu, I., et al. (2020). Prescription of concomitant medications in patients treated with nifurtimox eflornithine combination therapy (NECT) for T.b. gambiense second stage sleeping sickness in the democratic republic of the congo. *PLoS Negl. Trop. Dis.* 14:e0008028. doi: 10.1371/journal.pntd.0008028

Kumar, P., and Bose, P. P. (2019). Macrophage ghost entrapped amphotericin B: a novel delivery strategy towards experimental visceral leishmaniasis. *Drug. Deliv. Transl. Res.* 9, 249–259. doi: 10.1007/s13346-018-00602-1

Kupetz, E., Preu, L., Kunick, C., and Bunjes, H. (2013). Parenteral formulation of an antileishmanial drug candidate - tackling poor solubility, chemical instability, and polymorphism. *Eur. J. Pharm. Biopharm.* 85, 511–20. doi: 10.1016/j.ejpb.2013.02.001

Li, X., Tsibouklis, J., Weng, T., Zhang, B., Yin, G., Feng, G., et al. (2017). Nano carriers for drug transport across the blood-brain barrier. *J. Drug Target.* 25, 17–28. doi: 10.1080/1061186X.2016.1184272

Liu, Y., Xie, X., Chen, H., Hou, X., He, Y., Shen, J., et al. (2020). Advances in next-generation lipid-polymer hybrid nanocarriers with emphasis on polymer-modified functional liposomes and cell-based-biomimetic nanocarriers for active ingredients and fractions from chinese medicine delivery. *Nanomedicine* 29:102237. doi: 10.1016/j.nano.2020.102237

Lopes, R., Eleutério, C. V., Gonçalves, L. M., Cruz, M. E., and Almeida, A. J. (2012). Lipid nanoparticles containing oryzalin for the treatment of leishmaniasis. *Eur. J. Pharm. Sci.* 45, 442–450. doi: 10.1016/j.ejps.2011.09.017

Lopes, R., Gaspar, M. M., Pereira, J., Eleutério, C. V., Carvalheiro, M., Almeida, A. J., et al. (2014). Liposomes versus lipid nanoparticles: comparative study of lipid-based systems as oryzalin carriers for the treatment of leishmaniasis. *J. Biomed. Nanotechnol.* 10, 3647–3657. doi: 10.1166/jbn.2014.1874

Malvy, D., and Chappuis, F. (2011). Sleeping sickness. *Clin. Microbiol. Infect.* 7, 986–995. doi: 10.1111/j.1469-0691.2011.03536.x

Marquele-Oliveira, F., Torres, E. C., Barud, H., da, S., Zoccal, K. F., Faccioli, L. H., et al. (2016). Physicochemical characterization by AFM, FT-IR and DSC and biological assays of a promising antileishmania delivery system loaded with a natural Brazilian product. *J. Pharm. Biomed. Anal.* 123, 195–204. doi: 10.1016/j.jpba.2016.01.045

Maya Berg 1, Manu Vanaerschot, Andris Jankevics, Bart Cuypers, Ilse Maes, Sandip Mukherjee, Basudha Khanal, Suman Rijal, Syamal Roy, Fred Opperdoes, Rainer Breitling, Jean-Claude Dujardin

Maya, D. J., Cassels, B. K., Iturriaga-Vásquez, P., Ferreira, J., Faúndez, M., Galanti, N., et al. (2007). Mode of action of natural and synthetic drugs against *Trypanosoma cruzi* and their interaction with the mammalian host. *Comp. Biochem. Phys. A* 146, 601–620. doi: 10.1016/j.cbpa.2006.03.004

Mazur, K. L., Feuser, P. E., Valério, A., Poester Cordeiro, A., de Oliveira, C. I., Assolini, J. P., et al. (2019). Diethyldithiocarbamate loaded in beeswax-copaiba oil nanoparticles obtained by solventless double emulsion technique promote promastigote death *in vitro*. *Colloid. Surface. B.* 176, 507–512. doi: 10.1016/j.colsurfb.2018.12.048

Mecca, M. M., de, Bartel, L. C., Castro, C. R., and de, Castro, J. A. (2008). Benznidazole biotransformation in rat heart microsomal fraction without observable ultrastructural alterations: comparison to nifurtimox-induced cardiac effects. *Mem. I. Oswaldo Cruz.* 103, 549–553. doi: 10.1590/S0074-02762008000600007

Miranda-Verastegui, C., Tulliano, G., Gyorkos, T. W., Calderon, W., Rahme, E., Ward, B., et al. (2009). First-line therapy for human cutaneous leishmaniasis in Peru using the TLR7 agonist imiquimod in combination with pentavalent antimony. *PLoS Negl. Trop. Dis.* 3:e491. doi: 10.1371/journal.pntd.0000491

Molina, I., Gómez I Prat, J., Salvador, F., Treviño, B., Sulleiro, E., Serre, N., et al. (2014). Randomized trial of posaconazole and benznidazole for chronic chagas' disease. *N Engl. J. Med.* 370, 1899–1908. doi: 10.1056/NEJMoa1313122

Moosavian, S. A., Fallah, M., and Jaafari, M. R. (2019). The activity of encapsulated meglumine antimoniate in stearylamine-bearing liposomes against cutaneous leishmaniasis in BALB/c mice. *Exp. Parasitol.* 200, 30–35. doi: 10.1016/j.exppara.2019.03.004

Morilla, M. J., Benavidez, P., Lopez, M., Bakas, L., and Romero, E. L. (2002). Development and in vitro characterisation of a benznidazole liposomal formulation. *Int. J. Pharm.* 249, 89–99. doi: 10.1016/S0378-5173(02)00453-2

Morilla, M. J., Montanari, J., Frank, F., Malchiodi, E., Corral, R., Petray, P., et al. (2005). Etanidazole in pH-sensitive liposomes: design, characterization and *in vitro/in vivo* anti-*Trypanosoma cruzi* activity. *J. Control. Release.* 103, 599–607. doi: 10.1016/j.jconrel.2004.12.012

Morilla, M. J., Montanari, J., Prieto, M., Lopez, M., Petray, P., and Romero, E. L. (2004). Intravenous liposomal benznidazole as trypanocidal agent: increasing drug delivery to liver is not enough. *Int. J. Pharm.* 278, 311–318. doi: 10.1016/j.ijpharm.2004.03.025

Morillo, C. A., Marin-Neto, J. A., Avezum, A., Sosa-Estani, S., Rassi, A., Rosas, F., et al. (2015). Randomized trial of benznidazole for chronic chagas' cardiomyopathy. *N. Engl. J. Med.* 373, 1295–1306. doi: 10.1056/NEJMoa1507574

Morillo, C. A., Waskin, H., Sosa-Estani, S., Bangher, M., del, C., Cuneo, C., et al. (2017). Benznidazole and posaconazole in eliminating parasites in asymptomatic *Trypanosoma cruzi* carriers: the STOP-CHAGAS trial. *J. Am. Coll. Cardiol.* 69, 939–947. doi: 10.1016/j.jacc.2016.12.023

Mukherjee, A., Waters, A. K., Kalyan, P., Achrol, A. C., Kesari, S., and Yenugonda, V. M. (2019). Lipid-polymer hybrid nanoparticles as a next-generation drug delivery platform: state of the art, emerging technologies, and perspectives. *Int. J. Nanomed.* 19, 1937–1952. doi: 10.2147/IJN.S198353

Nafari, A., Cheraghipour, K., Sepahvand, M., Shahrokhi, G., Gabal, E., and Mahmoudvand, H. (2020). Nanoparticles: new agents toward treatment of leishmaniasis. *Parasite Epidemiol. Control.* 10:e00156. doi: 10.1016/j.parepi.2020.e00156

Nagle, A., Biggart, A., Be, C., Srinivas, H., Hein, A., Caridha, D., et al. (2020). Discovery and characterization of clinical candidate LXE408 as a kinetoplastid-selective proteasome inhibitor for the treatment of leishmaniases. *J. Med. Chem.* 63, 10773–10781. doi: 10.1021/acs.jmedchem.0c00499

Nagle, A., Khare, S., Kumar, A. B., Supek, F., Buchynskyy, A., Mathison, C. J. N., et al. (2014). Recent developments in drug discovery for leishmaniasis and human African trypanosomiasis. *Chem. Rev.* 114, 11305–11347. doi: 10.1021/cr500365f

Neal, R. A., and van Bueren, J. (1988). Comparative studies of drug susceptibility of five strains of Trypanosoma cruzi *in vivo* and *in vitro*. *Trans. R. Soc. Trop. Med. Hyg.* 82, 709–714. doi: 10.1016/0035-9203(88)90208

Nok, A. J. (2003). Arsenicals (melarsoprol), pentamidine and suramin in the treatment of human African trypanosomiasis. *Parasitol. Res.* 90, 71–79. doi: 10.1007/s00436-002-0799-9

Nussbaum, K., Honek, J., Cadmus, C. M., and Efferth, T. (2010). Trypanosomatid parasites causing neglected diseases. *Curr. Med. Chem.* 17, 1594–1617. doi: 10.2174/092986710790979953

Nwaka, S., and Hudson, A. (2006). Innovative lead discovery strategies for tropical diseases. *Nat. Rev. Drug Discov.* 5, 941–955. doi: 10.1038/nrd2144

Omarch, G., Kippie, Y., Mentor, S., Ebrahim, N., Fisher, D., Murilla, G., et al. (2019). Comparative *in vitro* transportation of pentamidine across the blood-brain barrier using polycaprolactone nanoparticles and phosphatidylcholine liposomes. *Artif. Cells Nanomed. Biotechnol.* 47, 1428–1436. doi: 10.1080/21691401.2019.1596923

O'Shea, I. P., Shahed, M., Aguilera-Venegas, B., and Wilkinson, S. R. (2016). Evaluating 5-nitrothiazoles as trypanocidal agents. *Antimicrob. Agents Chemother.* 60, 1137–1140. doi: 10.1128/AAC.02006-15

Paillard, A., Passirani, C., Saulnier, P., Kroubi, M., Garcion, E., Benoît, J. P., et al. (2010). Positively-charged, porous, polysaccharide nanoparticles loaded with anionic molecules behave as 'stealth' cationic nanocarriers. *Pharm. Res.* 27, 126–133. doi: 10.1007/s11095-009-9986-z

Parra, F. L., Frank, F. M., Alliani, B. F., Romero, E. L., and Petray, P. B. (2020). Imiquimod-loaded nanoarchaeosomes as a promising immunotherapy against *Trypanosoma cruzi* infection. *Colloid. Surface. B* 189:110850. doi: 10.1016/j.colsurfb.2020.110850

Parthasarathy, A., and Kalesh, K. (2020). Defeating the trypanosomatid trio: proteomics of the protozoan parasites causing neglected tropical diseases. *RSC. Med. Chem.* 11, 625–645. doi: 10.1039/D0MD00122H

Parvez, S., Yadagiri, G., Gedda, M. R., Singh, A., Singh, O. P., Verma, A., et al. (2020). Modified solid lipid nanoparticles encapsulated with amphotericin B and paromomycin: an effective oral combination against experimental murine visceral leishmaniasis. *Sci. Rep.* 10:12243. doi: 10.1038/s41598-020-69276-5

Patel, P. A., and Patravale, V. B. (2011). AmbiOnp: solid lipid nanoparticles of amphotericin B for oral administration. *J. Biomed. Nanotechnol.* 7, 632–639. doi: 10.1166/jbn.2011.1332

Patterson, S., and Wyllie, S. (2014). Nitro drugs for the treatment of trypanosomatid diseases: past, present, and future prospects. *Trends. Parasitol.* 30, 289–298. doi: 10.1016/j.pt.2014.04.003

Pépin, J., and Milord, F. (1994). The treatment of human African trypanosomiasis. *Adv. Parasitol.* 33, 1–47. doi: 10.1016/S0065-308X(08)60410-8

Pereira, P. C. M., and Navarro, E. C. (2013). Challenges and perspectives of chagas disease: a review. *J. Venom. Anim. Toxins.* 19:34. doi: 10.1186/1678-9199-19-34

Prata, A. (2001). Clinical and epidemiological aspects of chagas disease. *Lancet Infect. Dis.* 1, 92–100. doi: 10.1016/S1473-3099(01)00065-2

Puri, A., Loomis, K., Smith, B., Lee, J. H., Yavlovich, A., Heldman, E., et al. (2009). Lipid-based nanoparticles as pharmaceutical drug carriers: from concepts to clinic. *Crit. Rev. Ther. Drug Carrier Syst.* 26, 523–580. doi: 10.1615/CritRevTherDrugCarrierSyst.v26.i6.10

Quezada, C. Q., Azevedo, C. S., Charneau, S., Santana, J. M., Chorilli, M., Carneiro, M. B., et al. (2019). Advances in nanocarriers as drug delivery systems in chagas disease. *Int. J. Nanomed.* 14, 6407–6424. doi: 10.2147/IJN.S206109

Raether, W., and Seidenath, H. (1983). The activity of fexinidazole (HOE 239) against experimental infections with *Trypanosoma cruzi*, trichomonads and *Entamoeba histolytica. Ann. Trop. Med. Parasit.* 77, 13–26. doi: 10.1080/00034983.1983.11811668

Rathore, A., Jain, A., Gulbake, A., Shilpi, S., Khare, P., Jain, A., et al. (2011). Mannosylated liposomes bearing amphotericin B for effective management of visceral leishmaniasis. *J. Liposome Res.* 21, 333–340. doi: 10.3109/08982104.2011.575381

Rivero Berti, I., Rodenak-Kladniew, B., Onaindia, C., Adam, C. G., Islán, G. A., Durán, N., et al. (2020). Assessment of in vitro cytotoxicity of imidazole ionic liquids and inclusion in targeted drug carriers containing violacein. *RSC Adv.* 10, 29336–29346. doi: 10.1039/D0RA05101B

Saleem, K., Khursheed, Z., Hano, C., Anjum, I., and Anjum, S. (2019). Applications of nanomaterials in leishmaniasis: a focus on recent advances and challenges. *Nanomaterials* 9:1749. doi: 10.3390/nano9121749

Sánchez-Valdez, F. J., Padilla, A., Wang, W., Orr, D., and Tarleton, R. L. (2018). Spontaneous dormancy protects trypanosoma cruzi during extended drug exposure. *Elife* 7:e34039. doi: 10.7554/eLife.34039

Sanderson, L., Dogruel, M., Rodgers, J., De Koning, H. P., and Thomas, S. A. (2009). Pentamidine movement across the murine blood-brain and blood-cerebrospinal fluid barriers: effect of trypanosome infection, combination therapy, P-glycoprotein, and multidrug resistance-associated protein. *J. Pharmacol. Exp. Ther.* 329, 967–977. doi: 10.1124/jpet.108.149872

Sbaraglini, M. L., Vanrell, M. C., Bellera, C. L., Benaim, G., Carrillo, C., Talevi, A., et al. (2016). Neglected tropical protozoan diseases: drug repositioning as a rational option. *Curr. Top. Med. Chem.* 16, 2201–2222. doi: 10.2174/1568026616666160216154309

Seifert, K., and Croft, S. L. (2006). *In vitro* and *in vivo* interactions between miltefosine and other antileishmanial drugs. *Antimicrob. Agents Chemother.* 50, 73–79. doi: 10.1128/AAC.50.1.73-79.2006

Singodia, D., Khare, P., Dube, A., Talegaonkar, S., Khar, R. K., and Mishra, P. R. (2011). Development and performance evaluation of alginate-capped amphotericin B lipid nanoconstructs against visceral leishmaniasis. *J. Biomed. Nanotechnol.* 7, 123–124. doi: 10.1166/jbn.2011.1232

Smith, L., Serrano, D. R., Mauger, M., Bolás-Fernández, F., Dea-Ayuela, M. A., and Lalatsa, A. (2018). Orally bioavailable and effective buparvaquone lipid-based nanomedicines for visceral leishmaniasis. *Mol. Pharm.* 15, 2570–2583. doi: 10.1021/acs.molpharmaceut.8b00097

Soto, J., and Soto, P. (2006). Miltefosine: oral treatment of Leishmaniasis. *Exp. Ver. Anti Infect. Therap.* 4, 177–185. doi: 10.1586/14787210.4.2.177

Soulat, D., and Bogdan, C. (2017). Function of macrophage and parasite phosphatases in leishmaniasis. *Front. Immunol.* 8:1838. doi: 10.3389/fimmu.2017.01838

Sousa-Batista, A. J., Poletto, F. S., Philipon, C. I. M. S., Guterres, S. S., Pohlmann, A. R., and Rossi-Bergmann, B. (2017). Lipid-core nanocapsules increase the oral efficacy of quercetin in cutaneous leishmaniasis. *Parasitology* 144, 1769–1774. doi: 10.1017/S003118201700097X

Souza, A. P., de Jelicks, L. A., Tanowitz, H. B., Olivieri, B. P., Medeiros, M. M., Oliveira, G. M., et al. (2010). The benefits of using selenium in the treatment of chagas disease: prevention of right ventricle chamber dilatation and reversion of *Trypanosoma cruzi*-induced acute and chronic cardiomyopathy in mice. *Mem. Inst. Oswaldo Cruz.* 105, 746–751. doi: 10.1590/S0074-02762010000600003

Spósito, P. Á., Mazzeti, A. L., de Oliveira Faria, C., Urbina, J. A., Pound-Lana, G., Bahia, M. T., et al. (2017). Ravuconazole self-emulsifying delivery system: in vitro activity against *Trypanosoma cruzi* amastigotes and in vivo toxicity. *Int. J. Nanomed.* 12, 3785–3799. doi: 10.2147/IJN.S133708

Stone, N. R. H., Bicanic, T., Salim, R., and Hope, W. (2016). Liposomal amphotericin B (AmBisome®): a review of the pharmacokinetics, pharmacodynamics, clinical experience and future directions. *Drugs* 76, 485–500. doi: 10.1007/s40265-016-0538-7

Streck, L., Sarmento, V., de Menezes, R., Fernandes-Pedrosa, M. F., Martins, A., and da Silva-Júnior, A. A. (2019). Tailoring microstructural, drug release properties, and antichagasic efficacy of biocompatible oil-in-water benznidazol-loaded nanoemulsions. *Int. J. Pharm.* 555, 36–48. doi: 10.1016/j.ijpharm.2018.11.041

Sundar, S., More, D. K., Singh, M. K., Singh, V. P., Sharma, S., Makharia, A., et al. (2000). Failure of pentavalent antimony in visceral leishmaniasis in India: report from the center of the Indian epidemic. *Clin. Infect. Dis.* 31, 1104–1107. doi: 10.1086/318121

Sundar, S., and Olliaro, P. L. (2007). Miltefosine in the treatment of leishmaniasis: clinical evidence for informed clinical risk management. *Ther. Clin. Risk. Manag.* 3, 733–740.

Tarral, A., Blesson, S., Mordt, O. V., Torreele, E., Sassella, D., Bray, M. A., et al. (2014). Determination of an optimal dosing regimen for fexinidazole, a novel oral drug for the treatment of human African trypanosomiasis: first-in-human studies. *Clin. Pharmacokinet.* 53, 565–580. doi: 10.1007/s40262-014-0136-3

Thomas, M. G., De Rycker, M., Ajakane, M., Albrecht, S., Álvarez-Pedraglio, A. I., Boesche, M., et al. (2019). Identification of GSK3186899/DDD853651 as a preclinical development candidate for the treatment of visceral leishmaniasis. *J. Med. Chem.* 62, 1180–1202. doi: 10.1021/acs.jmedchem.8b01218

Tomiotto-Pellissier, F., Bortoleti, B., Assolini, J. P., Gonçalves, M. D., Carloto, A., Miranda-Sapla, M., et al. (2018). Macrophage polarization in leishmaniasis: broadening horizons. *Front. Immunol.* 9:2529. doi: 10.3389/fimmu.2018.02529

Torrico, F., Gascon, J., Ortiz, L., Alonso-Vega, C., Pinazo, M. J., Schijman, A., et al. (2018). Treatment of adult chronic indeterminate chagas disease with benznidazole and three E1224 dosing regimens: a proof-of-concept, randomised, placebo-controlled trial. *Lancet. Inf. Dis.* 18, 419–430. doi: 10.1016/S1473-3099(17)30538-8

Urbina, J. A. (2017). Pharmacodynamics and follow-up period in the treatment of human *Trypanosoma cruzi* infections with posaconazole. *J. Am. Coll. Cardiol.* 70, 299–300. doi: 10.1016/j.jacc.2017.03.611

Urbina, J. A., and Docampo, R. (2003). Box 1. Pathogenesis of chagas disease: auto-immunity or parasite persistence? *Trends Parasitol.* 11, 495–501. doi: 10.1016/j.pt.2003.09.001

Urbina, J. A., Payares, G., Sanoja, C., Lira, R., and Romanha, A. J. (2003). *In vitro* and *in vivo* activities of ravuconazole on *Trypanosoma cruzi*, the causative agent of chagas disease. *Int. J. Antimicrob. Agents.* 21, 27–38. doi: 10.1016/S0924-8579(02)00273-X

Van Bocxlaer, K., Caridha, D., Black, C., Vesely, B., Leed, S., Sciotti, R. J., et al. (2019). Novel benzoxaborole, nitroimidazole and aminopyrazoles with activity against experimental cutaneous leishmaniasis. *Int. J. Parasitol. Drug* 11, 129–138. doi: 10.1016/j.ijpddr.2019.02.002

Van den Kerkhof, M., Mabille, D., Chatelain, E., Mowbray, C. E., Braillard, S., Hendrickx, S., et al. (2018). *In vitro* and *in vivo* pharmacodynamics of three novel antileishmanial lead series. *Int. J. Parasitol. Drugs* 8, 81–86. doi: 10.1016/j.ijpddr.2018.01.006

Veerareddy, P. R., Vobalaboina, V., and Ali, N. (2009). Antileishmanial activity, pharmacokinetics and tissue distribution studies of mannose-grafted amphotericin B lipid nanospheres. *J. Drug Target.* 17, 140–147. doi: 10.1080/10611860802528833

Villalta, F., and Rachakonda, G. (2019). Advances in preclinical approaches to chagas disease drug discovery. *Expert. Opin. Drug. Dis.* 14, 1161–1174. doi: 10.1080/17460441.2019.1652593

Vinuesa, T., Herráez, R., Oliver, L., Elizondo, E., Acarregui, A., Esquisabel, A., et al. (2017). Benznidazole nanoformulates: a chance to improve therapeutics for chagas disease. *Am. J. Trop. Med. Hyg.* 97, 1469–1476. doi: 10.4269/ajtmh.17-0044

Volpedo, G., Costa, L., Ryan, N., Halsey, G., Satoskar, A., and Oghumu, S. (2019). Nanoparticulate drug delivery systems for the treatment of neglected tropical protozoan diseases. *J. Venom. Anim. Toxins incl. Trop. Dis.* 25:e144118. doi: 10.1590/1678-9199-jvatitd-1441-18

Want, M. Y., Islammudin, M., Chouhan, G., Ozbak, H. A., Hemeg, H. A., Chattopadhyay, A. P., et al. (2017). Nanoliposomal artemisinin for the

treatment of murine visceral leishmaniasis. *Int. J. Nanomed.* 12, 2189–2204. doi: 10.2147/IJN.S106548

Wei, P., Ye, Z., Cao, S., Bai, S., Seeberger, P. H., Yin, J., et al. (2020). Combination therapy with amphotericin B and doxorubicin encapsulated in mannosylated nanomicelles for visceral leishmaniasis. *Colloid. Surface. A* 598:124804. doi: 10.1016/j.colsurfa.2020.124804

Wijnant, G. J., Croft, S., de la Flor, R., Alavijeh, M., Yardley, V., Braillard, S., et al. (2019). Pharmacokinetics and pharmacodynamics of the nitroimidazole DNDI-0690 in mouse models of cutaneous leishmaniasis. *Antimicrob. Agents Chemother.* 63, e00829–e00819. doi: 10.1128/AAC.00829-19

Wiwanitkit, V. (2012). Interest in paromomycin for the treatment of visceral leishmaniasis (kala-azar). *Therapeutics and clinical risk management. Ther. Clin. Risk. Manag.* 8, 323–328. doi: 10.2147/TCRM.S30139

World Health Organization (2020a). *Trypanosomiasis, human African (sleeping sickness) (factsheet)*. Available online at: https://www.who.int/news-room/fact-sheets/detail/trypanosomiasis-human-african-(sleeping-sickness) (assessed August 2020).

World Health Organization (2020b). *Chagas Disease (American Trypanosomiasis) (factsheet)*. Available online at: https://www.who.int/news-room/fact-sheets/detail/Chagas-disease-(american-trypanosomiasis) (assessed August 2020).

World Health Organization (2020c). *Leishmaniasis. (factsheet)*. Available online at: https://www.who.int/news-room/q-a-detail/Leishmaniasis (accessed August 2020).

World Health Organization (2020d). *Report of a meeting of the WHO Expert Committee on the Control of Leishmaniases (fact sheet 949)*. Available online at: https://www.who.int/neglected_diseases/resources/who_trs_949/en/ (accessed August 2020).

Wortmann, G., Zapor, M., Ressner, R., Fraser, S., Hartzell, J., Pierson, J., et al. (2010). Lipsosomal amphotericin B for treatment of cutaneous leishmaniasis. *Am. J. Trop. Med. Hyg.* 83, 1028–1033. doi: 10.4269/ajtmh.2010.10-0171

Wyllie, S., Brand, S., Thomas, M., De Rycker, M., Chung, C. W., Pena, I., et al. (2019). Preclinical candidate for the treatment of visceral leishmaniasis that acts through proteasome inhibition. *Proc. Natl. Acad. Sci. U.S.A.* 116, 9318–9323. doi: 10.1073/pnas.1820175116

Wyllie, S., Thomas, M., Patterson, S., Crouch, S., De Rycker, M., Lowe, R., et al. (2018). Cyclin-dependent kinase 12 is a drug target for visceral leishmaniasis. *Nature* 560. 192–197. doi: 10.1038/s41586-018-0356-z

Yang, S., Wenzler, T., Miller, P. N., Wu, H., Boykin, D. W., Brun, R., et al. (2014). Pharmacokinetic comparison to determine the mechanisms underlying the differential efficacies of cationic diamidines against first- and second-stage human African trypanosomiasis. *Antimicrob. Agents Chemother.* 58, 4064–4074. doi: 10.1128/AAC.02605-14

Yardley, V., and Croft, S. L. (1999). *In vitro* and *in vivo* activity of amphotericin B-lipid formulations against experimental *Trypanosoma cruzi* infections. *Am. J. Trop. Med. Hyg.* 61, 193–197. doi: 10.4269/ajtmh.1999.61.193

Yun, O., Priotto, G., Tong, J., Flevaud, L., and Chappuis, F. (2010). NECT is next: implementing the new drug combination therapy for *Trypanosoma brucei gambiense* sleeping sickness. *PLoS Negl. Trop. Dis.* 4:e720. doi: 10.1371/journal.pntd.0000720

Surface Plasmon Resonance as a Characterization Tool for Lipid Nanoparticles Used in Drug Delivery

Cecilia Yamil Chain*, María Antonieta Daza Millone*, José Sebastián Cisneros, Eduardo Alejandro Ramirez and María Elena Vela

Instituto de Investigaciones Fisicoquímicas Teóricas y Aplicadas (INIFTA- Universidad Nacional de La Plata (UNLP)- Consejo Nacional de Investigaciones Científicas y Técnicas (CONICET)), La Plata, Argentina

The development of drug carriers based in lipid nanoparticles (LNPs) aims toward the synthesis of non-toxic multifunctional nanovehicles that can bypass the immune system and allow specific site targeting, controlled release and complete degradation of the carrier components. Among label free techniques, Surface Plasmon Resonance (SPR) biosensing is a versatile tool to study LNPs in the field of nanotherapeutics research. SPR, widely used for the analysis of molecular interactions, is based on the immobilization of one of the interacting partners to the sensor surface, which can be easily achieved in the case of LNPs by hydrophobic attachment onto commercial lipid- capture sensor chips. In the last years SPR technology has emerged as an interesting strategy for studying molecular aspects of drug delivery that determines the efficacy of the nanotherapeutical such as LNPs' interactions with biological targets, with serum proteins and with tumor extracelullar matrix. Moreover, SPR has contributed to the obtention and characterization of LNPs, gathering information about the interplay between components of the formulations, their response to organic molecules and, more recently, the quantification and molecular characterization of exosomes. By the combination of available sensor platforms, assay quickness and straight forward platform adaptation for new carrier systems, SPR is becoming a high throughput technique for LNPs' characterization and analysis.

Keywords: lipid nanoparticles, drug carriers, Surface Plasmon Resonance, molecular target, protein corona

1. INTRODUCTION

Drug delivery has been improved over the years with continuous effort to develop new and more efficient carriers. Nowadays, drug carrier design points toward a non-toxic multifunctional nanoparticle (NP) that eludes the immune system and allows site-specific targeting, on-demand drug release and complete degradation of the carrier components (Choi and Han, 2018; Li et al., 2019; Yan et al., 2019; Zhao et al., 2019; Yeh et al., 2020).

Lipid-based nanoparticles (LNPs) bear the advantages for *in vivo* applications of being non-toxic and biodegradable (Puri et al., 2009) and they have probed their usefulness as vehicles for dermal, transdermal, mucosal, parenteral and ocular drug administration routes (Allen and Cullis, 2013; Desfrançois et al., 2018). Among them, phospholipid vesicles or "liposomes" were the first and so far most successful form of nanocarriers, with the larger number of approved formulations (Bozzuto and Molinari, 2015; Pattni et al., 2015; Bunker et al., 2016; Zylberberg and Matosevic, 2016; Li et al., 2019). Liposomes can be modified with a "stealth sheath," e.g., with poly- ethylene glycol (PEG), to avoid the complement activation of the immune system. Another strategy to evade

the immune system is to utilize natural vesicles such as exosomes (György et al., 2015; Ha et al., 2016; Wiklander et al., 2019). On the other hand, immunogenic properties can be exploited for targeting in virus-like particles (VLPs) that display effective cell entry properties due to their viral origin (Zdanowicz and Chroboczek, 2016; Rohovie et al., 2017). Nevertheless, all these vesicles lack of long-term storage stability and, if taken orally, they suffer a rapid degradation by stomach pH, bile salts or intestinal enzymes (Selvamuthukumar and Velmurugan, 2012). These difficulties and the need of compatible large-scale manufacturing lead to the development of solid lipid nanoparticles (SLNs) and, more recently, nanostructured lipid carriers (NLCs) (Naseri et al., 2015; Oner et al., 2020). NLCs incorporate small amounts of liquid lipids in the formulation diminishing matrix crystallization, increasing drug loading and preventing drug expulsion during storage and they have proved to be cytocompatible (Rodenak-Kladniew et al., 2019; Bueloni et al., 2020) and effective for different delivery routes.

The adequate characterization of LNPs is crucial to obtain drug vehicles and to understand their behavior in biological systems. The characterization methods should focused on the LNP's parameters that determine their usefulness in nanotherapeutics: particle size and zeta potential, drug loading and drug release, stability and biomolecular interactions, among others (Mehnert and Mäder, 2012). Most of the conventional methods to study biomolecular interactions require labeling, such as ELISA, fluorescence techniques or MicroScale Thermophoresis (MST) (Jerabek-Willemsen et al., 2014). Among label-free techniques, binding affinity can be assessed by Isothermal Titration Calorimetry (ITC) (Duff et al., 2011) or Biolayer Interferometry (BLI) (Weeramange et al., 2020) but, as they lack from dynamic flow conditions, kinetic parameters cannot be determined. Surface Plasmon Resonance (SPR) spectroscopy is a label free optical technique capable of real-time measuring through changes in the refractive index (RI) in the vicinity of a metal surface. To do so, one binding partner (ligand) is immobilized on a sensor chip while the free counterpart (analyte) from a sample solution is injected through a microfluidic setup (**Figure 1A**). Although similar information is provided by the quartz crystal microbalance (QCM), in this case the obtained data depends both on the analyte binding and on the water displacements that can occur due to the interaction, affecting the obtained results (Tonda-Turo et al., 2018).

The aim of this review is to outline the state of the art in SPR sensing of LNPs, describing its usefulness and challenges in the framework of drug delivery research.

2. SURFACE PLASMON RESONANCE

2.1. Principle

In order to achieve the SPR phenomenon, a material that exhibits a free electron behavior is required, as it occurs with the conduction band electrons in metals (Maier, 2007). Plasmons are quantized waves of the collective movement of electrons resulting from the interaction with photons from a *p*-polarized light source. The propagation of plasmons, now surface plasmon-polaritons (SPPs), produces alternating positive and negative

regions that in contact with a lower RI medium result in a confined evanescent field, that decays exponentially in the perpendicular direction at both sides of the interface (**Figure 1B**). Small changes in RI within the evanescent field will greatly alter the propagation properties of SPPs, reason why this phenomenon drew attention as an analytical technique.
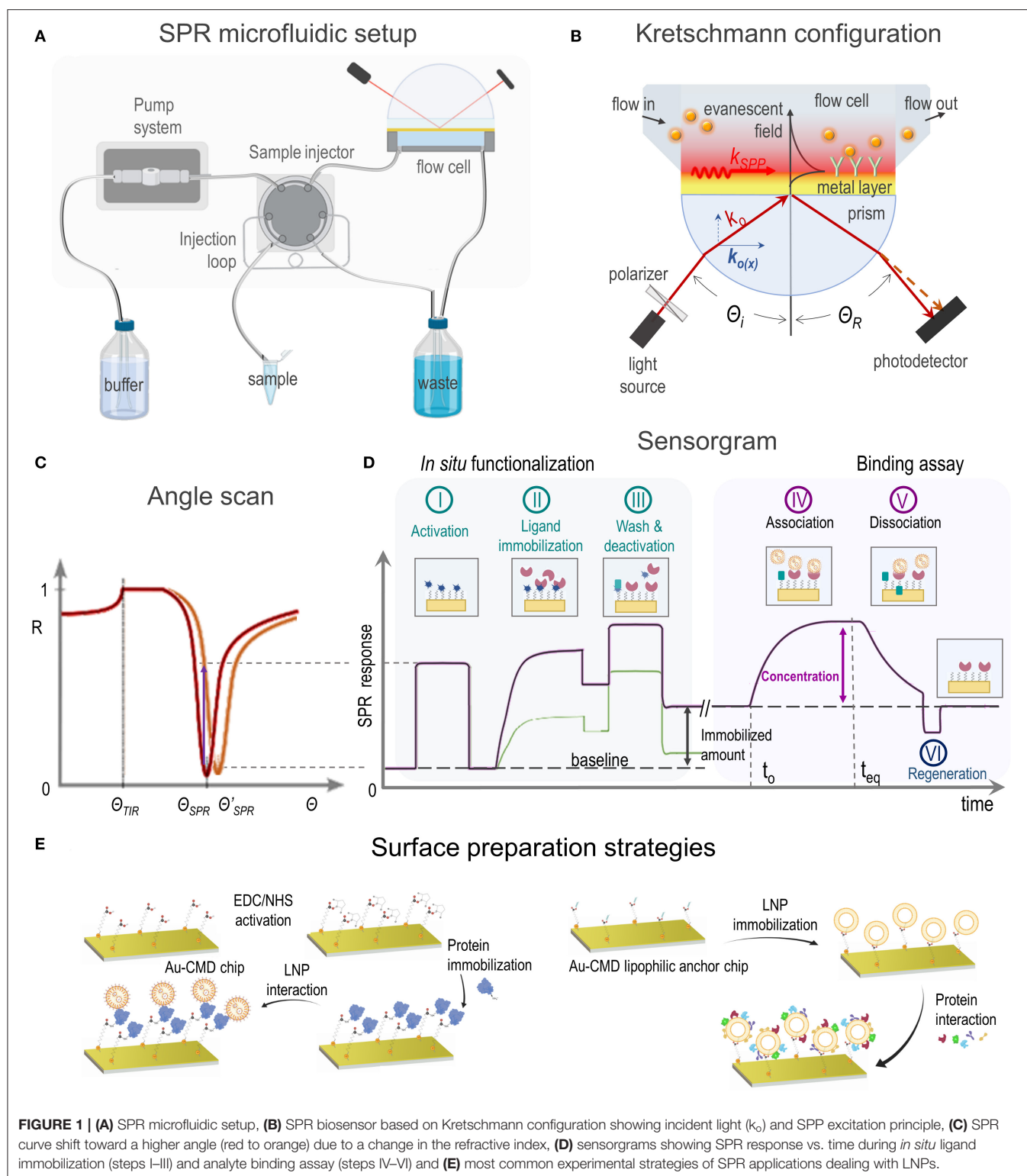
The resonant condition, where the largest number of photons can excite SPPs, will be reached when the light wavevector in the propagation direction $[k_{o(x)}]$ matches the wavevector of the SPPs (k_{SPP}). There are different strategies to achieve this matching, the most widely employed method in SPR instruments is the Kretschmann configuration (**Figure 1B**) where SPP excitation is attained through total internal reflection (TIR) (Schasfoort, 2017). Depending on the incident angle (Θ_i), the $k_{o(x)}$ light component is absorbed by SPPs, resulting in a drop of reflectivity (R) (**Figure 1C**). At a given RI in the medium, Θ_{SPR} allows the maximum light absorption by SPPs and the minimum reflected light. As RI changes, i.e., by molecules in a solution, k_{SPP} is modified and a different Θ_{SPR} is required to fulfill the new resonance condition. SPR measurements are usually carried out at a fixed Θ_i and changes expressed as SPR response (either ΔR or $\Delta \Theta$) are registered as a function of time (**Figure 1D**), yielding curves known as sensorgrams.

2.2. Measurement Data and Analysis

SPR sensors chips are usually gold coated glass plates. The optimal gold layer thickness of ~ 50 nm allows to achieve high sensitivity (Fontana, 2006) and the glass side is coupled to a prism through a RI matching fluid or polymer (**Figure 1B**). A flow cell is placed upon the gold surface enclosing one or more flow channels. The microfluidic SPR setup allows to infuse a running buffer and a sequential injection of small volume (50–1,000 μL) sample solutions that will interact with the sensor platform (**Figure 1A**). The adequate choice of the flow rate is critical to avoid mass transport limitations or shear stress effects.

Platform design should be optimized to prevent steric hindrance that can affect binding events. Depending on the application, the gold layer needs to be modified (section 3) and a biocompatible organic layer (thiol self-assembled monolayer—SAM- or polymer), eventually exhibiting anchor points for immobilization, is placed onto the surface (Gedig, 2017). Ligand immobilization can take place either *ex situ* or *in situ,* in the latter case the immobilized amount can be quantified (**Figure 1D**; Albers and Vikholm-Lundin, 2011). For immobilization by covalent attachment, crosslinker reagents are injected in the first place to activate the surface (**Figure 1D**, step I) and the ligand solution is subsequently passed over for a time period that allows conjugation (**Figure 1D**, step II). On the other side, a ligand solution can be directly injected without previous activation (**Figure 1D**, step II) if immobilization is based on physical attachment, i.e., by hydrogen bonding or hydrophobic forces. Finally, a washing procedure (**Figure 1D**, step III) is employed to either remove weakly bound material and/or deactivate the reactive functional groups generated in step I.

Once the surface is ready, a solution containing the analyte is injected allowing association (**Figure 1D**, step IV) and registering

FIGURE 1 | (A) SPR microfluidic setup, **(B)** SPR biosensor based on Kretschmann configuration showing incident light (k$_o$) and SPP excitation principle, **(C)** SPR curve shift toward a higher angle (red to orange) due to a change in the refractive index, **(D)** sensorgrams showing SPR response vs. time during *in situ* ligand immobilization (steps I–III) and analyte binding assay (steps IV–VI) and **(E)** most common experimental strategies of SPR applications dealing with LNPs.

afterwards the dissociation (**Figure 1D**, step V). Before the next analyte assay the surface must be regenerated (**Figure 1D**, step VI) with the mildest solution that releases the analyte without damaging the immobilized ligand, i.e., diluted acids

or bases, detergents, etc. As the amount of the SPR response at the steady state (t$_{eq}$) is related to the analyte concentration and possible matrix interferents, control experiments must be carefully designed in order to avoid data misinterpretation.

Moreover, to minimize unspecific adsorption, a blocking step to reduce non-specific binding can also be included before the assay, e.g., by using a well-known protein solution.

3. SURFACE PREPARATION STRATEGIES

Since SPR studies of LNPs cover a great variety of applications, several immobilization methods have been utilized, mainly based on covalent immobilization or hydrophobic attachment of one of the interacting entities onto organic layer covered- gold sensor surfaces (**Figure 1E**). High affinity capture of ligands by a specific binding molecule and adsorption onto bare gold sensor chips have also been reported. In this section, a brief description of each immobilization method utilized in SPR studies of LNPs is presented. Reference papers corresponding to each subsection are listed in **Table 1**.

3.1. Covalent Immobilization

Among conjugation techniques to immobilize ligands to SPR surfaces, amide linkage (Hermanson, 2013) is the most employed strategy. Functional carboxylic groups are included in carboxymethyl dextran (CMD) or alginate coated commercial gold sensor chips or they can be obtained from bare sensor surfaces adequately covered with thiol SAMs (**Table 1**) based on the robust covalent bond that is established between S and Au (Vericat et al., 2010).

Although covalent coupling easily provides stable ligand immobilization to the sensor surface, it may modify active sites of proteins potentially affecting the analyte binding activity. In cases where the covalent immobilization of the ligand is unsuitable, capturing methods provide an alternative approach.

3.2. Capturing Approaches

Ligand immobilization based on high affinity streptavidin- biotin capture has also been reported in SPR studies dealing with LNPs. The surface preparation relies on the adequate attachment of streptavidin onto the sensor surface either through reaction with biotinylated alkanethiols (Meierhofer et al., 2010; Rupert et al., 2016), thiolated PEG (Im et al., 2017) or amide coupling (Al-Ahmady et al., 2014) and in the previous ligand's conjugation to biotin (Hermanson, 2013).

3.3. Hydrophobic Attachment

Immobilization of LNPs to SPR chips through hydrophobic interactions can be achieved by alkane chains incorporated in a polymeric coating, commercially referred to as "Au- lipid capture chips" or prepared by covering bare sensor chips with alkanethiol- SAMs (**Table 1**).

Most of SPR applications focused on surface attached LNPs are based on Au- lipid capture chips coated with CMD and functionalized with lipophilic substituents (**Table 1**), as these platforms yield the immobilization of "intact" LNPs (**Figure 1E**, right; Hodnik and Anderluh, 2013). On the other side sensor surfaces coated with alkanethiol groups, either obtained commercially (Tamiaki et al., 2006) or prepared by chemical modification of bare gold sensor chips (Malmsten, 1999; Efremova et al., 2000), have also been used to immobilize LNPs,

with the limitation that NPs fuse to the surface generating a lipid monolayer onto the alkanethiol (Hodnik and Anderluh, 2013).

3.4. Physical Adsorption

Some SPR applications dealing with immobilized LNPs are based on simple physical attachment to SPR bare gold chips (**Table 1**) as some biomolecules show a strong spontaneous adsorption on gold surfaces (Hodnik and Anderluh, 2013). Nevertheless, the reorganization or uncontrolled exchange of the adsorbed entities to attain the most favorable thermodynamic state have been reported (Hodnik and Anderluh, 2013) which can result in unreliable assays.

4. APPLICATIONS OF SPR-BASED BIOSENSORS IN THE STUDY OF LNPs

SPR-based sensors are increasingly used to study a variety of LNPs such as liposomes, SLNs, NLCs, VLPs, exosomes and hybrid systems. In this section, examples of applications of SPR biosensing on drug LNPs' carriers in different areas of nanotherapeutics research are presented.

4.1. LNPs' Interactions Involved in Drug Delivery

4.1.1. Interaction With Biological Targets

One of the major challenges of nanotherapeutics is to selectively deliver NPs to the desired biological target. With this aim, NPs are functionalized with adequate targeting ligands resulting in decorated nanovehicles with enhanced capacity to direct selective binding. Analyses of interactions between LNPs and their biological molecular targets is a well-established research area of SPR, either by using isolated proteins, cell membranes or entire cells as target models (**Table 1**).

SPR experiments have been defining in the obtention of decorated liposomes with high affinity to amyloid-β peptide (Gobbi et al., 2010; Mourtas et al., 2011; Gregori et al., 2017), contributing to the development of very promising vectors for the targeted delivery of potential new diagnostic and therapeutic molecules for Alzheimer's disease. SPR sensing based on surface immobilization of the target protein onto Au- CMD chips (**Figure 1E**, left) has also contributed to the elucidation of the interplay of decorated liposomes or SLNs and membrane proteins that are overexpressed in malignant tissues (Nielsen et al., 2002; Terada et al., 2007; Mizrahy et al., 2011; Shi et al., 2015a; Huang et al., 2019), in disease-supporting macrophages (Etzerodt et al., 2012; Rafique et al., 2019) or in T-cells involved in autoimmune diseases (Ding et al., 2015). Moreover, SPR studies based on immobilized liposomes (**Figure 1E**, right) have shed light on the complex mechanism for the interaction of lectins with glycoliposomes specially designed to target sugar-binding proteins (Tamiaki et al., 2006; Sandoval-Altamirano et al., 2017).

The interplay between LNPs and cell membranes or entire cells as biological targets have also been investigated by SPR (**Table 1**). In this regard, SPR has been applied to study the interaction of liposomes in solution and immobilized bacterial

TABLE 1 | Summary of SPR studies on LNPs: research area, subject of study, immobilized ligand and analyte in solution, surface preparation strategy, and reference papers.

Lipid nanoparticle	Research area	Subject of study	Immobilized ligand/analyte in solution	Sensor chip and surface immobilization chemistry	References
Liposomes	Molecular interactions involved in drug delivery	Interaction with biological targets (4.1.1)	Target protein/LNP	Au-CMD chip, amide coupling (3.1)	Laukkanen et al., 1994; Nielsen et al., 2002; Terada et al., 2007; Mizrahy et al., 2011; Etzerodt et al., 2012; Ding et al., 2015; Shi et al., 2015a,b; Xiang et al., 2015; Gregori et al., 2017; Huang et al., 2019
				Au-alginate chip, amide coupling (3.1)	Gobbi et al., 2010; Mourtas et al., 2011
				Au chip, biotinylated thiol layer (3.2)	Viitala et al., 2012
				Au-CMD chip, amide coupling, streptavidin (3.2)	Al-Ahmady et al., 2014
			LNP/target protein	Au 1-octadecanethiol SAM chip (3.3)	Tamiaki et al., 2006
				Au chip, 11-mercapto 1- undecanol SAM (3.3)	Sandoval-Altamirano et al., 2017
			Cell membrane model/LNP	Au lipid- capture chip (3.3)	Cai et al., 2014; Wang et al., 2014
			Cell/LNP	Au-CMD chip, amide coupling (3.1)	Guo et al., 2014
			Bacterial biofilm/LNP	Au chip, incubation with diluted bacterial culture suspensions	Sugano et al., 2016
		Interaction with serum proteins (4.1.2)	LNP/protein	Au lipid- capture chip (3.3)	Akita et al., 2015; Shibata et al., 2015; Kari et al., 2017
				Au chip, 1-octadecanethiol SAM (3.3)	Malmsten, 1999; Efremova et al., 2000
				Au chip, biotinylated thiol layer, streptavidin (3.2)	Meierhofer et al., 2010
			Protein/LNP	Au-CMD chip, amide coupling (3.1)	Crielaard et al., 2011
				Au-alginate chip, amide coupling (3.1)	Canovi et al., 2012
		Interaction with ECM matrix (4.1.3)	Protein/ LNP	Au-CMD chip, amide coupling (3.1)	Wadajkar et al., 2019
	Obtention and characterization of LNP's formulations	Interaction between components of the formulations (4.2.1)	LNP/protein	Au lipid- capture chip (3.3)	Rauscher et al., 2014; Skyttner et al., 2019
			LNP/PEG	Au chip (3.4)	Zhao et al., 2010
			Protein/LNP	Au-CMD chip, amide coupling (3.1)	Yatuv et al., 2009
		Response to organic molecules (4.2.2)	LNP/detergent	Au-lipid capture chip (3.3)	Shibata et al., 2012
			LNP/ glucose	Au chip (3.4)	Seong et al., 2003
Hybrid NPs	Obtention and characterization of LNP's formulations	Interaction between components of the formulations (4.2.1)	Hybrid NP/targeting peptide	Au lipid- capture chip (3.3)	Soman et al., 2008; Pan et al., 2011
			Liposome/polymeric NP	Au lipid- capture chip (3.3)	Gao et al., 2014
	Molecular interactions involved in drug delivery	Interaction with biological targets (4.1.1)	Hybrid NP/cell	Au lipid. capture chip (3.3)	Soman et al., 2009
Exosomes	Quantification and molecular characterization of exosomes	Quantification of exosomes (4.3)	Specific biotinylated antibody/exosome	Au chip, biotinylated thiol layer, streptavidin (3.2)	Rupert et al., 2016
			Streptavidin/ biotinylated exosome	Au chip, biotinylated thiol layer (3.2)	Rupert et al., 2014

(Continued)

TABLE 1 | Continued

Lipid nanoparticle	Research area	Subject of study	Immobilized ligand/analyte in solution	Sensor chip and surface immobilization chemistry	References
		Identification of exosomal proteins (4.3)	Specific biotinylated antibody/exosome	Au chip, thiolated PEG /streptavidin (3.2)	Im et al., 2017
SLN	Molecular interactions involved in drug delivery	Interaction with biological targets (4.1.1)	Protein/LNP	Au-alginate chip, amide coupling (3.1)	Gobbi et al., 2010
		Interaction with serum proteins (4.1.2)	Protein/LNP	Au chip, 11-mercaptoundecanoic acid SAM, amide coupling (3.1)	Di Ianni et al., 2017
NLC	Molecular interactions involved in drug delivery	Interaction with biological targets (4.1.1)	Protein/LNP	Au-CMD chip, amide coupling (3.1)	Rafique et al., 2019
VLP	Molecular interactions involved in drug delivery	Interaction with biological targets (4.1.1)	Cell membrane model/LNP	Au lipid- capture chip (3.3)	Jedynak et al., 2018

Parentheses indicate subsections where subjects of study and surface immobilization chemistries are described.

biofilms (Sugano et al., 2016) or tumoral cell lines (Guo et al., 2014), and a work describing the application of SPR to assess the interaction of immobilized hybrid NPs and eukaryotic cells in solution has been reported (Soman et al., 2009).

4.1.2. Interaction With Serum Proteins
It is well-known that the interaction of drug nanocarriers with serum proteins can alter the pharmacokinetics of the nanovehicles either affecting the cellular uptake or the clearance of the particles by the immune system (Pearson et al., 2014). SPR has been applied to study the interplay between NPs and isolated serum proteins in order to optimize LNP's formulation design (**Table 1**). SPR has contributed to study fibrinogen, human serum albumin and bovine pancreatic trypsin inhibitor adsorption onto both neutral and negatively charged PEG-decorated liposomes (Efremova et al., 2000). Interestingly, the observed reduction in protein adsorption as PEG densities in the nanovehicles increases agreed with theoretical predictions. These results suggest that SPR studies could contribute to establish the physical basis of the different interactions of LNPs with proteins and cells. Moreover, particular proteins of the NPs' corona were identified by means of SPR experiments on LNPs preincubated with serum (Canovi et al., 2012) and the real-time protein corona formation was followed on surface-immobilized NPs (Kari et al., 2017).

4.1.3. Interaction With Tumor ECM
Therapeutic efficacy of drug nanovehicles for cancer applications is significantly impaired by limited tumor tissue penetration due to a physical barrier formed by extracellular matrix (ECM) proteins. In this regard, SPR has been recently expanded as a method to examine the interfacial properties of liposomes, by analyzing their binding properties toward surface immobilized tumor ECM proteins as a surrogate for their ability to penetrate solid tumors (Wadajkar et al., 2019).

4.2. Obtention and Characterization of LNPs' Formulations
4.2.1. Interaction Between Components of the LNPs' Formulation
Stability, targeting specificity and drug release efficiency of nanosized drug carriers can be improved by nanovehicle's surface functionalization. In this sense, SPR has contributed to the optimization of LNP- based drug delivery systems by providing a rapid screening method to assess the interaction between LNP and potential binding molecules to be included in the final NP formulation (**Table 1**). Soman et al., by way of illustration, incorporated the peptide melittin in the outer lipid monolayer of perfluorocarbon (PFC) NPs and demonstrated the tight binding of this potential cancer chemotherapeutic with the nanocarriers from the SPR data (Soman et al., 2008).

4.2.2. LNPs' Response to Organic Molecules
LNPs can be easily captured on SPR chips by means of lipophilic anchors (Del Vecchio and Stahelin, 2016) as described in section 3.3 and the obtained sensor surfaces can be used to investigate the interplay of the immobilized nanovehicles and organic molecules in aqueous solutions (Seong et al., 2003; Shibata et al., 2015). For instance, Shibata et al. utilized SPR to study the interaction of different detergents (two bile salts and Triton X-100) and PEGylated liposomes that were immobilized to the surface of a lipid- capture chip (Shibata et al., 2012). The authors observed that the detergents were either bound to or partitioned into lipid bilayers and they subsequently solubilized and dissociated from the chip. These results suggest that SPR can provide an automatized method to simply address the solubilization and interaction of detergents with LNPs.

4.3. Quantification and Molecular Characterization of Exosomes

The increasing interest of the scientific community in using exosomes as drug nanovehicles has generated a growing need for sensitive methods capable of quantifying and characterizing these nanosized cell- secreted vesicles. Recent SPR reports in the field of exosome's investigation are based on the immobilization of specific antibodies against exosomal proteins onto the sensor surface and the measuring of SPR response as exosomes in solution are injected into the setup (**Table 1**). A thorough review of the use of SPR as a method for sensitive detection and molecular characterization of exosomes can be found in the literature (Rojalin et al., 2019).

5. CONCLUSIONS

SPR technology has emerged as an interesting strategy for studying different aspects of LNPs intended to deliver bioactive molecules, from the physicochemical characterization and quantification of lipid- based drug carriers to the study of the interaction of nanovehicles with the biological entities that they will encounter in therapeutic applications.

Although SPR technique is a well-established tool for studying molecular interactions, the experiment's reliability is based on the adequate immobilization of one of the interacting partners on the sensor surface and in the absence of interferences that could affect the resulting signals. Concerning LNPs, chemical constraints that may appear in the sensor surface preparation can be easily overcome as lipid based nanovehicles can be directly immobilized onto commercial lipid- capture chips by hydrophobic attachment.

Regardless of the numerous reports presented in this review, SPR still remains as an underexploited technique in the field of LNP development and analysis. Measurement's simplicity and quickness should position SPR as a high-throughput technique for LNPs' characterization, providing preliminary information about biomolecular interactions that LNPs experiment in therapeutic applications and allowing to tune formulations before *in vivo* experiments. Finally, given the universal SPR detection principle, assays can be straight forward adapted to new drug carriers, a trend that with the incorporation of VLPs, exosomes and hybrid systems is in continuous growth.

AUTHOR CONTRIBUTIONS

CYC, MADM, JSC, EAR, and MEV wrote and revised the manuscript and approved it for publication. All authors contributed to the article and approved the submitted version.

FUNDING

ACKNOWLEDGMENTS

REFERENCES

Akita, H., Nakatani, T., Kuroki, K., Maenaka, K., Tange, K., Nakai, Y., et al. (2015). Effect of hydrophobic scaffold on the cellular uptake and gene transfection activities of DNA-encapsulating liposomal nanoparticles via intracerebroventricular administration. *Int. J. Pharm* 490, 142–145. doi: 10.1016/j.ijpharm.2015.05.043

Al-Ahmady, Z. S., Chaloin, O., and Kostarelos, K. (2014). Monoclonal antibody-targeted, temperature-sensitive liposomes: In vivo tumor chemotherapeutics in combination with mild hyperthermia. *J. Controll. Release* 196, 332–343. doi: 10.1016/j.jconrel.2014.10.013

Albers, W. M., and Vikholm-Lundin, I. M. (2011). "Surface plasmon resonance on nanoscale organic films," in *Nano-Bio-Sensing*, ed S. Carrara (New York, NY: Springer), 4–10.

Allen, T. M., and Cullis, P. R. (2013). Liposomal drug delivery systems: from concept to clinical applications. *Adv. Drug Deliv. Rev.* 65, 36–48. doi: 10.1016/j.addr.2012.09.037

Bozzuto, G., and Molinari, A. (2015). Liposomes as nanomedical devices. *Int. J. Nanomedicine* 10, 975–999. doi: 10.2147/IJN.S68861

Bueloni, B., Sanna, D., Garribba, E., Castro, G. R., León, I. E., and Islan, G. A. (2020). Design of nalidixic acid-vanadium complex loaded into chitosan hybrid nanoparticles as smart strategy to inhibit bacterial growth and quorum sensing. *Int. J. Biol. Macromol.* 161, 1568–1580. doi: 10.1016/j.ijbiomac.2020.07.304

Bunker, A., Magarkar, A., and Viitala, T. (2016). Rational design of liposomal drug delivery systems, a review: combined experimental and computational studies of lipid membranes, liposomes and their PEGylation. *Biochim. Biophys. Acta* 1858, 2334–2352. doi: 10.1016/j.bbamem.2016.02.025

Cai, D., Gao, W., He, B., Dai, W., Zhang, H., Wang, X., et al. (2014). Hydrophobic penetrating peptide PFVYLI-modified stealth liposomes for doxorubicin delivery in breast cancer therapy. *Biomaterials* 35, 2283–2294. doi: 10.1016/j.biomaterials.2013.11.088

Canovi, M., Lucchetti, J., Stravalaci, M., Re, F., Moscatelli, D., Bigini, P., et al. (2012). Applications of surface plasmon resonance (SPR) for the characterization of nanoparticles developed for biomedical purposes. *Sensors* 12, 16420–16432. doi: 10.3390/s121216420

Choi, Y. H., and Han, H.-K. (2018). Nanomedicines: current status and future perspectives in aspect of drug delivery and pharmacokinetics. *J. Pharm. Invest.* 48, 43–60. doi: 10.1007/s40005-017-0370-4

Crielaard, B. J., Yousefi, A., Schillemans, J. P., Vermehren, C., Buyens, K., Braeckmans, K., et al. (2011). An *in vitro* assay based on surface plasmon resonance to predict the *in vivo* circulation kinetics of liposomes. *J. Controll. Release* 156, 307–314. doi: 10.1016/j.jconrel.2011.07.023

Del Vecchio, K., and Stahelin, R. V. (2016). "Using surface plasmon resonance to quantitatively assess lipid–protein interactions," in *Methods in Molecular Biology*, ed J. M. Walker (New York, NY: Humana Press), 141–153.

Desfrançois, C., Auzély, R., and Texier, I. (2018). Lipid nanoparticles and their hydrogel composites for drug delivery: a review. *Pharmaceuticals* 11:118. doi: 10.3390/ph11040118

Di Ianni, M. E., Islan, G. A., Chain, C. Y., Castro, G. R., Talevi, A., and Vela, M. E. (2017). Interaction of solid lipid nanoparticles and specific proteins

of the corona studied by surface plasmon resonance. *J. Nanomater.* 2017:11. doi: 10.1155/2017/6509184

Ding, Q., Si, X., Liu, D., Peng, J., Tang, H., Sun, W., et al. (2015). Targeting and liposomal drug delivery to CD40L expressing T cells for treatment of autoimmune diseases. *J. Controll. Release* 207, 86–92. doi: 10.1016/j.jconrel.2015.03.035

Duff, M. R. Jr., Grubbs, J., and Howell, E. E. (2011). Isothermal titration calorimetry for measuring macromolecule-ligand affinity. *J. Vis. Exp.* 55:2796. doi: 10.3791/2796

Efremova, N. V., Bondurant, B., O'brien, D. F., and Leckband, D. E. (2000). Measurements of interbilayer forces and protein adsorption on uncharged lipid bilayers displaying poly(ethylene glycol) chains. *Biochemistry* 39, 3441–3451. doi: 10.1021/bi992095r

Etzerodt, A., Maniecki, M. B., Graversen, J. H., Moller, H. J., Torchilin, V. P., and Moestrup, S. K. (2012). Efficient intracellular drug-targeting of macrophages using stealth liposomes directed to the hemoglobin scavenger receptor CD163. *J. Controll. Release* 160, 72–80. doi: 10.1016/j.jconrel.2012.01.034

Fontana, E. (2006). Thickness optimization of metal films for the development of surface-plasmon-based sensors for nonabsorbing media. *Appl. Opt.* 45, 7632–7642. doi: 10.1364/AO.45.007632

Gao, L.-Y., Liu, X.-Y., Chen, C.-J., Wang, J.-C., Feng, Q., Yu, M.-Z., et al. (2014). Core-Shell type lipid/rPAA-Chol polymer hybrid nanoparticles for *in vivo* siRNA delivery. *Biomaterials* 35, 2066–2078. doi: 10.1016/j.biomaterials.2013.11.046

Gedig, E. T. (2017). "Chapter 6 surface chemistry in SPR technology," in *Handbook of Surface Plasmon Resonance*, ed R. B. M. Schasfoort (London: The Royal Society of Chemistry), 171–254.

Gobbi, M., Re, F., Canovi, M., Beeg, M., Gregori, M., Sesana, S., et al. (2010). Lipid-based nanoparticles with high binding affinity for amyloid-β1-42 peptide. *Biomaterials* 31, 6519–6529. doi: 10.1016/j.biomaterials.2010.04.044

Gregori, M., Taylor, M., Salvati, E., Re, F., Mancini, S., Balducci, C., et al. (2017). Retro-inverso peptide inhibitor nanoparticles as potent inhibitors of aggregation of the Alzheimer's Aβ peptide. *Nanomedicine* 13, 723–732. doi: 10.1016/j.nano.2016.10.006

Guo, Z., He, B., Jin, H., Zhang, H., Dai, W., Zhang, L., et al. (2014). Targeting efficiency of RGD-modified nanocarriers with different ligand intervals in response to integrin αvβ3 clustering. *Biomaterials* 35, 6106–6117. doi: 10.1016/j.biomaterials.2014.04.031

György, B., Hung, M. E., Breakefield, X. O., and Leonard, J. N. (2015). Therapeutic applications of extracellular vesicles: clinical promise and open questions. *Annu. Rev. Pharmacol. Toxicol.* 55, 439–464. doi: 10.1146/annurev-pharmtox-010814-124630

Ha, D., Yang, N., and Nadithe, V. (2016). Exosomes as therapeutic drug carriers and delivery vehicles across biological membranes: current perspectives and future challenges. *Acta Pharm. Sin. B* 6, 287–296. doi: 10.1016/j.apsb.2016.02.001

Hermanson, G. T. (2013). "Chapter 3 - the reactions of bioconjugation," in *Bioconjugate Techniques, 3rd Edn,* ed G. T. Hermanson (Boston, MA: Academic Press), 229–258.

Hodnik, V., and Anderluh, G. (2013). Surface plasmon resonance for measuring interactions of proteins with lipid membranes. *Methods Mol. Biol.* 974, 23–36. doi: 10.1007/978-1-62703-275-9_2

Huang, Z. R., Tipparaju, S. K., Kirpotin, D. B., Pien, C., Kornaga, T., Noble, C. O., et al. (2019). Formulation optimization of an ephrin A2 targeted immunoliposome encapsulating reversibly modified taxane prodrugs. *J. Controll. Release* 310, 47–57. doi: 10.1016/j.jconrel.2019.08.006

Im, H., Yang, K., Lee, H., and Castro, C. M. (2017). Characterization of extracellular vesicles by surface plasmon resonance. *Methods Mol. Biol.* 1660, 133–141. doi: 10.1007/978-1-4939-7253-1_11

Jedynak, M., Worch, R., Podsiadła-Białoskórska, M., Chroboczek, J., and Szołajska, E. (2018). Cholesterol and phosphatidylserine are engaged in adenoviral dodecahedron endocytosis. *Biochim. Biophys. Acta Biomembr.* 1860, 2215–2223. doi: 10.1016/j.bbamem.2018.09.002

Jerabek-Willemsen, M., André, T., Wanner, R., Roth, H. M., Duhr, S., Baaske, P., et al. (2014). MicroScale thermophoresis: interaction analysis and beyond. *J. Mol. Struct.* 1077, 101–113. doi: 10.1016/j.molstruc.2014.03.009

Kari, O. K., Rojalin, T., Salmaso, S., Barattin, M., Jarva, H., Meri, S., et al. (2017). Multi-parametric surface plasmon resonance platform for studying liposome-serum interactions and protein corona formation. *Drug Deliv. Transl. Res.* 7, 228–240. doi: 10.1007/s13346-016-0320-0

Laukkanen, M. L., Alfthan, K., and Keinänen, K. (1994). Functional immunoliposomes harboring a biosynthetically lipid-tagged single-chain antibody. *Biochemistry* 33, 11664–11670. doi: 10.1021/bi00204a031

Li, C., Wang, J., Wang, Y., Gao, H., Wei, G., Huang, Y., et al. (2019). Recent progress in drug delivery. *Acta Pharm. Sin. B* 9, 1145–1162. doi: 10.1016/j.apsb.2019.08.003

Maier, S. A. (2007). "Electromagnetics of metals," in *Plasmonics: Fundamentals and Applications*, ed S. A. Maier (New York, NY: Springer), 5–19.

Malmsten, M. (1999). Studies of serum protein adsorption at phospholipid surfaces in relation to intravenous drug delivery. *Colloids Surf. A Physicochem. Eng. Aspects* 159, 77–87. doi: 10.1016/S0927-7757(99)00164-8

Mehnert, W., and Mäder, K. (2012). Solid lipid nanoparticles: production, characterization and applications. *Adv. Drug Deliv. Rev.* 64, 83–101. doi: 10.1016/j.addr.2012.09.021

Meierhofer, T., van den Elsen, J. M. H., Cameron, P. J., Muñoz-Berbel, X., and Jenkins, A. T. A. (2010). The interaction of serum albumin with cholesterol containing lipid vesicles. *J. Fluoresc.* 20, 371–376. doi: 10.1007/s10895-009-0522-7

Mizrahy, S., Raz, S. R., Hasgaard, M., Liu, H., Soffer-Tsur, N., Cohen, K., et al. (2011). Hyaluronan-coated nanoparticles: the influence of the molecular weight on CD44-hyaluronan interactions and on the immune response. *J. Controll. Release* 156, 231–238. doi: 10.1016/j.jconrel.2011.06.031

Mourtas, S., Canovi, M., Zona, C., Aurilia, D., Niarakis, A., La Ferla, B., et al. (2011). Curcumin-decorated nanoliposomes with very high affinity for amyloid-β1-42 peptide. *Biomaterials* 32, 1635–1645. doi: 10.1016/j.biomaterials.2010.10.027

Naseri, N., Valizadeh, H., and Zakeri-Milani, P. (2015). Solid lipid nanoparticles and nanostructured lipid carriers: structure, preparation and application. *Adv. Pharm. Bull.* 5, 305–313. doi: 10.15171/apb.2015.043

Nielsen, U. B., Kirpotin, D. B., Pickering, E. M., Hong, K., Park, J. W., Refaat Shalaby, M., et al. (2002). Therapeutic efficacy of anti-ErbB2 immunoliposomes targeted by a phage antibody selected for cellular endocytosis. *Biochim. Biophys. Acta Mol. Cell Res.* 1591, 109–118. doi: 10.1016/S0167-4889(02)00256-2

Oner, E., Kotmakci, M., and Kantarci, A. G. (2020). A promising approach to develop nanostructured lipid carriers from solid lipid nanoparticles: preparation, characterization, cytotoxicity and nucleic acid binding ability. *Pharm. Dev. Technol.* 25, 936–948. doi: 10.1080/10837450.2020.1759630

Pan, H., Ivashyna, O., Sinha, B., Lanza, G. M., Ratner, L., Schlesinger, P. H., et al. (2011). Post-formulation peptide drug loading of nanostructures for metered control of NF-κB signaling. *Biomaterials* 32, 231–238. doi: 10.1016/j.biomaterials.2010.08.080

Pattni, B. S., Chupin, V. V., and Torchilin, V. P. (2015). New developments in liposomal drug delivery. *Chem. Rev.* 115, 10938–10966. doi: 10.1021/acs.chemrev.5b00046

Pearson, R. M., Juettner, V. V., and Hong, S. (2014). Biomolecular corona on nanoparticles: a survey of recent literature and its implications in targeted drug delivery. *Front. Chem.* 2:108. doi: 10.3389/fchem.2014.00108

Puri, A., Loomis, K., Smith, B., Lee, J.-H., Yavlovich, A., Heldman, E., et al. (2009). Lipid-based nanoparticles as pharmaceutical drug carriers: from concepts to *clinic. Crit. Rev. Ther. Drug Carrier Syst.* 26, 523–580. doi: 10.1615/CritRevTherDrugCarrierSyst.v26.i6.10

Rafique, A., Etzerodt, A., Graversen, J. H., Moestrup, S. K., Dagnæs-Hansen, F., and Møller, H. J. (2019). Targeted lipid nanoparticle delivery of calcitriol to human monocyte-derived macrophages *in vitro* and *in vivo*: investigation of the anti-inflammatory effects of calcitriol. *Int. J. Nanomedicine* 14, 2829–2846. doi: 10.2147/IJN.S192113

Rauscher, A., Frindel, M., Maurel, C., Maillasson, M., Le Saëc, P., Rajerison, H., et al. (2014). Influence of pegylation and hapten location at the surface of radiolabelled liposomes on tumour immunotargeting using bispecific antibody. *Nucl. Med. Bio.* 41, e66–e74. doi: 10.1016/j.nucmedbio.2013.12.012

Rodenak-Kladniew, B., Scioli Montoto, S., Sbaraglini, M. L., Di Ianni, M., Ruiz, M. E., Talevi, A., et al. (2019). Hybrid Ofloxacin/eugenol co-loaded solid lipid nanoparticles with enhanced and targetable antimicrobial properties. *Int. J. Pharm.* 569:118575. doi: 10.1016/j.ijpharm.2019.118575

Rohovie, M. J., Nagasawa, M., and Swartz, J. R. (2017). Virus-like particles: next-generation nanoparticles for targeted therapeutic

delivery. *Bioeng. Transl. Med.* 2, 43–57. doi: 10.1002/btm2.
10049

Rojalin, T., Phong, B., Koster, H. J., and Carney, R. P. (2019). Nanoplasmonic
approaches for sensitive detection and molecular characterization of
extracellular vesicles. *Front. Chem.* 7:729. doi: 10.3389/fchem.2019.00279

Rupert, D. L. M., Lässer, C., Eldh, M., Block, S., Zhdanov, V. P., Lotvall,
J. O., et al. (2014). Determination of exosome concentration in solution
using surface plasmon resonance spectroscopy. *Anal. Chem.* 86, 5929–5936.
doi: 10.1021/ac500931f

Rupert, D. L. M., Shelke, G. V., Emilsson, G., Claudio, V., Block, S., Lässer, C., et al.
(2016). Dual-wavelength surface plasmon resonance for determining the size
and concentration of sub-populations of extracellular vesicles. *Anal. Chem.* 88,
9980–9988. doi: 10.1021/acs.analchem.6b01860

Sandoval-Altamirano, C., Sanchez, S. A., Ferreyra, N. F., and Gunther, G.
(2017). Understanding the interaction of concanavalin a with mannosyl
glycoliposomes: a surface plasmon resonance and fluorescence study. *Colloids
Surf. B Biointerfaces* 158, 539–546. doi: 10.1016/j.colsurfb.2017.07.026

Schasfoort, R. B. M. (2017). "Chapter 1: introduction to surface plasmon
resonance," in *Handbook of Surface Plasmon Resonance*, ed R. B.
M. Schasfoort (London: The Royal Society of Chemistry), 1–26.
doi: 10.1039/9781788010283-00001

Selvamuthukumar, S., and Velmurugan, R. (2012). Nanostructured lipid carriers:
a potential drug carrier for cancer chemotherapy. *Lipids Health Dis.* 11:59.
doi: 10.1186/1476-511X-11-159

Seong, H., Choi, W. M., Kim, J. C., Thompson, D. H., and Park, K.
(2003). Preparation of liposomes with glucose binding sites: liposomes
containing di-branched amino acid derivatives. *Biomaterials* 24, 4487–4493.
doi: 10.1016/S0142-9612(03)00352-1

Shi, K., Li, J., Cao, Z., Yang, P., Qiu, Y., Yang, B., et al. (2015a). A pH-responsive
cell-penetrating peptide-modified liposomes with active recognizing of integrin
αvβ3 for the treatment of melanoma. *J. Controll. Release* 217, 138–150.
doi: 10.1016/j.jconrel.2015.09.009

Shi, K., Long, Y., Xu, C., Wang, Y., Qiu, Y., Yu, Q., et al. (2015b).
Liposomes combined an integrin αvβ3-specific vector with ph-responsible
cell-penetrating property for highly effective antiglioma therapy through
the blood-brain barrier. *ACS Appl. Mater. Interfaces* 7, 21442–21454.
doi: 10.1021/acsami.5b06429

Shibata, H., Saito, H., Yomota, C., Kawanishi, T., and Okuda, H. (2012).
Alterations in the detergent-induced membrane permeability and
solubilization of saturated phosphatidylcholine/cholesterol liposomes: effects
of poly(ethylene glycol)-conjugated lipid. *Chem. Pharm. Bull.* 60, 1105–1111.
doi: 10.1248/cpb.c12-00153

Shibata, H., Yoshida, H., Izutsu, K. I., Haishima, Y., Kawanishi, T., Okuda, H., et al.
(2015). Interaction kinetics of serum proteins with liposomes and their effect
on phospholipase-induced liposomal drug release. *Int. J. Pharm.* 495, 827–839.
doi: 10.1016/j.ijpharm.2015.09.053

Skyttner, C., Selegård, R., Larsson, J., Aronsson, C., Enander, K., and Aili, D.
(2019). Sequence and length optimization of membrane active coiled coils for
triggered liposome release. *Biochim. Biophys. Acta Biomember.* 1861, 449–456.
doi: 10.1016/j.bbamem.2018.11.005

Soman, N. R., Baldwin, S. L., Hu, G., Marsh, J. N., Lanza, G. M., Heuser, J. E., et al.
(2009). Molecularly targeted nanocarriers deliver the cytolytic peptide melittin
specifically to tumor cells in mice, reducing tumor growth. *J. Clin. Invest.* 119,
2830–2842. doi: 10.1172/JCI38842

Soman, N. R., Lanza, G. M., Heuser, J. M., Schlesinger, P. H., and Wickline, S. A.
(2008). Synthesis and characterization of stable fluorocarbon nanostructures
as drug delivery vehicles for cytolytic peptides. *Nano Lett.* 8, 1131–1136.
doi: 10.1021/nl073290r

Sugano, M., Morisaki, H., Negishi, Y., Endo-Takahashi, Y., Kuwata, H., Miyazaki,
T., et al. (2016). Potential effect of cationic liposomes on interactions
with oral bacterial cells and biofilms. *J. Liposome Res.* 26, 156–162.
doi: 10.3109/08982104.2015.1063648

Tamiaki, H., Azefu, Y., Shibata, R., Sato, R., and Toma, K. (2006). Oligomethylene
spacer length dependent interaction of synthetic galactolipids incorporated
in phospholipid layers with ricin. *Colloids Surf B Biointerfaces* 53, 87–93.
doi: 10.1016/j.colsurfb.2006.08.001

Terada, T., Mizobata, M., Kawakami, S., Yamashita, F., and Hashida, M.
(2007). Optimization of tumor-selective targeting by basic fibroblast growth

factor-binding peptide grafted PEGylated liposomes. *J. Control. Release* 119,
262–270. doi: 10.1016/j.jconrel.2007.01.018

Tonda-Turo, C., Carmagnola, I., and Ciardelli, G. (2018). Quartz crystal
microbalance with dissipation monitoring: a powerful method to predict the
in vivo behavior of bioengineered surfaces. *Front. Bioeng. Biotech.* 6:158.
doi: 10.3389/fbioe.2018.00158

Vericat, C., Vela, M. E., Benitez, G., Carro, P., and Salvarezza, R. C. (2010). Self-
assembled monolayers of thiols and dithiols on gold: new challenges for a
well-known system. *Chem. Soc. Rev.* 39, 1805–1834. doi: 10.1039/b907301a

Viitala, T., Liang, H., Gupta, M., Zwinger, T., Yliperttula, M., and Bunker,
A. (2012). Fluid dynamics modeling for synchronizing surface plasmon
resonance and quartz crystal microbalance as tools for biomolecular and
targeted drug delivery studies. *J. Colloid Interface Sci.* 378, 251–259.
doi: 10.1016/j.jcis.2012.04.012

Wadajkar, A. S., Dancy, J. G., Carney, C. P., Hampton, B. S., Ames, H. M.,
Winkles, J. A., et al. (2019). Leveraging surface plasmon resonance to dissect
the interfacial properties of nanoparticles: implications for tissue binding and
tumor penetration. *Nanomedicine* 20:102024. doi: 10.1016/j.nano.2019.102024

Wang, X., Chen, X., Yang, X., He, B., Dai, W., Wang, X., et al. (2014). A mechanism
study on the tamoxifen mediated cellular internalization of liposomes. *J. Chin.
Pharm. Sci.* 23, 595–600. doi: 10.5246/jcps.2014.09.076

Weeramange, C. J., Fairlamb, M. S., Singh, D., Fenton, A. W., and Swint-Kruse,
L. (2020). The strengths and limitations of using biolayer interferometry to
monitor equilibrium titrations of biomolecules. *Protein Sci.* 29, 1004–1020.
doi: 10.1002/pro.3827

Wiklander, O. P. B., Brennan, M. Á., Lötvall, J., Breakefield, X. O., and Andaloussi,
S. E. L. (2019). Advances in therapeutic applications of extracellular vesicles.
Sci. Transl. Med. 11:eaav8521. doi: 10.1126/scitranslmed.aav8521

Xiang, Y., Kiseleva, R., Reukov, V., Mulligan, J., Atkinson, C., Schlosser, R.,
et al. (2015). Relationship between targeting efficacy of liposomes and the
dosage of targeting antibody using surface plasmon resonance. *Langmuir* 31,
12177–12186. doi: 10.1021/acs.langmuir.5b01386

Yan, L., Zhao, F., Wang, J., Zu, Y., Gu, Z., and Zhao, Y. (2019). A safe-by-
design strategy towards safer nanomaterials in nanomedicines. *Adv. Mater.*
31:e1805391. doi: 10.1002/adma.201805391

Yatuv, R., Carmel-Goren, L., Dayan, I., Robinson, M., and Baru, M. (2009). Binding
of proteins to PEGylated liposomes and improvement of G-CSF efficacy in
mobilization of hematopoietic stem cells. *J. Controll. Release* 135, 44–50.
doi: 10.1016/j.jconrel.2008.12.004

Yeh, Y.-C., Huang, T.-H., Yang, S.-C., Chen, C.-C., and Fang, J.-Y. (2020). Nano-
based drug delivery or targeting to eradicate bacteria for infection mitigation:
a review of recent advances. *Front. Chem.* 8:286. doi: 10.3389/fchem.2020.
00286

Zdanowicz, M., and Chroboczek, J. (2016). Virus-like particles as drug delivery
vectors. *Acta Biochim. Pol.* 63, 469–473. doi: 10.18388/abp.2016_1275

Zhao, F., Cheng, X., Liu, G., and Zhang, G. (2010). Interaction of hydrophobically
end-capped polyethylene glycol with phospholipid vesicles: The hydrocarbon
end-chain length dependence. *J. Phys. Chem. B* 114, 1271–1276.
doi: 10.1021/jp910024n

Zhao, Z., Ukidve, A., Krishnan, V., and Mitragotri, S. (2019). Effect of
physicochemical and surface properties on in vivo fate of drug nanocarriers.
Adv. Drug Deliv. Rev. 143, 3–21. doi: 10.1016/j.addr.2019.01.002

Zylberberg, C., and Matosevic, S. (2016). Pharmaceutical liposomal drug
delivery: a review of new delivery systems and a look at the regulatory
landscape. *Drug Deliv.* 23, 3319–3329. doi: 10.1080/10717544.2016.
1177136

Check for updates

Optimizing the Intracellular Delivery of Therapeutic Anti-inflammatory TNF-α siRNA to Activated Macrophages Using Lipidoid-Polymer Hybrid Nanoparticles

Abhijeet Lokras[1], Aneesh Thakur[1], Abishek Wadhwa[1], Kaushik Thanki[1†], Henrik Franzyk[2] and Camilla Foged[1*]

[1] Department of Pharmacy, Faculty of Health and Medical Sciences, University of Copenhagen, Copenhagen, Denmark,
[2] Department of Drug Design and Pharmacology, Faculty of Health and Medical Sciences, University of Copenhagen, Copenhagen, Denmark

RNA interference (RNAi) has an unprecedented potential as a therapeutic strategy for reversibly silencing the expression of any gene. Therapeutic delivery of the RNAi mediator, i.e., small interfering RNA (siRNA), can be used to address diseases characterized by gene overexpression, for example inflammatory conditions like chronic obstructive pulmonary disease (COPD). Macrophages play a key role in COPD pathogenesis and are recruited to the airways and lung parenchyma, where they release proinflammatory cytokines, e.g., tumor necrosis factor-alpha (TNF-α). Hence, targeting TNF-α with siRNA is a promising therapeutic approach for COPD management. However, a safe and effective delivery system is required for delivery of TNF-α siRNA into the cytosol of hard-to-transfect macrophages. The purpose of this study was to optimize the intracellular delivery of TNF-α siRNA to the lipopolysaccharide-activated murine macrophage cell line RAW 264.7 using lipidoid-polymer hybrid nanoparticles (LPNs) composed of the lipid-like transfection agent lipidoid 5 (L_5) and the biodegradable polymer poly (D,L-lactide-co-glycolide). Applying a quality-by-design approach, the influence of critical formulation variables, i.e., the L_5 content and the L_5:siRNA ratio (w/w), on critical quality attributes (CQAs) was investigated systematically using risk assessment and design of experiments, followed by delineation of an optimal operating space (OOS). The CQAs were identified based on the quality target product profile and included size, polydispersity index, zeta potential, encapsulation efficiency and loading for achieving efficient and safe TNF-α gene silencing in activated RAW 264.7 cells. Formulations inducing efficient gene silencing and low cytotoxicity were identified, and the optimal formulations displayed L_5 contents of 15 and 20% (w/w), respectively, and an L_5:siRNA weight ratio of 15:1. All tested formulations within the OOS mediated efficient and sequence-specific TNF-α gene silencing in RAW 264.7 cells at TNF-α-siRNA concentrations, which were significantly lower than the concentrations required

of non-encapsulated TNF-α-siRNA, highlighting the benefit of the delivery system. The results also demonstrate that increasing the loading of siRNA into the delivery system does not necessarily imply enhanced gene silencing. This opens new avenues for further exploitation of LPNs as a robust platform technology for delivering TNF-α siRNA to macrophages, e.g., in the management of COPD.

INTRODUCTION

RNA interference (RNAi) is a regulatory pathway in eukaryotic cells in which gene expression is inhibited at the messenger RNA (mRNA) level by sequence-specific double-stranded RNA, for example small interfering RNA (siRNA) (Ryther et al., 2005). In principle, any disease characterized by protein overexpression may be treated using synthetic molecules harnessing the RNAi pathway by Watson-Crick base-pairing, e.g., siRNA directed against a specific mRNA. Although the ability of double-stranded RNA to mediate silencing of gene expression was discovered in *Caenorhabditis elegans* more than two decades ago (Elbashir et al., 2001), only four drugs based on siRNA have been approved to date, i.e., patisiran (Adams et al., 2018), givosiran (Balwani et al., 2020), lumasiran (McGregor et al., 2020), and inclisiran (Raal et al., 2020; Ray et al., 2020) used for systemic treatment of the polyneuropathy of hereditary transthyretin amyloidosis, acute hepatic porphyria, and elevated LDL cholesterol respectively. Major hurdles for unlocking of the full potential of siRNA for therapeutic applications are delivery-related challenges (Dammes and Peer, 2020). These include, but are not limited to, (i) protection of siRNA against degradation by exo- and endonucleases, (ii) cellular uptake, and (iii) endosomal escape and siRNA release in the cytosol after cellular internalization (Haussecker, 2014). Some of these challenges have been partially overcome by chemical modification of the siRNA, which has enhanced the resistance to nucleases (Place et al., 2012). However, while chemical modification has certainly improved the drug properties of siRNA, the adoption of delivery technologies has also appeared to be essential for overcoming barriers related to siRNA delivery (Whitehead et al., 2009).

One example of a disease that can be targeted via the RNAi pathway is chronic obstructive pulmonary disease (COPD). More than 210 million people are affected by COPD, and by 2030, COPD is expected to be the fourth largest cause of death worldwide (Bousquet and Kaltaev, 2007). COPD severely compromises breathing, which causes a general decline in organ function, eventually resulting in chronic co-morbid conditions, including cardiovascular diseases, diabetes, and hypertension (Mannino et al., 2008). The pathophysiology of COPD is relatively complex and ranges from cellular inflammation to structural remodeling (Chung and Adcock, 2008). Tumor necrosis factor-alpha (TNF-α), along with interleukin 1-beta (IL-1β), plays a critical role in the inflammatory cascades during exacerbations of COPD (Matera et al., 2010; Cazzola et al., 2012). However, two clinical trials indicated no immediate

or long-term benefit for patients with moderate to severe COPD of systemic treatment with the anti-TNF-α monoclonal antibody Infliximab (Rennard et al., 2007, 2013). Also, there was no significant difference between subjects treated with the corticosteroid prednisone compared to the TNF inhibitor Etanercept (Aaron et al., 2013). Hence, there is an urgent need to design novel treatment approaches for COPD, mainly focusing on the underlying inflammatory and irreversibly destructive phases. Targeting alveolar macrophages through RNAi mediated by siRNA represents one strategy to knock down the expression of inflammatory genes in COPD, e.g., TNF-α (Barnes, 2003; Peer and Lieberman, 2011). Therefore, we have previously exploited the RNAi machinery inherent in macrophages to ameliorate the gene expression of TNF-α with subsequent reduction of lipopolysaccharide (LPS)-induced inflammation (Jansen et al., 2019).

Overall, two types of delivery technologies are commonly used to deliver siRNA across the cell membrane into the cytosol (Roberts et al., 2020): i.e., (i) delivery systems like lipoplexes (Schroeder et al., 2010), lipid nanoparticles (LNPs) (Xu and Wang, 2015), cyclodextrin polymeric nanoparticles (Dominique et al., 2016), and lipid-polymer hybrid nanoparticles (LPNs) (Hadinoto et al., 2013), and (ii) conjugates (Kanasty et al., 2013), e.g., N-acetyl-D-galactosamine (GalNAc)-siRNA conjugates, which are used for liver targeting in the clinic (givosiran patisiran, lumasiran, and inclisiran) by actively targeting the internalizing asialoglycoprotein receptor 1 expressed by hepatocytes (Balwani et al., 2020). In general, LNPs represent the most clinically advanced delivery system for nucleic acids (Cullis and Hope, 2017), and patisiran, the siRNA in Onpattro, is delivered to liver hepatocytes using an LNP formulation (Adams et al., 2018). Lipid-based delivery systems are biocompatible and display high loading and transfection efficiency, but a drawback is their premature drug leakage and poor colloidal stability. Lipids with single or multiple cationic centers have been used as carriers for siRNA (Schroeder et al., 2010; Zhi et al., 2013). LNPs containing a single amine-based cationic lipid, a polyethylene glycol-lipid, and helper lipids, were first reported for intracellular delivery of siRNA (Heyes et al., 2005). Lipid-like materials referred to as lipidoids have also been developed for siRNA delivery, and they contain one or several amine centers and multiple hydrophobic tails (Akinc et al., 2009). Lipidoids consist of an alkylated tetraamine backbone, and depending on the degree of alkylation, different subtypes are obtained, e.g., the penta-substituted lipidoid, which is referred to as L_5 (Akinc et al., 2009). To improve the efficiency of siRNA delivery, amino

alcohol-based lipidoids have been developed (Love et al., 2010). On the other hand, delivery systems based on polymeric matrix systems, e.g., poly(lactic-co-glycolic acid) (PLGA) nanoparticles, display higher structural integrity and collidal stability, and enables sustained release of siRNA, but they display poor loading capacity and low transfection efficiency (Cun et al., 2010, 2011).

Therefore, we have designed LPNs for delivering siRNA by combining lipidoids with PLGA (Thanki et al., 2017) to exploit the advantages of both lipids and polymers. Hence, siRNA-loaded lipidoid-modified PLGA nanoparticle are biocompatible, have high loading and transfection efficiency, high colloidal stability, and allow for sustained siRNA release (Thanki et al., 2019a). In these LPNs, the anionic siRNA is complexed with the outer lipidoid shell, and also with the PLGA core by incorporating some of the net-neutral lipophilic complexes of siRNA and lipidoid (Colombo et al., 2015). Recent mechanistic uptake studies suggest that LPNs are taken up *via* macropinocytosis (Jansen et al., 2019) and probably because of leaky macropinosomes (Meier et al., 2002), improve lipidoid-mediated siRNA delivery and the resulting gene silencing (Love et al., 2010). However, bulk lipidoids are potent agonists for toll-like receptor (TLR) 4 and activate murine antigen-presenting cells (APCs) *in vitro* (de Groot et al., 2018). The agonistic effect was also confirmed *in silico*. Interestingly, this agonistic effect was abrogated when L_5 was formulated as LPNs loaded with siRNA. However, no systematic studies have been performed to date to investigate the effect of the L_5 content and the L_5:TNF-α siRNA weight ratio on the *in vitro* safety and gene silencing effect of LPNs. Hence, we used a systematic quality-by-design (QbD) approach implementing risk assessment and design of experiments (DoE) for optimizing the loading of therapeutically relevant TNF-α siRNA in LPNs. The QbD approach and DoE are valuable tools as maximal information is provided from the least number of experiments. The QbD process involves the following steps: (i) identification of the quality target product profile (QTPP) i.e., the product attributes that are critical to stability, safety and efficacy; (ii) identification of the critical quality attributes (CQA); (iii) identification of critical process parameters (CPP), and (iv) layout and implementation of DoE to establish the relationship between the CQAs and the CPPs. This information is used to define a process design space i.e., the optimal operating space (OOS) that will result in an end product of the desired QTPP (Ingvarsson et al., 2013; Colombo et al., 2018). We also evaluated the safety and gene silencing mediated by TNF-α siRNA-loaded LPNs *in vitro* in the murine macrophage cell line RAW 264.7 and show that loading a higher dose of siRNA in the LPNs does not correlate with higher gene silencing *in vitro*.

MATERIALS AND METHODS

Materials

2′-*O*-Methyl-modified dicer substrate asymmetric siRNA duplexes directed against TNF-α siRNA (17928.334 g/mol) and negative control siRNA were generously provided by GlaxoSmithKline (Stevenage, UK) as dried, purified and desalted duplexes (**Supplementary Table 1**). The siRNA duplexes were re-annealed according to a standard protocol recommended

by Integrated DNA Technologies (IDT) (Coralville, IA, USA). PLGA (lactide:glycolide molar ratio 75:25, M_w: 20 kDa) was obtained from Wako Pure Chemical Industries (Osaka, Japan). L_5 was synthesized, purified, and characterized as previously reported (Akinc et al., 2008). Polyvinylalcohol (PVA) 403 with an average molecular weight of 30–70 kDa (87–90% degree of hydrolysis) was purchased from Sigma-Aldrich (St. Louis, MO, USA). Heparin and octyl β-D-glucopyranoside (OG) were obtained from Biochrom GmbH (Berlin, Germany) and Sigma-Aldrich, respectively. Quant-iT™ RiboGreen® RNA Reagent and Tris–EDTA buffer (TE buffer, 10 mM Tris, 1 mM EDTA, pH 8.0) were acquired from Molecular Probes, Invitrogen (Paisley, UK). Primers (**Supplementary Table 1**) were obtained from TAG Copenhagen (Copenhagen, Denmark). RNase-free diethyl pyrocarbonate (DEPC)-treated Milli-Q water was used for all buffers and dilutions. Additional chemicals were of analytical grade and purchased from Sigma-Aldrich and Merck (Copenhagen, Denmark).

Preparation and Physicochemical Characterization of LPNs

L_5-modified LPNs loaded with TNF-α siRNA were prepared using the double emulsion solvent evaporation (DESE) method, essentially as reported previously (Thanki et al., 2017, 2019b; Dormenval et al., 2019). The L_5 content relative to the total solid content (L_5 + PLGA) was varied from 15 to 25% (w/w), and the L_5:TNF-α siRNA ratio ranged from 5.0:1 to 15.0:1 (w/w). The final batch size per formulation was 15 mg. The physicochemical properties (z-average, PDI, zeta potential, encapsulation efficiency, and siRNA loading) of the LPNs were determined as described previously (Thanki et al., 2017, 2019b; Dormenval et al., 2019).

Statistical Optimization of LPNs

Initially, the effect of L_5:TNF-α siRNA ratio was investigated on the physicochemical properties by keeping the L_5 content constant and vice versa. Based on these experiments, 12 and 23-run response surfaces were constructed for TNF-α gene silencing, i.e., the half-maximal inhibitory concentration (IC_{50}) values and physicochemical properties, respectively, using an I-optimal design with two critical independent variables, i.e., L_5 content and L_5:TNF-α siRNA weight ratio (**Supplementary Table 2**). The L_5 content ranged from 15 to 25% (w/w), while the latter ranged from 5.0:1 to 15.0:1 (**Table 1**). Seven responses [z-average, PDI, zeta potential, encapsulation efficiency, siRNA loading, and the effective concentration for half- maximal gene silencing (IC_{50})] to the independent variables were measured. Critical responses

TABLE 1 | Formulation design space.

Factor	Low level	Center level	Center-high level	High level
L_5 content (%, w/w LPNs)	15	20	-	25
L_5:TNF-α siRNA weight ratio	5.0:1	7.5:1	10.0:1	15.0:1

were identified and subjected to model fitting by using analysis of variance (ANOVA), and the best model fit was selected based on statistical parameters, i.e., the p-value, the R^2, the difference between adjusted and predicted R^2, and the adequate precision. The results were further optimized numerically and graphically to construct desirability and overlay plots, respectively. Statistical optimization was performed using Design Expert (version 12.0.1, Stat-Ease Inc., Minneapolis, MN, USA).

In vitro Gene Silencing

The murine macrophage cell line RAW 264.7 was purchased from the American Type Culture Collection (TIP71, Manassas, VA, USA). The cells were maintained in Dulbecco's Modified Eagle's Medium with high (4.5 g/L) glucose (DMEM+, Fisher Scientific Biotech Line, Slangerup, Denmark) supplemented with 100 U/mL penicillin, 100 μg/mL streptomycin, 2 mM glutamine (all from Sigma-Aldrich), and 10% (v/v) fetal bovine serum (FBS, Gibco, Life Technologies). The cells were grown in a 5% CO_2-95% atmospheric air incubator at 37°C, the growth medium was renewed every second day, and the cells were subcultured twice a week by detaching them from the culture flask (75 cm^2, Sigma Aldrich) using a cell scraper. Cells were seeded in 6-well tissue culture plates (Sigma Aldrich) at a density of 1.0×10^6 cells/well. Subsequently, nanoparticle suspensions were added to each well resulting in final siRNA concentrations of 2.8, 5.6, 11.3, 27.9, and 55.8 nM, respectively, in duplicates, followed by incubation for 21 h. To each well, 5 ng/mL (final concentration) lipopolysaccharide (LPS, Sigma-Aldrich) was added, and the cells were subsequently incubated for additional 3 h. After 24 h, the cells were lysed with 350 μL NucleoSpin cell lysis buffer (Macherey-Nagel, Düren, Germany), and total RNA was isolated and purified using the NucleoSpin RNA Plus kit (Macherey-Nagel). Total RNA was checked for purity and quantified by UV-Vis spectroscopy (Nanodrop 2000, ThermoFisher Scientific). Purified RNA was reverse transcribed using the iScript cDNA synthesis kit (Bio-Rad Laboratories, Hercules, CA, USA). The real-time polymerase chain reaction (PCR) or quantitative PCR (qPCR) was performed in duplicate for the reference housekeeping genes [β-actin (ACTB) and β-glucuronidase (GUSB)] and in triplicate for the TNF-α gene using a LightCycler[®] 480 (Roche, Basel, Switzerland) and the SYBR I Green[®] Master Mix (Roche) as reported previously (Jensen et al., 2012) with slight modifications. The concentrations of the primers for ACTB, GUSB, and TNF-α in the reaction mixture were 1.0, 0.5, and 1.0 μM, respectively. The LightCycler[®] 480 software v.1.5.0 (Roche) was used for crossing point (CP) analysis, followed by quantification relative to LPS-treated cells using the comparative $\Delta\Delta CP$ method (Pfaffl, 2001).

Cell Viability

RAW 264.7 cells were seeded in a 96-well plate at a density of 5,000 cells/well in a final volume of 180 μL and allowed to adhere by incubation for 4 h. Subsequently, the cells were incubated for 24 h with 20 μL test formulations in quadruplicates at eight different TNF-α siRNA concentrations

(1.38–222.8 nM). The final volume in the well was 200 μL. At 24 h, the cell culture medium was withdrawn from each well. Adherent cells were washed with PBS, followed by the addition of 180 μL cell culture medium and 20 μL freshly prepared 12 mM methylthiazolyldiphenyl-tetrazolium bromide (MTT) (Sigma Aldrich). The plates were incubated for 2 h at 37°C in 5% CO_2-95% atmospheric air. At 26 h, the cell culture medium containing MTT was removed from the wells, and the plate was thoroughly air-dried overnight in the dark before adding 200 μL dimethyl sulfoxide to solubilize formazan MTT crystals. The cell viability was determined based on the amount of formazan crystals formed in cells incubated with the test formulations vs. the control cells by measuring the absorbance at 570 nm using a microplate reader (FLUOstar OPTIMA, BMG Labtech, Germany).

Statistical Analysis

Data were analyzed using GraphPad Prism (GraphPad Software version 8, La Jolla, CA, USA) and represented as mean values ± standard deviation (SD). Statistically significant differences were assessed by one-way analysis of variance (ANOVA) followed by a Tukey's post-hoc multiple comparison test. A p-value ≤ 0.05 was considered statistically significant.

RESULTS

Identification of QTPP and CQAs

The QTPP of the TNF-α siRNA-loaded LPNs was defined (**Table 2**) to ensure that the desired product properties were engineered into the nanoparticles already during the design phase (Colombo et al., 2018). Hence, the QTPP served as a guide for the optimization of formulation and process parameters to ensure that CQAs were within the desired range. The selected CQAs define the criteria of the liquid formulation encompassing safety, efficacy, and quality. The following CQAs were identified: (i) z-average, (ii) PDI, (iii) zeta potential, (iv) encapsulation efficiency, (v) loading of siRNA, (vi) in vitro transfection efficiency, and (vii) in vitro cell viability.

TABLE 2 | Quality target product profile (QTPP) of TNF-α siRNA-loaded lipidoid-polymer hybrid nanoparticles (LPNs).

Response	Target	Explanation
z-average	<200 nm	Maximal uptake by macrophages
PDI	<0.200	Predictable particle behavior
Zeta potential	>0.0 mV	Enhanced interaction with macrophages
Encapsulation efficiency	>60.0%	Pharmacoeconomic consideration
Loading efficiency	>6.0 μg/mg LPNs	Reduced effective dose of siRNA and delivery system
Gene silencing efficiency (IC_{50})	<20.0 nM	
Cell viability	>200 nM	

TABLE 3 | Physicochemical properties of the formulations used for the I-optimal design. Data are shown as mean values ± SD of three independent formulation batches and three technical replicates ($N = 3$ and $n = 3$).

L_5 content (%, w/w)	L_5:TNF-α siRNA weight ratio	z-average (nm)	PDI	Zeta potential (mV)	Encapsulation efficiency (%)	TNF-α siRNA loading (μg siRNA/mg LPNs)	Fold reduction in IC_{50} value for TNF-α gene silencing[^]
15	5.0:1	202.5 ± 12.6[#]	0.126 ± 0.038[#]	6.7 ± 0.6*	71.6 ± 8.6[#]	23.7 ± 0.6***	3.4
	7.5:1	195.0 ± 1.5	0.102 ± 0.014	13.8 ± 2.0	64.4 ± 13.0	12.9 ± 2.6**	1.7
	10.0:1	194.6 ± 1.9	0.100 ± 0.027	13.7 ± 3.0	67.2 ± 2.8	10.1 ± 0.4	3.3
	15.0:1	194.2 ± 3.2	0.113 ± 0.024	19.6 ± 1.7	67.1 ± 4.3	6.7 ± 0.4	4.5 ± 1.2[#]
20	5.0:1	202.0 ± 11.4	0.119 ± 0.010	19.5 ± 1.8	73.5 ± 3.6	29.4 ± 1.4***	3.1
	7.5:1	188.2 ± 4.4	0.106 ± 0.032	22.2 ± 8.6	73.8 ± 9.4	19.7 ± 2.5***	1.6
	10.0:1	189.7 ± 2.9	0.116 ± 0.028	26.5 ± 2.7	76.7 ± 9.4	15.3 ± 1.8***	2.6
	15.0:1	190.7 ± 1.9	0.125 ± 0.038	30.9 ± 1.0*	78.0 ± 5.0	10.4 ± 0.7	3.22 ± 0.6[¤]
25	5.0:1	186.0 ± 9.8	0.118 ± 0.009	21.5 ± 5.0	71.8 ± 2.8	35.9 ± 1.4***	3.3
	7.5:1	187.9 ± 12.0	0.175 ± 0.082	32.0 ± 4.8*	73.8 ± 9.6	24.6 ± 3.2***	1.3
	10.0:1	181.2 ± 7.3	0.148 ± 0.051	33.3 ± 7.2**	74.3 ± 9.5	18.6 ± 2.4***	1.9
	15.0:1	181.0 ± 16.8	0.166 ± 0.009	39.0 ± 5.7***	74.3 ± 3.0	12.4 ± 0.5**	4.6

[^]Reduction relative to non-encapsulated TNF-α siRNA, where the IC_{50} value for silencing TNF-α expression for non-encapsulated TNF-α is 63.7 nM. [#]$N = 3$, [¤]$N = 4$. *$p < 0.05$, **$p < 0.01$, ***$p < 0.001$ compared to 15%, 15.0:1.

Effect of Independent Variables on the Physicochemical Properties of LPNs

To investigate the effect of one of the independent variables, i.e., the L_5 content (15, 20, and 25%), on the physicochemical properties of the LPNs, the other variable, i.e., the L_5:TNF-α siRNA ratio, was kept constant at four different levels (5.0:1, 7.5:1, 10.0:1, and 15.0:1) (**Table 3**). Significant differences were not observed in the z-average and PDI, and the values were within the range of the QTPP. A ∼1.9-fold increase in the loading was observed when the L_5 content was increased from 15 to 25% at L_5:TNF-α siRNA ratios from 7.5:1 to 15.0:1. However, the loading dropped to 1.5-fold when the ratio was 5.0:1. As expected, the zeta potential increased with the L_5:TNF-α siRNA ratio due to an increase in the content of cationic L_5.

The physicochemical properties of the formulations were explored further by keeping the L_5 content constant and varying the L_5:TNF-α siRNA ratio. The z-average and PDI of the LPNs remained almost constant at all tested L_5:TNF-α siRNA ratios (**Table 3**). In contrast, a significant decrease in the zeta potential was observed as the L_5:TNF-α siRNA ratio was decreased (corresponding to a higher amount of siRNA without increasing the L_5 content). Hence, the L_5 content and the L_5:TNF-α siRNA ratio influence the zeta potential and the siRNA loading. The encapsulation efficiency was neither affected by the L_5 content nor the L_5:TNF-α siRNA ratio, and no significant differences were observed. However, the responses were within the QTPP (>60%). Based on these results, the L_5 content relative to the final batch weight (%, w/w, 15, 20, and 25%) and the L_5:TNF-α siRNA ratio (5.0:1, 7.5:1, 10.0:1, and 15.0:1) were selected for inclusion in a systematic DoE.

Effect of TNF-α siRNA-Loaded LPNs on TNF-α mRNA Expression

The TNF-α gene silencing activity was evaluated at the mRNA level in the murine macrophage cell line RAW 264.7 activated with LPS. The TNF-α siRNA-loaded LPNs induced concentration-dependent TNF-α gene silencing (**Figure 1**). However, the magnitude of the silencing effect was specific for each formulation. Overall, both the L_5 content and the L_5:TNF-α siRNA ratio affected the gene silencing. At an siRNA concentration of 5.6 nM for LPNs having 15% L_5 content, the TNF-α mRNA expression was ∼60%. In contrast, the expression was at least 80% with the remaining LPNs. At the highest tested siRNA concentration (55.8 nM), the TNF-α mRNA expression generally decreased as the L_5 content increased (**Figure 1**) at a constant L_5:TNF-α siRNA ratio. At a constant L_5 level, as the amount of siRNA increased in the LPNs, the TNF-α mRNA expression decreased from 15.0:1 to 7.5:1. Interestingly, cells incubated with LPNs having a ratio of 5.0:1 had lower TNF-α mRNA expressed for reasons that need to be investigated. As expected, a decrease in the LPS concentration used for activation of the macrophages from 5 to 1.25 ng/mL resulted in only 50% TNF-α mRNA expression when treated with LPNs composed of 15% L_5 and having an L_5:TNF-α siRNA ratio of 15.0:1 at 5.6 nM (**Figure 1A**). Even though the cells incubated with LPNs having an L_5:TNF-α siRNA ratio of 7.5:1 expressed higher TNF-α gene levels compared to cells incubated with other LPNs, it was interesting to note that at an siRNA concentration of 55.6 nM, the TNF-α mRNA expression was ∼44.6 (**Figure 1A**), 37.7 (**Figure 1B**), and 46.0% (**Figure 1C**), hence displaying a sharp increase in the silencing effect relative to lower concentrations. The TNF-α mRNA levels were reduced by 93.8% in cells incubated with the formulation containing 25% L_5 and an L_5:TNF-α siRNA ratio of 15.0:1 at the highest tested TNF-α siRNA concentration (**Figure 1C**). It appears that as the L_5 content increases, the TNF-α mRNA expression increases at the lower siRNA concentrations tested (**Figure 1**). Overall, LPNs containing an L_5 content of 15, 20, and 25% with L_5:TNF-α siRNA ratio of 15:1 were most efficient in causing a significant concentration-dependent decrease in TNF-α mRNA expression.
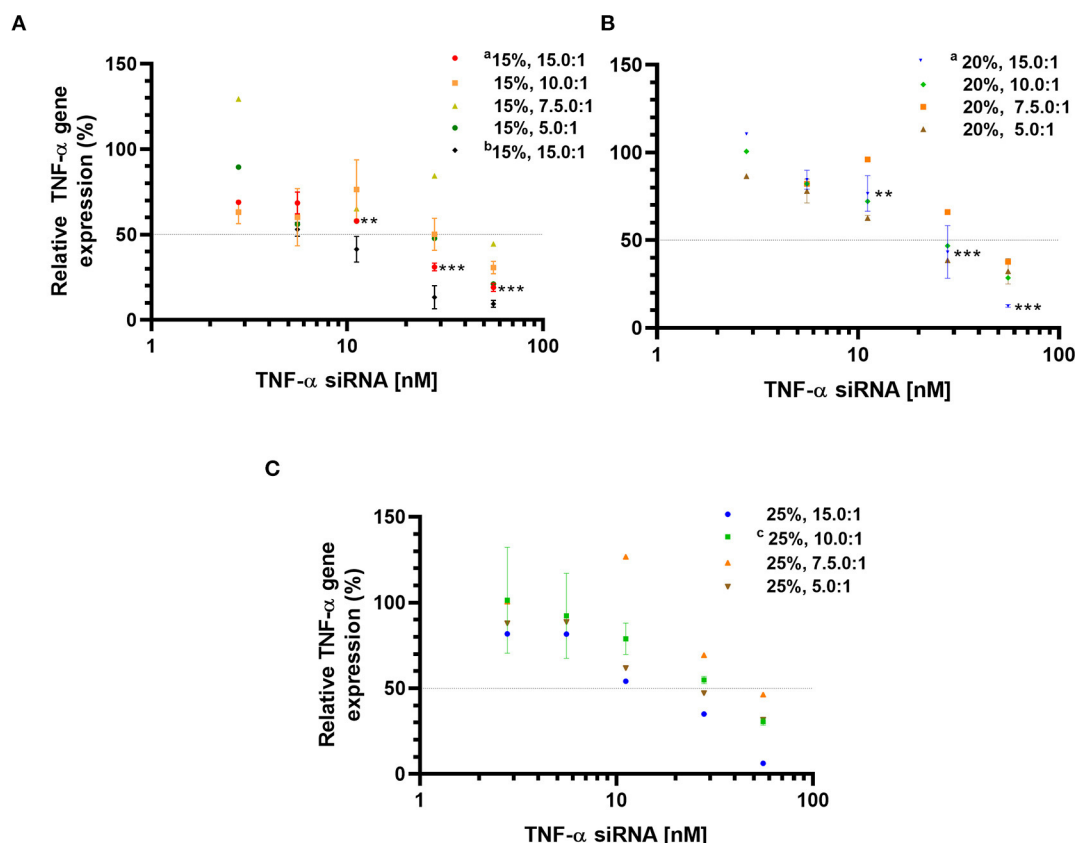
FIGURE 1 | Relative TNF-α mRNA expression determined by qPCR in LPS-activated RAW 264.7 macrophages incubated with TNF-α siRNA loaded formulations. Formulations with an L_5 content of 15% **(A)**; 20% **(B)**, and 25% **(C)**. Data is normalized to non-transfected, LPS-treated cells (100% TNF-α mRNA expression). Data is represented as mean values ± SD ([a]$N = 3$, $n = 3$, [c]$N = 2$, $n = 3$, 5 ng LPS/mL; [b]$N = 3$, $n = 3$, 1.25 ng LPS/mL and unmarked $N = 1$, $n = 3$), where $N =$ independent formulations with duplicates of each concentration during transfection, $n =$ technical replicates. **p < 0.01, ***p < 0.001 compared to 5.58 nM TNF-α siRNA concentration in LPNs.
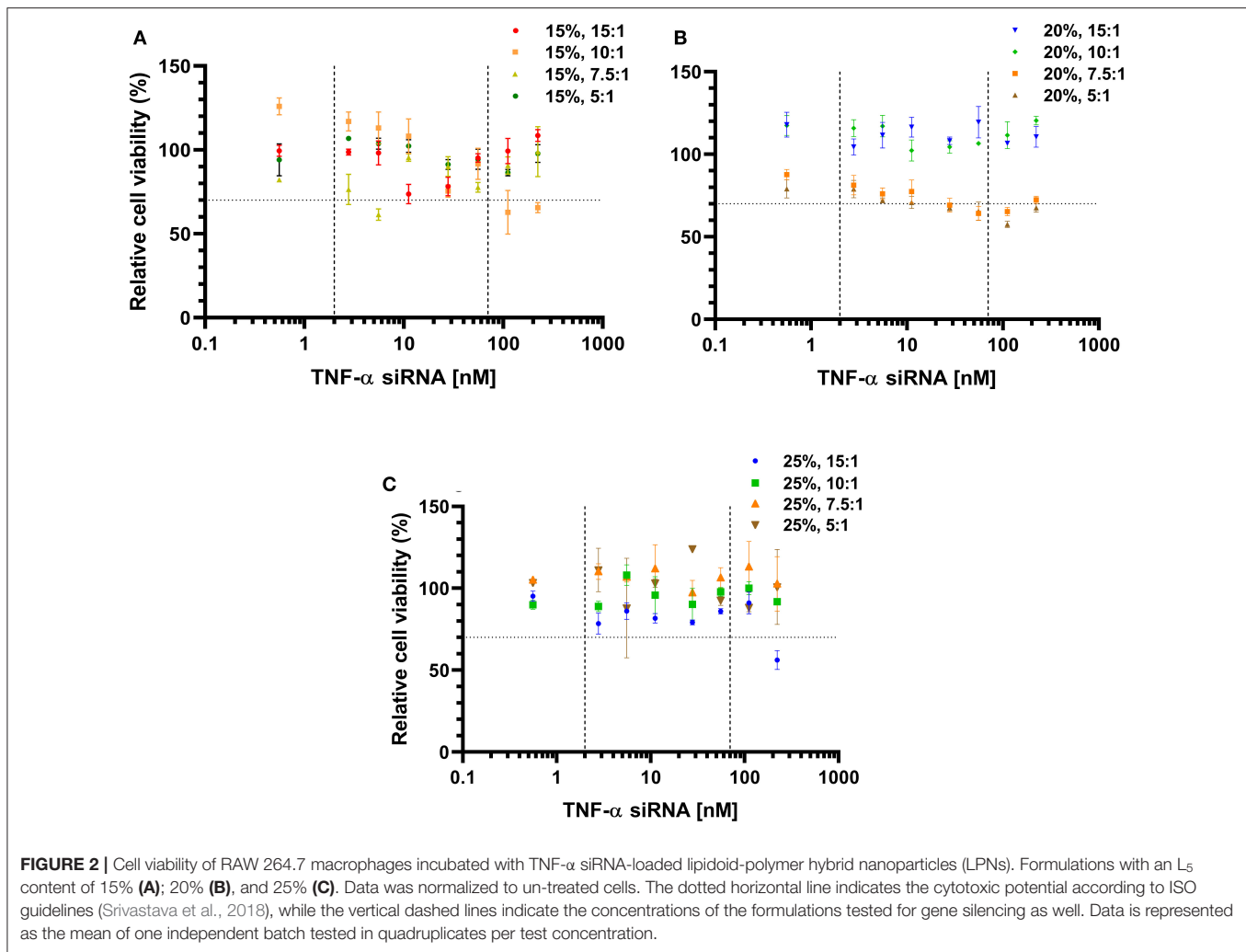
Effect of TNF-α siRNA-Loaded LPNs on Cell Viability

To investigate whether incubation with TNF-α siRNA-loaded LPNs influenced the viability of RAW 264.7 macrophages and hence affect the measured TNF-α gene silencing effect, the viability was quantified using the MTT assay. The cell viability appeared to drop between 5.6 and 55.8 nM siRNA concentrations for all formulations with an L_5 content of 15% (**Figure 2**). However, for the formulations displaying an L_5:TNF-α siRNA wt. ratio of 10.0:1, the viability dropped at 27.8 nM and continued to decrease below 70% after a brief increase at 55.8 nM (**Figure 2A**). Formulations having an L_5 content of 20% and L_5:TNF-α siRNA ratios of 15.0:1 and 10.0:1 exhibited no cytotoxicity, evident by almost 100% cell viability at all tested concentrations. Between TNF-α siRNA concentrations of 11.2 and 222.8 nM, the cell viability was ∼70% and appeared to increase from 111.4 nM (**Figure 2B**). Formulations having an L_5 content of 25% did not appear to be cytotoxic based on the nearly constant cell viability >80% at all tested siRNA concentrations. However, for the formulation having a wt. ratio of 15.0:1, the viability was above 75% up to 111.4 nM siRNA concentration but then the

viability steeply declined to around 56% (**Figure 2C**). Of all the LPNs tested for cell viability, only a few of them (15%, 10.0:1 and 7.5:1; 20%, 7.5:1, and 5.0:1; 25% 15.0:1) seemed to have cytotoxic potential (**Figure 2**) but none of them caused >50% loss in cell viability even at 222.8 nM. Thus, in terms of cytotoxicity and TNF-α gene silencing effect, formulations having an L_5 content and L_5:TNF-α siRNA wt. ratio of 15%, 15.0:1 and 20%, 15.0:1 exhibited a balanced profile and were consequently used for model validation.

Contour Profiling of Response Variables

Formulations from the design space (**Table 1**) were prepared, and responses to the independent variables were assessed and compared to the QTPP (**Table 2**). Contour plots were constructed for each of the response variables as a function of the L_5 content (%w/w) and the L_5:TNF-α siRNA ratio (**Figure 3**). The differences in z-average were not significant in the design space (**Figure 3A**). This suggests that the z-average is not affected by the independent variables but may rather be dependent on the process parameters for preparing the particles. However, the z-average decreased considerably when the L_5 content was

FIGURE 2 | Cell viability of RAW 264.7 macrophages incubated with TNF-α siRNA-loaded lipidoid-polymer hybrid nanoparticles (LPNs). Formulations with an L_5 content of 15% **(A)**; 20% **(B)**, and 25% **(C)**. Data was normalized to un-treated cells. The dotted horizontal line indicates the cytotoxic potential according to ISO guidelines (Srivastava et al., 2018), while the vertical dashed lines indicate the concentrations of the formulations tested for gene silencing as well. Data is represented as the mean of one independent batch tested in quadruplicates per test concentration.

higher than 20% and the L_5:TNF-α siRNA ratio was >7.5:1, and vice versa. There was a gradual increase in the PDI (from ~0.100 to 0.175) as the L_5 content increased from 15 to 25% (**Figure 3B**). A minor increase in the PDI was observed when the L_5:TNF-α siRNA ratio decreased at an L_5 content of 15%. The zeta potential increased gradually from 6.7 mV to a maximum of 39.0 mV (**Figure 3C**). The encapsulation efficiency remained almost constant (64–78%) throughout the design space (**Figure 3D**), which may indicate that the encapsulation efficiency is more dependent on the process of preparing the LPNs rather than on the independent variables. The siRNA loading was affected by both independent variables (**Figure 3E**). The L_5:TNF-α siRNA ratio displayed a greater impact on the loading, which was expected as a higher amount of siRNA would correspond to increased loading per weight of LPNs. To test the performance of the formulations loaded with TNF-α siRNA in a biologically relevant system, the IC_{50} values were calculated as a function of the TNF-α siRNA concentration in formulations responsible for half maximal inhibition of TNF-α mRNA expression in macrophages (**Figure 3F**). The IC_{50} values for transfection efficiency of all formulations ranged from

10.2 to 50.0 nM. Formulations displaying the highest L_5:TNF-α siRNA wt. ratio, i.e., least amount of TNF-α siRNA relative to L_5, at 15, 20, and 25% L_5 had transfection efficiencies below 20 nM. The IC_{50} value for naked TNF-α siRNA was found to be 63.7 nM. Fold-change in TNF-α mRNA inhibition relative to naked siRNA was obtained by the ratio of IC_{50} values of TNF-α siRNA-loaded LPNs and naked TNF-α siRNA. This corresponds to an siRNA dose-reduction in obtaining similar responses. At a constant L_5 content, the fold-change increased as per the quadratic model fitting (**Tables 3, 4**) from 7.5:1 to 15.0:1 ratio. When the L_5:TNF-α ratio was kept constant, the fold-change generally increased with an increase in the L_5 content. Interestingly, LPNs with an L_5 content of 15 and 25% had similar IC_{50} values.

Mathematical Modeling of Responses

The obtained responses (**Supplementary Table 3**) were fitted with an appropriate, non-aliased model using ANOVA. Although the model was significant for the z-average and the PDI ($p = 0.0042$ and 0.0177), the R^2 was only −0.3 and 0.27, respectively, hence these responses were excluded from the
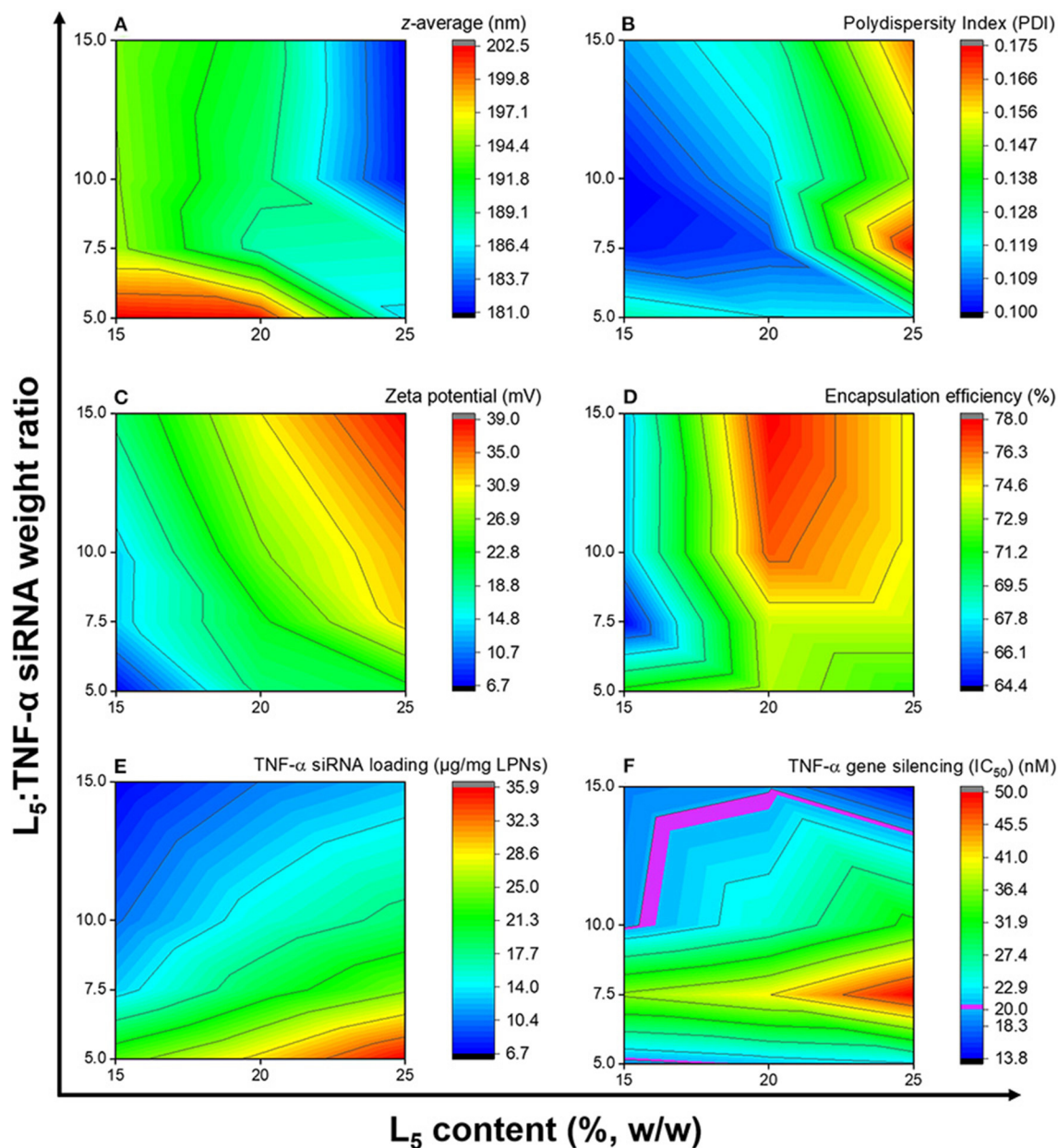
FIGURE 3 | Contour plots showing the effects of the independent variables on the z-average **(A)**, polydispersity index **(B)**, zeta potential **(C)**, encapsulation efficiency **(D)**, TNF-α siRNA loading **(E)**, and TNF-α gene silencing **(F)**. Data is based on the mean of three independent formulations ($N = 3$, $n = 3$) for **(A–E)**, while for **(F)** it is based on mean of duplicates of transfection well and triplicates of qPCR reaction for one formulation.

analysis. For all modeled responses (**Table 4**), the adjusted R^2 was in reasonable agreement with the predicted R^2 (the difference was <0.2), while the adequate precision was higher than four. In addition, the lack of fit was not significant for all modeled responses. Formulations displaying an L_5:TNF-α siRNA wt. ratio of 5.0:1 were excluded from the mathematical modeling because the IC_{50} values for gene silencing fit the model equations linearly from 7.5:1 to 15.0:1 ratio.

Identification of the Optimal Operating Space

A desirability plot was constructed with parameter inputs (**Supplementary Table 3**) from the QTPP (except cell viability, for which the IC_{50} could not be determined due to negligible effects if the formulations on cell viability) and the prediction model analyzed using ANOVA (**Figure 4**). The region shaded toward dark yellow (**Figure 4A**) constitutes the optimal L_5 content and L_5:TNF-α siRNA weight ratio where all the responses

show the most optimal values. The edge of failure is the boundary between the dark blue region and the other colored regions, where either one or several responses do not fulfill the set criteria. The light blue shaded region (**Figure 4A**) indicates that all criteria defined in the QTPP were met but were less optimal relative to the green and yellow region. Ten formulations displaying a desirability score ranging from 0.671 to 0.796 were identified (**Supplementary Table 4**). An overlay plot (**Figure 4B**) was constructed, which shows all possible combinations of L_5 content and L_5:TNF-α siRNA ratio (**Table 4**). In other words, this is the OOS, and a formulation selected from this region is most likely to have the desired characteristics.

Validation of Responses

Although the desirability scores (**Figure 4A**) show that the point formulations with the most desirable properties are 15%, 13.5:1 and 25%, 15.0:1, they do not account for the cell viability since the IC_{50} values could not be calculated due to lack of typical log dose-response relationship at the tested concentrations. To exclude potential cytotoxic formulations at the tested concentrations (**Figure 2**), two formulations having L_5 contents and L_5:TNF-α

TABLE 4 | Model fitting parameters for significant responses[*].

Parameter	Zeta potential	siRNA loading	Gene silencing (IC_{50})
p-value	<0.0001	<0.0001	0.0013
R^2	0.739	0.940	0.938
Adjusted R^2	0.719	0.922	0.893
Predicted R^2	0.657	0.900	0.768
Adequate precision	12.8	23.4	13.0
Model	2FI	Quadratic	Quadratic

*Formulations displaying an L_5:TNF-α siRNA wt. ratio of 5.0:1 were excluded from the design.

siRNA wt. ratios of 15 and 20%, 15.0:1 were formulated in triplicates to validate the OOS. The physicochemical properties of the formulations and the IC_{50} values for TNF-α gene silencing were determined and compared to the point formulations from numerical optimization using specific criteria (**Tables 4, 5**). Using one-way ANOVA, no statistically significant differences were observed between the z-average, PDI, and TNF-α gene silencing for these two formulations (**Table 5**). However, there was a significant difference between the zeta potential ($p < 0.05$). The IC_{50} values of TNF-α siRNA-loaded LPNs with L_5 content of 15 and 20% having an L_5:TNF-α siRNA ratio of 15.0:1 relative to non-encapsulated siRNA were 4.5 ± 1.2 and 3.2 ± 0.6-fold times lower, respectively (**Table 5**).

DISCUSSION

Adopting a QbD approach ensures the quality of medicines by employing statistical, analytical, and risk management methodologies in the design, development, and manufacturing of medicines (Lawrence et al., 2014). Such an approach helps in identifying all potential sources of variability that may affect a process and/or a formulation and aids in meeting the predefined characteristics from the very beginning. Thus, applying these principles when designing a formulation of TNF-α siRNA-loaded LPNs may ensure a high-quality and robust formulation displaying high siRNA loading, optimal physicochemical properties, high gene silencing efficiency, and low toxicity. Hence, the specific purpose of this study was to optimize the loading of TNF-α siRNA in LPNs using a QbD approach, where the L_5 content relative to the PLGA content in the formulation was varied, along with the L_5:TNF-α siRNA weight ratio, by keeping the total weight of the solids (L_5 + PLGA) constant. This was followed by assessment of all formulations for their effect on TNF-α gene silencing and cell viability in activated RAW 264.7 macrophages.
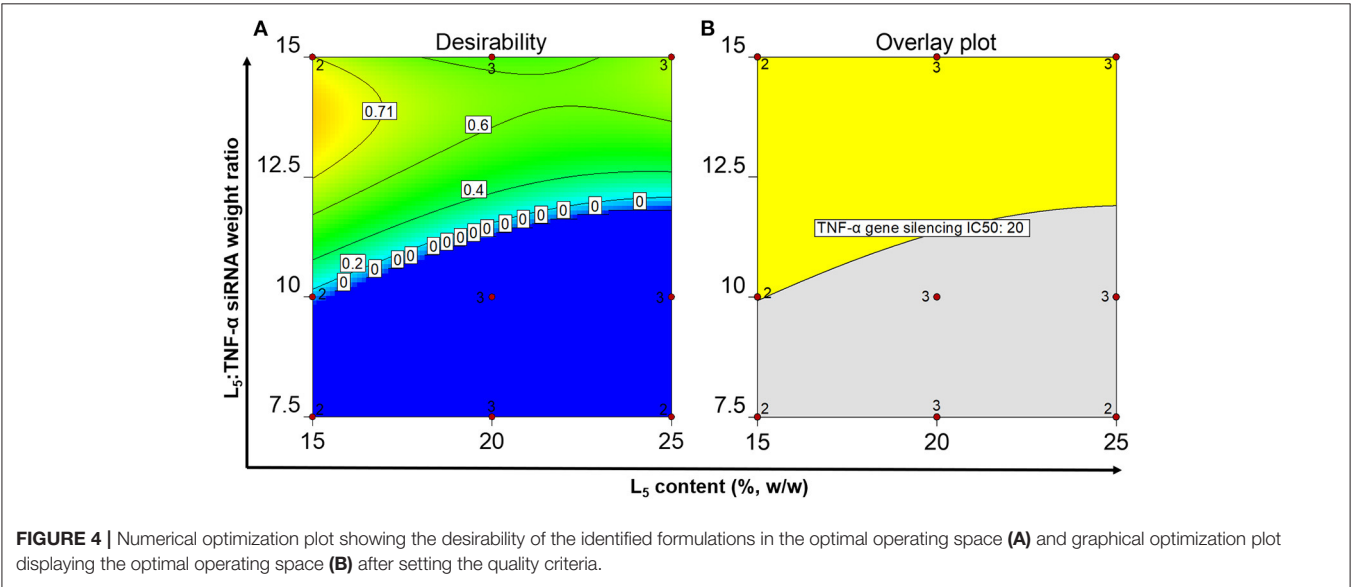

FIGURE 4 | Numerical optimization plot showing the desirability of the identified formulations in the optimal operating space **(A)** and graphical optimization plot displaying the optimal operating space **(B)** after setting the quality criteria.

TABLE 5 | Validation of two, point formulations from the optimal operating space.

L_5 content (%, w/w)	L_5: TNF-α wt. ratio	z-average (nm)	PDI	Zeta potential (mV)	Encapsulation efficiency (%)	TNF-α siRNA loading (μg/mg LPNs)	TNF-α gene silencing IC_{50} (nM)	Desirability	Fold reduction in IC_{50} value for TNF-α gene silencing
15.0	15.0:1	194.7 ± 3.3	0.113 ± 0.024	19.6 ± 1.7	67.1 ± 4.3	6.7 ± 0.4	15.1 ± 4.1	0.712	4.5 ± 1.2
20.0	15.0:1	190.7 ± 1.9	0.125 ± 0.038	30.9 ± 1.0	78.1 ± 5.1	10.4 ± 0.7	20.9 ± 4.6	0.569	3.2 ± 0.6

Data are represented as mean values ± SD of independent formulations (N = 3–4).

The physicochemical properties of the LPNs were dependent on the starting amounts of lipid and siRNA. First, the effect of the L_5 content on various responses was identified by keeping the L_5:TNF-α siRNA ratio constant. Based on these one-factor-at-a-time experiments, it was established that the L_5 content significantly affects the zeta potential and, in some cases, the z-average and PDI. The z-average for LPNs formulated using the optimized DESE method used in this study is expected to be ∼200 nm. To confirm the effect on z-average and PDI at higher L_5 content (30 and 40%) by keeping the L_5:TNF-α siRNA ratio 15.0:1, two formulations were prepared, and it was found that the z-averages were 159.1 and 154.8 nm with PDIs of 0.216 and 0.272, respectively (**Supplementary Table 2**). These differences were statistically significant ($p < 0.01$). One explanation could be that as the amount of L_5 is increased, the PLGA content decreases, which means a lower concentration of the latter in the organic phase during the preparation process and consequently a reduction in particle size. This may be attributed to a decrease in solvent viscosity, increase in diffusion coefficient, and the decrease in PLGA content in the droplets of the organic phase resulting in smaller particles after solvent evaporation (Feczkó et al., 2011). The PLGA concentration in the organic phase is shown to influence particle size. An increase in the lipid content could lead to a heterogeneous population of lipoplexes and LPNs, thus increasing the PDI. This can be explained by the fact that at a lipid:polymer weight ratio of 10:90, the amount of lipid is within a range to cover the entire surface of the hydrophobic PLGA core. Similar observations have been reported previously, where the excess lipids have been speculated to increase above the critical micellar concentration, resulting in the assembly of liposomes, hence suggesting the coexistence of liposomes and hybrid nanoparticles (Zhang et al., 2008).

The encapsulation efficiency remained in the range of 60–80%, which is similar to the encapsulation efficiency of enhanced green fluorescent protein (eGFP) siRNA-loaded LPNs as we have reported previously (Thanki et al., 2017). However, the inclusion of L_5 in the nanoparticles significantly increased the encapsulation efficiency compared to the encapsulation efficiency in non-modified PLGA nanoparticles (data not shown), in agreement with previous reports (Thanki et al., 2017). PLGA is a hydrophobic polymer composed of lactic and glycolic acid monomers with pK_a values of 3.86 and 3.83, respectively (Yoo and Mitragotri, 2010). The pH value of the water phase during LPN preparation is ∼6.5. Hence, at this pH, the carboxylic acid end groups of PLGA exist in a deprotonated state. These anionic residues are not favorable for interaction with the negatively charged phosphate backbone of siRNA. Differences between

z-average and encapsulation efficiencies were not significant and were within the desirable limits.

An increase in the L_5 content from 15 to 25% resulted in ∼2 to 4-fold increase in the zeta potential at all tested L_5:TNF-α siRNA ratios (**Table 3**). The zeta potential is an indirect measure of the surface charge of the nanoparticles. It is one of the physicochemical properties that influences particle uptake by macrophages (Alexis et al., 2008). In one study, it was found that both positive and negative surface charges were promoting uptake of carboxymethyl hydrochloride-grafted polymeric nanoparticles (He et al., 2010). These results suggest that surface charge-dependent uptake is highly variable and depends on the type of formulation, uptake mechanisms, and the biological system. Since the LPNs are composed of cationic lipids, it is imperative to know the zeta potential as it can have a possible effect on the uptake of particles and for this reason, it was set to >0 mV in the QTPP (**Table 2**). In addition, the zeta potential is also a measure of particle colloidal stability, where higher magnitude suggests enhanced colloidal electrostatic stability (Shah et al., 2015). Furthermore, the intended site of action of these LPNs is the alveoli, which houses the alveolar macrophages (Byrne et al., 2015). These LPNs have been engineered as spray-dried particles intended for inhalable alveolar delivery to silence TNF-α gene in macrophages (Dormenval et al., 2019), thus circumventing the barriers of systemic delivery related to excess surface charge. Overall, the results are in agreement with previous reports where the zeta potential increased linearly with an increase in the molar composition of cationic lipids (Smith et al., 2017).

When keeping the L_5 content constant and varying the L_5:TNF-α siRNA ratio, it was observed that the siRNA loading decreased 3-fold when the L_5:TNF-α siRNA ratio was increased from 5.0:1 to 15.0:1. The L_5:TNF-α siRNA ratio displayed a greater impact on the siRNA loading, which was expected as a higher initial amount of siRNA would correspond to an increased loading per weight of the LPNs. The encapsulation efficiency increased (from 64.4 to ∼80%) as the L_5 content increased from 15 to 25%, highlighting the role of L_5 in electrostatic interactions with siRNA. The relatively lower encapsulation efficiency could be due to the high pH (7.5) during the emulsification process as L_5 might not be fully protonated (de Groot et al., 2018). In addition to the amount of cationic lipid, the overall performance of the system is also dependent on the dose of siRNA that reaches the cytosol of the cell. Thus, siRNA loading is a response worth investigating. The loading was expected to increase because even at the same weight ratio and a higher L_5 content, the absolute amount of siRNA was higher. Thus, to have a direct comparison,

formulations with L_5 contents of 15 and 20% with L_5:TNF-α siRNA ratios of 7.5:1 and 10.0:1, respectively, contained equal amounts of TNF-α siRNA (300 μg). No statistically significant differences were observed with respect to TNF-α siRNA loading between the two formulations. Similar results were obtained for LPNs loaded with an antisense oligonucleotide (ASO) (Thanki et al., 2019c). The encapsulation efficiency is important in terms of performance and pharmacoeconomics. Hence, a value higher than 60% was set for the encapsulation efficiency, while a higher siRNA loading (>6 μg siRNA/mg LPNs) would have a positive impact on the gene silencing effect and reduction in cytotoxicity. The increase in loading without compromising the particle properties suggests that the electrostatic charge condensation between the siRNA and the amine headgroups of L_5 is not complete and that more siRNA could be complexed. However, in general, excess siRNA may not necessarily translate into higher gene silencing because the cationic character of the lipid decreases, eventually resulting in poor transport across the cell membrane and thus poor transfection (Fröhlich, 2012). Based on these observations, it is evident that both the L_5 content and the L_5:TNF-α siRNA ratio affect the physicochemical properties of the LPNs, hence they were included in the systematic QbD-based optimization of the LPNs.

Nucleic acid delivery has traditionally been hindered by the toxicity associated with their delivery systems. In the past years, novel carrier systems and analogs have been developed to overcome this problem (Love et al., 2010). *In vitro* studies using the MTT assay exhibit that the LPNs, in general, do not have a cytotoxic potential at the measured concentration ranges. The toxicity is predominantly induced by the positively charged lipid component of the nanoparticulate carrier. However, the use of synthetic lipids or lipidoids help overcome these delivery challenges (Akinc et al., 2008). No differences in cell viability were found (except at 11.2 nM) between the LPNs having the highest (5.0:1 wt. ratio, 6.5 $\pm$ 0.6 mV) and least amount of siRNA (15.0:1 wt. ratio, 20.4 $\pm$ 1.5 mV) highlighting that the zeta potential of a formulation measured in the dispersion medium is not the only determinant of the toxicity. Dose response of siRNA LPNs demonstrated lack of cytotoxic potential for different formulations tested at certain concentrations for gene silencing (**Figures 2A–C**), and only a few of them (15%, 10.0:1 and 7.5:1; 20%, 7.5:1; 25% 15.0:1) seemed to have cytotoxic potential. The possibility of potential apoptotic and necrotic effects of the particles should not be disregarded since it may not be apparent from the MTT assay. However, at TNF-α siRNA concentrations of 100 and 200 nM, no significant apoptotic or necrotic cells were observed for 15%, 15.0:1 LPNs (Jansen et al., 2019).

In the present study, we identified the effect of the independent variables on the cell viability where all the tested formulations had comparable siRNA concentrations. It was found that non-encapsulated TNF-α siRNA and scrambled siRNA did not affect the cell viability at the tested concentrations. Thus, the toxicity of the formulations is most likely caused by the L_5 component. It has been reported that certain lipidoids. e.g., DLinDMA, at a concentration of 1 μg/mL of siRNA induce a significant increase in apoptotic macrophages (Basha et al., 2011). Cytotoxicity is highly affected by various factors, and one of

them is the cell type (Nakamura et al., 2016). The concentration of TNF-α siRNA in the most optimal formulations required to knock down between 60 and 69% of TNF-α was found to be 27.8 nM, while a concentration of 55.8 nM was required for >80% knockdown. At these concentrations, none of the most optimal formulations displayed any cytotoxic potential. The TNF-α gene silencing profile was found to be quite similar to previously published results (Jansen et al., 2019).

To study the effect of the independent variables on the TNF-α mRNA expression, 12 formulations with different L_5 content and L_5:TNF-α siRNA ratios were tested at five concentrations of encapsulated TNF-α siRNA. All formulations, except the ones displaying an L_5:TNF-α siRNA ratio of 7.5:1, exhibited IC_{50} values 2.6- to 4.6-fold lower than the LPNs loaded with negative control siRNA and the non-loaded TNF-α siRNA. These results show that using LPNs as a delivery system is clearly advantageous and the silencing is due to the specific sequence of TNF-α siRNA. This may be due to the fact that non-loaded TNF-α siRNA cannot cross the cell membrane (De Paula et al., 2007; Kim et al., 2010). The silencing mediated by non-encapsulated siRNA might be related to damage of the cell membranes upon harvesting, as the siRNA (and also the LPNs) are incubated with cells immediately after harvesting (Jensen et al., 2012). We found a linear increase in TNF-α gene silencing effect when the L_5:TNF-α siRNA ratio was increased from 7.5:1 to 15.0:1 at 15, 20, and 25% L_5 content. Interestingly, LPNs with a 5.0:1 ratio silenced TNF-α gene expression more efficiently than 7.5:1. We do not fully understand the reason for these results, which needs to be addressed in future studies. Although the IC_{50} values are quite different for every formulation, it is evident that at the highest tested concentration of siRNA, the gene expression of TNF-α in LPS-activated macrophages treated with LPNs containing 15, 20, and 25% L_5 and having an L_5:TNF-α siRNA ratio of 15.0:1 was only 19, 12, and 6%, respectively. Similar observations have been documented previously where increasing the lipidoid content resulted in more efficient silencing of Factor VII mRNA (Akinc et al., 2009; Basha et al., 2011). This suggests that the positive charge of the lipid is not the only determinant of transfection efficiency and thus gene silencing, and that endosomal escape can also be a greater factor governing the efficacy (Raemdonck et al., 2008). The IC_{50} values are highly variable and depend on many factors, including the composition of the formulation (Thanki et al., 2017) and the cell lines used (Nakamura et al., 2016), hence comparison seems valid when all other variables are kept constant. Based on the current observations, LPNs composed of 15, 20, and 25% L_5 having an L_5: TNF-α siRNA ratio of 15.0:1 were found to be most optimal for gene silencing in macrophages, as determined from their IC_{50} values (**Table 3**).

To date, several different lipid carriers have been studied for siRNA delivery. It is generally challenging to compare silencing and non-specific effects obtained in different studies due to highly variable experimental conditions, e.g., cell type, LPS concentration, incubation time, and presence of serum proteins. These tend to destabilize cationic nanoparticles and thus invalidate the observations, since the actual amount of siRNA that reaches the cytosol may vary (Buyens et al., 2010). In a recent study the 15%, 15.0:1 formulation was used a

lead formulation to investigate critical formulation and process parameters involved in spray drying of liquid LPN dispersions into nanocomposite microparticles. The resulting spray-dried microparticles were resuspended and compared to the original liquid LPN dispersions, and no significant differences were found in their performance in terms of physicochemical properties and *in vitro* gene silencing (Dormenval et al., 2019). Also, this formulation was dosed at a TNF-α siRNA concentration of only 5.58 nM and was shown to have a remarkable gene silencing activity *in vivo* (Jansen et al., 2019). It is interesting to compare the OOS of TNF-α siRNA loaded LPNs with that of single-stranded ASO (Thanki et al., 2019c) and an siRNA directed against eGFP (Thanki et al., 2017). The *z*-average, PDI, zeta potential, siRNA loading, and encapsulation efficiencies are almost identical with the latter, which may be due to comparable nucleotide length and similar modification patterns (**Supplementary Table 1**), whereas the gene silencing effect depends on both the L_5 content and the L_5:TNF-α siRNA weight ratio as shown from the coefficients (**Supplementary Table 5**). Recently, we performed a detailed mechanistic evaluation of the release kinetics of fluorescently labeled siRNA from LPNs *in vitro* and *in vivo* after pulmonary administration, which demonstrated that the sustained release of siRNA from LPNs correlates well with cell uptake and *in vivo* biodistribution (Thanki et al., 2019a). It is expected that the optimal formulations identified in the current study display *in vitro* and *in vivo* release kinetics, which is highly comparable to our previously reported findings (Thanki et al., 2019a).

The OOS was constructed based on the results obtained from the above experiments and on the criteria set in the QTPP. Ten formulations displaying a desirability score from 0.671 to 0.796 were identified. The desirability values are between 0 and 1, the latter being the most desirable. However, this term may be misinterpreted because the desirability function is fully dependent on how close the upper and lower limits are set in the QTPP. The goal of optimization is how well the set conditions meet the goals and not about gaining the highest desirability (Desirability Function, 2018).

CONCLUSION

In conclusion, we demonstrate the application of a systematic QbD approach for loading therapeutic TNF-α siRNA into LPNs with optimal *in vitro* gene silencing effect and safety. We show that both the L_5 content and the L_5:TNF-α siRNA ratio significantly affect the zeta potential, siRNA loading and TNF-α gene silencing. It was also found that the responses to the independent variables were complex, but in general there seemed to be an optimal range for loading siRNA into LPNs. QbD with statistical analysis facilitated the modeling of these responses with a high coefficient of determination, which can be useful in predicting responses based on user input of the independent variables. The LPN formulations loaded with TNF-α siRNA showed a 1.3- to 4.6-fold reduction in the effective dose for *in vitro* gene silencing as compared to the dose required for gene silencing by non-encapsulated TNF-α siRNA, highlighting the importance of a delivery system. It was also shown that the zeta potential is not the only determinant of toxicity of a formulation and that reducing the positive surface charge does not necessarily imply reduced gene silencing in every scenario. We further show that higher siRNA loading does not necessarily correlate with higher gene silencing *in vitro*. Finally, an OOS was identified based on graphical optimization, and point formulations displaying L_5 contents of 15 and 20% and L_5:TNF-α siRNA weight ratio of 15.0:1 were identified that satisfied all the criteria set in the QTPP and had a balanced toxicity/efficacy profile. These results demonstrate the importance of systematic formulation design for loading therapeutic TNF-α siRNA in LPNs with optimal gene silencing and safety and support our ongoing efforts for TNF-α siRNA-mediated therapeutic management of COPD in preclinical animal models.

DATA AVAILABILITY STATEMENT

The original contributions presented in the study are included in the article/**Supplementary Material**, further inquiries can be directed to the corresponding author.

AUTHOR CONTRIBUTIONS

FUNDING

ACKNOWLEDGMENTS

SUPPLEMENTARY MATERIAL

The Supplementary Material for this article can be found online at: https://www.frontiersin.org/articles/10.3389/fbioe.2020.601155/full#supplementary-material

REFERENCES

Aaron, S. D., Vandemheen, K. L., Maltais, F., Field, S. K., Sin, D. D., Bourbeau, J., et al. (2013). TNFα antagonists for acute exacerbations of COPD: a randomised double-blind controlled trial. *Thorax* 68:142. doi: 10.1136/thoraxjnl-2012-202432

Adams, D., Gonzalez-Duarte, A., O'Riordan, W. D., Yang, C. C., Ueda, M., Kristen, A. V., et al. (2018). Patisiran, an RNAi therapeutic, for hereditary transthyretin amyloidosis. *N. Engl. J. Med.* 379, 11–21. doi: 10.1056/NEJMoa1716153

Akinc, A., Goldberg, M., Qin, J., Dorkin, J. R., Gamba-Vitalo, C., Maier, M., et al. (2009). Development of lipidoid–sirna formulations for systemic delivery to the liver. *Mol. Therapy* 17:874. doi: 10.1038/mt.2009.36

Akinc, A., Zumbuehl, A., Goldberg, M., Leshchiner, E. S., Busini, V., Hossain, N., et al. (2008). A combinatorial library of lipid-like materials for delivery of RNAi therapeutics. *Nat. Biotechnol.* 26:567. doi: 10.1038/nbt1402

Alexis, F., Pridgen, E., Molnar, L. K., and Farokhzad, O. C. (2008). Factors affecting the clearance and biodistribution of polymeric nanoparticles. *Mol. Pharm.* 5, 511–513. doi: 10.1021/mp800051m

Balwani, M., Sardh, E., Ventura, P., Peiro, P. A., Rees, D. C., Stolzel, U., et al. (2020). Phase 3 trial of RNAi therapeutic givosiran for acute intermittent porphyria. *N. Engl. J. Med.* 382, 2289–2301. doi: 10.1056/NEJMoa1913147

Barnes, P. J. (2003). Chronic obstructive pulmonary disease * 12: new treatments for COPD. *Thorax* 58:804. doi: 10.1136/thorax.58.9.803

Basha, G., Novobrantseva, T. I., Rosin, N., Tam, Y. Y. C., Hafez, I. M., Wong, M. K., et al. (2011). Influence of cationic lipid composition on gene silencing properties of lipid nanoparticle formulations of siRNA in antigen-presenting cells. *Mol. Ther.* 19, 2191–2193. doi: 10.1038/mt.2011.190

Bousquet, J., and Kaltaev, N. (2007). "Global surveillance, prevention and control of chronic respiratory diseases: a comprehensive approach," in *Global Alliance against Chronic Respiratory Diseases*, eds J. Bousquet, and N. Khaltaev (Geneva: World Health Organization), 14–90.

Buyens, K., Meyer, M., Wagner, E., Demeester, J., De Smedt, S. C., and Sanders, N. N. (2010). Monitoring the disassembly of siRNA polyplexes in serum is crucial for predicting their biological efficacy. *J. Control. Release* 141, 40–41. doi: 10.1016/j.jconrel.2009.08.026

Byrne, A. J., Mathie, S. A., Gregory, L. G., and Lloyd, C. M. (2015). Pulmonary macrophages: key players in the innate defence of the airways. *Thorax* 70, 1189–1196. doi: 10.1136/thoraxjnl-2015-207020

Cazzola, M., Page, C. P., Calzetta, L., and Matera, M. G. (2012). Emerging anti-inflammatory strategies for COPD. *Eur. Resp. J.* 40:727. doi: 10.1183/09031936.00213711

Chung, K. F., and Adcock, I. M. (2008). Multifaceted mechanisms in COPD: inflammation, immunity, and tissue repair and destruction. *Eur. Resp. J.* 31:1337. doi: 10.1183/09031936.00018908

Colombo, S., Beck-Broichsitter, M., Botker, J. P., Malmsten, M., Rantanen, J., and Bohr, A. (2018). Transforming nanomedicine manufacturing toward Quality by Design and microfluidics. *Adv. Drug Deliv. Rev.* 128, 115–131. doi: 10.1016/j.addr.2018.04.004

Colombo, S., Cun, D., Remaut, K., Bunker, M., Zhang, J., Martin-Bertelsen, B., et al. (2015). Mechanistic profiling of the siRNA delivery dynamics of lipid–polymer hybrid nanoparticles. *J. Control. Release* 201:28. doi: 10.1016/j.jconrel.2014.12.026

Cullis, P. R., and Hope, M. J. (2017). Lipid nanoparticle systems for enabling gene therapies. *Mol. Ther.* 25, 1467–1475. doi: 10.1016/j.ymthe.2017.03.013

Cun, D., Foged, C., Yang, M., Frokjaer, S., and Nielsen, H. M. (2010). Preparation and characterization of poly(DL-lactide-co-glycolide) nanoparticles for siRNA delivery. *Int. J. Pharm.* 390, 70–75. doi: 10.1016/j.ijpharm.2009.10.023

Cun, D., Jensen, D. K., Maltesen, M. J., Bunker, M., Whiteside, P., Scurr, D., et al. (2011). High loading efficiency and sustained release of siRNA encapsulated in PLGA nanoparticles: quality by design optimization and characterization. *Eur. J. Pharm. Biopharm.* 77, 26–35. doi: 10.1016/j.ejpb.2010.11.008

Dammes, N., and Peer, D. (2020). Paving the road for RNA therapeutics. *Trends Pharmacol. Sci.* 41, 755–775. doi: 10.1016/j.tips.2020.08.004

de Groot, A. M., Thanki, K., Gangloff, M., Falkenberg, E., Zeng, X., van Bijnen, D. C. J., et al. (2018). Immunogenicity testing of lipidoids *in vitro* and *in silico*: modulating lipidoid-mediated TLR4 activation by nanoparticle design. *Mol. Therapy Nucleic Acids* 11:165. doi: 10.1016/j.omtn.2018.02.003

De Paula, D., Bentley, M. V. L. B., and Mahato, R. I. (2007). Hydrophobization and bioconjugation for enhanced siRNA delivery and targeting. *RNA* 13, 438–439. doi: 10.1261/rna.459807

Desirability Function (2018). Available online at: https://www.statease.com/docs/v11/contents/optimization/desirability-function/#:$\sim$\$:text=Desirability%20is%20an%20objective%20function,adjusting%20the%20weight%20or%20importance (accessed August 2, 2020).

Dominique, D., Roberta, C., and Ruxandra, G. (2016). Cyclodextrin-based Polymeric nanoparticles as efficient carriers for anticancer drugs. *Curr. Pharm. Biotechnol.* 17, 248–255. doi: 10.2174/1389201017666151030104944

Dormenval, C., Lokras, A., Cano-Garcia, G., Wadhwa, A., Thanki, K., Rose, F., et al. (2019). Identification of factors of importance for spray drying of small interfering rna-loaded lipidoid-polymer hybrid nanoparticles for inhalation. *Pharm. Res.* 36:3. doi: 10.1007/s11095-019-2663-y

Elbashir, S. M., Harborth, J., Lendeckel, W., Yalcin, A., Weber, K., and Tuschl, T. (2001). Duplexes of 21-nucleotide RNAs mediate RNA interference in cultured mammalian cells. *Nature* 411:497. doi: 10.1038/35078107

Feczkó T., Tóth, J., Dósa, G., and Gyenis, J. (2011). Influence of process conditions on the mean size of PLGA nanoparticles. *Chem. Eng. Process. Process Intensifcat.* 50:849. doi: 10.1016/j.cep.2011.05.006

Fröhlich, E. (2012). The role of surface charge in cellular uptake and cytotoxicity of medical nanoparticles. *Int. J. Nanomedicine* 7, 5584–5585. doi: 10.2147/IJN.S36111

Hadinoto, K., Sundaresan, A., and Cheow, W. S. (2013). Lipid–polymer hybrid nanoparticles as a new generation therapeutic delivery platform: a review. *Eur. J. Pharm. Biopharm.* 85:440. doi: 10.1016/j.ejpb.2013.07.002

Haussecker, D. (2014). Current issues of RNAi therapeutics delivery and development. *J. Control. Release* 195, 52–53. doi: 10.1016/j.jconrel.2014.07.056

He, C., Hu, Y., Yin, L., Tang, C., and Yin, C. (2010). Effects of particle size and surface charge on cellular uptake and biodistribution of polymeric nanoparticles. *Biomaterials* 31, 3661–3664. doi: 10.1016/j.biomaterials.2010.01.065

Heyes, J., Palmer, L., Bremner, K., and MacLachlan, I. (2005). Cationic lipid saturation influences intracellular delivery of encapsulated nucleic acids. *J. Control. Release* 107, 276–287. doi: 10.1016/j.jconrel.2005.06.014

Ingvarsson, P. T., Yang, M., Mulvad, H., Nielsen, H. M., Rantanen, J., and Foged, C. (2013). Engineering of an inhalable DDA/TDB liposomal adjuvant: a quality-by-design approach towards optimization of the spray drying process. *Pharm. Res.* 30, 2772–2784. doi: 10.1007/s11095-013-1096-2

Jansen, M. A. A., Klausen, L. H., Thanki, K., Lyngsø J., Skov Pedersen, J., Franzyk, H., et al. (2019). Lipidoid-polymer hybrid nanoparticles loaded with TNF siRNA suppress inflammation after intra-articular administration in a murine experimental arthritis model. *Eur. J. Pharm. Biopharm.* 142:43. doi: 10.1016/j.ejpb.2019.06.009

Jensen, L. B., Griger, J., Naeye, B., Varkouhi, A. K., Raemdonck, K., Schiffelers, R., et al. (2012). Comparison of polymeric siRNA nanocarriers in a murine LPS-activated macrophage cell line: gene silencing, toxicity and off-target gene expression. *Pharm. Res.* 29:674. doi: 10.1007/s11095-011-0589-0

Kanasty, R., Dorkin, J. R., Vegas, A., and Anderson, D. (2013). Delivery materials for siRNA therapeutics. *Nat. Mater.* 12, 972–974. doi: 10.1038/nmat3765

Kim, S.-S., Ye, C., Kumar, P., Chiu, I., Subramanya, S., Wu, H., et al. (2010). Targeted delivery of siRNA to macrophages for anti-inflammatory treatment. *Mol. Ther.* 18:994. doi: 10.1038/mt.2010.27

Lawrence, X. Y., Gregory, A., Mansoor, A. K., Stephen, W. H., James, P., Raju, G. K., et al. (2014). Understanding pharmaceutical quality by design. *AAPS J.* 16, 771–783. doi: 10.1208/s12248-014-9598-3

Love, K. T., Mahon, K. P., Levins, C. G., Whitehead, K. A., Querbes, W., Dorkin, J. R., et al. (2010). Lipid-like materials for low-dose, *in vivo* gene silencing. *Proc. Nat. Acad. Sci. U. S. A.* 107:1867. doi: 10.1073/pnas.0910603106

Mannino, D. M., Thorn, D., Swensen, A., and Holguin, F. (2008). Prevalence and outcomes of diabetes, hypertension and cardiovascular disease in COPD. *Eur. Resp. J.* 32:968. doi: 10.1183/09031936.00012408

Matera, M. G., Calzetta, L., and Cazzola, M. (2010). TNF-α inhibitors in asthma and COPD: we must not throw the baby out with the bath water. *Pulm. Pharmacol. Therap.* 23, 122–123. doi: 10.1016/j.pupt.2009.10.007

McGregor, T. L., Hunt, K. A., Yee, E., Mason, D., Nioi, P., Ticau, S., et al. (2020). Characterising a healthy adult with a rare HAO1 knockout to

support a therapeutic strategy for primary hyperoxaluria. *Elife* 9:e54363. doi: 10.7554/eLife.54363

Meier, O., Boucke, K., Hammer, S. V., Keller, S., Stidwill, R. P., Hemmi, S., et al. (2002). Adenovirus triggers macropinocytosis and endosomal leakage together with its clathrin-mediated uptake. *J. Cell Biol.* 158:1122. doi: 10.1083/jcb.200112067

Nakamura, T., Kuroi, M., Fujiwara, Y., Warashina, S., Sato, Y., and Harashima, H. (2016). Small-sized, stable lipid nanoparticle for the efficient delivery of siRNA to human immune cell lines. *Sci. Rep.* 6, 2–3. doi: 10.1038/srep37849

Peer, D., and Lieberman, J. (2011). Special delivery: targeted therapy with small RNAs. *Gene Ther.* 18:1128. doi: 10.1038/gt.2011.56

Pfaffl, M. W. (2001). A new mathematical model for relative quantification in real-time RT–PCR. *Nucleic Acids Res.* 29:e45. doi: 10.1093/nar/29.9.e45

Place, R. F., Wang, J., Noonan, E. J., Meyers, R., Manoharan, M., Charisse, K., et al. (2012). Formulation of small activating RNA into lipidoid nanoparticles inhibits xenograft prostate tumor growth by inducing p21 expression. *Mol. Therapy Nucleic Acids* 1:3. doi: 10.1038/mtna.2012.5

Raal, F. J., Kallend D., Ray, K. K., Turner, T., Koenig, W., Wright, R. S., et al. (2020). Inclisiran for the treatment of heterozygous familial hypercholesterolemia. *N. Engl. J. Med.* 382, 1520–1530. doi: 10.1056/NEJMoa1913805

Raemdonck, K., Vandenbroucke, R. E., Demeester, J., Sanders, N. N., and De Smedt, S. C. (2008). Maintaining the silence: reflections on long-term RNAi. *Drug Discov. Today* 13:928. doi: 10.1016/j.drudis.2008.06.008

Ray, K. K., Wright, R. S., Kallend, D., Koenig, W., Leiter, L. A., Raal, F. J., et al. (2020). Two phase 3 trials of inclisiran in patients with elevated LDL cholesterol. *N. Engl. J. Med.* 382, 1507–1519. doi: 10.1056/NEJMoa1912387

Rennard, S. I., Flavin, S. K., Agarwal, P. K., Lo, K. H., and Barnathan, E. S. (2013). Long-term safety study of infliximab in moderate-to-severe chronic obstructive pulmonary disease. *Respir. Med.* 107, 424–432. doi: 10.1016/j.rmed.2012.11.008

Rennard, S. I., Fogarty, C., Kelsen, S., Long, W., Ramsdell, J., Allison, J., et al. (2007). The safety and efficacy of infliximab in moderate to severe chronic obstructive pulmonary disease. *Am. J. Respir. Crit. Care Med.* 175:926. doi: 10.1164/rccm.200607-995OC

Roberts, T. C., Langer, R., and Wood, M. J. A. (2020). Advances in oligonucleotide drug delivery. *Nat. Rev. Drug Discov.* 19, 673–694. doi: 10.1038/s41573-020-0075-7

Ryther, R. C. C., Flynt, A. S., Phillips, J. A., and Patton, J. G. (2005). siRNA therapeutics: big potential from small RNAs. *Gene Ther.* 12, 5–11. doi: 10.1038/sj.gt.3302356

Schroeder, A., Levins, C. G., Cortez, C., Langer, R., and Anderson, D. G. (2010). Lipid-based nanotherapeutics for siRNA delivery. *J. Intern. Med.* 267:13. doi: 10.1111/j.1365-2796.2009.02189.x

Shah, R., Eldridge, D., Palombo, E., and Harding, I. (2015). *Physicochemical Stability. Lipid Nanoparticles: Production, Characterization and Stability.* Cham: Springer International Publishing, 79. doi: 10.1007/978-3-319-10711-0

Smith, M. C., Crist, R. M., Clogston, J. D., and McNeil, S. E. (2017). Zeta potential: a case study of cationic, anionic, and neutral liposomes. *Anal. Bioanal. Chem.* 409:5783. doi: 10.1007/s00216-017-0527-z

Srivastava, G. K., Alonso-Alonso, M. L., Fernandez-Bueno, I., Garcia-Gutierrez, M. T., Rull, F., Medina, J., et al. (2018). Comparison between direct contact and extract exposure methods for PFO cytotoxicity evaluation. *Sci. Rep.* 8:1425. doi: 10.1038/s41598-018-19428-5

Thanki, K., Papai, S., Lokras, A., Rose, F., Falkenberg, E., Franzyk, H., et al. (2019c). Application of a quality-by-design approach to optimise lipid-polymer hybrid nanoparticles loaded with a splice-correction antisense oligonucleotide: maximising loading and intracellular delivery. *Pharm. Res.* 36:12. doi: 10.1007/s11095-018-2566-3

Thanki, K., van Eetvelde, D., Geyer, A., Fraire, J., Hendrix, R., Van Eygen, H., et al. (2019a). Mechanistic profiling of the release kinetics of siRNA from lipidoid-polymer hybrid nanoparticles *in vitro* and *in vivo* after pulmonary administration. *J. Control. Release* 310, 82–93. doi: 10.1016/j.jconrel.2019.08.004

Thanki, K., Zeng, X., and Foged, C. (2019b). Preparation, characterization, and *in vitro* evaluation of lipidoid-polymer hybrid nanoparticles for siRNA delivery to the cytosol. *Methods Mol. Biol.* 1943, 141–152. doi: 10.1007/978-1-4939-9092-4_9

Thanki, K., Zeng, X., Justesen, S., Tejlmann, S., Falkenberg, E., Van Driessche, E., et al. (2017). Engineering of small interfering RNA-loaded lipidoid-poly(DL-lactic-co-glycolic acid) hybrid nanoparticles for highly efficient and safe gene silencing: a quality by design-based approach. *Eur. J. Pharm. Biopharm.* 120:25. doi: 10.1016/j.ejpb.2017.07.014

Whitehead, K. A., Langer, R., and Anderson, D. G. (2009). Knocking down barriers: advances in siRNA delivery. *Nat. Rev. Drug Discov.* 8:134. doi: 10.1038/nrd2919-c1

Xu, C.-f., and Wang, J. (2015). Delivery systems for siRNA drug development in cancer therapy. *Asian J. Pharm. Sci.* 10:7. doi: 10.1016/j.ajps.2014.08.011

Yoo, J. W., and Mitragotri, S. (2010). Polymer particles that switch shape in response to a stimulus. *PNAS* 107, 11205–11210. doi: 10.1073/pnas.1000346107

Zhang, L., Chan, J. M., Gu, F. X., Rhee, J.-W., Wang, A. Z., Radovic-Moreno, A. F., et al. (2008). Self-assembled lipid–polymer hybrid nanoparticles: a robust drug delivery platform. *ACS Nano* 2:1698. doi: 10.1021/nn800275r

Zhi, D., Zhang, S., Cui, S., Zhao, Y., Wang, Y., and Zhao, D. (2013). The headgroup evolution of cationic lipids for gene delivery. *Bioconjug. Chem.* 24, 487–519. doi: 10.1021/bc300381s

In silico and *in vitro* Evaluation of Mimetic Peptides as Potential Antigen Candidates for Prophylaxis of Leishmaniosis

Deborah Carbonera Guedes [1†], Manuel Hospinal Santiani [1†], Joyce Carvalho [1], Carlos Ricardo Soccol [1], João Carlos Minozzo [1,2], Ricardo Andrez Machado de Ávila [3], Juliana Ferreira de Moura [1], Eliezer Lucas Pires Ramos [1], Guillermo Raul Castro [4,5], Carlos Chávez-Olórtegi [6] and Vanete Thomaz-Soccol [1*]

[1] Programa de Pós-Graduação Strictu Sensu em Engenharia de Bioprocessos e Biotecnologia, Universidade Federal do Paraná, Curitiba, Brazil, [2] Centro de Produção e Pesquisa de Imunobilógicos, Secretaria De Saúde do Estado do Paraná, Piraquara, Brazil, [3] Programa de Pós Graduação em Ciência da Saúde, Universidade do Extremo Sul Catarinense, Criciúma, Brazil, [4] Laboratorio de Nanobiomateriales, CINDEFI, Departamento de Química, Facultad de Ciencias Exactas, Universidad Nacional de La Plata (UNLP)-CONICET (CCT La Plata), La Plata, Argentina, [5] Max Planck Laboratory for Structural Biology, Chemistry and Molecular Biophysics of Rosario (MPLbioR, UNR-MPIbpC), Partner Laboratory of the Max Planck Institute for Biophysical Chemistry (MPIbpC, MPG), Centro de Estudios Interdisciplinarios (CEI), Universidad Nacional de Rosario, Rosario, Argentina, [6] Departamento de Bioquímica e Imunologia, Instituto de Ciência Biológicas, Universidade Federal de Minas Gerais, Belo Horizonte, Brazil

Antigen formulation is the main feature for the success of leishmaniosis diagnosis and vaccination, since the disease is caused by different parasite species that display particularities which determine their pathogenicity and virulence. It is desirable that the antigens are recognized by different antibodies and are immunogenic for almost all *Leishmania* species. To overcome this problem, we selected six potentially immunogenic peptides derived from *Leishmania* histones and parasite membrane molecules obtained by phage display or spot synthesis and entrapped in liposome structures. We used these peptides to immunize New Zealand rabbits and determine the immunogenic capacity of the chimeric antigen. The peptides induced the production of antibodies as a humoral immune response against *L. braziliensis* or *L. infantum*. Next, to evaluate the innate response to induce cellular activation, macrophages from the peptide mix-immunized rabbits were infected *in vitro* with *L. braziliensis* or *L. infantum*. The peptide mix generated the IFN-γ, IL-12, IL-4 and TGF-β that led to Th1 and Th2 cellular immune responses. Interestingly, this mix of peptides also induced high expression of iNOS. These results suggest that the mix of peptides derived from histone and parasites membrane molecules was able to mimic parasites proteins and induce cytokines important to CD4+ T cell Th1 and Th2 differentiation and effector molecule to control the parasite infection. Finally, this peptide induced an immune balance that is important to prevent immunopathological disorders, inflammatory reactions, and control the parasite infection.

Keywords: mimetic peptides, cytokines, *in vitro* infection, vaccines, leishmaniasis

INTRODUCTION

Despite all the advances in the field of immunization and different strategies to identify new antigenic molecules, there is still no antigen capable of inducing *Leishmania* spp. control and protecting individuals against leishmaniosis. Moreover, the large number of *Leishmania* species, responsible for cutaneous and visceral forms, and the differences among them make the diagnosis of these pathologies harder (Maroof et al., 2012). Thus, it is essential to search for new technologies to develop antigen candidates for diagnosis or a vaccine to induce the control of these diseases in individuals who reside in at risk regions (De Brito et al., 2018).

Given this scenario, an attractive alternative is peptide-based antigens that use epitopes of immunogenic proteins, which can stimulate a long-lasting immune response against the pathogen. This approach is a promising strategy, since it could even promote protection against *Leishmania*, it is a potent therapeutic tool to treat the disease (Skwarczynski and Toth, 2016; De Brito et al., 2018), could be applied in diagnosis (Link et al., 2017), and used to develop antigens to stimulate cellular immunity for potential use in vaccine protocols (Hamrouni et al., 2020). Furthermore, peptides are easier to produce and show greater stability. These antigens are produced by chemical synthesis, reducing problems with biological contamination. Antigens can be characterized as chemical molecules, similar to classical drugs, their production is reproducible, simple, cost-effective and fast, and low cost to scale-up (Joshi et al., 2014). Concerning immunity, these antigens can be customizing to generate specific responses and can be combined to design multi-epitopes or multi-specific antigens to target different *Leishmania* species or immunogenic molecules from different stages of the parasite life cycle. Despite all the advantages, this approach has some challenges, such as enhancing the immunogenicity of the peptides. One of the strategies to overcome this challenge is to design a multi-epitope-based antigen, which consists of incorporating multiple epitopes that allows for better coverage of natural pathogen antigen diversity (Moyle and Toth, 2013; De Brito et al., 2018).

The effectivity of a vaccine to promote a long-lasting cell mediated immune response also depends on the molecules used as antigens in the different production approaches. A high diversity of virulent *Leishmania* molecules have been tested as antigens, including gp63 (glycoprotein leishmaniolysin), SLA (soluble *Leishmania* antigen), LPG (lipophosphoglycan), histones, and several other purified antigens (Khamesipour et al., 2006; Olivier et al., 2012; Chamakh-Ayari et al., 2014; Martínez Salazar et al., 2014; Link et al., 2017).

Among these molecules, histones are potential candidates against leishmaniosis, since they constitute structural proteins that are important in the organization and regulation of the parasite genes. There are four major *Leishmania* histone classes –H2A, H2B, H3, and H4– that are basic component units of chromatin, the nucleosome (Requena et al., 2000). These molecules are highly conserved antigens, produced by several *Leishmania* species, which are non-secreted, but are able to induce an intense immune response (Santarem et al., 2007).

These proteins are released during the infection process after the elimination of intracellular amastigotes by active macrophages. Moreover, they can modulate the host immune response, since they do not suffer selective pressure by the host immunity, unlike surface secreted proteins of *Leishmania* (Chang et al., 2003).

The identification and selection of an epitope are crucial stages to develop a peptide-based antigen. It is necessary to map the whole protein of interest to identify suitable sequences that can induce a strong and permanent cellular immunity response against *Leishmania* parasites. These epitopes can be identified *in silico* and analyzed by bioinformatics tools that focus on T and B cell epitopes prediction, identification of conserved *Leishmania* species sequences, and location of the sequence on the protein quaternary conformation (Herrera-Najera et al., 2009; Freitas et al., 2016). The second approach is *in vitro* analysis of the epitopes by biotechnological and biochemical tools, such as phage display and spot synthesis techniques (Pini et al., 2005; Rhaiem and Houimel, 2016).

Our research group has been working in these areas to improve and develop diagnosis and prophylaxis techniques for the different neglected tropical diseases (NTDs). Some of these previous works have shown great promise regarding the evaluation of mimetic peptides as antigens for leishmaniosis diagnosis and vaccines (Seger, 2014; Link et al., 2017; Guedes et al., 2019). Based on previously obtained results with three mimetic peptides selected by phage display and chemically synthesized as soluble molecules, their potential as antigens was evaluated in skin tests. The peptides, individually (PA1, PA2, and PA3) or in a mix (PA1,2,3-Mix), were tested on an animal model (*Cavia porcellus*) immunized with dead *L. amazonensis* or *L. braziliensis* and compared with the standard skin test antigen. The results showed that the peptides, individually or in a mix, promoted induration reactions 48 and 72 h after inoculation (Guedes et al., 2019). These results indicate that these peptides can recruit and maintain a desired immune response and that they can be applied as antigens for immune prophylaxis purposes. Based on these findings, this work proposed the investigation of new active peptides derived from histone proteins of *Leishmania* spp. though the production of a chimeric molecule with the three peptides previously selected by our group. The biological activity of this chimeric molecule was investigated to verify its potential to activate a satisfactory immune response for diagnosis or as a candidate vaccine.

MATERIALS AND METHODS

The method used in this work consists of two main steps illustrated in **Figures 1**, **2**. The first involved the selection, synthesis, and evaluation of peptides. The second included experimental procedures to evaluate the immunogenicity of these peptides by analyzing humoral and macrophages immune responses. Regarding the first step, seven intracellular immunogenic proteins from *Leishmania* spp. (histone classes H2A, H2B, H3 and H4, and HP1) were selected and spot synthesized, followed by the selection of reactive peptides by immunodetection assay (**Figure 1**, step 1). The reactive spots
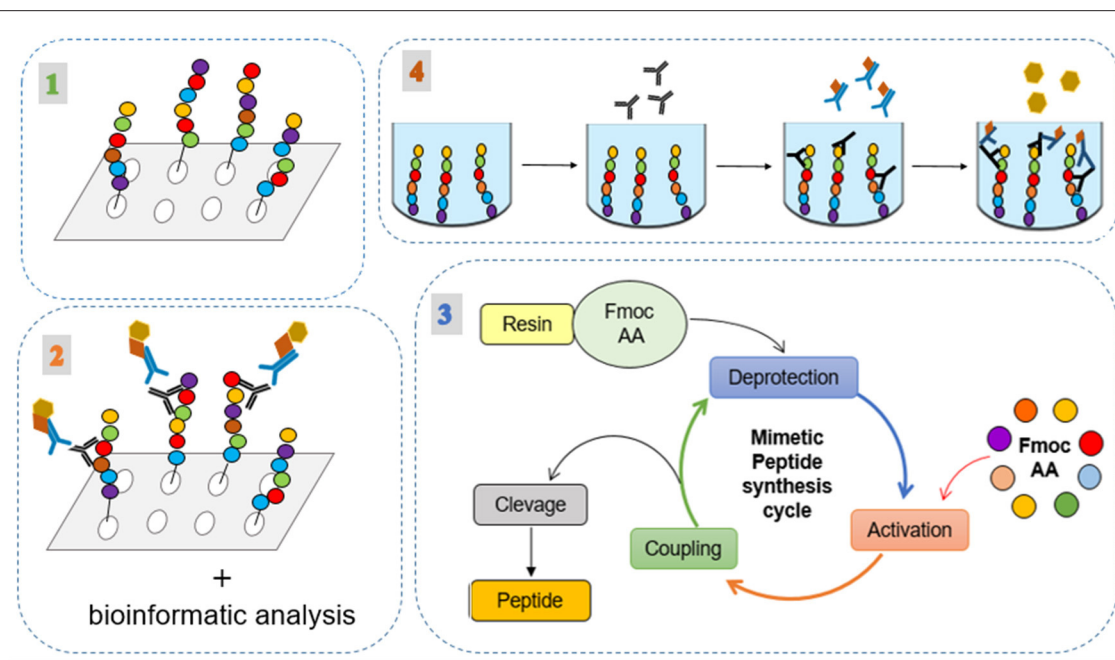
FIGURE 1 | Experimental processes for the selection, synthesis, and evaluation of the peptides. (1) Spot synthesis of the intracellular immunogenic proteins from Leishmania spp.; (2) Immunodetection assay of reactive spots; (3) their analysis by bioinformatic tools; and (4) application of the peptides in indirect ELISA method using human serum.
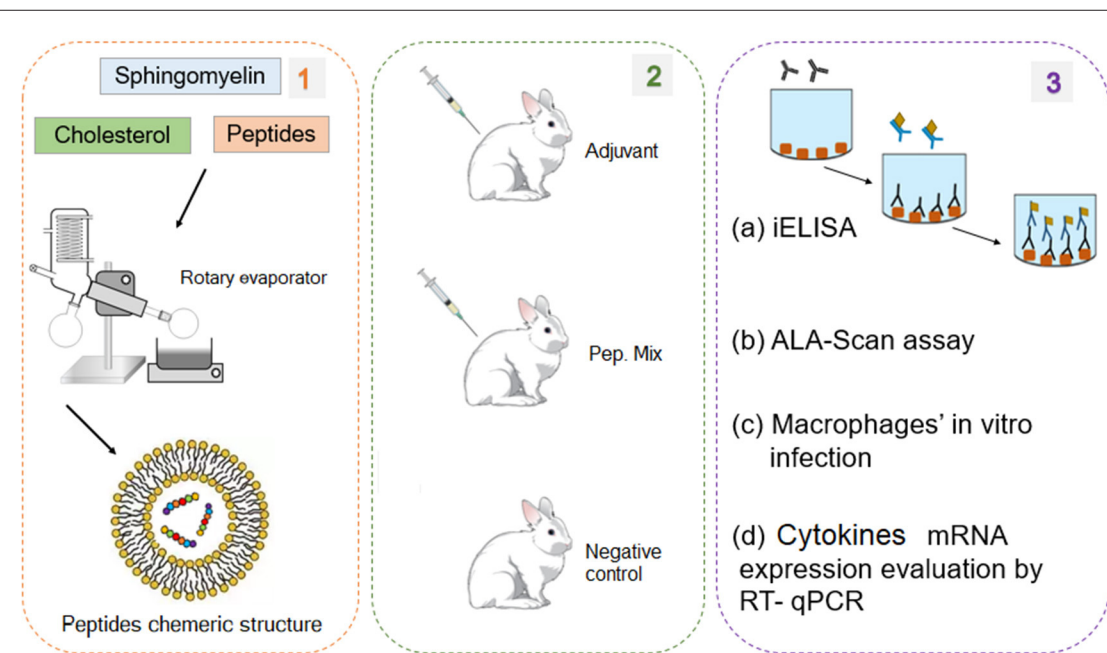
FIGURE 2 | Experimental processes for the production and evaluation of the peptide chimeric molecules. (1) Peptides encapsulation in liposomes. (2) Rabbits immunization with mix of six peptides (chimeric molecule) to produce anti-peptide polyclonal antibodies. (3) Evaluation of the peptides immunogenic capacity to induce immune response: (a) ELISA assay to evaluate IgG antibody production profile; (b) Evaluation of ALA scanning peptides with rabbit anti-peptide polyclonal antibodies; (c) in vitro experimental infection of macrophages from rabbits immunized with peptides; (d) Evaluation of cytokines mRNA expression profile by RT-qPCR.

were analyzed by bioinformatics tools to evaluate their chemical and structural characteristics to verify protein regions that manifest epitope-like features (**Figure 1**, step 2). The selected peptides were chemically synthesized (**Figure 1**, step 3) and encapsulated in liposome structures (**Figure 2**, step 1), with the other three previously selected peptides, to formulate

the peptide-based antigen (see section Results). In sequence, the peptide-based antigen was used to immunize a group of New Zealand rabbits (**Figure 2**, step 2) and *in vitro* analyses were performed to evaluate the capacity of the peptide-based antigen to stimulate humoral and macrophage responses against *L. braziliensis* or for *L. infantum* (**Figure 2**, step 3). Other analyses were performed to verify the peptide characteristics that contributed to their selection (**Figure 2**, step 3).

All applicable international, national, and institutional guidelines for the care and use of animals were followed. The study was approved by the Research Ethics Committee of the Federal University of Parana (process no. 23075.085350/2015-54 and 107/11).

Peptide Selection

The proteins selected for this study were immunogenic intracellular molecules derived from *L. amazonensis* and *L. braziliensis* histones. The sequences of histones were accessed on the UniProt database and identified as HP1 (UniProt accession number: Q9NL78), HP2 (Q9NL77), HP3 (Q9BMY8), HP4 (A4H9W0), HP5 (A4HBV1), HP6 (O44009), and HP7 (A4HNK4). The homology of the protein sequences among *Leishmania* sp. (*L. amazonensis*, *L braziliensis* and *L. infantum*) were verified by EMBOSS Needle pairwise sequence alignment (Rice et al., 2000).

The seven selected protein sequences were spot synthesized by overlapping pentadecapeptides, with an offset of three amino acids, scanning aimed at selecting and evaluating the reactivity of epitopes on these sequences. The spot synthesis was performed on a cellulose membrane with fluorenylmethyloxycarbonyl (Fmoc) protection using an automated spot peptide synthesizer (Intavis Bioanalytical Instruments, Nattermannallee, Germany) (Frank, 2002). For the immunodetection assay to select and evaluate the reactive spots, the cellulose membrane was firstly blocked, for non-specific binding, by overnight agitation with 3% (w/v) casein and 0.5% (w/v) sucrose dissolved in TBS-T (0.1% Tween 20 (v/v) in TBS) at 4°C. Afterwards, the membrane was washed with 0.1% TBS-T for 10 min under agitation, and probed, for 90 min at 37°C, with patients serum containing antibodies for *L. braziliensis* or *L. infantum*, or negative control diluted 1:100 in blocking buffer (3% (w/v) casein, 0.5% (w/v) sucrose, and 0.1% TBS-T). The membrane was washed again and incubated with biotin-labeled secondary antibody (1:30,000) diluted in blocking buffer for 60 min at 37°C, followed by an incubation step with streptavidin (1:10,000) diluted in blocking buffer for 60 min at 37°C. After two washes, positive spots were visualized by electrochemiluminescence (ECL^{TM} system).

To complement the selection of reactive peptides, the protein sequences were analyzed using bioinformatics tools such as Peptide 2.0 (https://www.peptide2.com/main_about.php), IPC (Kozlowski, 2016) and PepCalc (https://pepcalc.com/) to evaluate characteristics like molecular weight, isoelectric point, net charge, and hydrophobicity. Other tools, such as Epitopia server (Rubinstein et al., 2009), ABCpred (Saha and Raghava, 2006), and IEDB Analysis Resource (Vita et al., 2015), were used to verify protein regions that manifest epitope-like characteristics. Additionally, the 3D structure of proteins was obtained by

a homology-modeling server, SwissModel (Guex and Peitsch, 1997), using the histones X-ray diffraction structure as templates and the predicted epitopes were analyzed by Swiss-Pdb Viewer (Guex and Peitsch, 1997). Analyses of the 3D structures of the proteins were performed to evaluate where the reactive peptides (their sequences) were located on the protein structure, which contributed to verifying whether they are more exposed or internal. Finally, the peptide sequences were BLASTed against *Leishmania* spp. protein sequences, using TriTrypDB to analyze the similarities between them (Aslett et al., 2010).

Chemical Synthesis of Selected Peptides

The peptides selected by immunodetection assay and analyzed by bioinformatics tools were chemically synthesized according standard protocol by Fmoc strategy (9-fluorenylmethyloxycarbonyl) using a resin as insoluble solid support (Merrifield, 1969) with a MultiPep RS automated peptide synthesizer (Intavis Bioanalytical Instruments, Nattermannallee, Germany). After the final synthesis cycle, the peptides were released from the resin by trifluoracetic acid treatment, filtered and precipitated with cold ethyl ether, yielding the peptides. After centrifugation, the ether was discarded and peptides were lyophilized, weighed, dissolved in ultrapure water, and stored at −20°C until the next step.

To reduce the number of peptides selected by the bioinformatics tools after chemical synthesis, they were tested by indirect ELISA (iELISA) for humoral response using serum from human patients with anti-*L. braziliensis* or anti-*L. infantum* antibodies. The aim was to determine whether the peptides induce a mimicked response to the parasite.

Reactive Peptides Encapsulation in Liposome

The immunogenic peptides (selected in this work by spot synthesis) plus three peptides previously selected by our research group (selection determined by phage display and hypersensitivity reaction named P1, P2, and P3 for detail, see Link et al., 2017; Guedes et al., 2019), were encapsulated in liposome according to Toledo-Machado et al. (2015), producing the peptide-based antigen. Briefly, the encapsulated peptides were produced by dissolving sphingomyelin (25 mg) and cholesterol (6.5 mg) in 5 mL solution containing methanol and chloroform (1:2). The solvent was removed by flash evaporation on a rotatory evaporator at 37°C and dried for 80 min under reduced pressure. Next, an aqueous phase containing the six peptides (500 µg of each peptide) diluted in 3 mL of PBS pH 7.4 was added to lipid film composing the liposome structures with the six peptides encapsulated. To dislodge and retrieve the liposomes they were treated three times with ultrasonic vibration for 20 s. To remove no encapsulated peptides, the liposome suspension was washed twice by centrifugation (10 min, 8,000 g at 4°C) and resuspended in PBS pH 7.4. After washing, the liposomes were lyophilized and stored at 4°C.

Polyclonal Antibody Production

To produce polyclonal antibodies, five adult female New Zealand White rabbits (NZW), weighing 2.1–2.6 kg were used. The rabbits

were housed in single cages in a standard animal room (20°C and 55% humidity) and fed a balanced diet and water ad libitum. The rabbits were divided in three groups: Group 1, immunized with the adjuvant (aluminum hydroxide); Group 2, immunized with the peptides mix entrapped in liposome; and Group 3, no immunization (uninfected group). For the first immunization (day 0), Group 1 was submitted to intramuscular injection with 1 mL of aluminum hydroxide; Group 2 was submitted to intramuscular injection with 500 μg/rabbit (Melo et al., 2020) of entrapped peptides mix dissolved in PBS buffer (pH 7.4) and 1 mL of aluminum hydroxide (adjuvant); and Group 3 (negative control) was not immunized. The other immunizations were performed under the same conditions on days 15, 30, 45, 60, and 90 after the first immunization (a.f.i.). On day 90, the rabbits were bled, euthanized and macrophages were collected for the *in vitro* assay.

Blood samples for polyclonal antibody reactivity evaluation were obtained before every immunization (days 0, 15, 30, 45, and 60), by vein puncture from the marginal ear vein of the rabbits and transferred to vacutainer blood collection tubes. For cytokines evaluation, blood samples were collected at 48 and 72 h a.f.i. (day 0) and transferred to vacutainer blood collection tubes containing 200 μL of TRIzol. After each sample collection, they were centrifuged at 448 x g, for 10 min, at room temperature, resuspended in red blood cell (RBC) lysis buffer pH 7.3 (89.9 g of NH_4Cl; 10 g of $KHCO_3$; 2 mL of EDTA 0.5M), incubated for 5 min and centrifuged for 2 min, 1,008 x g at room temperature. The supernatant was discarded, and the pellet was resuspended in PBS, centrifuged for 2 min, 1,008 x at room temperature and resuspended in 400 μL of TRIzol. The samples were stored at −80°C.

Anti-IgG Antibody Production Profile

An indirect ELISA assay was performed to evaluate the profile of the polyclonal antibody reactivity obtained during the rabbits' immunization period. The microtiter plates were coated with *L. braziliensis* or *L. infantum* protein extracts at a concentration of 1 μg/well prepared according to Link et al. (2017). Rabbit sera, with anti-peptide polyclonal antibodies, and the second antibody (anti-rabbit IgG (whole molecule) peroxidase–Sigma Aldrich) were respectively diluted 1:200 and 1:7,500 in plates coated with *L. braziliensis* protein extract, and 1:100 and 1:10,000 in plates coated with *L. infantum* protein extract.

In vitro Experimental Infection of Macrophages From Rabbits Immunized With the Peptides Chimeric

Macrophages *in vitro* Infection With *L. braziliensis* and *L. infantum* Promastigote Forms

After 90 days post immunization, the rabbits were euthanized, and the macrophages were obtained by inoculation of 120 mL cold PBS buffer 1x (pH 7.4) in the peritoneal cavity. The PBS was collected and transferred to a tube and maintained on ice. The material collected was centrifuged at 1,800 x g, for 10 min at 4°C. The pellet was washed with PBS buffer 1x (pH 7.4), and centrifuged (1,800 x g, for 10 min at 4°C). The pellet

was resuspended in RPMI 1640 + 20% FBS + 10% penicillin-streptomycin and counted in a Neubauer chamber. For *in vitro* infection, the parasites were obtained from cultures of *L. braziliensis* and *L. infantum* separately cultivated in biphasic brain heart infusion medium until stationary phage (5 days). The parasites were harvested from culture media, centrifuged twice with PBS for 15 min, 1,000 x g at 10°C, resuspended in RPMI 1640 + 20% FBS + 10% penicillin-streptomycin, and counted in a Neubauer chamber. For the *in vitro* infection, 500 μL of parasite suspension were added to each well containing the adhered macrophage cells (1×10^5 cells/well). The parasites were added in a proportion of 15:1 (parasites: cells) (1.5×10^6 parasites/well) and were incubated at 37°C and 5% CO_2. Next, the RNA was extracted 48 and 72 h post infection (p.i.) to analyze cytokines, inducible nitric oxide synthase (iNOS) expression, and the parasite load.

Evaluation of Cytokines and iNOS mRNA Expression by Real Time PCR (RT-qPCR)

A reverse transcriptase and quantitative real time PCR (RT-qPCR) was performed to assess the expression of mRNAs of cytokines and iNOS in blood samples, collected between 48 and 72 h a.f.i. in rabbits, and the peritoneal macrophages from immunized rabbits (90 days a.f.i.) after the *in vitro* infection.

Total RNA of the samples was extracted using RNeasy Mini Kit (QIAGEN®), according to the manufacturer's instructions. To remove contaminating genomic DNA from RNA samples, a TURBO DNase-free kit (Invitrogen®) was used. The samples were quantified by spectophometers, and 150 ng of isolated RNA was reverse transcribed to cDNA using a First Strand cDNA Synthesis kit (Thermo Scientific®) with oligos dT_{15}. Complementary DNA was mixed with 10 pmol of each gene-specific marker and 2.5 μL of SYBR Green PCR Master Mix (Applied Biosystem). The mRNA expression of cytokines and iNOS was assessed using StepOnePlus Real-Time PCR System (Thermo Scientific). Data analysis was performed by the Livak method ($2^{-\Delta\Delta Ct}$) (Livak and Schmittgen, 2001) using the housekeeping genes glyceraldehyde 3-phosphate dehydrogenase (GAPDH) and beta-actin (ACTB) to normalize mRNA expression.

DNA Extraction From *in vitro* Macrophage Infection

Total DNA of samples was extracted using the Dynabeads™ DNA DIRECT™ Universal kit (Invitrogen, Vilnius, Lituania), according to the manufacturer's instructions. The DNA eluate was stored at −20°C until its use in qPCR analysis.

Parasite Load by Quantitative Real-Time PCR (qPCR)

The qPCR reactions were performed with 5 μL DNA; 2X KAPA Probe Fast ABI Prism® from KapaBiosystem; 200 nM DpolyAF (5′ GACDGTGAATTACAGGHTGC 3′) and DpolyAR (5′ ATACTTGCAGCAGCACATCG 3′) primers and 100 nM DpolyAS probe (5′FAM- TCACTTGCACHCCAGATK -NFQ-MGB3′) specific for the DNA polymerase A of *Leishmania* sp. Cycling conditions were a first step at 95°C for 10 min, followed by 40 cycles at 94°C for 30 sec and 58°C for 30 min. The amplifications were performed in a QuantStudio™ 3 (Applied
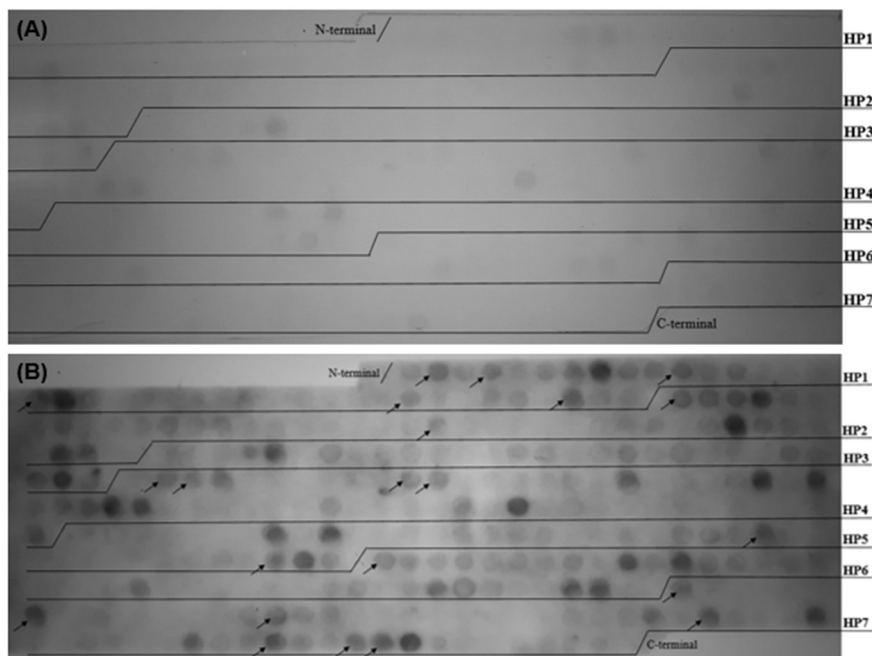
FIGURE 3 | Histone proteins sequences were spot synthesized by overlapping pentadecapeptides offset by three amino acids aimed at selecting and evaluating the reactivity of epitopes on these sequences. Reactivity of peptides originated from histone proteins of *Leishmania* spp. with anti-*L. braziliensis* immunoglobulins G. **(A)** Reactivity of peptides with healthy patient serum without anti-*Leishmania* spp. IgG. **(B)** Reactive spots immunodetected by patient serum with antibodies for *L. braziliensis* and not cross-reacted with healthy patient serum (without anti-*Leishmania* spp. IgG). The arrows indicate the 22 peptides selected by the immunoassay.

Biosystems, USA). Standard calibration curves were constructed by serial dilution of DNA extracted samples of *L. braziliensis* from 10 to 0.001 ng.

Statistics Analyses

The results were presented as means ± SD. Differences in antibody titers, parasite load and cytokine production were assessed by a two-way ANOVA followed by a Tukey HSD comparison test. All statistical analysis was performed using GraphPad Prism version 7.0 software. A *p*-value of <0.05 was considered statistically significant.

RESULTS

Peptide Selection: *In silico* and *in vitro* Analysis

First, the proteins HP1 and HP2 from *L. amazonensis* were compared with the protein HP6 from *L. braziliensis*; all three proteins correspond to the histone subunit H3. The analysis showed that between the proteins HP1 and HP6 similarity is 84.6% and identity is 94.6%. For proteins HP2 and HP6, similarity is 85.4% and identity is 95.4%. Consequently, the similarity and identity of the protein sequences were analyzed with *L. infantum* histone subunit fractions. The parameters of similarity and identity were not analyzed for HP3, because the protein sequence of histone subunit fraction H1 was not found for *L. braziliensis* and *L. infantum*.

Immunodetection

The spot synthesis of the seven histone sequences (HP1, HP2, HP3, HP4, HP5, HP6, and HP7) generated 302 spots, such that each spot was a different pentadecapeptide. The reactive epitopes were immunodetected by patient serum with anti-*L. braziliensis* antibodies. Twenty-two spots were selected, derived from almost all seven histone sequences analyzed. The 22 spots were named P_H2, P_H4, P_H11, P_H17, P_H31, P_H37, P_H40, P_H61, P_H109, P_H110, P_H118, P_H119, P_H190, P_H202, P_H205, P_H245, P_H251, P_H260, P_H276, P_H290, P_H293, and P_H294. The membrane was tested with serum from volunteer healthy patients, without antibodies for *Leishmania* spp., to verify that these reactions were specific (**Figure 3**).

In silico Analysis of Peptide Sequences

Bioinformatics tools (Peptide 2.0, IPC, PepCalc) enabled the analysis of peptide sequences and those with a hydrophobicity lower than 55% were selected for the next steps of the study (**Table 1**). In fact, hydrophobic peptides are insoluble hindering their use. The *Leishmania* spp. histone proteins sequences used in this study were 3D modeled using the X-ray diffraction structure of histones as templates. The structures of HP1, HP2 and HP6 were constructed by homology with histone H3. The tridimensional structure HP4 was constructed with histone H2B; histone H2A was used for HP5; and for HP7, the template was constructed by homology with histone H4.

TABLE 1 | *In silico* analysis of reactive peptides.

Peptides	Molecular weight (g/mol)	Iso-electric Point	Net charge	Hydrophobicity (%)	Peptide source	CD4 T cell immunogenicity prediction	T cell class I pMHC immunogenicity prediction
P_H2*	1649.89	9.66	4	20	H3.1	71.85	−0.27
P_H4*	1535.79	9.76	5	26.67	H3.1	51.16	−1.18
P_H11*	1864.19	11.37	3	40	H3.1	63.99	0.61
P_H17*	1747.03	9.1	1.9	40	H3.1	45.92	−0.02
P_H31*	1599.83	3.29	−2.1	53.33	H3.1	46.20	−0.16
P_H37*	1779.14	10.55	3	46.67	H3.1	59.58	−0.10
P_H40*	1750.04	11.55	4	26.67	H3.2	60.96	0.06
P_H61*	1727.96	10.36	2	33.33	H3.1	54.26	−0.29
P_H109*	1627.88	5.21	−0.1	53.33	H2B	55.89	−0.11
P_H110*	1659.97	5.21	−0.1	53.33	H2B	46.26	−0.47
P_H118	1825.12	9.95	1.2	60	H2B	47.46	0.15
P_H119	1865.16	6.59	0	60	H2B	55.34	0.32
P_H190*	1807.24	12.14	4.1	53.33	H2A	46.71	0.01
P_H202*	1610.94	9.84	6.1	20	H2A	60.08	−0.87
P_H205*	1766.04	11.55	4	20	H3	72.93	−0.12
P_H245	1605.95	5.83	−0.1	66.67	H4	72.28	0.34
P_H251*	1523.69	10.47	1.1	46.67	H4	56.31	−0.34
P_H260*	1827.16	11.15	2.2	40	H4	43.00	−0.24
P_H276*	1713	10.66	5	26.67	H4	84.88	−1.10
P_H290*	1882.12	4.79	−1	40	H4	42.78	0.17
P_H293*	1719.87	3.96	−2.1	33.33	H4	46.25	0.24
P_H294*	1776.92	4.57	−1.1	26.67	H4	53.46	0.15

The evaluated parameters are mass weight, iso-electric point, net charge, and hydrophobicity. The (*) indicates the peptides that present hydrophobicity lower than 55%.

According to these alignments, the tridimensional structures of the proteins HP1, HP2, HP5, and HP7 were constructed (**Figure 4**). The alignment of HP1 and HP2 sequences was made with the same template from histone H3, so these two proteins have the same 3D structure. After constructing the tridimensional structures by homology modeling, the peptides were located on the structures using the Swiss-PDB Viewer program. For HP1, the reactive peptides P_H11, P_H17, P_H31, P_H37, and P_H61 were highlighted on the histone protein structure. The same was performed for HP5 with peptides P_H190 and P_H202, and for HP7 with peptides P_H276, P_H290, P_H293, and P_H294. After these analyses, the reactive peptides were evaluated by Epitopia server (**Figure 5**) and IEDB Analysis Resource to verify their immunogenic characteristics (**Table 1**). After all these analyses, the amino acid sequences of the selected peptides were BLASTed against *Leismania* spp. histone proteins sequences to verify the identity between them.

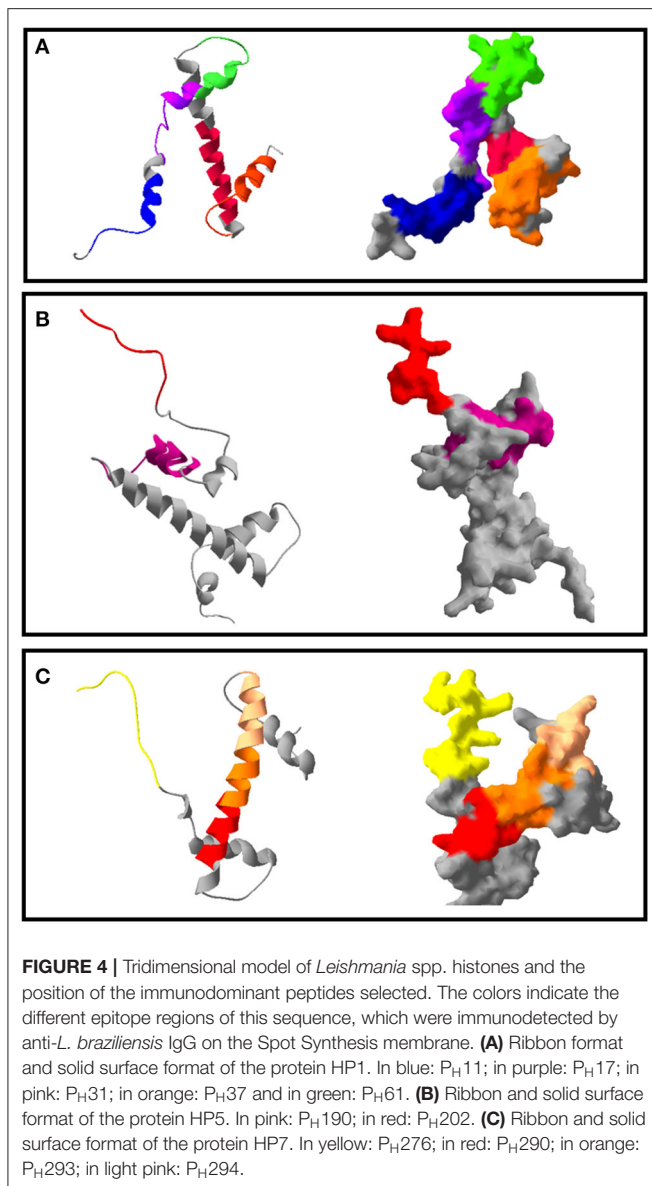## Chemical Synthesis of Selected Peptides and Their Evaluation by Indirect ELISA

The synthesis of peptides resulted in 2.5 mg of each soluble molecule, which were resuspended in 1 mL of ultrapure water. Each peptide was tested as an antigen in an iELISA assay at concentrations of 0.25, 0.5, and 1 μg/mL.

The results showed that all the peptides showed immunoreactivity in patient serum for anti-*L. braziliensis* ($n = 13$) and for anti- *L. infantum* ($n = 10$) antibodies. In the

iELISA test for patient serum with anti- *L. braziliensis* antibodies, the best results were observed for peptides P_H31, and P_H293, which reached an absorbance 2.5-fold higher than the positive and negative controls. These results were observed for the peptides tested under the conditions of 0.25 μg/mL of antigen, 1:100 of serum and 1:7,500 of conjugate in the case of P_H31; and of 0.5 μg/mL of antigen, 1:200 of serum and 1:10,000 of conjugate for P_H293 (**Table 2**). For anti- *L. infantum* antibodies, the best results were observed for P_H202 and P_H293 under the same conditions of 0.5 μg/mL of antigen, 1:200 of serum, 1:10,000 of conjugate, where the absorbance was 2.5 times higher from positive and negative controls (**Table 2**). According to these test results, the peptides P_H31, P_H202, and P_H293 were selected and analyzed in biological assays as antigen candidates.

Production and Evaluation of Peptides Chimeric Structure

The encapsulation of peptides resulted in five samples of chimeric molecules at a concentration of 500 μg/mL. To formulate the antigen for animal immunization, each sample was resuspended in 1 mL of adjuvant resulting in a final concentration of 500 μg/mL. The antibody response with the entrapped mix of peptides, evaluated by iELISA test showed that producing anti-peptides polyclonal antibodies 15 days a.f.i. was feasible. This production was detected by all the kinetics evaluated (until 90 days a.f.i.) for both *L. braziliensis* and *L. infantum* protein extracted antigen (**Figure 6**).

FIGURE 4 | Tridimensional model of *Leishmania* spp. histones and the position of the immunodominant peptides selected. The colors indicate the different epitope regions of this sequence, which were immunodetected by anti-*L. braziliensis* IgG on the Spot Synthesis membrane. **(A)** Ribbon format and solid surface format of the protein HP1. In blue: P_H11; in purple: P_H17; in pink: P_H31; in orange: P_H37 and in green: P_H61. **(B)** Ribbon and solid surface format of the protein HP5. In pink: P_H190; in red: P_H202. **(C)** Ribbon and solid surface format of the protein HP7. In yellow: P_H276; in red: P_H290; in orange: P_H293; in light pink: P_H294.

Cytokines and Effector Molecule Induction by the Chimeric Molecules

To understand how the immunization could activate the immune response in the different groups, the expression of inflammatory Th-1 inductor cytokines (IL-12, IFN-γ), Th2 inductor cytokine (IL-4), regulatory cytokine (IL-10) and effector molecule (nitric oxide) inductor (iNOS) was measured 48 and 72 h a.f.i. in the blood of the rabbits. The peptide mix (Group 2) induced high expression of all the molecules evaluated 72 h a.f.i., compared with the other groups; this was significant, with a P-value > 0.01. High expression of IL-12 and iNOS was observed in the control group 48 h a.f.i. Group 1 (adjuvant) only induced iNOS expression 48 h a.f.i. (**Figure 7A**).

After the collection of peritoneal macrophages, from rabbits previously immunized with the peptides mix, infection in culture

with *L. braziliensis* was performed and analyzed after 48 and 72 h. High expression was observed in the rabbits immunized with the peptide mix, showing a significant difference compared with the other groups (P-value > 0.01) at 48 h p.i., which decreased by 72 h p.i. In addition, the IFN-γ expression was increased in this group 72 h p.i. and showed a significant difference in relation to the negative control group, while iNOS expression was the same at both times evaluated. The peptide mix group (Group 2) also induced IL-4 and TGF-β 72 h p.i. and showed a significant difference in relation with the other groups (P-value > 0.1). The adjuvant group (Group 1) showed increased expression of all the cytokines evaluated and iNOS 72 h p.i., while the control group only induced the expression of iNOS 72 h p.i. (**Figure 7B**).

Peritoneal macrophages were also infected in culture with *L. infantum* and high expression of IL-12, TGF-β and iNOS was observed 48 h p.i., showing a significant difference compared with the other groups (P-value > 0.01), while IL-4 and IFN-γ also increased 72 h p.i. in the peptide mix group (Group 2). No significant expression was observed in the other groups after infection by this parasite (**Figure 7C**).

Regarding parasite load, a significant reduction in the load of *Leishmania* was observed in macrophages from rabbits immunized with the peptide mix in relation to the negative control and adjuvant group at 48 h (P-value > 0.0001) and 72 h (P-value > 0.1) (**Figure 8**). The parasitism in macrophages from the adjuvant group showed an increase compared with the negative control group, which is probably related to a non-specific cellular activation caused by this compound that favors *Leishmania* infection in these cells. Finally, these results indicate an activation of the macrophages by the peptide mix, facilitating the neutralization of *Leishmania* amastigotes.

DISCUSSION

Leishmania spp. are intracellular parasites that have complex mechanisms to survive and multiply inside the host system of phagocytic mononuclear cells. The production of antibodies and/or cellular immunity during host infection is induced because most *Leishmania* antigens are recognized by the host system. However, the immune response to some of these antigens does not protect the host. In other cases, it may contribute to intensifying the pathological response, due to cross-reaction with the host's biomolecules (Handman, 2001). In addition, some studies report that the capacity to respond to *Leishmania* antigens varies from individual to individual. Thus, the diagnosis of our vaccine against leishmaniosis requires different antigens (polyvalent) capable of inducing a protective immune response in most of the population and which can be produced in large scale (Mukherjee et al., 2013).

To achieve higher antigenicity, proteins were selected to target antigenic epitopes and then constructing a chimeric molecule that has greater antigenicity. Thus, seven protein sequences of *Leishmania* spp. histones were selected, which are one of the intracellular immunogenic molecules from this parasite. The core histone of eukaryotic species comprises two paired dimers H2A/H2B and H3/H4 and a linker histone H1, which constitute
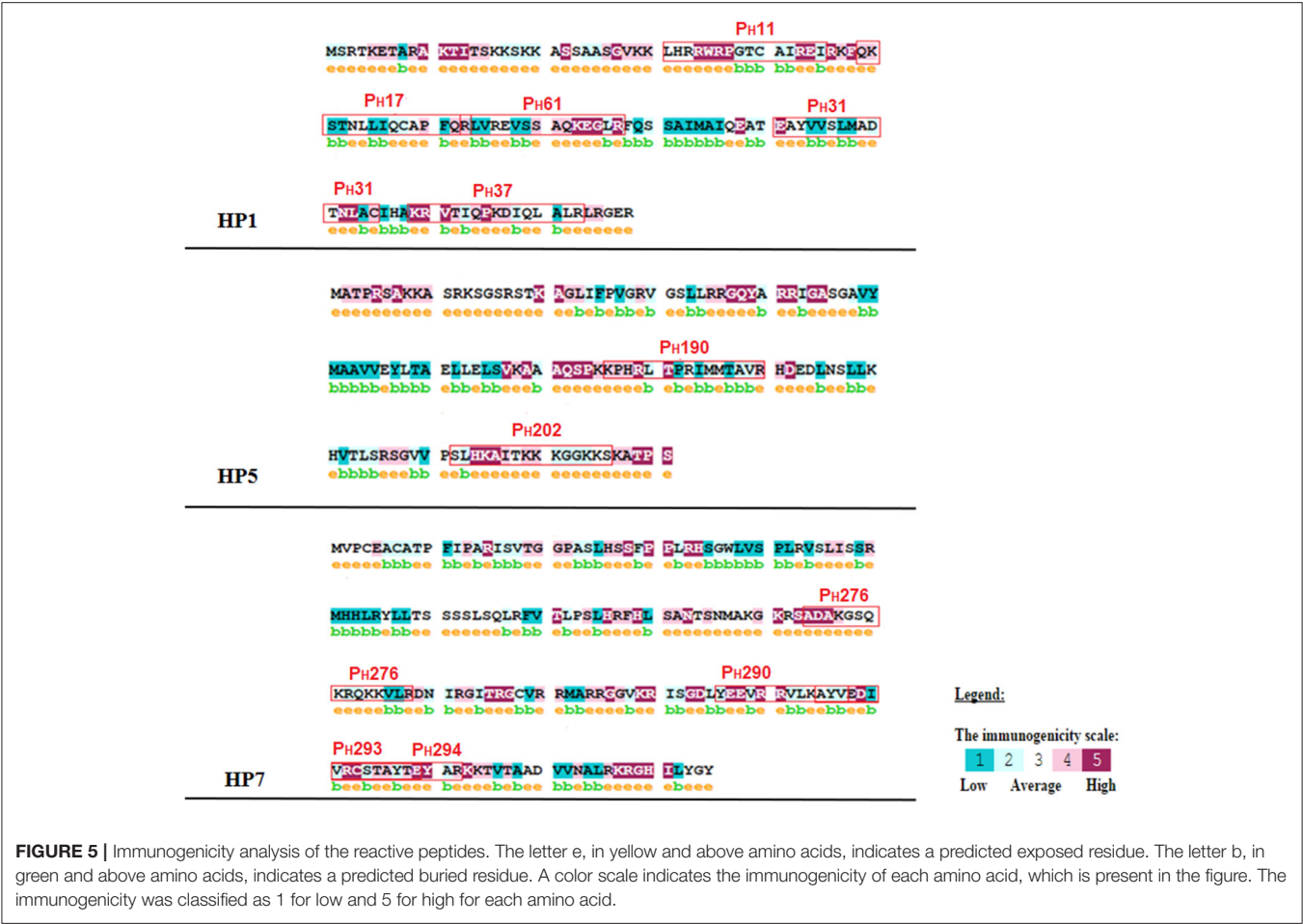
FIGURE 5 | Immunogenicity analysis of the reactive peptides. The letter e, in yellow and above amino acids, indicates a predicted exposed residue. The letter b, in green and above amino acids, indicates a predicted buried residue. A color scale indicates the immunogenicity of each amino acid, which is present in the figure. The immunogenicity was classified as 1 for low and 5 for high for each amino acid.
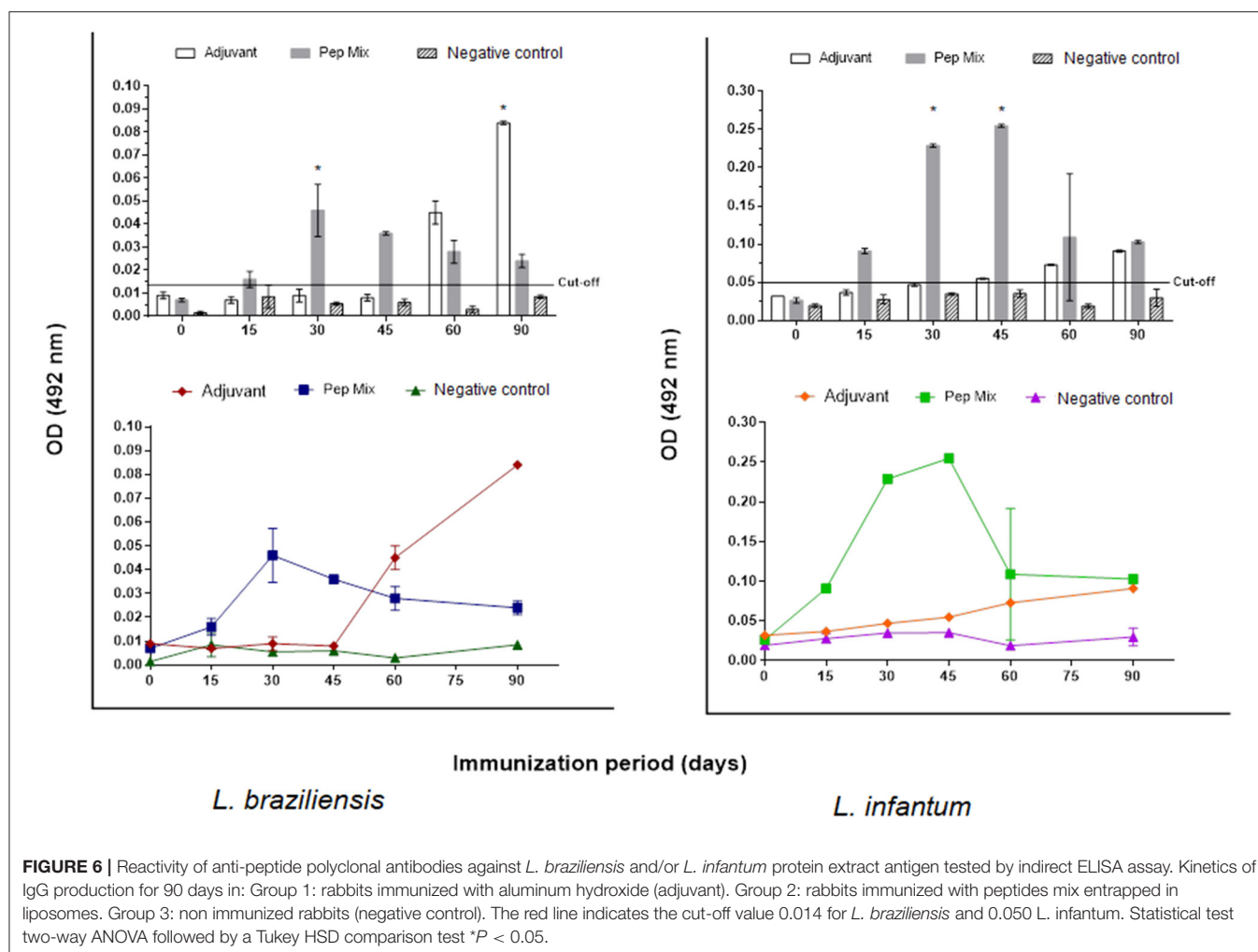
TABLE 2 | Indirect ELISA reaction parameters standardized for peptides PH31, PH202, and PH293.

	Peptide (μg/mL)[a]	Serum[b] (N = 23)	Second antibody[c]	Absorbance[d]
Anti–L. braziliensis IgG				
P_H31	0.25	1:100	1:7,500	0.132
P_H293	0.5	1:200	1:10,000	0.120
Anti–L. infantum IgG				
P_H202	0.5	1:200	1:10,000	0.123
P_H293	0.5	1:200	1:10,000	0.137

[a] Antigen (peptide) concentration on indirect ELISA assay; [b] Patients serum concentration; [c] Second antibody concentration; [d] The absorbance of negative serum samples was 0.05.

some of the most well-conserved molecules among these organisms. For these characteristics, these molecules are good protein candidates to screen conserved immunogenic epitopes among the different *Leishmania* spp. (Baharia et al., 2014). The histone protein sequences derived from *L. amazonensis* were named HP1, HP2, and HP3, while those derived from *L. braziliensis* were named HP4, HP5, HP6, and HP7. The proteins HP1, HP2, and HP6 correspond to histone fraction type H3, protein HP3 corresponds to H1, HP4 to H2B; HP5 to H2A, and protein HP7 corresponds to H4. These sequences were evaluated according to the similarity and identity among them. The results showed that the sequences have more than 84% similarity and 90% identity. When compared with *L. infantum* histones, the score varies from 52 to 92% similarity and 49 to 82% identity. The results indicate good similarity and identity between the *Leishmania* species, which is desirable to enable the selection of epitopes with amino acid sequences that can be recognized by different species from the parasite and formulate an antigen capable of inducing an immune response for different *Leishmania* species. In the last few years, several studies have described the isolation and application of different biomolecules that present protective activity and are potentially good antigen candidates for a leishmaniosis vaccine (Singh and Sundar, 2012; De Brito et al., 2018; Thomaz-Soccol et al., 2018). These antigens are originated from proteases and other molecules actively secreted by the parasites or from membrane and intracellular proteins. Among these molecules are histones, which are highly conserved antigens produced by *Leishmania* spp. and even though they are not secreted by the parasites they can induce a potent immune response. These antigens are released during infection after the elimination of intracellular

FIGURE 6 | Reactivity of anti-peptide polyclonal antibodies against *L. braziliensis* and/or *L. infantum* protein extract antigen tested by indirect ELISA assay. Kinetics of IgG production for 90 days in: Group 1: rabbits immunized with aluminum hydroxide (adjuvant). Group 2: rabbits immunized with peptides mix entrapped in liposomes. Group 3: non immunized rabbits (negative control). The red line indicates the cut-off value 0.014 for *L. braziliensis* and 0.050 L. infantum. Statistical test two-way ANOVA followed by a Tukey HSD comparison test *$P < 0.05$.

amastigotes by the active macrophage, or by the spontaneous cystolysis of amastigotes inside the infected cells (Carrión et al., 2009). Moreover, these antigens are capable of modulating the host immune response because they do not suffer from its immune selective pressure, unlike surface and secreted proteins (Chang et al., 2003).

The antigenicity of the core histones (H2B, H2A, H3, and H4) have been reported in studies as being recognized by sera from cutaneous (CL) and mucocutaneous leishmaniosis (MCL) human patients and by canine visceral leishmaniosis (CVL) (Soto et al., 1999; Meddeb-Garnaoui et al., 2010; Souza et al., 2013). The protein H2A has been described as the most antigenic core histone and one which can also be recognized by sera from VL human patients (Passos et al., 2005). Other studies report the analysis of histone H2A, H3, and H4 immunization against CL by applying the histones individually, in cocktails, or genetically fused to a plasmid. BALB/c mice genetically immunized with the individual histones showed a delay in the development of the lesion, and immunization with the plasmids encoding the histone and the cocktails provided protection against *L. major* (Carrion et al., 2008). A study by Iborra et al. (2004) evaluated the prophylactic activity of *L. infantum* histones in an animal

model for cutaneous leishmaniasis, and reported that the animals immunized with a mixture of the four plasmids encoding the histones H2A, H2B, H3, and H4 developed a specific Th1 response associated with histone-specific production of IFN-γ. Carneiro et al. (2012) also analyzed the immune protection conferred by nucleosomal histones of *L. infantum* in murine model infected with *L. braziliensis*, and concluded that histone are potential targets for vaccine formulation against *L. braziliensis* since they showed significant inhibition activity for the disease.

To select the most reactive and antigenic peptides from spot synthesized histones, this study evaluated whether the reactive peptides were located in immunogenic regions of the proteins and whether they were able to manifest epitope-like characteristics. The results showed that all the peptides were located in regions with an immunogenicity score higher than 70 % (**Table 1**) and the majority of the amino acids of the peptides were considered to be predicted exposed residues (**Figure 6**). In the last *in silico* analysis, the peptide sequences were BLASTed against *Leishmania* spp. protein to evaluate the identity rate between them and to analyze whether the peptide sequences were homologous to *Leishmania* histones. The results showed that all the peptides sequences analyzed presented more than
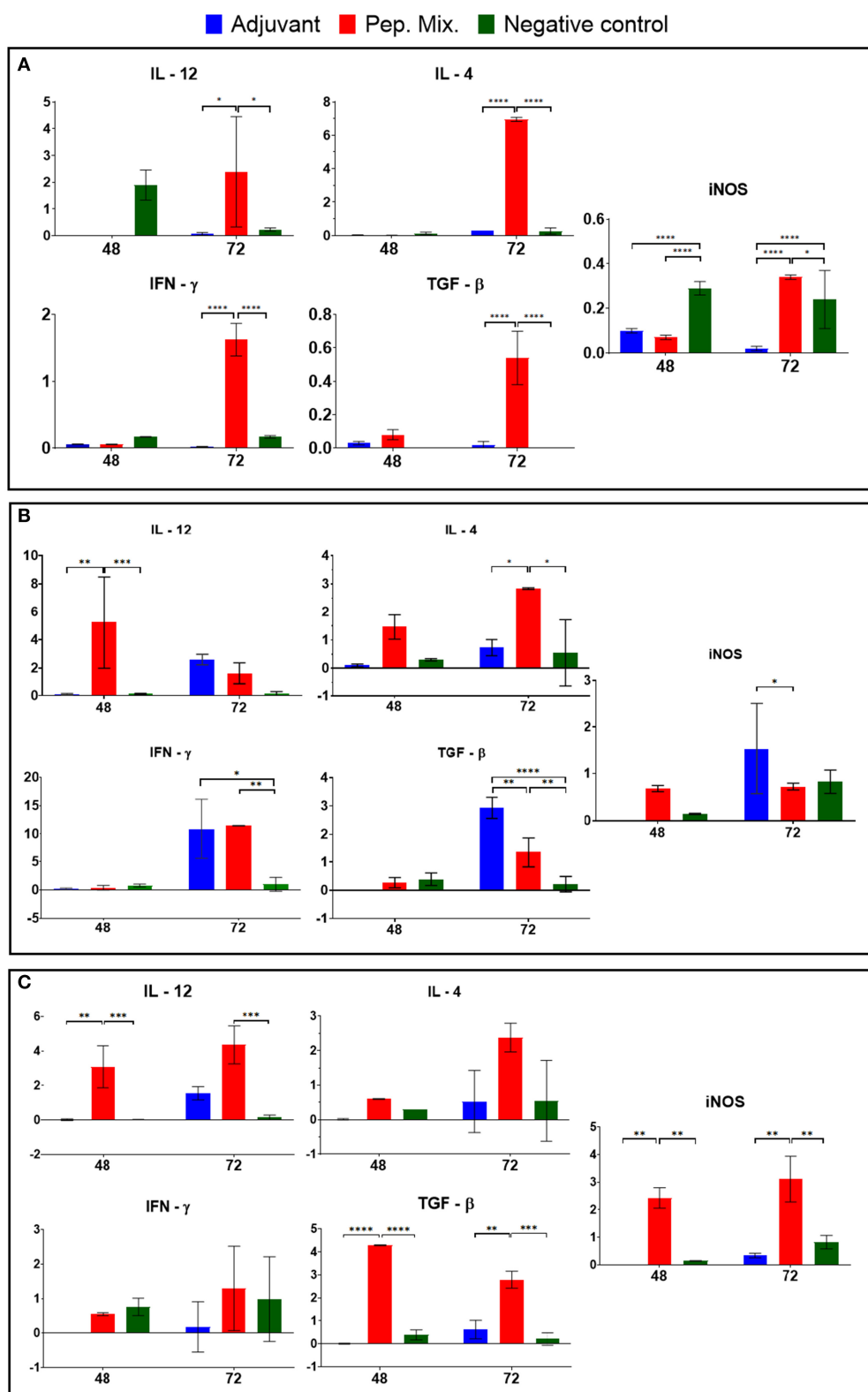
FIGURE 7 | Cytokine (IL-12, IFNγ, IL-4, and TGF-β) and iNOS mRNA expression were evaluated in blood samples **(A)** and macrophages from rabbits immunized with adjuvant, or peptides mix, and non-immunized (negative control) after infection by *L. braziliensis* **(B)** and *L. infantum* **(C)**. All the results are presented as the mean ± SD. Statistical test two-way ANOVA followed by a Tukey HSD comparison test *P < 0.05; **P < 0.01; ***P < 0.001; ****P < 0.0001, a comparison was with negative control.

90% identity with histone proteins from different *Leishmania* spp., mainly for *L. braziliensis* and *L. infantum*. The results also confirmed the identity of each peptide sequence with its own original histone sequence.

All these *in silico* analyses resulted in the selection of the peptides PH11, PH17, PH31, PH37, and PH61 (histone H3), PH190 and PH202 (histone H2A), and PH276, PH290, PH293, and PH294 (histone H4), which presented a response score for *in silico* CD4 analysis ranging from 42.78 to 84.9 (**Table 1**). The results of the iELISA study showed that some peptides did not show a satisfactory difference between serum positivity and negativity. It may not be able to induce a mimetic response like the parasite. Thus, the peptides selected according to these specifications were PH31, PH202, and PH293. Peptide PH31 showed good reactivity against anti-*L. braziliensis* antibodies, as did PH202 for anti-*L. infantum* antibodies. Peptide PH293 showed good reactivity against anti-*L. braziliensis* antibodies and for *L. infantum* IgG. We have shown here that the humoral response (optical density) was low compared with serological tests, where the differences between positive and negative are 8 to 10 times greater. However, the peptides were able to mimic the antigen. The milestone in *Leishmania* histone antigenicity studies was the screening of cDNA expression libraries using sera from infected dogs. The first report on a specific immune response against histones during infection was the identification of histone H2A from *L. infantum* by immunoscreening with CVL serum (Soto et al., 1992). Later, a study by Soto et al. (1994) reported the isolation of a cDNA clone coding *L. infantum* histone H3 by a strong immunoreaction with VL sera. In a subsequent study, the authors demonstrated that the histones H2B and H4 from *L. infantum* were also recognized by VL sera (Soto et al., 1999). Moreover, a study by Lakhal et al. (2012) reported the diagnostic performance of a crude *Leishmania* histone used as antigen in an ELISA assay in which the reactivity was accessed by sera from VL patients. The results showed the ability of this antigen to discriminate between VL cases and healthy controls. These studies report the ability and capability of histone proteins at being recognized by humoral immune molecules, which affirms their antigenicity potential for use as antigen molecules in diagnosis. This also corroborates our results for the anti-peptide histone humoral response tests, in which the reactivity of the peptides against human patient serum with anti- *L. braziliensis* or anti- *L. infantum* antibodies was verified. The peptides did not achieve the expected yield, as shown by *Leishmania* protein extract or recombinant proteins. This is because, in comparison to peptides, the protein extracts and recombinant proteins offer a greater variety of reactive epitopes, which consequently can recruit a greater immune response. This hypothesis reinforces the need for testing different combinations of molecules/peptides designed for anti-*Leishmania* vaccines to induce a strong immune response (Alonso and Soto, 2014).

After this step, we selected three reactive peptides (P_H31, P_H202, and P_H293) and added three more previously selected by our research group (Thomaz-Soccol et al., 2015; Link et al., 2017; Guedes et al., 2019), which were then encapsulated in liposome. This small vesicle structure was selected to encapsulate the peptides due to its properties of biocompatibility, low toxicity, size, and hydrophobic and hydrophilic character. Moreover,
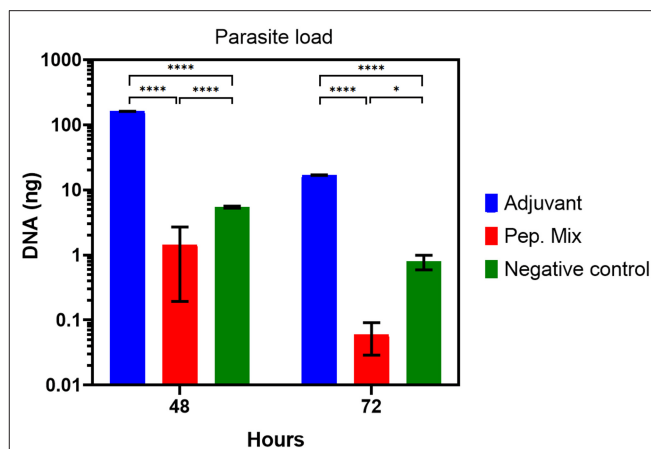

FIGURE 8 | Parasite load from *in vitro* infection with *Leishmania* of macrophages from rabbits immunized with adjuvant, or peptides mix, and non-immunized (negative control), 48 or 72 h post-infection. All the results are presented as the mean ± SD. Statistical test two-way ANOVA followed by a Tukey HSD comparison test *$P < 0.05$; **$P < 0.01$; ***$P < 0.001$, ****$P < 0.0001$.

liposome structures avoid decomposition of the entrapped molecules and release them at designed targets, which make them promising systems for drug delivery (Akbarzadeh et al., 2013; Alavi et al., 2017). The antibody response with the entrapped mix of peptides, evaluated by ELISA test, showed that producing anti-peptide polyclonal antibodies 15 days after the first immunization was feasible and this production was detected by all the kinetics evaluated for both *L. braziliensis* and *L. infantum* protein extract antigen (**Figure 6**). In both situations, a characteristic curve of antibody response kinetics with plateau phase between 30 and 45 days of immunization was observed. The first 30 days of immunization characterize the primary immune response, where immature B cells are stimulated by the antigen and become active, which induces a more specific antibody for the antigen. With repeated infection (45 days), the secondary immune response is induced when the same antigen stimulates the memory B cells leading to the production of greater quantities of specific antibodies than observed in the primary response (Abbas et al., 2015).

The group immunized only with adjuvant (aluminum hydroxide) presented anti-*Leishmania* immune response, which confirms its capacity for use as an antigen. Aluminum-based adjuvants are widely used throughout the world, and among the variants, aluminum hydroxide is the chemical most commonly used as an adjuvant. An important function of aluminum hydroxide is stimulating T cells activation and the expression of co-stimulators on antigen-presenting cells (APCs) (Abbas et al., 2015). Aluminum hydroxide mechanisms of action include depot formation, which facilitate the continued release of antigens, the formation of particulate structures promoting antigen phagocytes by macrophages and B cells, and inflammation induction that results in the activation and recruitment of macrophages (Mutiso et al., 2010; He et al., 2015). Thus, aluminum-based adjuvants can help boost the humoral immunity response by providing Th2 cells and the injection of

this adjuvant can result in the priming and persistence of Th2 cells producing IL-4, IL-5, and IL-10 (Awate et al., 2013; Beck et al., 2018).

Although the previous analyses were performed by selecting biomolecules that stimulate immune response type B, some tests were performed to evaluate the cytokine profile stimulated by these peptides. These evaluations of cellular immune response sought to verify whether the peptides were capable of inducing a profile of cytokines that can lead to their application as antigens for vaccines. A protocol of *in vitro* infection was developed to identify the pattern of cytokines expressed during the immunization period and to verify whether differentiated expression of these cytokines occurred to promote a cellular immune response generated by these peptides. The results showed that the peptides induced high expression of iNOS, IL-12, and IFN-γ, 72 h after first immunization, although there were also increases in the IL-4 and TGF-β expression. This means that the peptide mix was able to induce cellular immune response in rabbits with a cytokine profile that stimulated T helper 1 (Th1) and T helper 2 (Th2) responses, but the principal information is that this immunization induced the increase of iNOS, the main NO inductor. The expression of iNOS is induced by IFN-γ in macrophages and its activation contributes to controlling the death or replication of intracellular pathogens. High-levels of iNOS are associated with the adaptive phase of immune response and its function of co-factor can contribute to the activation of IL-12 and IFN-γ in natural killer (NK) cells (Bogdan, 2015). Although transforming growth factor–beta (TGF-β) is related to the regulatory functions of the immune system, it is known that multifunctional cytokines are implicated in a variety of biological processes by enhancing cellular proliferation, activation, and stimulating cytokines of effector Th17 cells. Th17 cells show an inflammatory profile with the recruitment of neutrophils. These cells are important at the onset of infection since they can recruit more cells to the infection site and favor control of the infection (Oh and Li, 2013; Okamura et al., 2015).

The differentiation of Th1 cells is promoted mainly by IL-12 and IFN-γ and occurs in response to pathogens that activate dendritic cells, macrophages and NK cells. This profile of cytokines stimulates phagocytosis, oxidative burst and intracellular pathogen killing, regulates the expression of major histocompatibility complex (MHC), classes I and II, and thus stimulates antigen presentation to T cells (Spelberg and Junior, 2001; Abbas et al., 2015; Cortés et al., 2017). Th2 differentiation is promoted by IL-4, which stimulates high titers of antibody production and activates B cell proliferation. Moreover, Th2 plays an important role in the inflammatory process by activating mast cells and eosinophils (Spelberg and Junior, 2001; Cortés et al., 2017). Both subclasses of CD4^{+} cells are important and desired for host defense against different infectious pathogens.

The quantification of interleukins expressed by macrophages *in vitro* infected with *L. braziliensis* or *L. infantum*, showed that the peptide mix was capable of inducing a cytokine profile, which presented an increase in all the cytokines tested compared with the control group. Our data also revealed that the levels of IL-12, IFN-γ and IL-4 mRNA expression by macrophages infected with *L. braziliensis* or *L. infantum* suggests the ability

of these peptides to induce Th1 and Th2 polarization that can lead to a balanced response, no inflammatory pathologies, and protective immune response. According to the literature, the host immunity to a parasite is determined by a suitable Th1 response characterized by IL-12 and IFN-γ production, and induction of iNOS in infected macrophages, which contributes to the control of parasite proliferation (Costa et al., 2002). Regarding the use of biomolecules as vaccine candidates, some studies reported an increase in the levels of IL-12 and IFN-γ in animals immunized with ribosomal protein and infected with *L. infantum* and *L. amazonensis* (Chávez-Fumagalli et al., 2010). Martins et al. (2019) tested the immunogenicity of specific protein from *Leishmania* against *L. major* and *L. braziliensis* infection, and reported that the vaccination induced a Th1 response characterized by the production of IL-12 and IFN-γ.

Although immunity against *Leishmania* is well-known and defined as complex due to the mechanisms used by the parasite to survive in the host immune system. It is well-documented that Th1 response is responsible for inducing resistance to leishmaniosis through the production of inflammatory cytokines, such as IL-12 and IFN-γ, leading to the activation of macrophages and the killing of parasites. On the other hand, susceptibility to infection is related to Th2 development and IL-4 cytokine production, which leads to parasite resistance and replication (Chávez-Fumagalli et al., 2010).

The performance of immune response in immunopathology and the immunoprotection of leishmaniosis remain a paradox. For example, some studies report that, even though the Th1 response induces inflammatory cytokine production and plays a crucial role in the immunoprotection of leishmaniosis, their excessive production can lead to severe immunopathology in the disease (Sacks and Noben-Trauth, 2002; Martin and Leibovich, 2005; Nylén and Eidsmo, 2012). However, apart from inducing the persistence of the parasite at the site of injection, the Th2 response is able to induce anti-inflammatory cytokine production at lower levels, which can mitigate inflammatory reactions and accelerate the healing process (Nylén and Eidsmo, 2012; Pasparakis et al., 2014). These studies suggest that a balance between pro- and anti-inflammatory cytokines is essential, and desirable, to prevent immunopathological disorders and inflammatory reactions and can control the infection. This fact reinforces and corroborates our results that the peptide mix was able to induce the production of a cytokine profile that leads to a Th1 and Th2 immune response. In addition, the parasite load showed a reduction in the parasite. The next step of this study should be to evaluate the peptides in an *in vivo* model.

CONCLUSIONS

It was possible to encapsulate the peptides in the liposomes permitting the use of these molecules to entrap the peptides and delivering them for recognition as immunogenic epitopes by the immune mechanisms, while generating an appropriate immune response against these peptides. This indicates their ability to induce humoral immune response through the production of antibodies capable of reacting against *L. braziliensis* and *L.*

infantum. They also demonstrate the ability to generate cellular immune response through the expression of cytokines that induce Th1 and Th2 polarization of T CD4+ cells, which leads to a balanced response, preventing immunopathological disorders and inflammatory reactions. Most of all, the peptides can lead to the expression of iNOS, the pivotal inductor of the effector molecule NO that controls parasite infection. Finally, these results suggest that the peptides can mimic the parasites proteins that present an important role in the host-parasite interaction, such as histones, and are targets to generate immunity against the parasites. In summary the mix of mimetic peptides tested in this work, by *in vitro* infection, demonstrated a satisfactory development for use as a potential candidate for leishmaniosis vaccines.

DATA AVAILABILITY STATEMENT

The original contributions presented in the study are included in the article/supplementary material, further inquiries can be directed to the corresponding author.

ETHICS STATEMENT

The animal study was reviewed and approved by Comissão de Ética no Uso de Animais Universidade Federal do Paraná.

AUTHOR CONTRIBUTIONS

DG, MS, JC, and JCM performed the animal experiments. RM performed *in silico* analyses. VT-S, CS, JFM, and CC-O performed the conception and design of the work. VT-S and RM synthesized peptides. MS performed the assay qPCR for cytokines and parasites load. DG, VT-S, MS, GC, CS, and ER analyzed the data and wrote the draft of the manuscript. VT-S and CS corrected the final manuscript. VT-S supervised the entire project. All authors contributed to the article and approved the submitted version.

FUNDING

ACKNOWLEDGMENTS

REFERENCES

Abbas, A. K., Lichtman, A. H., and Pillai, S. (2015). *Imunologia Celular e Molecular.* 8th Edn. Amsterdam: Elsevier, 239–263.

Akbarzadeh, A., Rezaei-Sadabady, R., Davaran, S., Woo Joo, S., Zarghami, N., and Hanifehpour, Y. (2013). Liposome: classification, preparation, and applications. *Nanoscale Res. Lett.* 8:102. doi: 10.1186/1556-276X-8-102

Alavi, M., Karimi, N., and Safaei, M. (2017). Application of various types of liposomes in drug delivery systems. *Adv. Pharm. Bull.* 7, 3–9. doi: 10.15171/apb.2017.002

Alonso, C., and Soto, M. (2014). Development of anti-*Leishmania* vaccines: contribution of Spanish researchers. *An. Real Acad. Farm.* 80, 250–264. Available online at: https://core.ac.uk/download/pdf/230311897.pdf

Aslett, M., Aurrecoechea, C., Berriman, M., Brestelli, J., Brunk, B. P., and Carrington, M. (2010). TriTrypDB: a functional genomic resource for the Trypanosomatidae. *Nucleic Acids Res.* 38, 457–462. doi: 10.1093/nar/gkp851

Awate, S., Babiuk, L. A., and Mutwiri, G. (2013). Mechanisms of action of adjuvants. *Front. Immunol.* 4:114. doi: 10.3389/fimmu.2013.00114

Baharia, R. K., Tandon, R., Sahasrabuddhe, A. A., Sundar, S., and Dube, A. (2014). Nucleosomal histone proteins of *L. donovani*: a combination of recombinant H2A, H2B, H, and H4 proteins were highly immunogenic and offered optimum prophylactic efficacy against *Leishmania* challenge in hamsters. *PLoS ONE* 9:e97911. doi: 10.1371/journal.pone.0097911

Beck, Z., Torres, B. O., Matyas, G. R., Lanar, D. E., and Alving, C. R. (2018). Immune response to antigen adsorbed to aluminum hydroxide particles: effects of co-adsorption of ALF or ALFQ adjuvant to the aluminum-antigen complex. *J. Control Release* 275, 12–19. doi: 10.1016/j.jconrel.2018.02.006

Bogdan, C. (2015). Nitric oxide synthase in innate and adaptive immunity: an update. *Trends Immunol.* 36, 161–178. doi: 10.1016/j.it.2015.01.003

Carneiro, M. W., Santos, D. M., Fukutani, K. F., Clarencio, J., Miranda, J. C., and Brodskyn, C. (2012). Vaccination with *L. infantum chagasi* nucleosomal histones confers protection against new world cutaneous *Leishmania*sis is caused by *Leishmania braziliensis*. *PLoS ONE* 7:e52296. doi: 10.1371/journal.pone.0052296

Carrion, J., Folgueira, C., and Alonso, C. (2008). Transitory or long-lasting immunity to *Leishmania* major infection: the result of immunogenicity and multicomponent properties of histone DNA vaccines. *Vaccine* 26, 1155–1165. doi: 10.1016/j.vaccine.2007.12.051

Carrión, J., Folgueira, C., and Alonso, C. (2009). Development of Immunization Strategies against Leishmaniosis based on the *Leishmania* histones pathoantigens. *Procedia Vaccinol.* 1, 101–103. doi: 10.1016/j.provac.2009.07.018

Chamakh-Ayari, R., Bras-Golçalves, R., Bahi-Jader, N., Petitdidier, E., Markikou-Ouni, W., and Aoun, K. (2014). *In vitro* evaluation of a soluble *Leishmania* promastigote surface antigen as a potential vaccine candidate against human *Leishmania*sis. *PLoS ONE* 9:e92708. doi: 10.1371/journal.pone.0092708

Chang, K. P., Reed, S. G., Mcgwire, B. S., and Soong, L. (2003). *Leishmania* model for microbial virulence: the relevance of parasite multiplication and pathoantigenicity. *Acta Trop.* 85, 375–390. doi: 10.1016/S0001-706X(02)00238-3

Chávez-Fumagalli, M. A., Costa, M. A., Oliveira, D. M., Ramirez, L., Costa, L. E., and Duarte, M. C. (2010). Vaccination with the *Leishmania infantum* ribosomal protein induces protection in BALB/c mice against *Leishmania chagasi* and *Leishmania amazonensis* challenge. *Microbes Infect.* 12, 967–977. doi: 10.1016/j.micinf.2010.06.008

Cortés, A., Muñoz-Antoli, C., Esteban, J. G., and Toledo, R. (2017). Th2 and Th1 responses: clear and hidden sides of immunity against intestinal helminths. *Trends Parasitol.* 33, 679–693. doi: 10.1016/j.pt.2017.05.004

Costa, C. H., Stewart, J. M., Gomes, R. B., Garcez, L. M., Ramos, P. K., and Bozza, M. (2002). Assymptomatic human carriers of *Leishmania chagasi*. *Am. J. Trop. Med. Hyg.* 66, 334–337. doi: 10.4269/ajtmh.2002.66.334

De Brito, R. C. F., De O Cardoso, J. M., Reis, L. E. S., Vieira, J. F., Mathias, F. A. S., Roatt, B. M., et al. (2018). Peptide vaccines for *Leishmania*sis. *Front. Immunol.* 9:1043. doi: 10.3389/fimmu.2018.01043

Frank, R. (2002). The spot-synthesis technique. Synthetic peptide arrays on membrane supports–principles and applications. *J. Immunol. Methods* 267, 13–26. doi: 10.1016/S0022-1759(02)00137-0

Freitas, E., Silva, R., Ferreira, L. F., Hernandes, M. Z., De Brito, M. E., and De Oliveira, B. C. (2016). Combination of *in silico* methods in the search for potential CD4(+) and CD8(+) T cell epitopes in the proteome of *Leishmania braziliensis*. *Front. Immunol.* 7:327. doi: 10.3389/fimmu.2016.00327

Guedes, D. C., Pasquali, A. K. S., Minozzo, J. C., Faulds, C., Petterle, R. R., Soccol, C. R., et al. (2019). Biological evaluation of mimetic peptides as active molecules for a new and simple skin test in an animal model. *Parasitol. Res.* 118, 317–324. doi: 10.1007/s00436-018-6128-8

Guex, N., and Peitsch, M. C. (1997). SWISS-MODEL and the Swiss-PdbViewer: an environment for comparative protein modeling. *Electrophoresis* 18, 2714–2723. doi: 10.1002/elps.1150181505

Hamrouni, S., Bras-Gonçalves, R., Kidar, A., Aoun, K., Chamakh-Ayari, R., Petitdidier, E., et al. (2020). Design of multi-epitope peptides containing HLA class-I and class-II-restricted epitopes derived from immunogenic *Leishmania* proteins, and evaluation of CD4+ and CD8+ T cell responses induced in cured cutaneous leishmaniasis subjects. *PLoS Negl. Trop. Dis.* 14:e0008093. doi: 10.1371/journal.pntd.0008093

Handman, E. (2001). *Leishmania*sis: current status of vaccine development. *Clin. Microbiol. Rev.* 14, 229–243. doi: 10.1128/CMR.14.2.229-243.2001

He, P., Zou, Y., and Hu, Z. (2015). Advances in aluminum hydroxide-based adjuvant research and its mechanism. *Hum. Vaccin. Immunother.* 11, 477–488. doi: 10.1080/21645515.2014.1004026

Herrera-Najera, C., Pina-Aguilar, R., Xacur-Garcia, F., Ramirez-Sierra, M. J., and Dumonteil, E. (2009). Mining the *Leishmania* genome for novel antigens and vaccine candidates. *Proteomics* 9, 1293–1301. doi: 10.1002/pmic.200800533

Iborra, S., Soto, M., Carrion, J., Alonso, C., and Requena, J. M. (2004). Vaccination with a plasmid DNA cocktail encoding the nucleosomal histones of *Leishmania* confers protection against murine cutaneous leishmaniosis. *Vaccine* 22, 3865–3876. doi: 10.1016/j.vaccine.2004.04.015

Joshi, S., Rawat, K., Yadav, N. K., Kumar, V., Siddiqi, M. I., and Dube, A. (2014). Visceral leish-maniasis: advancements in vaccine development via classical and molecular approaches. *Front. Immunol.* 5:380. doi: 10.3389/fimmu.2014.00380

Khamesipour, A., Rafati, S., Davoudi, N., Maboudi, F., and Modabber, F. (2006). *Leishmania*sis vaccine candidates for development: a global overview. *Indian J. Med. Res.* 123, 423–438.

Kozlowski, L. P. (2016). IPC—isoelectric point calculator. *Biol. Direct* 11:55. doi: 10.1186/s13062-016-0159-9

Lakhal, S., Mekki, S., Ben-Abda, I., Mousli, M., Amri, F., and Aoun, K. (2012). Evaluation of an Enzyme-linked immunosorbent assay based on crude *Leishmania* histone proteins for serodiagnosis of human infantile visceral *Leishmania*sis. *Clin. Vaccine Immunol.* 19, 1487–1491. doi: 10.1128/CVI.00257-12

Link, J. S., Alban, S. M., Soccol, C. R., Pereira, G. V. M., and Thomaz-Soccol, V. (2017). Synthetic peptides as potential antigens for cutaneous leishmaniosis diagnosis. *J. Immunol. Res.* 2017:5871043. doi: 10.1155/2017/5871043

Livak, K. J., and Schmittgen, T. D. (2001). Analysis of relative gene expression data using real-time quantitative PCR and the $2^{-\Delta\Delta cT}$ Method. *Methods* 25, 402–408. doi: 10.1006/meth.2001.1262

Maroof, A., Brown, N., Smith, B., Hodgkinson, M. R., Maxwell, A., and Losch, F. O. (2012). Therapeutic vaccination with recombinant adenovirus reduces splenic parasite burden in experimental visceral leishmaniasis. *J. Infect. Dis.* 205, 853–863. doi: 10.1093/infdis/jir842

Martin, P., and Leibovich, S. J. (2005). Inflammatory cells during wound repair: the good, the bad, and the ugly. *Trends Cell Biol.* 15, 599–607. doi: 10.1016/j.tcb.2005.09.002

Martínez Salazar, M. B., Delgado Domínguez, J., Silva Estrada, J., González, C. B., and Becker, I. (2014). Vaccination with *Leishmania mexicana* LPG induces 81 PD-1 in CD8+ and PD-L2 in macrophages thereby suppressing the immune response: a model to assess vaccine efficacy. *Vaccine* 32, 1259–1265. doi: 10.1016/j.vaccine.2014.01.016

Martins, T., Lage, D. P., Duarte, M. C., Costa, L. E., Chavez-Fumagalli, M. A., and Roatt, B. M. (2019). Cross-protective efficacy from an immunogen firstly identified in *Leishmania infantum* against tegumentary leishmaniasis. *Parasite Immunol.* 38, 108–117. doi: 10.1111/pim.12304

Meddeb-Garnaoui, A., Toumi, A., Ghelis, H., Mahjoub, M., Louzir, H., and Chenik, M. (2010). Cellular and humoral responses induced by *Leishmania* histone H2B and its divergent and conserved parts in cutaneous and visceral *Leishmania*sis patients, respectively. *Vaccine* 28, 1881–1886. doi: 10.1016/j.vaccine.2009.11.075

Melo, P. D. V., Lima, S. A., Araujo, P., Santos, T. M., Gonzalez, E., Belo, A. A., et al. (2020). Immunoprotection against lethal effects of Crotalus durissus snake venom elicited by synthetic epitopes trapped in liposomes. *Int. J. Biol. Macromol.* 161, 299–307. doi: 10.1016/j.ijbiomac.2020.05.171

Merrifield, R. (1969). Solid-phase peptide synthesis. *Adv. Enzymol. Relat. Areas Mol. Biol.* 32, 221–296. doi: 10.1002/9780470122778.ch6

Moyle, P. M., and Toth, I. (2013). Modern subunit vaccines: development, components, and research opportunities. *ChemMedChem* 8, 360–376. doi: 10.1002/cmdc.201200487

Mukherjee, S., Zhu, J., Zikherman, J., Parameswaran, R., Kadlecek, T. A., and Wang, Q. (2013). Monovalent and multivalent ligation of the B cell receptor exhibit differential dependence upon syk and src family kinases. *Sci. Signal.* 6:ra1. doi: 10.1126/scisignal.2003220

Mutiso, J. M., Macharia, J. C., and Gicheru, M. M. (2010). A review of adjuvants for *Leishmania* vaccine candidates. *J. Biomed. Res.* 24, 16–25. doi: 10.1016/S1674-8301(10)60004-8

Nylén, S., and Eidsmo, L. (2012). Tissue damage and immunity in cutaneous leishmaniasis. *Parasite Immunol.* 34, 551–561. doi: 10.1111/pim.12007

Oh, S. A., and Li, M. O. (2013). TGF-β3: guardian of t-cell function. *J. Immunol.* 191, 3973–3979. doi: 10.4049/jimmunol.1301843

Okamura, T., Morita, K., Iwasaki, Y., Inoue, M., Komai, T., Fujio, K., et al. (2015). Role of TGF-β3 in the regulation of immune responses. *Clin. Exp. Rheumatol.* 34, 63–69.

Olivier, M., Atayde, D., Isnard, A., Hassani, K., and Shio, M. (2012). T. *Leishmania* virulence factors: focus on the metalloprotease GP63. *Microbes Infect.* 14, 1377–1389. doi: 10.1016/j.micinf.2012.05.014

Pasparakis, M., Haasen, I., and Nestle, F. O. (2014). Mechanisms regulating skin immunity and inflammation. *Nat. Rev. Immunol.* 15, 289–301. doi: 10.1038/nri3646

Passos, S., Carvalho, L. P., Orge, G., Jeronimo, S. M., Bezerra, G., and Soto, M. (2005). Recombinant *Leishmania* antigens for serodiagnosis of visceral *Leishmania*sis. *Clin. Diagn. Lab. Immunol.* 12, 1164–1167. doi: 10.1128/CDLI.12.10.1164-1167.2005

Pini, A., Giuliani, A., Falciani, C., Runci, Y., Ricci, C., and Lelli, B. (2005). Antimicrobial activity of novel dendrimeric peptides obtained by phage display selection and rational modification. *Antimicrob. Agents Chemother.* 49, 2665–2672. doi: 10.1128/AAC.49.7.2665-2672.2005

Requena, J. M., Alonso, C., and Soto, M. (2000). Evolutionarily conserved proteins as prominent immunogens during *Leishmania* infections. *Parasitol. Today* 16, 246–250. doi: 10.1016/S0169-4758(00)01651-3

Rhaiem, R. B., and Houimel, M. (2016). Targeting *Leishmania major* parasite with peptides derived from a combinatorial phage display library. *Acta Trop.* 159, 11–19. doi: 10.1016/j.actatropica.2016.03.018

Rice, P., Longden, I., and Bleasby, A. (2000). EMBOSS: The European Molecular Biology Open Software Suite. *Trends Genet.* 16, 276–277. doi: 10.1016/S0168-9525(00)02024-2

Rubinstein, N. D., Mayrose, I., Martz, E., and Pupko, T. (2009). Epitopia: a web-server for predicting B-cell epitopes. *BMC Bioinformatics* 10:287. doi: 10.1186/1471-2105-10-287

Sacks, D., and Noben-Trauth, N. (2002). The immunology of susceptibility and resistance to *Leishmania major* in mice. *Nat. Rev. Immunol.* 2, 845–858. doi: 10.1038/nri933

Saha, S., and Raghava, G. P. S. (2006). Prediction of continuous B-cell epitopes in an antigen using recurrent neural network. *Proteins* 65, 40–48. doi: 10.1002/prot.21078

Santarem, N., Silvestre, R., Tavares, J., Silva, M., Cabral, S., Maciel, J., et al. (2007). Immune response regulation by *Leishmania* secreted and nonsecreted antigens. *J. Biomed. Biotechnol.* 2007:85154. doi: 10.1155/2007/85154

Seger, J. (2014). *Peptídeos sintéticos para diagnóstico e imunoprofilaxia da leishmaniose tegumentar americana* (Dissertation). Federal University of Parana, Curitiba, Brazil.

Singh, B., and Sundar, S. (2012). *Leishmania*sis: vaccine candidates and perspectives. *Vaccine* 30, 3834–3842. doi: 10.1016/j.vaccine.2012.03.068

Skwarczynski, M., and Toth, I. (2016). Peptide-based synthetic vaccines. *Chem. Sci.* 7, 842–854. doi: 10.1039/C5SC03892H

Soto, M., Requena, J. M., Gomez, L. C., Navarrete, I., and Alonso, C. (1992). Molecular characterization of a *Leishmania donovani infantum* antigen identified as histone H2A. *Eur. J. Biochem.* 205, 211–216. doi: 10.1111/j.1432-1033.1992.tb16770.x

Soto, M., Requena, J. M., Morales, G., and Alonso, C. (1994). The *Leishmania infantum* histone H3 possesses an extremely divergent N terminal domain. *Biochim. Biophys. Acta* 1219, 533–535. doi: 10.1016/0167-4781(94)90082-5

Soto, M., Requena, L. M., Quijana, L., Perez, M. L., Nieto, C. G., and Guzman, F. (1999). Antigenicity of the *Leishmania infantum* histones H2B and H4 during canine viscerocutaneous *Leishmania*sis. *Clin. Exp. Immunol.* 115, 342–349. doi: 10.1046/j.1365-2249.1999.00796.x

Souza, A. P., Soto, M., Costa, J. M., Boaventura, S., De Oliveira, C. I., and Cristal, J. R. (2013). Towards a more precise serological diagnosis of human tegumentary *Leishmania*sis using *Leishmania* recombinant proteins. *PLoS ONE* 8:e66110. doi: 10.1371/journal.pone.0066110

Spelberg, B., and Junior, J. E. E. (2001). Type 1/Type 2 immunity in infectious diseases. *Clin. Infect. Dis.* 32, 76–102. doi: 10.1086/317537

Thomaz-Soccol, V., Alban, S., and Seger, J. (2015). *Peptídeos miméticos de Leishmania sp. Processo para sua obtenção e aplicações*. Patent.

Thomaz-Soccol, V., Ferreira Da Costa, E. S., Karp, S. G., Junior Letti, L. A., Soccol, F. T., and Soccol, C. R. (2018). Recent advances in vaccines against *Leishmania* based on patent applications. *Recent Pat. Biotechnol.* 12, 21–32. doi: 10.2174/1872208311666170510121126

Toledo-Machado, C. M., Bueno, L. L., Menezes-Souza, D., Machado-De-Avila, R. A., Nguyen, C., and Granier, C. (2015). Use of phage display technology in development of canine visceral Leishmaniasis vaccine using synthetic peptide trapped in sphingomyelin/ cholesterol liposomes. *Parasit. Vectors* 8:133. doi: 10.1186/s13071-015-0747-z

Vita, R., Overton, J. A., Greenbaum, J. A., Ponomarenko, J., Clark, J. D., and Cantrell, J. R. (2015). The immune epitope database (IEDB) 3.0. *Nucleic Acids Res.* 43, 405–412. doi: 10.1093/nar/gku938

Rapamycin-Loaded Lipid Nanocapsules Induce Selective Inhibition of the mTORC1-Signaling Pathway in Glioblastoma Cells

Delphine Séhédic[1], Loris Roncali[1], Amel Djoudi[1], Nela Buchtova[1], Sylvie Avril[1], Michel Chérel[2], Frank Boury[1], Franck Lacoeuille[1], François Hindré[1] and Emmanuel Garcion[1]*

[1] Univ Angers, Université de Nantes, Inserm, CRCINA, SFR ICAT, Angers, France, [2] Université de Nantes, Inserm, CNRS, CRCINA, Nantes, France

Inhibition of the PI3K/Akt/mTOR signaling pathway represents a potential issue for the treatment of cancer, including glioblastoma. As such, rapamycin that inhibits the mechanistic target of rapamycin (mTOR), the downstream effector of this signaling pathway, is of great interest. However, clinical development of rapamycin has floundered due to the lack of a suitable formulation of delivery systems. In the present study, a novel method for the formulation of safe rapamycin nanocarriers is investigated. A phase inversion process was adapted to prepare lipid nanocapsules (LNCs) loaded with the lipophilic and temperature sensitive rapamycin. Rapamycin-loaded LNCs (LNC-rapa) are ~110 nm in diameter with a low polydispersity index (<0.05) and the zeta potential of about −5 mV. The encapsulation efficiency, determined by spectrophotometry conjugated with filtration/exclusion, was found to be about 69%, which represents 0.6 wt% of loading capacity. Western blot analysis showed that LNC-rapa do not act synergistically with X-ray beam radiation in U87MG glioblastoma model *in vitro*. Nevertheless, it demonstrated the selective inhibition of the phosphorylation of mTORC1 signaling pathway on Ser2448 at a concentration of 1 μM rapamycin in serum-free medium. Interestingly, cells cultivated in normoxia (21% O_2) seem to be more sensitive to mTOR inhibition by rapamycin than those cultivated in hypoxia (0.4% O_2). Finally, we also established that mTOR phosphorylation inhibition by LNC-rapa induced a negative feedback through the activation of Akt phosphorylation. This phenomenon was more noticeable after stabilization of HIF-1α in hypoxia.

Keywords: rapamycin, nanoparticles, radiation, hypoxia, mTOR, Akt, HIF-1α, cancer

INTRODUCTION

Glioblastoma (GB) is the most common and deadly primary brain tumor in adults (Ostrom et al., 2017). Despite remarkable advances in surgical techniques and treatment options including chemotherapy and radiotherapy, the prognosis of this disease remains very poor with a median survival under 15 months (Stupp et al., 2005, 2009). Therefore, the understanding of the molecular mechanisms that drive malignancy in glioblastoma is seriously needed for the development of new agents specifically targeting tumor cells and the tumor microenvironment (Touat et al., 2017; Najberg et al., 2019).

The phosphatidylinositol 3-kinase (PI3K)/protein kinase B (Akt)/mechanistic target of rapamycin (mTOR) intracellular signaling pathway plays a central role in the regulation of cell proliferation, growth, differentiation, and survival (Sonoda et al., 2001; Bjornsti and Houghton, 2004; Knobbe et al., 2005; Castellino and Durden, 2007; Jiang and Liu, 2009). Stimulation of this pathway results in the activation of a receptor tyrosin kinase (RTK) by a cytokine or a growth factor, which drive a sequential phosphorylation of PI3K, Akt, and mTOR. mTOR regulates cell growth and survival *via* two different multiprotein complexes, mTORC1 and mTORC2. The complex mTORC1 is composed of mTOR, regulatory-associated protein of mTOR (Raptor), mammalian lethal with Sec13 protein 8 (mLST8), proline-rich AKT substrate 40 kDa (PRAS40), and DEP-domain-containing mTOR-interacting protein (Deptor) (Saxton and Sabatini, 2017). mTORC1 activates the eukaryotic initiation factor 4E (eIF4E)-binding protein, releasing the transcription factor eIF4E and the p70 ribosomal S6 kinase 1 (S6K1 or p70S6K) implicated in translation (Heimberger et al., 2005).

This pathway can be activated through numbers of mechanisms, including growth factors, overexpression or amplification of Akt family members, inactivation of the inhibitory effects of PTEN (phosphatase and tensin homolog) tumor suppressor or by non-canonical Wnt pathway (Saxton and Sabatini, 2017). Furthermore, radiation can also activate mTOR signaling in vascular endothelium and in glioblastoma cell lines (Eshleman et al., 2002; Shinohara et al., 2005; Anandharaj et al., 2011). Consequently, mutations in the PI3K or AKT genes, loss of PTEN, epigenetic modifications, or constitutive activation of upstream tyrosine kinase receptors will lead to dysregulation of this pathway in a variety of tumors, including GB (Engelman, 2009; Bai et al., 2011; Wick et al., 2011; Mao et al., 2012). As such, there are marked associations between alterations in the PI3K/AKT/mTOR pathway and the poor clinical survival (Engelman, 2009). Therefore, inhibition of the PI3K/Akt/mTOR signaling pathway has been widely investigated as a potential therapy for cancer including glioblastoma (Li et al., 2016). Interestingly, tumor cells in which the PI3K/Akt/mTOR pathway is dysregulated are more susceptible to the inhibition of mTOR, the downstream effector of this signaling pathway, than normal cells (Courtney et al., 2010). Hence, mTOR inhibitors such as rapamycin and its derivatives provide a new class of active agents and therapeutics for GB.

Rapamycin (Sirolimus) is a natural macrolide antibiotic (firstly isolated from samples of Streptomyces hygroscopicus found on Easter Island), which binds to FK506 binding protein 12 (FKBP12). The rapamycin-FKBP12 complex inhibits mTOR and prevents further phosphorylation of proteins involved in the transcription, translation, and cell cycle control (Heimberger et al., 2005). Anandharaj et al. studied three PTEN-null GB cell lines and demonstrated that rapamycin combined with radiotherapy inhibited the inhibitor of apoptosis protein (IAP) family protein surviving through repression of phospho-Akt. Thus, targeting Akt through mTOR with rapamycin increased the radiation sensitivity (Anandharaj et al., 2011). Preclinical trials showed that PTEN deficient tumors and those dependent on PI3K overexpression were most sensitive to rapamycin

(Bjornsti and Houghton, 2004). These results provide a strong basis for investigation of mTOR inhibitors as potential tumor-selective therapeutic agents. Rapamycin and its derivatives, CCI-779 and RAD001, specifically inhibit the function of mTOR by blocking the phosphorylation of downstream molecules, such as p70S6 kinase (p70S6K) and eukaryotic initiation factor 4E-binding protein 1 (4E-BP1), leading to G1-phase cell cycle arrest. Accumulating evidence from preclinical and early clinical studies suggests that these mTOR inhibitors, alone or in combination, would be directly and indirectly effective as growth inhibitors against a broad range of tumors including GB (Mecca et al., 2018; Hsu et al., 2020; Wanigasooriya et al., 2020).

Despite the potency of rapamycin in preclinical studies, clinical development of rapamycin floundered due to the lack of suitable formulations. The low oral bioavailability (<15%) (Yatscoff et al., 1995) precludes tablet formulation except for low dosage treatments such as immunosuppression. Rapamycin's poor solubility in water, ca. 2.6 μg/mL, and common excipients make intravenous (i.v.) formulation difficult (Simamora et al., 2001). In addition, pharmacokinetic studies found that rapamycin strongly partition into the erythrocytes (Kd ca. 20) from where it may not readily access to solid tumors (Yatscoff et al., 1995). This led to the development of ester derivatives, e.g., Temsirolimus or CCI-779, which were more easily formulated. Despite the promise of CCI-779 for mTOR inhibition, intravenous formulations required ethanol that may cause hemolysis (Raymond et al., 2004). Furthermore, phase I trials established that the CCI-779 prodrug was rapidly hydrolyzed in the plasma back into rapamycin thus favoring again potential partition into erythrocytes and unsupportive for tumor accumulation. More recent evolutions with the derivative Everolimus in phase II leads to increase treatment-related toxicities (Chinnaiyan et al., 2018).

In order to improve rapamycine biodistribution, nanovectorization strategies have been developed. They provide a physical protection and allow freeing from solubility problems. In this work, lipid nanocapsules loaded with rapamycin (LNC-rapa) were developed as new nanocarriers for the treatment of GB. We demonstrated that encapsulated rapamycin keeps its biological effect and efficiently inhibits mTOR phosphorylation. LNC-rapa were more cytotoxics than rapamycin alone but, in association with 8Gy radiation, no synergistic effect were observed. This result could be explained by the complexity of the PI3k/Akt/mTOR in GB as demonstrated by activation of phosphorylated Akt with mTOR inhibition and dependence from oxic status.

MATERIALS AND METHODS

Materials

Lipoïd® S75-3 (soybean lecithin at 69% of phosphatidylcholine) and Solutol® HS15 (a mixture of polyethylene glycol 660 and polyethylene glycol 660 hydroxystearate) were kindly provided by LipoïdGmbh (Ludwigshafen, Germany) and BASH (Ludwigshafen, Germany), respectively. NaCl and DMSO were provided by Sigma Aldrich (St-Quentin, Fallavier, France). Deionized water was obtained from a Milli-Q plus

system (Millipore, Paris, France). Lipophilic Labrafac® CC (caprylic-capric acid triglycerides) was provided by Gattefosse S.A. (Saint-Priest, France). Rapamycin was purchased from Interchim (Montluçon, France).Captex® 8000 (Triglyceride of caprylic acid), Transcutol® HP (Diethylene glycol monoethyl ether), and Miglyol® 812 (caprylic/capric triglyceride) were purchased, respectively, from Abitec (Janesville, WI, USA), Gattefosse S.A. (Saint-Priest, France) and Sasol Germany GmbH (Marl, Germany).

Reagents and Antibodies

Rapamycin was dissolved in DMSO. The final concentration of DMSO in the culture medium did not exceed 0.2%. Anti-phospho-mTOR (ab109268, diluted 1:2,000) and anti-HIF-1α (ab51608, diluted 1:2,000) were from Abcam (Cambridge, UK). Anti-phospho-Akt (#4058, diluted 1:1,000) was from Cell Signaling Technology (Beverly, MA, USA) and anti-HSC70 (sc7298, diluted 1:10,000) was from Santa Cruz biotechnology (Dallas, TX, USA). Peroxidase-conjugated anti-mouse (#32430, diluted 1:2,000) and anti-rabbit (#32460, diluted 1:2,000) secondary antibody were from ThermoScientific (Waltham, MA, USA). Lysis buffer: [50 mM Hepes (pH 7.5), 150 mM sodium chloride, 1 mM EDTA (pH 8), 2.5 mM EGTA (pH 7.4), 0.1% Tween 20, 10% glycerol, 0.1 mM sodium orthovanadate, 1 mM sodium fluoride and 10 mM β-glycerophosphate] plus Protease inhibitor cocktail (#539134 Calbiochem, Darmstadt, Germany), PMSF and Phosphatase inhibitor Cocktail Set II (#524636 Calbiochem).

Solubility Assays

Rapamycin solubility assays were performed in different oils: Captex® 8000, Labrafac® CC and Miglyol® 812. Five microgram of rapamycine were dissolved in 250 mg of oil and kept under magnetic stirring during 3 h at room temperature (RT) or at 90°C. Rapamycin concentration was determined by reverse-phase high-performance liquid chromatography (RP-HPLC) after 24 h settling at 4°C, using μBondapack C18 column (Waters Corporation, Milford, MA) with an ultraviolet detector at 278 nm. The mixture of 90% acetonitrile and 10% water (v/v) was used as a mobile phase, and delivered at a flow rate of 2.0 mL/min. The injection volume was 10 μL and the retention time was about 2.3 min.

For spectral analysis of the stability of rapamycin in Labrafac®, rapamycin was solubilized at 1 mg/mL in Labrafac® under magnetic stirring before being submitted to 3 to 6 short cycles of heating (70°C for <1 min) and cooling (RT) or incubated for 1 to 3 h at 70°C in Labrafac. Spectral analysis was then made by use of the CLARIOstar microplate reader (BMG Labtech, Champigny-sur-Marne, France).

Formulation and Physico-Chemical Characterization of Empty (LNCs) and Rapamycin-Loaded Lipid Nanocapsules (LNC-rapa)

LNCs were prepared according to a phase-inversion process adapted from Heurtault et al. (2002). This process involves

the formation of an oil/water microemulsion containing an oily/fatty phase (triglycerides: Labrafac® WL 1349), a non-ionic hydrophilic surfactant (polyethylene glycol hydroxystearate: Solutol® HS15), and a lipophilic surfactant (lecithin: Lipoïd® S75-3). Briefly, 21 mg of Lipoïd® S75-3, 138 mg of Solutol® HS15, 345 mg of Labrafac®, 104 mg of NaCl and 898 mg of deionized water were mixed by magnetic stirring. 5 mg of rapamycin were added to other reagents for a final concentration of 1 mg/mL. Three cycles of progressive heating and cooling between 30 and 70°C were then carried out and followed by an irreversible shock, induced by addition of 3.6 mL of 0°C deionized water. Afterwards, slow magnetic stirring was applied to the suspension for 5 min. LNCs were filtered through a Minisart® 0.2 μm filter (Sartorius, Goettingen, Germany) and kept at 4°C. The average diameter and polydispersity index were determined using Malvern Zetasizer® Nano Serie DTS 1060 (Malvern instruments S.A., Worcestershire, UK).

Encapsulation of drug: For determination of drug encapsulation yield, three samples of filtrate were prepared by dissolution of an exact quantity of LNC dispersion in a 96/4 (v/v) methanol/tetrahydrofurane solution. Free rapamycin (non-soluble) was removed by the filtration performed through the Minisart® 0.2 μm filter and its concentration measured by spectrophotometry at 289 nm. Quantification was achieved by comparison between observed peak area ratios of rapamycin of the samples and a calibration curve performed using the same conditions. Samples were performed in triplicate and the loading capacity (LC) was calculated using the following equation:

$$\text{Drug content (wt\%)} = \frac{\text{mass of encapsulated drug}}{\text{mass of encapsulated drug + mass of LNC excipients}} \times 100 \qquad (1)$$

The encapsulation efficiency (EE) of rapamycin was calculated using the Equation (2):

$$\text{Encapsulation efficiency (wt\%)} = \frac{\text{mass of encapsulated drug}}{mass\ of\ initial\ drug} \times 100 \qquad (2)$$

For electrical conductivity measurements, an electrical conductivity meter (Cond 330i/SET, WTW, Germany) was used in non-linear temperature compensation mode according to EN 27888. The conductivity variations were followed as a function of temperature to determine the emulsion inversion zone.

Cell Culture and Exposure to Hypoxia

Human malignant glioma cell lines U87MG were purchased from American Tissue Culture Collection (Rockville, MD). Tumor cells were cultured in Dulbecco's modified Eagle's medium 4.5 g/L glucose and L-glutamine (DMEM, Lonza, Verviers, Belgium) supplemented with 10% of heat-inactivated fetal bovine serum (FBS, Lonza) and 1% antibiotics suspension (10

units/mL of penicillin, 10 mg/mL streptomycin and $25\,\mu g$/mL amphotericin B, Sigma-Aldrich, Saint-Louis, MO, USA). Tumor cells were incubated at 37°C in 5% CO_2 and 21% (normoxia) or 0.4% O_2 (hypoxia). Hypoxia conditions were obtained by use of an InVivO$_2$ 400 SCI-tive hypoxia workstation (Ruskinn Technology, Ltd., Leeds, UK).

Irradiation Procedure

Irradiation was performed with the CP-160 cabinet x-ray system (Faxitron, Edimex, Le Plessis Grammoire, Angers, France) which delivers a dose of 1,5 grays by min. Irradiation was performed during 5.33 min in order to reach the dose of 8 grays. Irradiation was performed with cells covered. Depending on the condition considered, the cells were placed throughout the experiment in a conventional 21% O_2 incubator at 37°C/5% CO_2 (normoxia) or 0.4% O_2 (hypoxia) at 37°C/5% CO_2 in an InVivO2 400 SCI-tive hypoxia workstation (Ruskinn); they are only placed in an isolated flask for the duration of the irradiations.

Cytotoxicity Evaluation

Two assays were performed to determine the cytotoxicity effect of LNC-rapa on the glioblastoma cell line U87MG:MTS (3-(4,5-dimethylthiazol-2-yl)-5-(3-carboxymethoxyphenyl)-2-(4-sulfophenyl)-2H-tetrazolium) (Promega, Charbonnières, France) and clonogenic assay by crystal violet coloration (Sigma-Aldrich).

For the MTS assay, U87MG cells (5×10^4 cells/mL) harvested in the exponential growth phase were seeded in a 24-well plate in DMEM medium with 10% FBS, in humidified atmosphere (5% CO_2) at 37°C. Once the cells incubated in the exponential growth phase, serum-contained medium was removed and replaced by serum-deprived DMEM supplemented with 1% N1 supplement (Sigma-Aldrich). Free rapamycin dissolved in DMSO (1/10,000, non-toxic) was applied at various concentrations (0.04; 0.2; 1; 5; 10; 20; 100; $200\,\mu$M) for 4 h. 8Gy radiation was performed 6 h after the onset of initial treatment by Faxitron CP-160 (Faxitron X-rays, Lincolnshire, UK). Medium was changed every day. Forty-eight hours following the treatment, MTS reagent was diluted (1:5) in U87MG cell medium and incubated for 2 h at 37°C. The absorbance was measured at 492 nm using Multiskan$^\circledR$ microplate spectrophotometer (Thermo Scientific).

For the clonogenic assay, U87MG cells (10^3 cells/mL) harvested in the exponential growth phase were seeded in a 6-well plate in DMEM medium with 10% FBS, in humidified atmosphere (5% CO_2) at 37°C. Once the cells incubated in the exponential growth phase, serum-contained medium was removed and replaced by serum-deprived DMEM supplemented with 1 % N1 supplement. Cells were treated for 4 h with rapamycin, LNC-rapa at $1\,\mu$M (IC50 LNC-rapa at 21% O_2 corresponding to a 1/1,000 dilution from initial suspension) and with empty LNCs at the same dilution than LNC-rapa. 8Gy radiation was performed 6 h after the treatment by Faxitron CP-160. Ten days after treatment, colonies were colorized by crystal violet and their number was evaluated with ImageJ Software version 1.43.

Depending on the condition considered, the cells were placed throughout the experiment in a conventional 21% O_2 incubator at 37°C/5% CO_2 (normoxia) or 0.4% O_2 (hypoxia) at 37°C/5% CO_2 in an InVivO2 400 SCI-tive hypoxia workstation (Ruskinn); they are only placed in isolated flasks for the duration of the irradiations.

Western Blotting

U87MG cells (2.4×10^5 cells/mL) harvested in the exponential growth phase were seeded in dishes in DMEM medium with 10% FBS, at 37°C in humidified atmosphere containing 5% CO_2 and 21 or 0.4% O_2. Once the cells incubated in the exponential growth phase, serum-contained medium was removed and replaced by serum-deprived DMEM supplemented with 1% N1 supplement. Cells were treated with rapamycin, LNC-rapa at $1\,\mu$M and with empty LNCs at the same dilution than LNC-rapa. 8Gy radiation was performed 6 h after the treatment by Faxitron CP-160 (cf. section Irradiation Procedure).

Sixteen hours after rapamycin initial treatment (untreated, rapamycin, LNC, LNC-rapa), soluble proteins for immunobloting were harvested from tumor cells lysed in $300\,\mu$L lysis buffer on ice. Cells were scrapped and lysed by sonication for 10 s.

Equal amounts of protein from each sample, estimated by the Bio-Rad Protein Assay (Richmond, CA), were separated by electrophoresis through a 4–20% SDS-polyacrylamide gel (Mini-protean$^\circledR$ TGX^{TM} Ge, BioRad), transferred to PVDF membranes (AmershamHybond, GE Healthcare, Buckinghamshire, UK) and blocked with 4% non-fat dry milk in 1X TBS plus 0.1% Tween 20 at RT for 1 h. The membranes were washed and incubated with a primary antibody diluted in 2% BSA in 1X TBS plus 0.1% Tween 20 overnight at 4°C. The membranes were then washed and incubated again for 1 h at RT with peroxidase-conjugated anti-rabbit or anti-mouse secondary antibody. The bound antibody was detected using the enhanced chemiluminescence reagent kit SuperSignal West Femto (Thermo Scientific, Waltham, MA, USA) and read with a bioluminescence detector Image Quant Las 4000 (GE Healthcare, USA).

Statistical Analysis

Three independent biological replicates were performed for all experiments described in this manuscript. Statistical analyses were performed with R software using two-way *analysis* of variance (ANOVA) test. Differences were considered significant if the *p*-value was ≤0.05.
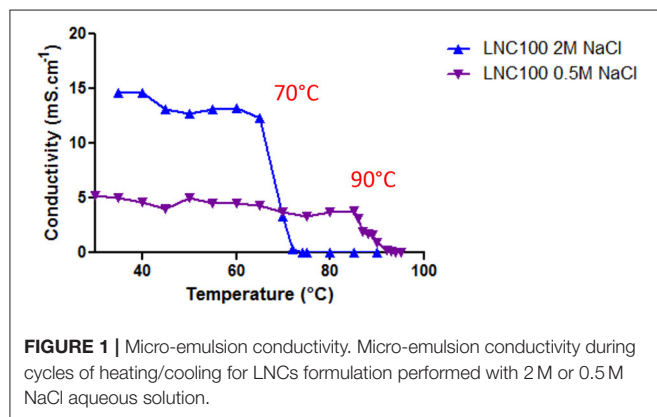
RESULTS

Formulation and Physicochemical Characterization of Rapamycin-Loaded LNCs

As a lipophilic molecule with logP = 4.3, rapamycin can be encapsulated in the lipophilic core of lipid nanocapsules. The formulation of LNCs *via* a phase-inversion process described by Heurtault et al. (2002) involves three cycles of heating/cooling between 60 and 90°C. However, rapamycin degrades at higher temperatures as observed during the solubility assay. Three different oils were tested for the dissolution of rapamycin at room temperature (RT) and at 90°C: Captex$^\circledR$ 8000, Miglyol$^\circledR$ 812

Oil	Temperature	Initial rapamycin (mg/mL)	Dissolved rapamycin (mg/mL)	Dissolution rate (%)
Captex® 8000	RT	19.0	1.8	9.5
	90°C	16.8	0	0
Miglyol® 812	RT	19.2	1.4	7.3
	90°C	17.1	0	0
Labrafac®	RT	24.0	1.5	6.3
	90°C	21.1	0	0

FIGURE 1 | Micro-emulsion conductivity. Micro-emulsion conductivity during cycles of heating/cooling for LNCs formulation performed with 2 M or 0.5 M NaCl aqueous solution.

and Labrafac®. Rapamycin concentration in the supernatant was determined by HPLC and the results are summarized in **Table 1**. At 90°C, rapamycin is completely degraded whatever the oil used. At RT, rapamycin has a comparable solubility in all three oils.

Finally, Labrafac®, pharmaceutically acceptable and in which the stability of rapamycin is confirmed during short cycles of heating and cooling at 70°C (**Supplementary Figure 1**), was used for the formulation of empty and rapamycin-loaded LNCs. Hence, a lower temperature (70°C) was employed in order to avoid rapamycin decomposition. To decrease the phase inversion temperature from 90 to 70°C, we increased the concentration of NaCl aqueous solution. Electrical conductivity of the micro-emulsion was measured as a function of temperature for the "classical formulation" with 0.5 M NaCl and for the formulation with 2 M NaCl (**Figure 1**). A steady state at a high conductivity value indicates that the continuous phase of the emulsion is water, whereas conductivity close to zero means that the continuous phase is oil. The region where the conductivity gradually changes with temperature represents the phase inversion from oil-in-water emulsion to water-in-oil emulsion. **Figure 1** shows that the phase inversion occurs at lower temperature (70°C) when 2 M NaCl aqueous solution is used as compared to 0.5 M NaCl solution (90°C). Thus, increasing NaCl concentration allows us to perform rapamycin encapsulation in non-degrading temperature range between 30 and 70°C.

Empty and rapamycin-loaded LNCs were characterized in terms of their average size and zeta potential. These values are presented in **Table 2**. LNC-rapa have an average size of 112.6 $\pm$ 8.4 nm with a polydispersity index (PDI) of 0.044 $\pm$ 0.011. The zeta potential is of -5.5 ± 0.4 mV. Rapamycin encapsulation efficiency and loading capacity were determined using the equations 1 and 2, these values are also reported in **Table 2**. The encapsulation efficiency is of 68.8 $\pm$ 7.1 wt% thus representing a loading capacity of the nanoparticle of 0.6 $\pm$ 0.1 wt%. This encapsulation efficiency rate was considered in the calculation of rapamycin concentration in biological assays. Insofar as low temperature-made LNC can exhibit fluctuations in their long-term stability with regard to preservation methods not yet fully elucidated, the LNCs used throughout of this work were prepared extemporaneously (**Supplementary Table 1**).

Effect of Rapamycin-Loaded LNCs (LNC-rapa) on mTOR Phosphorylation in U87MG Cells Depending on Oxic Condition and Exposure to Radiation Treatment

Rapamycin binds FKBP12 and the complex FKBP12/rapamycin inhibits mTOR phosphorylation that leads to 4E-BP1 dephosphorylation and inhibition of translation. To check if rapamycin encapsulated within LNCs keeps its biological proprieties, human U87MG glioblastoma cells, that are PTEN negative and thus overactive Akt/mTOR signals, were treated with empty LNCs, LNC-rapa and free rapamycin dissolved in DMSO. The cells were cultured in serum-free medium in atmosphere containing either 21% O_2 or 0.4% O_2.

As cytotoxicity assay performed by MTS with free rapamycin demonstrated a toxic effect only at high concentrations, with more impact in normoxia than in hypoxia (IC50 of 20.54 μM at 21% pO2 and 34.65 μM at 21% pO2 and 0.4% pO2, respectively, **Supplementary Figure 2**), the choice to use a relevant far much lower concentration while using the LNC nanocarrier was made. Hence a concentration of 1 μM (corresponding to the IC50 LNC-rapa at 21% O_2 and to a 1/1,000 dilution from the initial suspension while using LNC) was applied all throughout the work.
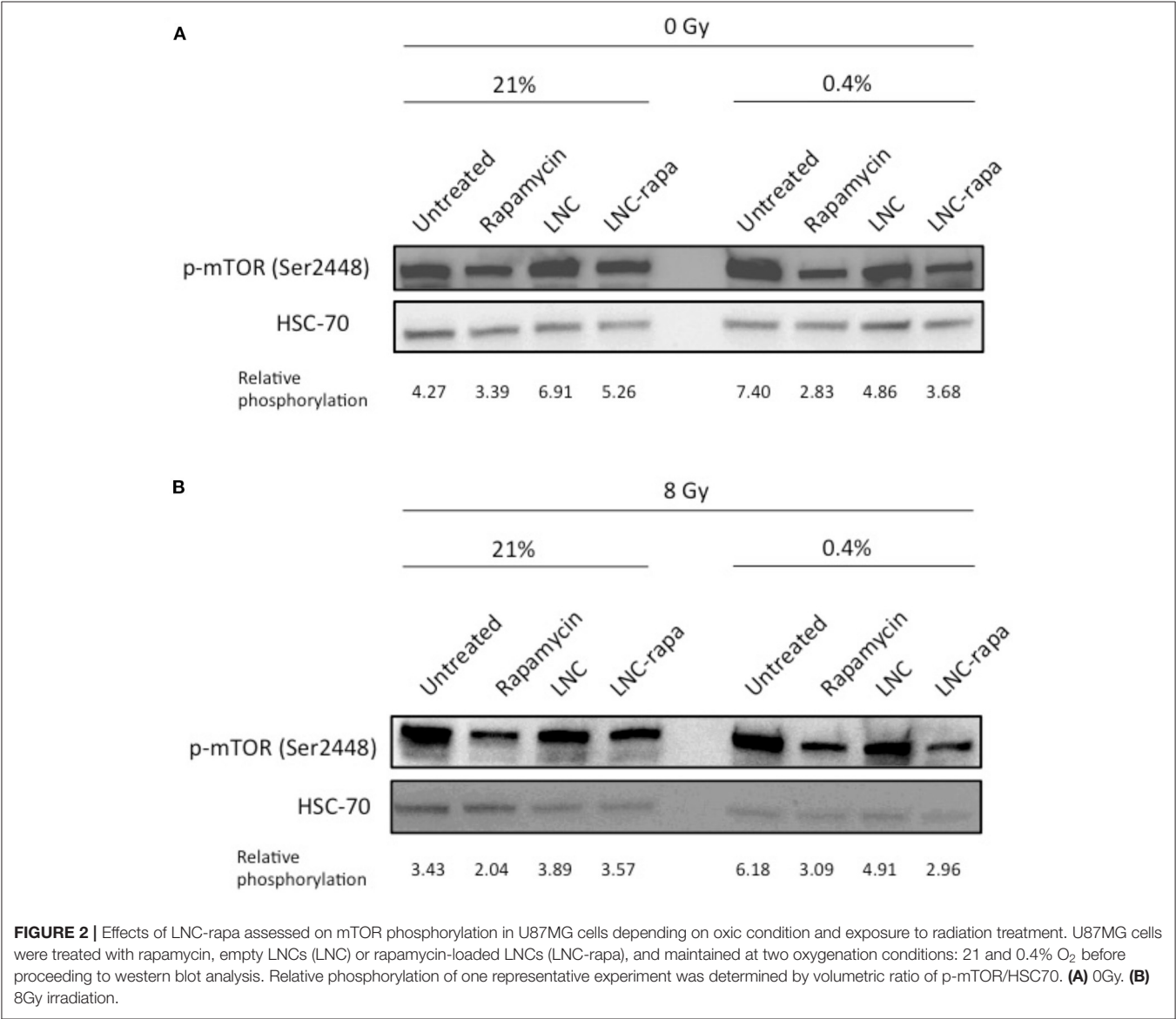
Western blot analysis was performed and relative phosphorylation was determined by volumetric ratio of p-mTOR/HSC70. The results presented in **Figure 2A** indicate that rapamycin-encapsulated within LNCs effectively inhibits mTOR phosphorylation (Ser2448) with modalities much more effective in hypoxia than in normoxia.

This observation is consistent with the one made by Brugarolas and coworkers who notably showed that hypoxia induced mTOR inhibition through TSC1/TSC2 tumor suppressor complex and the hypoxia-inducible gene REDD1/RTP801. They demonstrated that in contrast to energy depletion, mTOR inhibition by hypoxia does not require AMPK or LKB1 but depend on increased expression of the hypoxia inducible *REDD1* gene. They also showed that down-regulation of S6K, an mTOR target, phophorylation by Redd1 requires Tsc2 and Redd1 probably acts up-stream of the Tsc1/Tsc2 complex to down-regulate mTOR function in response to hypoxia (Brugarolas et al., 2004). Thus, at 0.4% oxygenation, mTOR is inhibited by rapamycin and hypoxia, with loaded-LNCs also exerting a higher effect in these conditions (**Figure 2A**).

TABLE 2 | Physicochemical parameters of LNC-rapa.

	Inversion phase (°C)	Size (nm)	PdI	Zeta-potential (mV)	Encapsulation efficiency (% w/w)	Loading capacity (%w/w)
LNC-rapa	70	112.6 ± 8.4	0.04 ± 0.01	−5.5 ± 0.5	68.8 ± 7,1	0.6 ± 0.1
LNC	90	92.3 ± 2.6	0.05 ± 0.02	−8.6 ± 0.6	0	0

Average particle size, PDI, zeta potential, encapsulation efficiency (EE) and loading capacity (LC) of empty and rapamycin-loaded LNCs.

FIGURE 2 | Effects of LNC-rapa assessed on mTOR phosphorylation in U87MG cells depending on oxic condition and exposure to radiation treatment. U87MG cells were treated with rapamycin, empty LNCs (LNC) or rapamycin-loaded LNCs (LNC-rapa), and maintained at two oxygenation conditions: 21 and 0.4% O_2 before proceeding to western blot analysis. Relative phosphorylation of one representative experiment was determined by volumetric ratio of p-mTOR/HSC70. **(A)** 0Gy. **(B)** 8Gy irradiation.

As various synergies have been tested and since the conventional treatment of glioblastoma involves beam radiation, the impact of LNC-rapa on mTOR phosphorylation in U87MG cells was also tested after exposure to 8Gy irradiation. Similar results to the non-irradiated condition are obtained (**Figure 2B**).

Effect of LNC-rapa on U87MG Cell Growth Depending on Oxic Condition and Exposure to Radiation Treatment

To determine the effect of rapamycin encapsulated within LNCs on cancer cell survival and growth depending on the oxygen status and exposure to radiation treatment, a clonogenic assay

was performed. Hence, U87MG cells were grown under two oxygenation conditions (21 or 0.4% O_2) and treaded with either empty LNCs, LNC-rapa or free rapamycin at 1 μM before being exposed, 6 h later, to 0 or 8Gy irradiation. They were then maintained in culture for 10 days and colorized by crystal violet (**Figure 3A**). Under all the conditions tested, a very clear effect of the irradiations, in normoxia (21% pO_2) as in hypoxia (0.4% O_2), was observed (**Figures 3B,C**). Rapamycin, nanovectorized or as free, exerts only moderate effects, however significant at 0.4% O_2, demonstrating the similarity of action of encapsulated LNC-rapa vs. the free form (**Figure 3C**). Interestingly, rapamycin and LNC-rapa do not exert any synergistic effect related to radiation treatment and even slight but significant inhibitory effects impacted radiation efficacy at 0.4% O_2 (**Figure 3C**).

Activation of Alternative Signaling Pathways in Response to Exposure to LNC-rapa in U87MG

The observed duality of the effects of rapamycin and LNC-rapa associating a strong inhibition of mTOR phosphorylation to a moderated cytotoxic effect whatever the environmental conditions used (low/high oxygen or irradiating) led us to focus on the mechanisms that control the PI3K/Akt/ mTOR pathway. Since HIF exerts negative feedback on mTOR (Brugarolas et al., 2004) and mTORC2 complex also exerts feedback control while capable to phosphorylate Akt (Sarbassov et al., 2005; O'Reilly et al., 2006), HIF-1α protein expression and phosphorylation of Akt on Ser473 (Akt-p) were evaluated. Western Blot presented in **Figure 4A** shows that HIF-1α protein expression is reduced when cells are treated with free rapamycin and LNC-rapa whatever oxygenation condition considered. Inversely, these treatments enhance Akt-p protein level. **Figure 4B** shows that at 8Gy, Akt-p protein expression is reduced related to HSC70 in comparison with the 0Gy control condition. Again the down regulation of HIF-1α protein expression by free rapamycin and LNC-rapa is observed concomitantly with the induction of phosphorylation of Akt, thus emphasizing the possible double edge sword impact of LNC-rapa due to the multiplicity of signals downstream mTOR inhibition.

DISCUSSION

This work demonstrated that a new safe formulation of rapamycin encapsulated in lipid nanocapsules at low temperature and without the use of organic solvent, allows keeping its activity while specifically inhibiting mTOR phosphorylation. These observations also established that the mechanism of action of rapamycin-loaded LNCs, to some extent like free rapamycin, involve distinct modalities of responses at 0.4 vs. 21% oxygenation. Indeed, protein expression analysis shows that, if mTOR phosphorylation inhibition is higher at 0.4% O_2, the up-stream effector of PI3k/Akt/mTOR pathway, Akt phosphorylation, is higher too. Furthermore, free rapamycin and

LNC-rapa inhibit HIF-1α expression at 21% O_2 and to a lesser extent at 0.4% O_2. This difference is linked to HIF-1α stabilization under hypoxia.

LNC-rapa as a New Safe Nanocarrier of Rapamycin

In the present study, we developed lipid nanocapsules capable to efficiently encapsulate rapamycin with yield close to 70%. The formulation was done between 30 and 70°C, a temperature range that protects rapamycin from thermal degradation. Capable to cope with poor water solubility of rapamycin and bioavailability due to their capability to effectively reached intracellular cell compartment (Paillard et al., 2010), rapamycin-loaded LNCs keep rapamycin biological proprieties with an effective inhibition of mTOR phosphorylation. Although this tool fulfills its role as a vector, it does not strengthen the activity of rapamycin or one of its selective aspects in our *in vitro* model tested as well as through multiple conditions (8Gy irradiation, 0.4% hypoxia, 21% normoxia).

In the plethora of new rapamycin nanovector formulations currently available, the loading capacities of each of them, their application methods and loco-regional bioavailability should make it possible to resolve the problem of efficiency and possibly synergy with conventional treatments. Thus a loading capacity of 0.6% for LNC-rapa remains low compared to other systems such as polysorbate 80-coated PLGA nanoparticles (Escalona-Rayo et al., 2019), lipid-polyaniline nanoparticles (Wang J. P. et al., 2016) or PEO/PDLLA electrospun nanofibers (Wang B. L. et al., 2016). Comparative studies in particular *in vivo* should make it possible to understand the rationale which makes one of these vectors an appropriate tool or not.

Forrest and coworkers have developed poly(ethylene glycol)-b-poly(ε-caprolactone) (PEG-PCL) micelles loaded with rapamycin and showed that this drug was efficiently loaded within PEG-PCL up to 10 wt% (more than 1 mg/mL) (Forrest et al., 2006). Other group also demonstrated that rapamycin encapsulation within poly(ethylene glycol)-Block-poly(2-methyl-2-benzoxycarbonyl-propylene carbonate) (PEG-b-PBC) micelles reduced its toxicity (Lu et al., 2011). Shi et al. (2013) developed elastin-based protein polymer nanoparticles loaded with rapamycin and decorated with its ligand FKBP. They showed that these objects slowed down the drug release as compared to non-decorated nanoparticles. Moreover, rapamycin elastin-like polypeptide nanoparticles decreased the gross toxicity and enhanced the anti-cancer activity on human breast cancer mice model (Dhandhukia et al., 2017a,b; Peddi et al., 2020). Finally, Tyler and coworkers incorporated rapamycin into biodegradable caprolactone-glycolide (35:65) polymer beads (Tyler et al., 2011). *In vitro*, rapamycin was cytotoxic toward 9L cells (rat glioma cells), causing growth inhibition at a concentration of 0.01 μg/mL. No *in vivo* toxicity was observed at 0.3, 3, and 30% loading doses implanted intracranially. Animals treated with the highest dose of rapamycin beads (30%) consistently demonstrated
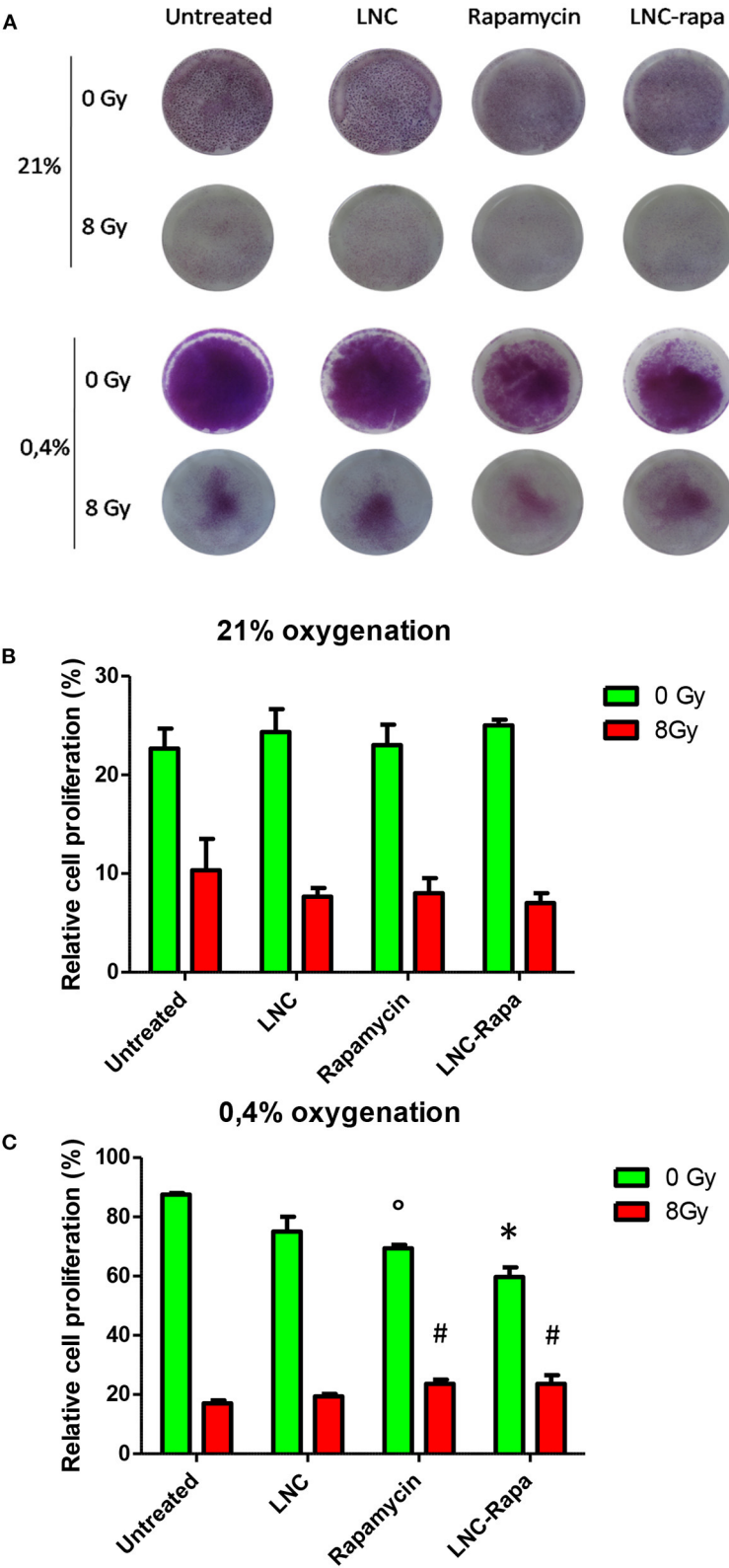
FIGURE 3 | Effects of LNC-rapa assessed by clonogenic assay on U87MG cell growth depending on oxic condition and exposure to radiation treatment. **(A)** Photography of 6-wells plates containing U87MG cells treated with LNCs, rapamycin or LNC-rapa, radiated at 0 Gy (top row) or 8Gy (bottom row) at 21 and 0.4% p0$_2$
(Continued)

FIGURE 3 | and stained with crystal violet. **(B,C)** Cell survival was determined by measuring crystal violet staining of wells exposed to 0 and 8Gy at 21% pO$_2$ **(B)** or 0.4% pO2 **(C)**. Data show the average values from a combination of three independent experiments and error bars display the standard deviation. Two-way ANOVA test was performed between LNC-rapa condition compared to LNC condition (*$p \leq 0.05$) or between rapamycin treatment condition and untreated control condition (°$p \leq 0.05$) or between rapamycin treatment condition and untreated condition (#$p \leq 0.05$).
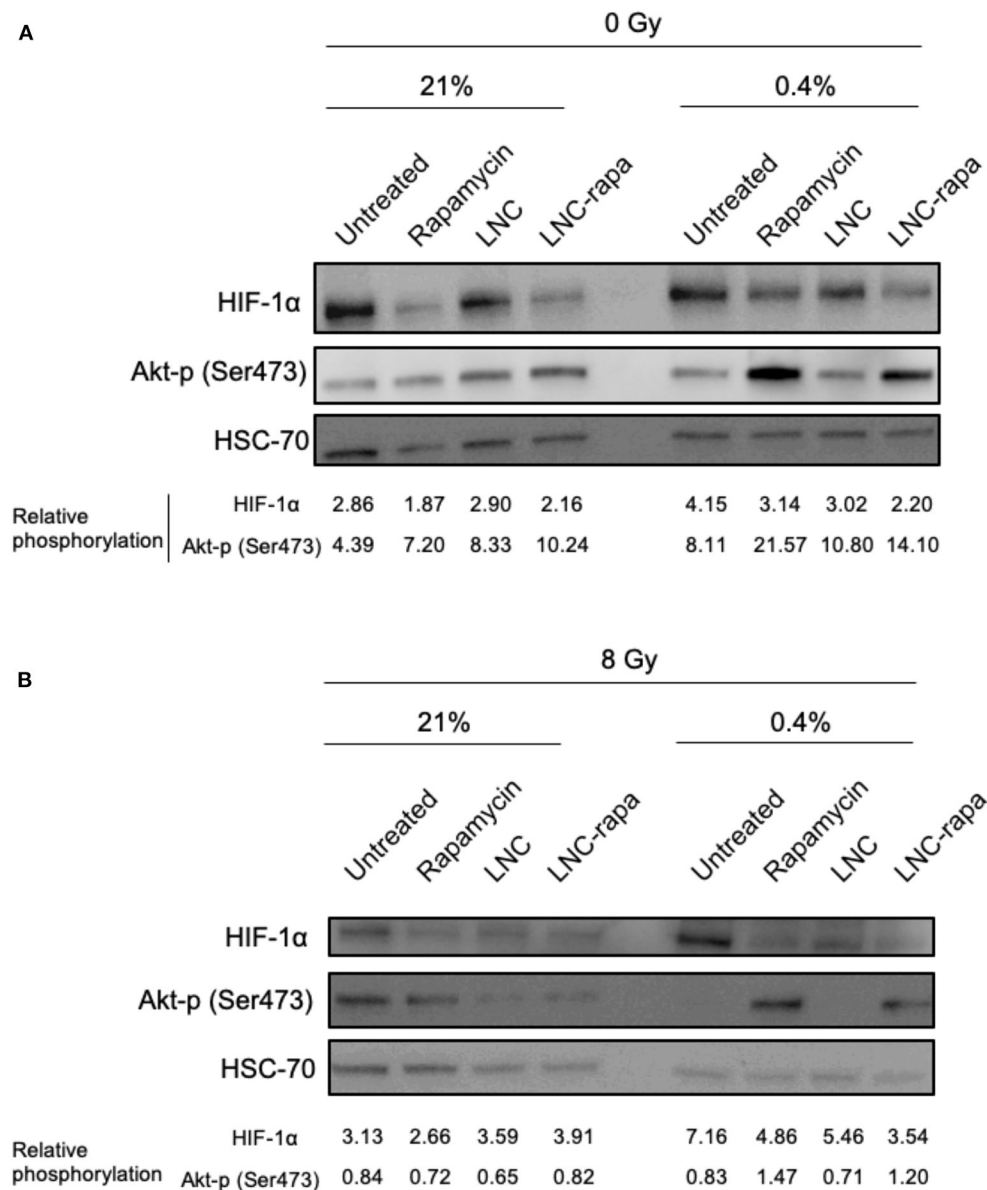
FIGURE 4 | Activation of alternative signaling pathways in response to exposure to LNC-rapa in U87MG. **(A,B)** U87MG cells were treated with free rapamycin, empty LNCs or LNC-rapa, radiated at 0 Gy **(A)** or 8Gy **(B)** and maintained at two oxygenation conditions: 21 and 0.4% before proceeding to western blot analysis. Relative phosphorylation of one representative experiment was measured by volumetry ratio of p-mTOR/HSC70.

significantly longer survival duration than the control and placebo groups. They also showed that radiation therapy in addition to the simultaneous treatment with 30% rapamycin beads led to significantly longer survival duration than each therapy alone.

Vectorized Rapamycin: A Double-Edge Sword "Interactor" in Cancer Cells

The result we obtained on mTOR phosphorylation by rapamycin and LNC-rapa associated with of HIF-1α down regulation and Akt phosphorylation can be linked to the observation made

FIGURE 5 | Rapamycin a likely double-edge sword molecular interactor in U87MG glioblastoma cells. Nanovectorized rapamycin (LNC-rapa) or rapamycin as free, solubilized in DMSO, inhibits the stabilization and transcriptional activity of HIF1α which in turn inhibits the TSC1/TSC2 inhibitor and thus promotes the activation of mTOR. On the other hand, rapamycin inhibits mTORC1 but not mTORC2, which in turn induces Akt phosphrylation. Finally, by inhibiting mTORC1, rapamycin lifts the inhibition exerted by p70s6k on IRS-1, which stabilizes this protein and induces Akt phosphorylation *via* the IGF-1 receptor.

by Hudson et al. who reported that rapamycin inhibits both stabilization of HIF-1α and the transcriptional activity of HIF-1 in hypoxic cancer cells and mTOR dependent signals stimulate HIF-1α accumulation and HIF-1 mediated transcription in cells exposed to hypoxia or hypoxia-mimetic agent (Zhong et al., 2000). Rapamycin-sensitive functions of mTOR are not essential for the accumulation of HIF-1α but are needed for maximal expression of this protein, as well as for optimal HIF-1-dependent gene expression under hypoxic conditions. The notion that mTOR is a nutrient sensor may be particularly relevant to HIF-1 function, since decrease oxygen tensions are almost inevitable accompanied by limited supplies of glucose and amino-acids in mammalian tissues (Hudson et al., 2002). *In vivo*, rapamycin enhance thrombosis and also an increase in the hypoxic zone (Weppler et al., 2007). Hypoxia causes activation of the TSC1/2 complex, which functions to inhibit mTOR. This can occur both *via* induction of the HIF-dependent gene REDD1, and/or through activation of AMPK (Brugarolas et al., 2004; Liu et al., 2006). Rapamycin may be less effective in hypoxic regions of tumors since mTOR may already be at least partially inactivated by TSC. Thus the amount of hypoxia present at the start of

treatment may play a part in determining sensitivity to rapamycin *in vivo* (Weppler et al., 2007) (**Figure 5**).

The higher Akt phosphorylation at 0.4% could also explain that cells are less sensitive to rapamycin than at 21%. Indeed, U87MG cell line is PTEN *null* that drives to a constitutive activation of the PI3K/Akt/mTOR pathway and could explains its radioresistance. Thus, mTOR inhibition could restore radiosensitivity but our results show that maximal cytotoxic effect was observed with 8Gy radiation and rapamycin or LNC-rapa were not sufficient to improve the cytotoxicity at the concentration of $1\,\mu$M. To well-understand this phenomenon, it is important to remind that mTOR exist in two complexes: mTORC1 and mTORC2. mTORC1 contains the mTOR, Raptor, mLST8/GβL, and PRAS40 proteins and controls cell size and protein translation *via* two major substrates, p70S6K and 4E-BP1. Activated S6 kinase causes feedback inhibition of insulin-like growth factor 1 (IGF-1)/insulin signaling by phosphorylating insulin receptor substrate 1 (IRS-1) and causing its degradation (Tremblay et al., 2007). mTORC2 has been shown to phosphorylate Akt at the serine 473 site, which enhances the catalytic activity of Akt already phosphorylated

on threonine 308 (Sarbassov et al., 2005). Rapamycin binds to FKBP-12 and this complex then binds to and causes the allosteric inhibition of mTORC1. Rapamycin effectively blocks S6K phosphorylation and also induces Akt S473 phosphorylation and Akt activity (O'Reilly et al., 2006). Physiologic activation of PI3k/Akt signaling is regulated by mTOR-dependent feed-back inhibition of IRS expression and, consequently, IGF-1 receptor (IGF-1R)/insulin receptor signaling (Tremblay et al., 2007). Rapamycin relieves this feedback and induces Akt S473 phosphorylation in an mTORC2-dependent manner, leading to Akt activation, which may attenuate its therapeutic effects (O'Reilly et al., 2006). Furthermore, mTOR inhibitory drug rapamycin up-regulates IRS-1 protein levels and induces Akt phosphorylation that increase IGF—IR/IRS-1/PI3K signaling to Akt (O'Reilly et al., 2006) (**Figure 5**). In line with this, mTORC2, not inhibited by LNC-rapa, has recently been described as a downstream integrator of metabolic and epigenetic landscape leading to tumor cell survival and cancer durg resistance (Masui et al., 2019, 2020).

In response of those problems, Rodrik-Outmezguine et al. (2011) used a selective ATP-competitive mTOR kinase inhibitor AZD8055. This drug inhibits 4E-BP1 phosphorylation more effectively than rapamycin. It also inhibits mTORC2 and Akt S473 phosphorylation, which leads to Akt T308 dephosphorylation and suppression of Akt activity and downstream signaling. Unfortunately, even though mTORC2 inhibition is potent and persistent, inhibition of Akt T308 and Akt substrate phosphorylation is only transient. Authors demonstrated that this re-induction resulted from hyperactivation of PI3K. In cells in which mTOR kinase inhibitors relieve feedback inhibition of receptor tyrosine kinase, leading to activation of PI3K, the result is a new steady state in which mTORC1 is potently inhibited and Akt is phosphorylated on T308 but not on the S473. This Akt species is activated and able to phosphorylate key substrates in the cells. Induction of PI3K activation depends also from cell directory of activated tyrosine kinase receptors and from active ligands available (Rodrik-Outmezguine et al., 2011).

Alternatively, Kahn and coworkers showed *in vitro* that addition of AZD2014, another mTORC1/mTORC2 inhibitor, to culture media 1 h before irradiation enhanced the radiosensitivity of CD133+ and CD15+ glioblastoma stem-like cells (Kahn et al., 2014). The combination of AZD2014 and radiation delivered to mice bearing GSC-initiated orthotopic xenografts significantly prolonged survival of these animals as compared to individual treatments.

In parallel, dual PI3K/mTOR inhibitors were developed, notably the NVP-BEZ235. It demonstrated suppression of mTORC1 (S6K1, S6K, and 4E-BP1) and mTORC2 (AKT) downstream components resulting in cell cycle arrest and induced autophagy (Cerniglia et al., 2012). NVP-BEZ235 showed inhibited *in vivo* glioma proliferation and improved anti-tumor effects compared to rapamycin analogs. Mukherjee et al. (2012) showed that NVP-BEZ235 can inhibit DNA repair proteins ATM and DNA-PKC in GB that lead to a radiosensitizing effect. Nevertheless, because of the induction of autophagy that seems to be cytoprotective (Cerniglia et al.,

2012), combination therapies with NVP-BEZ235 have been explored. One strategy utilized NVP-BEZ235 with autophagy inhibitor chloroquine to show a synergistic effect in *in vivo* tumor apoptosis (Fan et al., 2010). In line with this, Heinze et al., underlined that under hypoxia and nutrient-poor conditions, second generation mTORC1/C2 inhibitors displayed even stronger cytoprotective effect by reducing oxygen and glucose consumption (Heinzen et al., 2019).

However, those experiences were performed mainly *in vitro* and could yield different results *in vivo*. Indeed, some groups have reported that rapamycin sensitized U87MG xenografts to fractionated radiation therapy. Eshleman and coworkers also showed that there were no radiosensitizing effects of rapamycin on U87MG in the radiation clonogenic survival assays, nevertheless, they observed a great effect in the U87 xenograft and spheroids models (Eshleman et al., 2002). They proposed that other factors could also be important for the sensitizing effect of rapamycin. For example, rapamycin induces significant changes in glucose and nitrogen metabolism, and the starvation-like metabolic state induced by rapamycin could potentially decrease oxygen consumption in solid tumors and improve overall tumor oxygenation (Hardwick et al., 1999). Any decrease in the proportion of radioresistant hypoxic cells should significantly increase the efficacy of radiation. The authors also suggested that rapamycin could inhibit host-dependent processes that contribute to the profound sensitizing effect of rapamycin in xenograft model. Furthermore, rapamycin is a potent inhibitor of endothelial cell proliferation *in vitro*, therefore its systemic administration can inhibit angiogenesis. It reduces VEGF production by tumor cells and the inhibition of VEGF-induced proliferation in endothelial cells (Guba et al., 2002).

In the same way, Weppler et al. (2007) investigated the combination of rapamycin with short course of fractionated radiotherapy to minimize the anti-proliferative effect of rapamycin and thus evaluate its potential to contribute to the direct cytotoxic effect of radiation. They found that rapamycin did not significantly improve radiation response but increased variability in tumor response to radiotherapy, with several individual tumors showing large increases in growth delay. Thus, they underlined the importance to determine the biological factors that mediated this differential response in order to potentially identify patients that may benefit from combination treatment.

CONCLUSION

To conclude, rapamycin-loaded lipid nanocapsules for peripheral or loco-regional administration developed in this study represent a new safe nanocarrier of rapamycin capable to convey rapamycin and preserves its biological activity on cancer cells. We showed that activation of a negative feedback following mTOR phosphorylation inhibition is a serious brake on rapamycin cytotoxicity. The first solution could consist of changing rapamycin for dual PI3K/mTOR inhibitors like the NVP-BEZ235 which has demonstrated effectiveness *in vivo* (Cerniglia et al., 2012), or mTORC1/mTORC2 inhibitor is

AZD2014 which radiosensitizes glioma (Kahn et al., 2014). Nevertheless, rapamycin radiosensitizer effect have been proved *in vivo* or using fractionated radiation protocol (Eshleman et al., 2002). Moreover, if patients are biologically screened to select the most responsive ones, as underlined by Weppler et al., LNC-rapa can potentially be effective with an adapted radiation protocol.

DATA AVAILABILITY STATEMENT

All data generated or analyzed during this study are included in this published article (and its **Supplementary Information** files).

AUTHOR CONTRIBUTIONS

DS and EG wrote the manuscript. EG, FH, MC, FB, and FL contributed to the conception, design, and funding of the work. DS and SA contributed to the experiments. DS, NB, LR, AD, and EG contributed to manuscript revisions. All authors read and approved the submitted version.

FUNDING

ACKNOWLEDGMENTS

SUPPLEMENTARY MATERIAL

The Supplementary Material for this article can be found online at: https://www.frontiersin.org/articles/10.3389/fbioe.2020.602998/full#supplementary-material

Supplementary Figure 1 | Spectral analysis of rapamycin stability in Labrafac®. **(A)** Labrafac spectra at RT. **(B)** Labrafac spectra after 3 h heating at 70°C. **(C)** Rapamycin spectra after 3 h at RT in Labrafac. **(D)** Rapamycin spectra after six short cycles of heating and cooling (70°C to RT) in Labrafac. **(E)** Rapamycin spectra after 1 h heating at 70°C in Labrafac. **(F)** Rapamycin spectra after 3 h heating at 70°C in Labrafac. **(G)** Spectra of rapamycin, previously dissolved in methanol (MeOH), after three short cycles of heating and cooling (70°C to RT) in Labrafac. **(H)** Spectra of rapamycin, previously dissolved in methanol (MeOH), after 3 h heating at 70°C in Labrafac. Each curve represents one representative analysis of a triplicate.

Supplementary Figure 2 | Survival of U87MG cells in response of free-rapamycin treatment assessed by use of MTS assay. **(A)** U87MG cells were treated with free rapamycin at 21% (green curve) and 0.4% (red curve) oxygenation. **(B)** Calculated IC50 at 21 and 0.4% oxygenation following rapamycin treatment.

Supplementary Table 1 | Stability of 50 nm blank and rapamycin loaded LNC during storage at different temperatures. Note the modification of size and loss of polydispersity after 7 days storage (boxes highlighted in gray).

REFERENCES

Anandharaj, A., Cinghu, S., and Park, W. Y. (2011). Rapamycin-mediated mTOR inhibition attenuates survivin and sensitizes glioblastoma cells to radiation therapy. *Acta Biochim. Biophys. Sin.* 43, 292–300. doi: 10.1093/abbs/gmr012

Bai, R. Y., Staedtke, V., and Riggins, G. J. (2011). Molecular targeting of glioblastoma: drug discovery and therapies. *Trends Mol. Med.* 17, 301–312. doi: 10.1016/j.molmed.2011.01.011

Bjornsti, M. A., and Houghton, P. J. (2004). The TOR pathway: a target for cancer therapy. *Nat. Rev. Cancer* 4, 335–348. doi: 10.1038/nrc1362

Brugarolas, J., Lei, K., Hurley, R. L., Manning, B. D., Reiling, J. H., Hafen, E., et al. (2004). Regulation of mTOR function in response to hypoxia by REDD1 and the TSC1/TSC2 tumor suppressor complex. *Genes Dev.* 18, 2893–2904. doi: 10.1101/gad.1256804

Castellino, R. C., and Durden, D. L. (2007). Mechanisms of disease: the PI3K-Akt-PTEN signaling node - an intercept point for the control of angiogenesis in brain tumors. *Nat. Clin. Pract. Neurol.* 3, 682–693. doi: 10.1038/ncpneuro0661

Cerniglia, G. J., Karar, J., Tyagi, S., Christofidou-Solomidou, M., Rengan, R., Koumenis, C., et al. (2012). Inhibition of autophagy as a strategy to augment radiosensitization by the dual phosphatidylinositol 3-kinase/mammalian target of rapamycin inhibitor NVP-BEZ235. *Mol. Pharmacol.* 82, 1230–1240. doi: 10.1124/mol.112.080408

Chinnaiyan, P., Won, M., Wen, P. Y., Rojiani, A. M., Werner-Wasik, M., Shih, H. A., et al. (2018). A randomized phase II study of everolimus in combination with chemoradiation in newly diagnosed glioblastoma: results of NRG oncology RTOG 0913. *Neuro Oncol.* 20, 666–673. doi: 10.1093/neuonc/nox209

Courtney, K. D., Corcoran, R. B., and Engelman, J. A. (2010). The PI3K pathway as drug target in human cancer. *J. Clin. Oncol.* 28, 1075–1083. doi: 10.1200/JCO.2009.25.3641

Dhandhukia, J. P., Li, Z., Peddi, S., Kakan, S., Mehta, A., Tyrpak, D., et al. (2017a). Berunda polypeptides: multi-headed fusion proteins promote subcutaneous administration of rapamycin to breast cancer *in vivo*. *Theranostics* 7, 3856–3872. doi: 10.7150/thno.19981

Dhandhukia, J. P., Shi, P., Peddi, S., Li, Z., Aluri, S., Ju, Y. P., et al. (2017b). Bifunctional elastin-like polypeptide nanoparticles bind rapamycin and integrins and suppress tumor growth *in vivo*. *Bioconjug. Chem.* 28, 2715–2728. doi: 10.1021/acs.bioconjchem.7b00469

Engelman, J. A. (2009). Targeting PI3K signalling in cancer: opportunities, challenges and limitations. *Nat. Rev. Cancer* 9, 550–562. doi: 10.1038/nrc2664

Escalona-Rayo, O., Fuentes-Vazquez, P., Jardon-Xicotencatl, S., Garcia-Tovar, C. G., Mendoza-Elvira, S., and Quintanar-Guerrero, D. (2019). Rapamycin-loaded polysorbate 80-coated PLGA nanoparticles: optimization of formulation variables and *in vitro* anti-glioma assessment. *J. Drug Deliv. Sci. Technol.* 52, 488–499. doi: 10.1016/j.jddst.2019.05.026

Eshleman, J. S., Carlson, B. L., Mladek, A. C., Kastner, B. D., Shide, K. L., and Sarkaria, J. N. (2002). Inhibition of the mammalian target of rapamycin sensitizes U87 Xenografts to fractionated radiation therapy. *Cancer Res.* 62, 7291–7297.

Fan, Q. W., Cheng, C., Hackett, C., Feldman, M., Houseman, B. T., Nicolaides, T., et al. (2010). Akt and autophagy cooperate to promote survival of drug-resistant glioma. *Sci. Signal.* 3:ra18. doi: 10.1126/scisignal.2001017

Forrest, M. L., Won, C. Y., Malick, A. W., and Kwon, G. S. (2006). *In vitro* release of the mTOR inhibitor rapamycin from poly(ethylene glycol)-b-poly(epsilon-caprolactone) micelles. *J. Control. Release* 110, 370–377. doi: 10.1016/j.jconrel.2005.10.008

Guba, M., von Breitenbuch, P., Steinbauer, M., Koehl, G., Flegel, S., Hornung, M., et al. (2002). Rapamycin inhibits primary and metastatic tumor growth by antiangiogenesis: involvement of vascular endothelial growth factor. *Nat. Med.* 8, 128–135. doi: 10.1038/nm0202-128

Hardwick, J. S., Kuruvilla, F. G., Tong, J. K., Shamji, A. F., and Schreiber, S. L. (1999). Rapamycin-modulated transcription defines the subset of nutrient-sensitive signaling pathways directly controlled by the Tor proteins. *Proc. Natl. Acad. Sci. U.S.A.* 96, 14866–14870. doi: 10.1073/pnas.96.26.14866

Heimberger, A. B., Wang, E., McGary, E. C., Hess, K. R., Henry, V. K., Shono, T., et al. (2005). Mechanisms of action of rapamycin in gliomas. *Neuro Oncol.* 7, 1–11. doi: 10.1215/S1152851704000420

Heinzen, D., Dive, I., Lorenz, N. I., Luger, A. L., Steinbach, J. P., and Ronellenfitsch, M. W. (2019). Second generation mTOR inhibitors as a double-edged sword in malignant glioma treatment. *Int. J. Mol. Sci.* 20:4474. doi: 10.3390/ijms20184474

Heurtault, B., Saulnier, P., Pech, B., Proust, J. E., and Benoit, J. P. (2002). A novel phase inversion-based process for the preparation of lipid nanocarriers. *Pharm. Res.* 19, 875–880. doi: 10.1023/A:1016121319668

Hsu, S. P. C., Chen, Y.-C., Chiang, H.-C., Huang, Y.-C., Huang, C.-C., Wang, H.-E., et al. (2020). Rapamycin and hydroxychloroquine combination alters macrophage polarization and sensitizes glioblastoma to immune checkpoint inhibitors. *J. Neurooncol.* 146, 417–426. doi: 10.1007/s11060-019-03360-3

Hudson, C. C., Liu, M., Chiang, G. G., Otterness, D. M., Loomis, D. C., Kaper, F., et al. (2002). Regulation of hypoxia-inducible factor 1 alpha expression and function by the mammalian target of rapamycin. *Mol. Cell. Biol.* 22, 7004–7014. doi: 10.1128/MCB.22.20.7004-7014.2002

Jiang, B. H., and Liu, L. Z. (2009). PI3K/PTEN signaling in angiogenesis and tumorigenesis. *Adv. Cancer Res.* 102, 19–65. doi: 10.1016/S0065-230X(09)02002-8

Kahn, J., Hayman, T. J., Jamal, M., Rath, B. H., Kramp, T., Camphausen, K., et al. (2014). The mTORC1/mTORC2 inhibitor AZD2014 enhances the radiosensitivity of glioblastoma stem-like cells. *Neuro Oncol.* 16, 29–37. doi: 10.1093/neuonc/not139

Knobbe, C. B., Trampe-Kieslich, A., and Reifenberger, G. (2005). Genetic alteration and expression of the phosphoinositol-3-kinase/Akt pathway genes PIK3CA and PIKE in human glioblastomas. *Neuropathol. Appl. Neurobiol.* 31, 486–490. doi: 10.1111/j.1365-2990.2005.00660.x

Li, X., Wu, C., Chen, N., Gu, H., Yen, A., Cao, L., et al. (2016). PI3K/Akt/mTOR signaling pathway and targeted therapy for glioblastoma. *Oncotarget* 7, 33440–33450. doi: 10.18632/oncotarget.7961

Liu, L. P., Cash, T. P., Jones, R. G., Keith, B., Thompson, C. B., and Simon, M. C. (2006). Hypoxia-induced energy stress regulates mRNA translation and cell growth. *Mol. Cell* 21, 521–531. doi: 10.1016/j.molcel.2006.01.010

Lu, W. L., Li, F., and Mahato, R. I. (2011). Poly(ethylene glycol)-block-poly(2-methyl-2-benzoxycarbonyl-propylene carbonate) micelles for rapamycin delivery: *in vitro* characterization and biodistribution. *J. Pharm. Sci.* 100, 2418–2429. doi: 10.1002/jps.22467

Mao, H., LeBrun, D. G., Yang, J. X., Zhu, V. F., and Li, M. (2012). Deregulated signaling pathways in glioblastoma multiforme: molecular

mechanisms and therapeutic targets. *Cancer Invest.* 30, 48–56. doi: 10.3109/07357907.2011.630050

Masui, K., Harachi, M., Cavenee, W. K., Mischel, P. S., and Shibata, N. (2020). mTOR complex 2 is an integrator of cancer metabolism and epigenetics. *Cancer Lett.* 478, 1–7. doi: 10.1016/j.canlet.2020.03.001

Masui, K., Harachi, M., Ikegami, S., Yang, H. J., Onizuka, H., Yong, W. H., et al. (2019). mTORC2 links growth factor signaling with epigenetic regulation of iron metabolism in glioblastoma. *J. Biol. Chem.* 294, 19740–19751. doi: 10.1074/jbc.RA119.011519

Mecca, C., Giambanco, I., Donato, R., and Arcuri, C. (2018). Targeting mTOR in glioblastoma: rationale and preclinical/clinical evidence. *Dis. Markers.* 2018:9230479. doi: 10.1155/2018/9230479

Mukherjee, B., Tomimatsu, N., Amancherla, K., Camacho, C. V., Pichamoorthy, N., and Burma, S. (2012). The dual PI3K/mTOR inhibitor NVP-BEZ235 is a potent inhibitor of ATM- and DNA-PKcs-mediated DNA damage responses. *Neoplasia* 14, 34–43. doi: 10.1593/neo.111512

Najberg, M., Haji Mansor, M., Boury, F., Alvarez-Lorenzo, C., and Garcion, E. (2019). Reversing the tumor target: establishment of a tumor trap. *Front. Pharmacol.* 10:887. doi: 10.3389/fphar.2019.00887

O'Reilly, K. E., Rojo, F., She, Q. B., Solit, D., Mills, G. B., Smith, D., et al. (2006). mTOR inhibition induces upstream receptor tyrosine kinase signaling and activates Akt. *Cancer Res.* 66, 1500–1508. doi: 10.1158/0008-5472.CAN-05-2925

Ostrom, Q. T., Gittleman, H., Liao, P., Vecchione-Koval, T., Wolinsky, Y., Kruchko, C., et al. (2017). CBTRUS statistical report: primary brain and other central nervous system tumors diagnosed in the united states in 2010–2014. *Neuro Oncol.* 19, v1–v88. doi: 10.1093/neuonc/nox158

Paillard, A., Hindre, F., Vignes-Colombeix, C., Benoit, J. P., and Garcion, E. (2010). The importance of endo-lysosomal escape with lipid nanocapsules for drug subcellular bioavailability. *Biomaterials* 31, 7542–7554. doi: 10.1016/j.biomaterials.2010.06.024

Peddi, S., Roberts, S. K., and MacKay, J. A. (2020). Nanotoxicology of an elastin-like polypeptide rapamycin formulation for breast cancer. *Biomacromolecules* 21, 1091–1102. doi: 10.1021/acs.biomac.9b01431

Raymond, E., Alexandre, J., Faivre, S., Vera, K., Materman, E., Boni, J., et al. (2004). Safety and pharmacokinetics of escalated doses of weekly intravenous infusion of CCI-779, a novel mTOR inhibitor, in patients with cancer. *J. Clin. Oncol.* 22, 2336–2347. doi: 10.1200/JCO.2004.08.116

Rodrik-Outmezguine, V. S., Chandarlapaty, S., Pagano, N. C., Poulikakos, P. I., Scaltriti, M., Moskatel, E., et al. (2011). mTOR kinase inhibition causes feedback-dependent biphasic regulation of AKT signaling. *Cancer Discov.* 1, 248–259. doi: 10.1158/2159-8290.CD-11-0085

Sarbassov, D. D., Guertin, D. A., Ali, S. M., and Sabatini, D. M. (2005). Phosphorylation and regulation of Akt/PKB by the rictor-mTOR complex. *Science* 307, 1098–1101. doi: 10.1126/science.1106148

Saxton, R. A., and Sabatini, D. M. (2017). mTOR signaling in growth, metabolism, and disease. *Cell* 168, 960–976. doi: 10.1016/j.cell.2017.02.004

Séhédic, D. (2014). *Development of new nano-medicine strategies for the targeting and the radiosensization of glioblastoma stem cells* (Université d'Angers). Available online at: https://www.theses.fr/2014ANGE0028

Shi, P., Aluri, S., Lin, Y. A., Shah, M., Edman, M., Dhandhukia, J., et al. (2013). Elastin-based protein polymer nanoparticles carrying drug at both corona and core suppress tumor growth *in vivo*. *J. Control. Release* 171, 330–338. doi: 10.1016/j.jconrel.2013.05.013

Shinohara, E. T., Cao, C., Niermann, K., Mu, Y., Zeng, F. H., Hallahan, D. E., et al. (2005). Enhanced radiation damage of tumor vasculature by mTOR inhibitors. *Oncogene* 24, 5414–5422. doi: 10.1038/sj.onc.1208715

Simamora, P., Alvarez, J. M., and Yalkowsky, S. H. (2001). Solubilization of rapamycin. *Int. J. Pharm.* 213, 25–29. doi: 10.1016/S0378-5173(00)00617-7

Sonoda, Y., Ozawa, T., Aldape, K. D., Deen, D. F., Berger, M. S., and Pieper, R. O. (2001). Akt pathway activation converts anaplastic astrocytoma to glioblastoma multiforme in a human astrocyte model of glioma. *Cancer Res.* 61, 6674–6678.

Stupp, R., Hegi, M. E., Mason, W. P., van den Bent, M. J., Taphoorn, M. J., Janzer, R. C., et al. (2009). Effects of radiotherapy with concomitant and adjuvant temozolomide vs. radiotherapy alone on survival in glioblastoma in

a randomised phase III study: 5-year analysis of the EORTC-NCIC trial. *Lancet Oncol.* 10, 459–466. doi: 10.1016/S1470-2045(09)70025-7

Stupp, R., Mason, W. P., van den Bent, M. J., Weller, M., Fisher, B., Taphoorn, M. J., et al. (2005). Radiotherapy plus concomitant and adjuvant temozolomide for glioblastoma. *N. Engl. J. Med.* 352, 987–996. doi: 10.1056/NEJMoa043330

Touat, M., Idbaih, A., Sanson, M., and Ligon, K. L. (2017). Glioblastoma targeted therapy: updated approaches from recent biological insights. *Ann. Oncol.* 28, 1457–1472. doi: 10.1093/annonc/mdx106

Tremblay, F., Brule, S., Um, S. H., Li, Y., Masuda, K., Roden, M., et al. (2007). Identification of IRS-1 Ser-1101 as a target of S6K1 in nutrient- and obesity-induced insulin resistance. *Proc. Natl. Acad. Sci. U.S.A.* 104, 14056–14061. doi: 10.1073/pnas.0706517104

Tyler, B., Wadsworth, S., Recinos, V., Mehta, V., Vellimana, A., Li, K., et al. (2011). Local delivery of rapamycin: a toxicity and efficacy study in an experimental malignant glioma model in rats. *Neuro Oncol.* 13, 700–709. doi: 10.1093/neuonc/nor050

Wang, B. L., Li, H. Y., Yao, Q. Y., Zhang, Y. L., Zhu, X. D., Xia, T. L., et al. (2016). Local *in vitro* delivery of rapamycin from electrospun PEO/PDLLA nanofibers for glioblastoma treatment. *Biomed. Pharmacother.* 83, 1345–1352. doi: 10.1016/j.biopha.2016.08.033

Wang, J. P., Guo, F., Yu, M., Liu, L., Tan, F. P., Yan, R., et al. (2016). Rapamycin/DiR loaded lipid-polyaniline nanoparticles for dual-modal imaging guided enhanced photothermal and antiangiogenic combination therapy. *J. Control. Release* 237, 23–34. doi: 10.1016/j.jconrel.2016.07.005

Wanigasooriya, K., Tyler, R., Barros-Silva, J. D., Sinha, Y., Ismail, T., and Beggs, A. D. (2020). Radiosensitising cancer using phosphatidylinositol-3-kinase (PI3K), protein kinase B (AKT) or mammalian target of rapamycin (mTOR) inhibitors. *Cancers* 12:1278. doi: 10.3390/cancers12051278

Weppler, S. A., Krause, M., Zyromska, A., Lambin, P., Baumann, M., and Wouters, B. G. (2007). Response of U87 glioma xenografts treated with concurrent rapamycin and fractionated radiotherapy: possible role for thrombosis. *Radiother. Oncol.* 82, 96–104. doi: 10.1016/j.radonc.2006.11.004

Wick, W., Weller, M., Weiler, M., Batchelor, T., Yung, A. W. K., and Platten, M. (2011). Pathway inhibition: emerging molecular targets for treating glioblastoma. *Neuro Oncol.* 13, 566–579. doi: 10.1093/neuonc/nor039

Yatscoff, R. W., Wang, P., Chan, K., Hicks, D., and Zimmerman, J. (1995). Rapamycin - distribution, pharmacokinetics, and therapeutic range investigations. *Ther. Drug Monit.* 17, 666–671. doi: 10.1097/00007691-199512000-00020

Zhong, H., Chiles, K., Feldser, D., Laughner, E., Hanrahan, C., Georgescu, M. M., et al. (2000). Modulation of hypoxia-inducible factor 1 alpha expression by the epidermal growth factor/phosphatidylinositol 3-kinase/PTEN/AKT/FRAP pathway in human prostate cancer cells: implications for tumor angiogenesis and therapeutics. *Cancer Res.* 60, 1541–1545.

Advantages of publishing in Frontiers

OPEN ACCESS
Articles are free to read for greatest visibility and readership

FAST PUBLICATION
Around 90 days from submission to decision

HIGH QUALITY PEER-REVIEW
Rigorous, collaborative, and constructive peer-review

TRANSPARENT PEER-REVIEW
Editors and reviewers acknowledged by name on published articles

REPRODUCIBILITY OF RESEARCH
Support open data and methods to enhance research reproducibility

DIGITAL PUBLISHING
Articles designed for optimal readership across devices

FOLLOW US
@frontiersin

IMPACT METRICS
Advanced article metrics track visibility across digital media

EXTENSIVE PROMOTION
Marketing and promotion of impactful research

LOOP RESEARCH NETWORK
Our network increases your article's readership